IL
NUOVO CIMENTO
ORGANO DELLA SOCIETÀ ITALIANA DI FISICA
SOTTO GLI AUSPICI DEL CONSIGLIO NAZIONALE DELLE RICERCHE

VOL. XX, N. 6 *Serie decima* 16 Giugno 1961

Polarization in Proton-Beryllium and Proton-Proton Scattering at 1.7 GeV.

P. BAREYRE, J. F. DETOEUF, L. W. SMITH (*), R. D. TRIPP (**) and L. VAN ROSSUM

Laboratoire de Physique Corpusculaire à Haute Energie, C.E.N. - Saclay

(ricevuto il 23 Gennaio 1961)

Summary. — The polarization in p-Be and p-p scattering has been measured by counter techniques at a proton kinetic energy of 1.74 GeV. The maximum polarization in p-Be scattering was found to be $P_{max} = 0.19 \pm 0.04$ and occurs at an angle $\theta_{max} \geqslant 3.5°$. Inelastic scatters were rejected when the inelastic momentum loss was more than about 1% in the first scatter (magnetic analysis) or more than about 5% in the second scatter (Čerenkov threshold counter). The maximum polarization in p-p scattering is $P_{max} = 0.30 \pm 0.09$ and occurs at an angle $35° < \theta_{max} < 55°$ (c.m.). The angular dependence of the polarization is consistent with a distribution proportional to $\sin 2\theta$ within large statistical errors. Optical model calculations applied to the data on p-Be scattering yield an almost all imaginary central potential of about 43 MeV and a spin-orbit potential of between 0.9 MeV and 2.0 MeV which is also almost all imaginary, in contrast with the predominantly real spin-orbit potential needed to explain the large polarization in the region of several hundred MeV.

1. – Introduction.

Polarization of nucleons in nuclear collisions has been extensively investigated in the energy region accessible to cyclotrons. In particular, the range from 100 MeV to 400 MeV has been most carefully studied because of the large polarization observed.

(*) Present adress: Brookhaven National Laboratory, Upton, L.I., N.Y.
(**) Present adress: Lawrence Radiation Laboratory, Berkeley, Cal.

Above 1 GeV experiments have been limited to the total proton cross-section on protons, neutrons and nuclei and to differential elastic cross-sections in proton-proton collisions.

In this paper we report the results of experiments on proton-proton and proton-beryllium polarization at 1.74 GeV done at the Saclay Proton-Synchrotron. A summary of these results was presented at the 1960 International Conference on High Energy Physics at Rochester.

2. – Experimental.

2·1. *Proton-beryllium double scattering.* – In a first experiment protons of $T_p = 1.74$ GeV were elastically scattered from two successive beryllium targets. Both scatterings are in the same plane. The left-right asymmetry of the differential cross-section in the second scattering was measured by a counter telescope (Fig. 1).

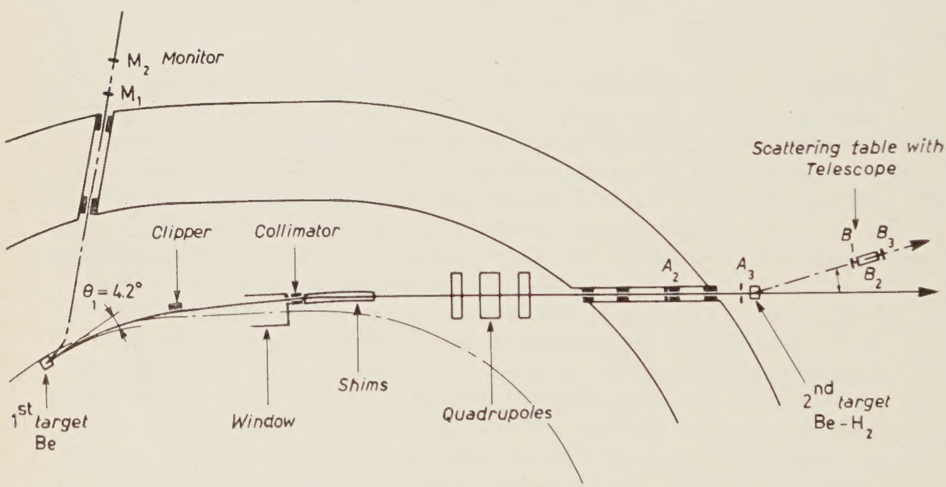

Fig. 1. – Layout of the 4.2° beam from beryllium.

The first scattering occurred at a scattering angle of 4.2° from an internal target in one of the magnet sections of the synchrotron. Beryllium was chosen as target material. At this energy the first diffraction minimum occurs at about 6°. The dimensions of the target were 3.0 cm (vertical), 1.5 cm (radial) and 3.3 cm (thickness).

The scattered beam was deflected by about 30° in the magnet section. At the following straight section the beam left the vacuum chamber, passed through a lead collimator, and was deflected again by about 4° in the fringing

field of the next magnet section. Along the beam path the gradient of the fringing field was modified by shims to prevent undesired focussing. The emerging beam was focussed by a triplet of 15 cm bore quadrupole lenses onto the second target located outside the main shielding wall.

The momentum dispersion $(1/p)\cdot(\mathrm{d}p/\mathrm{d}x)$ at the image, as calculated from the beam optics, was of the order of 1% per cm.

The aperture of the beam was defined by the opening in the collimator. Several additional iron collimators were placed along the passage through the shielding wall. From the exit of the lead collimator up to the second target the beam passed through helium filled bags to reduce multiple scattering.

The beam incident on the second target had a flux of $3.5\cdot10^5$ protons/10^{10} circulating protons and was approximately 2 cm in diameter. On the high momentum side the intensity fell to less than 1/50 of its peak value at 2.0 cm from the axis. On the low momentum side there was a tail of about $\frac{1}{7}$ peak value, due to protons scattered inelastically at the first target. These inelastic protons travelled from the target to the main collimator along trajectories with a smaller radius of curvature and could be intercepted by a clipper located in the magnet section outside the circulating beam. The position of the clipper was adjusted to achieve a symmetric intensity distribution at the second target.

The energy of this beam is variable and depends upon the energy of the protons incident on the internal target.

Since the same field deflects the incident and the scattered protons, the position of the beam is independent of momentum within the approximations:

a) that the ratio of incoming to outgoing momentum is independent of energy, and

b) that the relative value of the magnetic field along the path of the scattered beam is also independent of energy, *i.e.*, independent of the absolute value of the magnetic field.

The variation, with time, of the average momentum resulted in a shift of the beam center line because conditions *a*) and *b*) are only approximately satisfied. The beam incident on the second target moved by 0.07 cm during the 5 ms interval. False asymmetry, which could possibly result from this shift, was reduced by continuously observing that the time distribution of the beam intensity did not change during the experiment.

Definition in addition to collimators was achieved with two plastic scintillation detectors. Because of the high counting rate, « negative » defining counters were used, *i.e.*, the beam passed through a hole in the scintillator and the output of the detector produced a « veto » pulse. One of the scintillators (A_2), located in the shielding wall, excluded protons which could be scattered by the edge of the last iron collimators. The other one (A_3), close to the image, excluded particles which passed by the target.

The second target was a beryllium cylinder, 5.0 cm in diameter and 4.0 cm thick. Protons scattered in this target were detected by a counter telescope consisting of two plastic scintillators (B_1), (B_3) and an ethylene filled Čerenkov counter (B_2). The resolution of the Čerenkov counter and the energy spread of the beam were such that protons scattered with a loss of more than 80 MeV were excluded. The three counters were mounted on the moving arm of a scattering table. This arm could be swung left and right of the beam, rotating around a vertical axis which intersected the center line of the incident beam in the center of the second target. The first scintillation counter (B_1) was 3.0 cm wide and 7.0 cm high, at 280 cm from the target. Its angular position defined the scattering angle and was adjusted for each measurement to within one minute of arc with a theodolite located vertically above the pivot. The angle was measured with respect to the direction of the incident beam which was deduced from the beam profile as found when the whole telescope was moved through the forward direction. The results on the left-right asymmetry as a function of the scattering angle are given in Section **3**.

For the line-up procedure at the scattering table, which was repeated many times throughout the experiment, a small exploring telescope checked the position of the beam center line on the pivot and the main telescope checked the beam direction.

Because of the high counting rate in the scattered beam the protons incident on the second target could not be counted directly. A monitor telescope with a counting rate 160 times lower was set up in a beam of negative pions from the first target. These pions, emerging at forward angles, were deflected by 50° in the magnetic field of the accelerator. By positioning a collimator in the main shielding wall the average momentum was chosen to be about 400 MeV/c, close to the maximum of the pion production spectrum. The energy dependence of the ratio between the monitor beam and the scattered proton beam was checked and found to be small enough to be neglected.

2·2. *Proton-proton scattering in the* 4.2° *beam from beryllium.* – Once the polarization of the beam described in the previous section was measured by second scattering on beryllium, the same beam was used to study the polarization in proton-proton scattering, substituting hydrogen as second scatterer.

A 40 cm long liquid hydrogen target with styrofoam insulation and mylar windows was used for scattering up to c.m. angles of about 40°. The design of the target has been published previously (1).

Small angle proton-proton scattering was measured by the counter telescope (B_1), (B_2) and (B_3) as described above for scattering on beryllium, except

(1) P. Prugne, M. Marquet and M. Bougon *Onde Electrique*, **39**, 612 (1959).

2364

that the velocity threshold of the Čerenkov counter was adjusted for each scattering angle.

For scattering angles greater than 30° in the c.m. both outgoing protons could be detected in coincidence by plastic scintillators at conjugate angles, and the liquid hydrogen was replaced by a CH_2 target 3.0 cm in diameter and 7.0 cm thick. The coincidences due to scattering on nucleons in carbon were subtracted by comparaison with a carbon target in which discs of the same total stopping power were spaced such as to fill the same volume as the CH_2 target.

One of the scintillators (J_1), (7.0 cm wide and 14 cm high) was mounted on the main arm of the scattering table, at 130 cm from the pivot. On the shorter arm, at the conjugate angle, was mounted the second scintillator (J_2), at 95 cm from the pivot. The width and the height of (J_2) were different for the various scattering angles. The width was always chosen big enough such that (J_1) defined the angular interval of the scattering angle, whereas it was the height of (J_2) which defined the maximum angle between the scattering plane and the horizontal plane. In order to reduce accidental coincidences a third scintillator, (J_3), was used on the main arm, 4.0 cm back of (J_1), with 1 cm of Cu between (J_1) and (J_3).

The sensitivity to misalignment of (J_2) and the subtraction of coincidences from carbon were checked by moving the short arm to either side of its conjugate position. The efficiency for detecting the slow protons was checked at the largest angle for (J_3) by taking a range curve with Cu absorbers in front of (J_2).

When plotting the results which are given in Section **3**, the convention used is that the scattering angle is given by the angle of the proton detected in the counters on the main arm. The c.m. angle greater than 90° means that the slower proton was detected on the main arm.

2·3. *Proton-proton scattering in the* 18.3° *beam from* CH_2 *or* C. – The hydrogen results obtained in the experiment described in the previous section shows that a proton beam elastically scattered from hydrogen at an laboratory angle of 10° or 20° is at least as much polarized as that obtained by diffraction scattering on beryllium.

Experiments were therefore carried out in such a beam, with both first and second scatter on hydrogen or carbon, thus providing a check on the polarization in proton-proton scattering independent of the results obtained on beryllium (Fig. 2).

The first target was located in one of the straight sections of the proton synchrotron. Either a CH_2 target of 1.0 cm (vertical), 1.5 cm (radial), 8.0 cm (length), or a carbon target of the same dimensions was used.

Protons emerging at 18.3° were momentum-analysed by a magnet which

deflected the elastically scattered beam by 12°. A quadrupole doublet produced an image of about 2.5 cm (horizontal) by 5.0 cm (vertical) outside the main shielding wall, on the second target. The momentum dispersion, $(1/p)\cdot(\mathrm{d}p/\mathrm{d}x)$, at the image was about 0.6 % per cm.

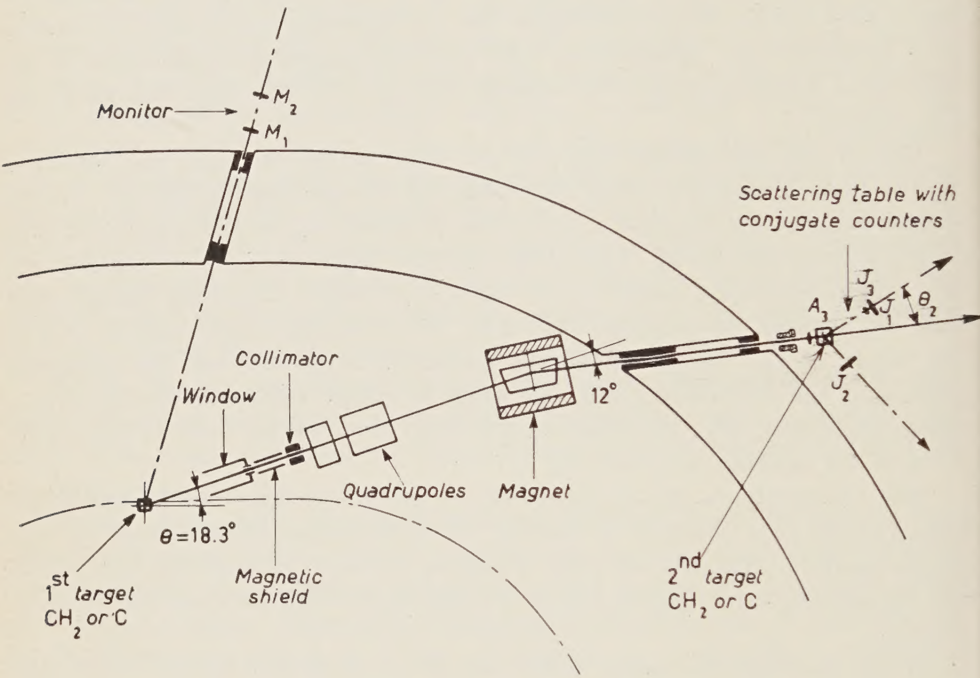

Fig. 2. – Lay-out of the 18.3° beam from CH_2 or C.

From the peak in the momentum spectrum of the protons, as measured by varying the magnet current, one could deduce that with CH_2 as first target about 70 % of the protons incident on the second target had been elastically scattered on free hydrogen, the remainder on nucleons in carbon. It was found necessary to use a defining counter in front of the second target. The beam flux incident on this counter (3.0 cm × 5.0 cm) was about 10^4 protons/10^{10} circulating protons, with CH_2 as first target.

The energy of the protons incident on the first target was chosen such that the energy in the first and in the second scattering (1.94 GeV and 1.58 GeV) were by roughly equal amounts above and below the energy at which the first experiments had been done (1.74 GeV).

The bombarding of the target was extended over 4 ms. In this interval the momentum of the incident protons varied by 0.5 %. The scattered beam being analysed by a d.c. magnetic field, the position of the elastic peak at the second target moved by about 0.8 cm during the 4 ms counting interval.

The time distribution of the intensity was again checked continuously in order to reduce possible false asymmetry arising from jitter in the average beam position.

The second scattering occured in a CH_2 target 3.5 cm wide, 5.5 cm high and 10 cm thick, or in a carbon target of the same stopping power in the same volume.

The left-right asymmetry was measured at only one angle (30° in the c.m.) by the proton-proton coincidence method as described in Section **2**'2, but requiring, in addition, a coincidence with the beam defining counter (A_3) in front of the target.

3. – Results and discussion of errors.

3'1. *Elastic cross-section on* Be. – The differential elastic cross-section for protons on Be is shown in Fig. 3. For scattering angles greater than 4° there is a significant contamination by inelastic scattering. Statistical errors are shown. We assign an additional systematic uncertainty of $\pm 10\%$ to the absolute cross-section. In order to deduce the 0° elastic differential cross-section following PRESTON *et al.* ([2]) (see also ([3])), we

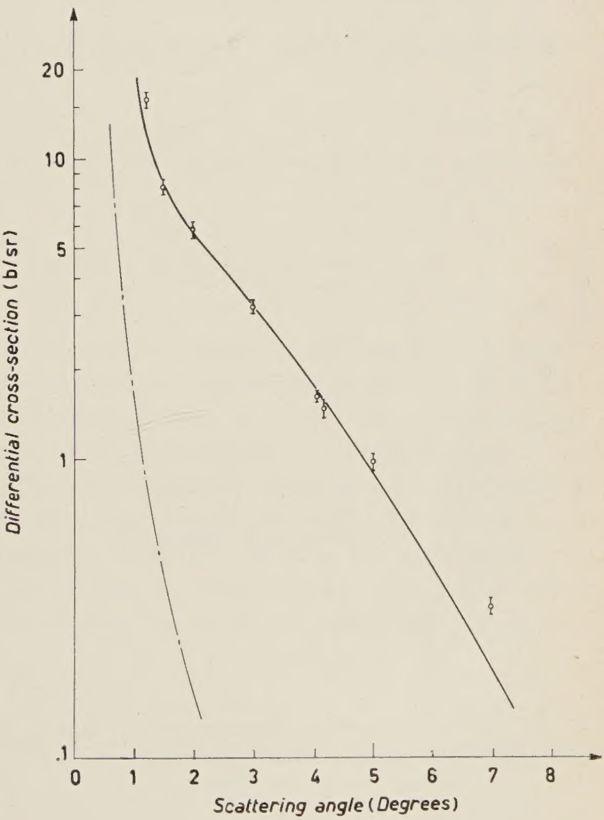

Fig. 3. – Differential elastic cross-section for 1.73 GeV protons on beryllium *vs.* laboratory scattering angle. The dashed line is the point-charge Coulomb scattering cross-section and the solid line is a fit to the data with a modified exponential nucleon density distribution: $\varrho(r)=\varrho(0)(1+r/a)\exp[-r/a]$, where $a = 0.55$ fermi, leading to a r.m.s. radius of 2.3 fermi.

([2]) W. M. PRESTON, R. WILSON and J. C. STREET: *Phys. Rev.*, **118**, 579 (1960).
([3]) H. A. BETHE: *Ann. Phys.*, **3**, 190 (1958).

2367

have fitted the curve between 2° and 4° by a formula of the type

$$\sigma(\theta) = [\sigma_n(0) + \sigma_c(0)] \cdot |F(k, \theta)|^2 ,$$

with: $\sigma_n(0)$ being the 0° nuclear cross-section,

$\sigma_c(0)$ the Coulomb point charge cross-section,

$F(k, \theta)$ a form factor related to the nucleon density distribution $\varrho(r)$ by

$$F(q) = \frac{4\pi}{q} \int_0^\infty \varrho(r) \cdot \sin qr \cdot r \, \mathrm{d}r .$$

Using a variety of density distributions we have found extrapolated 0° cross-sections in agreement with a value

$$\sigma_n(0) = (8 \pm 2) \text{ barn/steradian} .$$

3'2. *Asymmetry on* Be. – Fig. 4 shows as function of the scattering angle, the asymmetry

$$e = \frac{\sigma_L - \sigma_R}{\sigma_L + \sigma_R} ,$$

of the differential elastic cross-section for protons of the 4.2° beam from Be, scattered again on Be. Statistical errors only are shown. We estimate an additional instrumental uncertainty in the asymmetry of $\Delta e = \pm 0.014$. (See Table I).

From the angular dependence of the asymmetry it was concluded that the maximum of polarization occurs at some angle

$$\theta_{max} \geqslant 3.5° .$$

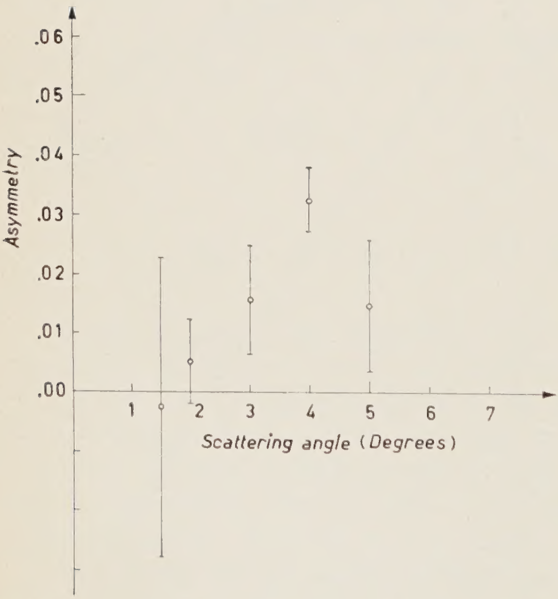

Fig. 4. – Proton-beryllium asymmetry *vs.* laboratory scattering angle. First scattering at 4.2°. Beam energy: 1.73 GeV.

Because of the larger contamination by inelastic events, the asymmetry observed at 5° was not considered to establish an upper limit for θ_{max}.

2368

TABLE I. – *Table of instrumental errors in the measurement of asymmetries.*

First target	Be	Be	CH_2, C	
Second target	Be	CH_2, C	CH_2, C	
Average slope of the differential cross-section $(\mathrm{d} \ln \sigma)/\mathrm{d}\theta$	0.60	0.25	0.25	degree^{-1}
Time shift of beam position at second target	0.014	0.014	0.20	cm ms^{-1}
Jitter in beam position corresponding to $\frac{1}{8}$ of gate width	0.012	0.012	0.13	cm
Distance from pivot to defining counter	280	130	120	cm
	Asymmetry Δe $(\cdot 10^2)$			
Uncertainty of 0.02° in beam direction	1.2	0.5	0.5	
Uncertainty from jitter in beam position	0.14	0.14	1.6	
Rate effects and drifts in coincidence efficiencies	0.70	0.32	0.32	
Angular misalignment of the conjugate counter	—	0.36	0.36	
Vertical misalignment of counters on both arms	—	0.01	0.01	
Total instrumental uncertainty	1.4	0.7	1.8	

3·3. *Polarization of the* 4.2° *beam.* – The square root of the 4.2° asymmetry yields the beam polarization:

$$P_{4.2}^{\mathrm{Be}} = \sqrt{e_{4.2}} = \sqrt{0.032 \pm 0.015} = 0.18^{+0.04}_{-0.05}\ .$$

This neglects the difference in the average energy at the first and the second scatter (about 10 MeV) and assumes that the contamination of inelastic events has the same effect on the polarization in both scatters. The statistical and the instrumental uncertainties have been combined. An independent measurement of the same quantity $P_{4.2}^{\mathrm{Be}}$ was obtained by measuring the polarization in proton-proton scattering with both first and second scattering on CH_2 or C (in the 18.3° beam) and by comparing these results with the asymmetry observed in the 4.2° beam when H_2 or CH_2 was used as second target. A table showing the various experiments is given in Table II. The following expressions and results were used:

$$K = \frac{\text{carbon flux}}{\mathrm{CH_2}\ \text{flux}} = 0.30 \pm 0.05 \ \text{(incident on the second target in experiment 4.)}$$

The relation:

$$P_{18.3}^{\mathrm{CH_2}} = K P_{18.3}^{\mathrm{C}} + (1-K) P_{18.3}^{\mathrm{H}}$$

2369

may be expanded into

$$(P^{\mathrm{Be}}_{4.2})^2 = \frac{e_1 \cdot e_2}{e_3} \cdot \frac{1 - K}{1 - K(e_4/e_3)}\,,$$

where

$$e_1 = P^{\mathrm{Be}}_{4.2} \cdot P^{\mathrm{H}}_{18.3} = 0.053 \pm 0.012 \quad \text{(experiment 3)}$$

$$e_2 = P^{\mathrm{Be}}_{4.2} \cdot P^{\mathrm{H}}_{14} = 0.069 \pm 0.013 \quad \text{(» 2 and 3)}$$

$$e_3 = P^{\mathrm{CH_2}}_{18.3} \cdot P^{\mathrm{H}}_{14} = 0.049 \pm 0.022 \quad \text{(» 4)}$$

$$e_4 = P^{\mathrm{C}}_{18.3} \cdot P^{\mathrm{H}}_{14} = 0.048 \pm 0.022 \quad \text{(» 5)}$$

TABLE II. – *Table of the various experiments.*

Exp. no.	First scatter				Second scatter				Results
	T_p GeV	tar-get	lab. angle	Selection of elastic events	T_p GeV	target	lab. angle	Selection of elastic events	
1	1.74	Be	4.2°	Synchrotron field	1.73	Be	1.5° to 5°	Čerenkov Ctr	Fig. 4
2	1.74	Be	4.2°	Synchrotron field	1.73	H_2	3° to 14°	Čerenkov Ctr	Fig. 7
3	1.74	Be	4.2°	Synchrotron field	1.73	CH_2	10° to 14°	p-p coincid.	Fig. 7
4	1.94	CH_2	18.3°	Fixed ext. field	1.58	CH_2—C	14°	p-p coincid.	$P^{18}_{\mathrm{CH_2}} P^{14}_{\mathrm{H}} = .049 \pm .022$
5	1.94	C	18.3°	Fixed ext. field	1.58	CH_2	14°	p-p coincid.	$P^{18}_{\mathrm{C}} P^{14}_{\mathrm{H}} = .048 \pm .022$

By this means one obtains $P^{\mathrm{Be}}_4 = 0.27 \pm 0.10$. The larger error in this result is due principally to the fact that the same fluctuations in the momentum of the protons incident on the internal target lead to a larger jitter in beam position for the 18.3 beam because it was deflected by a d.c. magnetic field. The instrumental uncertainty in experiments 4 and 5 were $\Delta e = \pm 0.018$ (See Table I).

The direct and the indirect measurement of the polarization of the 4.2° beam, when combined, yield

$$P^{4.2}_{\mathrm{Be}} = 0.19 \pm 0.04\,.$$

3·4. *Polarization in proton-proton scattering.* – Fig. 5 shows the asymmetry of the differential elastic cross-section (scale on the left) for protons of the 4.2° beam from Be scattered on hydrogen as second target. The circles represent small angle data obtained with liquid hydrogen and a Čerenkov counter to select elastic events. The larger angle data indicated by crosses are those found with a CH_2 target, both outgoing protons being detected in coincidence. The scale on the right gives the polarization in the scattering on hydrogen, assuming that the beam polarization was 0.19.

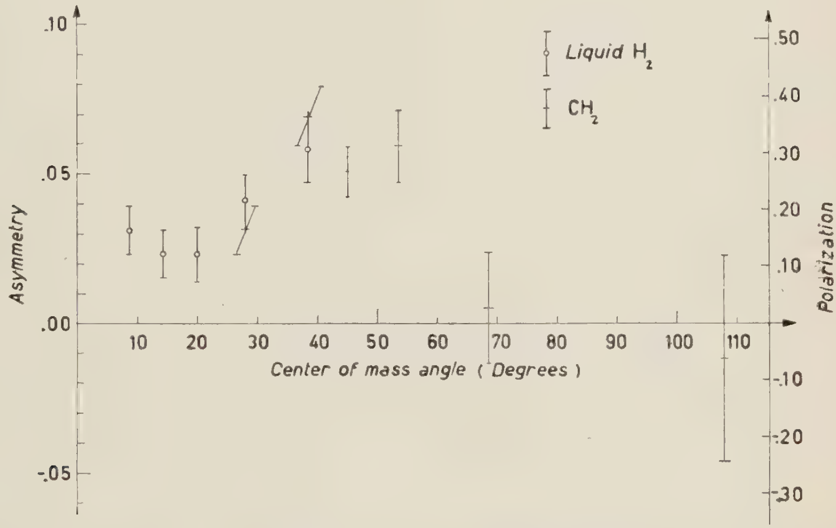

Fig. 5. – Proton-proton asymmetry *vs.* c.m. scattering angle. Polarization scale on the right corresponds to a beam polarization of 0.19.

Statistical errors only are shown. Additional instrumental errors in the measurement of the asymmetry amounted to

$$\Delta e = \pm\, 0.007\,, \quad \text{(see Table I)}\,.$$

The maximum of polarization appears to occur at a c.m. angle between 35° and 55°. Its value is

$$P_{\max} = 0.30 \pm 0.09\,.$$

The error includes the uncertainty of the beam polarization.

4. – Interpretation of results.

4·1. *Beryllium.* – The polarization in nucleon-nucleus scattering can be understood in terms of the optical model using a complex central and spin-orbit potential of the form

$$V(r) = V_c(r) + \lambda_\pi^2 \frac{1}{r} \cdot \frac{\mathrm{d}V_s(r)}{\mathrm{d}r} \boldsymbol{\sigma}\cdot\boldsymbol{L}\,, \tag{1}$$

where: $V_c = v_c \exp[i\varphi_c]$ = complex central potential

$V_s = v_s \exp[i\varphi_s]$ = complex spin-orbit potential

λ_π = pion Compton wave lenght.

As shown by FERMI [4], the calculation of the polarization when done in the Born approximation yields a particularly simple result. (The Born approximation calculation of the polarization has been justified for small angles and excluding the region of the diffraction minimum. It will be assumed for the sake of this discussion that the concept of a potential at relativistic energies continues to have some validity.) Evaluating the transition matrix of the above potential between plane wave incident and scattered states of wave numbers k and k' respectively, one obtains for the transition matrix

$$M = g(\theta) + \boldsymbol{\sigma}\cdot\boldsymbol{n}\, h(\theta)\,, \tag{2}$$

$$g(\theta) = \frac{m_p}{2\pi\hbar^2}\int V_c \exp[-i\Delta\boldsymbol{k}\cdot\boldsymbol{r}]\,\mathrm{d}\boldsymbol{r}\,, \tag{3}$$

$$h(\theta) = \frac{m_p}{2\pi\hbar^2}(-i\sin\theta\,\lambda_\pi^2 k^2)\int V_s \exp[-i\Delta\boldsymbol{k}\cdot\boldsymbol{r}]\,\mathrm{d}\boldsymbol{r}\,, \tag{4}$$

$$\Delta\boldsymbol{k} = \boldsymbol{k}' - \boldsymbol{k} = \text{momentum transfer}\,.$$

The polarization is given by

$$P = \frac{2\,\mathrm{Re}\, g^* h}{|g|^2 + |h|^2}\,. \tag{5}$$

Substituting eq. (3) and eq. (4) into eq. (5), one obtains

$$P = P_{\max} \frac{2\chi}{1+\chi^2}\,, \tag{6}$$

[4] E. FERMI: *Suppl. Nuovo Cimento*, **2**, 84 (1955).

2372

where

(7) $$P_{max} = \sin(\varphi_c - \varphi_s)$$

(8) $$\chi = \frac{\sin\theta}{\sin\theta_{max}}, \qquad \theta = \text{scattering angle}$$

$$\sin\theta_{max} = \left(\frac{m_\pi c}{R}\right)^2 \left| \frac{\int V_c \exp[-i\Delta\boldsymbol{k}\cdot\boldsymbol{r}]\,\mathrm{d}\boldsymbol{r}}{\int V_s \exp[-i\Delta\boldsymbol{k}\cdot\boldsymbol{r}]\,\mathrm{d}\boldsymbol{r}} \right|,$$

where: θ_{max} = angle of maximum polarization,

R = momentum of the incident proton.

Taking the same radial dependence for V_c and V_s, eq. (8) is simply

(9) $$\sin\theta_{max} = \left(\frac{m_\pi c}{R}\right)^2 \frac{v_c}{v_s},$$

From these expressions we see that the polarization is independent of nuclear size and that:

a) the maximum value of polarization depends only on the phase angle between the central and spin orbit potentials;

b) the angle at which the maximum polarization occurs is inversely proportional to the momentum squared if the potentials are independent of momentum.

We shall now discuss the specification of these potentials. The imaginary part of the central potential arises from inelastic processes occuring in the nuclear collision. It is given by [5]

(10) $$\mathrm{Im}[V_c] = \frac{\hbar v \bar{\sigma}}{(8/3)\pi R_0^3},$$

where: v = nucleon laboratory velocity,

$$\bar{\sigma} = \tfrac{1}{2}\gamma(\sigma_{pp} + \sigma_{np}).$$

γ is a factor accounting for the suppression of inelastic collisions with small momentum transfer due to the Pauli principle. For energies greater than 100 MeV, $\gamma \approx 1$.

At 1.74 GeV $\sigma_{pp} = 45$ mb, $\sigma_{np} = 41$ mb. Using $R_0 = 1.3\cdot 10^{-13}$ cm one finds $\mathrm{Im}[V_c] = 43$ MeV.

---

[5] W. B. Riesenfeld and K. M. Watson: *Phys. Rev.*, **102**, 1157 (1956).

A measure of the real central potential can be obtained by means of the optical theorem from a comparison of the total cross-section and the forward scattering cross-section. The optical theorem states

$$\operatorname{Im} g(0) = \frac{k}{4\pi}\,\sigma_{\text{tot.}}\,.$$

Extrapolating the proton-beryllium total cross-section results of CHEN, LEAVITT and SHAPIRO [6] to 1.74 GeV one obtains

$$\sigma_{\text{tot}} = (0.28 \pm 0.03)\ \text{barn}\,.$$

This yields $|\operatorname{Im} g(0)|^2 = (8.2 \pm 2.0)$ barn/sr.

If we compare this value to our experimental result for the 0° elastic differential cross-section of Section 3·1:

$$\sigma_n(0) = (8 \pm 2)\ \text{barn/sr}\,,$$

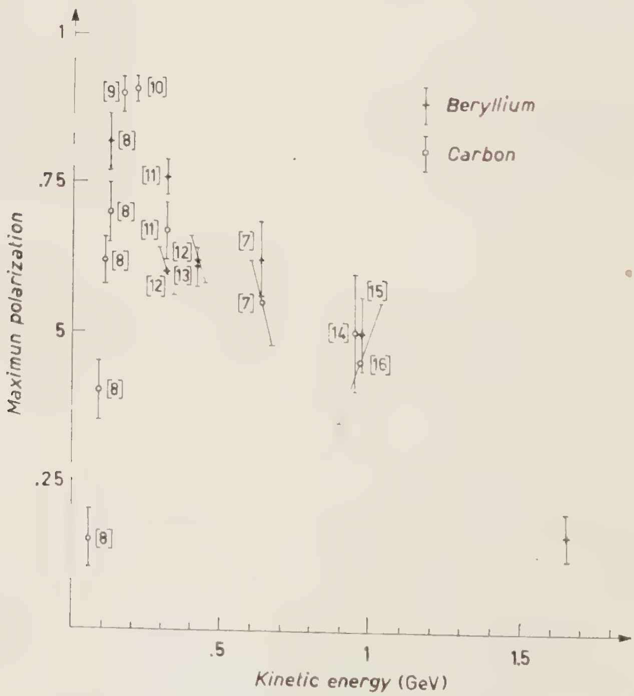

Fig. 6. – Maximum polarization in scattering on nuclei at various energies (see references). The data at about 1 GeV are deduced from the published asymmetries assuming that the polarization of the beam was 0.33 [24].

---

(6) F. F. CHEN, C. P. LEAVITT and A. M. SHAPIRO: *Phys. Rev.*, **99**, 857 (1955).

2374

we conclude from

$$\sigma_n(0) = |\operatorname{Re} g(0)|^2 + |\operatorname{Im} g(0)|^2$$

that $\operatorname{Re} g(0)$ is consistent with zero.

In the Born approximation, the real and imaginary parts of $g(0)$ (eq. (3)) are proportional respectively to the real and imaginary parts of the central potential. Thus one can conclude that very nearly all of the central potential is imaginary.

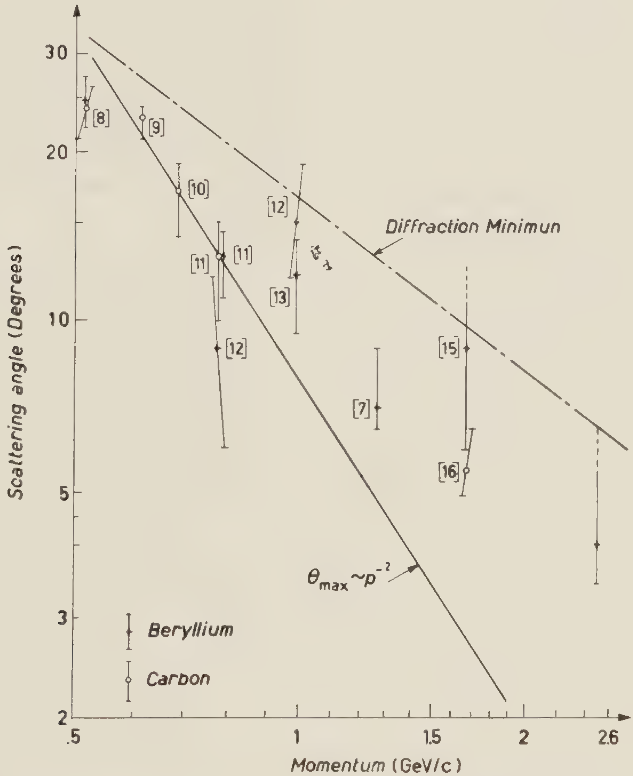

Fig. 7. – Angle of maximum polarization in scattering on nuclei *vs.* momentum (see references).

At lower energies, in the region of the several hundred MeV, the central potential is also found to be nearly imaginary, but of the order of 20 MeV in depth. (See for example (7)).

---

(7) M. G. Mescheriakov, S. B. Nurushev and G. D. Stoletov: *Soviet Physics JETP*, **4**, 337 (1957).

2375

From eq. (7) one can obtain the phase angle between the central and spin orbit potentials. $P_{\max} = 0.19 \pm 0.04$ yields $\varphi_c - \varphi_s = (11 \pm 3)^\circ$. Thus at high energies the spin-orbit potential, like the central potential, appears to be nearly all imaginary. This could arise from the strong spin dependence of meson

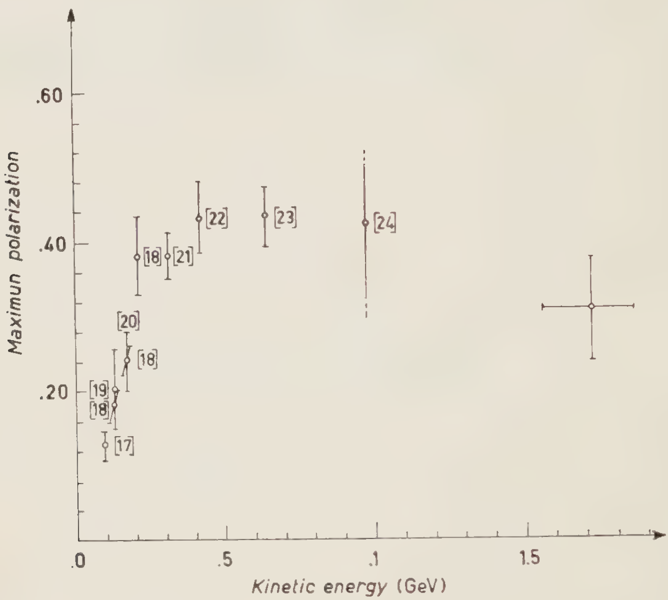

Fig. 8. – Maximum polarization in scattering on hydrogen *vs.* energy (see references).

production processes and is in sharp contrast with the predominantly real spin-orbit potential needed to explain the large polarizations observed in the region of several hundred MeV. A graph showing the maximum polarization as a function of energy using targets of beryllium and carbon appears in Fig. 6 ([7-16]).

([8]) J. M. Dickson, B. Rose and D. C. Salter: *Proc. Phys. Soc.*, **68**, 381 (1955).

([9]) P. Hilmann, A. Johansson and H. Tyren: *Nucl. Phys.*, **4**, 648 (1957).

([10]) W. G. Chesnut, E. M. Hafner and A. Roberts: *Phys. Rev.*, **104**, 449 (1956).

([11]) O. Chamberlain, E. Segrè, R. D. Tripp, C. Wiegand and T. Ypsilantis: *Phys. Rev.*, **96**, 807 (1954) and **102**, 1659 (1956).

([12]) H. G. De Carvalho, J. Marshall and L. Marshall: *Phys. Rev.*, **96**, 1081 (1954).

([13]) E. Heiberg, U. Kruse, J. Marshall, L. Marshall and F. Solmitz: *Phys. Rev.*, **97**, 250 (1955).

([14]) N. E. Booth, F. L. Hereford, M. Huq, G. W. Hutchinson, M. E. Law, A. M. Segar and D. H. White: *Proc. of Int. Conf. on High Energy Physics at CERN* (1958), p. 307.

([15]) C. J. Batty, W. O. Lock and P. V. March: *Proc. Phys. Soc.*, **73**, 100 (1959).

([16]) C. J. Batty and S. J. Goldsack: *Proc. Phys. Soc.*, **72**, 1130 (1958).

These data, as those in Fig. 7 and Fig. 8 ([17-24]), are a compilation of the results of many laboratories. The data at about 1 GeV are deduced from the published asymmetries assuming that the polarization of the beam was 0.33 ([24]).

The magnitude of the spin orbit potential can be deduced from eq. (9). Fig. 7 shows a log-log plot of the angle of maximum polarization *vs.* momentum for beryllium and carbon targets. It is clear that the angle of maximum polarization varies less rapidly than p^{-2}, as would be the case if the ratio v_c/v_s were independent of momentum. This experiment puts a lower limit on θ_{max} of about 3.5°, but because of the rapid decrease of the elastic scattering in the region of the diffraction minimum and consequent large inelastic contamination, we cannot measure the upper limit well. However by extrapolating the lower energy results it appears unreasonable that θ_{max} can be larger than 8°. (See Fig. 7). This yields a spin-orbit potential of between 0.9 and 2.0 MeV.

The 300 MeV scattering results require a spin-orbit potential of about 2 MeV ([25]).

4'2. *Hydrogen.* – Previous experiments on the p-p interaction in the GeV region consisted of measurements of the total cross-section, the differential elastic cross-section and a study of the Coulomb nuclear interference. Using the optical theorem and the total and differential p-p cross-sections, BARGE *et al.* ([26]) have concluded that the forward scattering cross-section is significantly greater than the square of the imaginary part of the forward scattering amplitude at 2.0 and 2.94 GeV. This would imply that either there is an appreciable spin flip amplitude in the p-p interaction or that the forward scattering amplitude contains some real part. PRESTON *et al.* ([2]), on the other hand, have found no Coulomb-nuclear interference in studying small angle p-p scattering, which, since the Coulomb amplitude is nearly real, indicates

([17]) A. E. TAYLOR: *Proc. of the VI Ann. Intern. Rochester Conference on High Energy Physics*, p. 13.

([18]) E. BASKIR, E. M. HAFNER, A. ROBERTS and J. H. TINLOT: *Phys. Rev.*, **106**, 564 (1957).

([19]) J. M. DICKSON and D. C. SALTER: *Nature*, **173**, 946 (1954).

([20]) D. FISHER and J. BALDWIN: *Phys. Rev.*, **100**, 1445 (1955).

([21]) O. CHAMBERLAIN, E. SEGRÈ, R. D. TRIPP, C. WIEGAND and T. YPSILANTIS: *Phys. Rev.*, **105**, 288 (1957).

([22]) J. A. KANE, R. A. STALLWOOD, R. B. SUTTON, T. H. FIELDS and J. G. FOX: *Phys. Rev.*, **95**, 1694 (1954).

([23]) M. G. MESCHERIAKOV, S. B. NURUSHEV and G. D. STOLETOV: *Soviet Physics JETP*, **6**, 28 (1958).

([24]) R. J. HOMER, G. W. HUTCHINSON, W. K. MCFARLANE, A. W. O'DELL, R. RUBINSTEIN and E. J. SACHARIDIS: *Nuovo Cimento*, **16**, 1132 (1960).

([25]) H. FESHBACH: *Ann. Rev. Nucl. Sci.*, **8**, 49 (1958).

([26]) BARGE *et al.*: private communication.

the absence of any significant real nuclear forward scattering amplitude. It has therefore been concluded that the p-p interaction is spin-dependent.

The present experiment confirms this conclusion, indicating the presence of spin-dependent forces in a more direct way.

Because of the large number of partial waves involved ($p_{cm} = 900$ MeV/c), a phase shift analysis at this energy would require not only the angular distribution and polarization measured with considerable precision, but triple scattering experiments and a knowledge of the inelastic channels as well. A less ambitious program might be to fit the data with an optical model potential. This has been done for the angular distribution and total cross-section with some success by several authors using a spin-independent interaction. Introduction of spin-dependent terms into the optical potential could no doubt account for the observed polarization.

Fig. 8 shows a plot of the maximum p-p polarization as a function of energy. The maximum of the curve occurs at a somewhat higher energy than for scattering from nuclei and decreases more slowly with energy. The angle for maximum polarization is forward of 45° c.m. at lower energies. At 970 MeV HOMER *et al.* [24] have found a maximum around 50°, while our data indicate a maximum at $(45 \pm 10)°$.

* * *

The authors wish to thank J. C. BRISSON and the electronics group for their continuous help during the experiment and J. TICHIT who took care of the hydrogen target.

They also wish to acknowledge the effort of R. LÉVY-MANDEL and the operating and maintenance crews of the synchrotron, as well as P. STICKEL and the group responsible for the experimental facilities.

Two of us, L.S. and R.T., express their gratitude to Prof. A. BERTHELOT for his kind hospitality at « Saturne ».

RIASSUNTO (*)

Abbiamo misurato con la tecnica dei contatori la polarizzazione nello scattering p-Be e p-p con protoni di 1.74 GeV di energia cinetica. Abbiamo trovato che la massima polarizzazione nello scattering p-Be è $P_{max} = 0.19 \pm 0.04$ e si ha per un angolo $\theta_{max} \approx 3.5°$. Abbiamo scartato gli scattering anelastici quando la perdita anelastica dell'impulso era più dell'1% circa nel primo scattering (analisi magnetica) o più del 5% circa nel secondo scattering (contatore di soglia di Čerenkov). La polarizzazione massima nello scattering p-p è $P_{max} = 0.30 \pm 0.09$ e si ha per un angolo di $35° < \theta_{max} < 55°$ (c. m.). La dipendenza angolare della polarizzazione è coerente con una distribuzione proporzionale a $\sin 2\theta$ entro ampi errori statistici. Calcoli del modello ottico applicati ai dati dello scattering p-Be danno un potenziale centrale, quasi tutto immaginario, di 43 MeV circa ed un potenziale spin-orbita compreso fra 0.9 MeV e 2.0 MeV, che è anche quasi tutto immaginario, in contrasto con il potenziale spin-orbita predominantemente reale necessario per spiegare la forte polarizzazione nella zona delle parecchie centinaia di MeV.

(*) *Traduzione a cura della Redazione.*

Further Studies on the Decay of ^{132}Cs.

S. Jha, R. K. Gupta, H. G. Devare and G. C. Pramila

Tata Institute of Fundamental Research - Bombay

(ricevuto il 30 Gennaio 1961)

Summary. — 6.48-day ^{132}Cs has been made by the neutron-irradiation of natural Ba and chemical separation of Cs from Ba, and by 90 MeV proton bombardment of Cs. The following γ-rays were observed in a scintillation spectrometer: 670 keV (100), (1040 ± 20) keV (0.25 ± 0.03), (1140 ± 20) keV (0.55 ± 0.06), (1320 ± 20) keV (0.75 ± 0.08), (1700 ± 30) keV (0.01 ± 0.005), (1800 ± 30) keV (0.02 ± 0.005) and (1980 ± 30) keV (0.04 ± 0.01). By conventional coincidence and summing technique studies, the feeding of the following levels in ^{132}Xe is inferred: 670 keV (93%), 1320 keV (1%), 1450 keV (0.1%), 1700 keV (0.6%), 1800 keV (1.2%) and 1980 keV (0.6%). These levels have perhaps the spin and parity 2^+, 2^+, 4^+, 2, 2, and 2 respectively. The positron branching to the 670 keV state is about 1.2%. The β^--decay to the 470 keV state of ^{132}Ba is less than 3%. The decay energy of ^{132}Cs is inferred to be about 2100 keV. A decay scheme is suggested.

1. – Introduction.

It is well known that $^{132}_{55}$Cs decays with a half-life of (6.48 ± 0.03) days ([1,2]) by orbital electron-capture, accompanied mainly by the emission of a 670 keV γ-ray. On the presence of higher energy γ-rays, the reports ([3,4]) are rather sketchy. Since the earlier report ([3]) was published, it has been possible to obtain this isotope from different sources. Now a consistent picture emerges.

([1]) D. Strominger, J. M. Hollander and G. T. Seaborg: *Rev. Mod. Phys.*, **30**, 585 (1960).

([2]) G. N. White, Balraj Sharma and W. H. Taylor: *Canad. Journ. Phys.*, **38**, 877 (1960).

([3]) B. L. Robinson and R. W. Fink: *Phys. Rev.*, **98**, 221, 231 A (1955).

([4]) K. S. Bhatki, R. K. Gupta and S. Jha: *Nuovo Cimento*, **4**, 1519 (1956).

2. – Preparation of the source.

The source of ^{132}Cs was made (5) by the neutron-irradiation of 100 mg of natural $BaCO_3$ for two weeks in Dido, Harwell and subsequent chemical separation of Cs from Ba. This source, although mixed with ^{131}Cs, was carrier-free. ^{132}Cs, in this technique, was formed presumably by the reaction $^{130}_{56}Ba(n, \gamma)\,^{131}_{56}Ba \to ^{131}_{55}Cs(n, \gamma)\,^{132}_{55}Cs$. The confirmatory experiment of irradiating pure ^{131}Cs in a reactor to produce ^{132}Cs has not been done yet. For this reason, the alternative mode $^{132}_{56}Ba(n, p)\,^{132}_{55}Cs$, although improbable because of the extremely low natural abundance of ^{132}Ba, cannot be ruled out.

The source of ^{132}Cs has been made, for our experiments, also by the bombardment of about a gram of CsCl with about 90 MeV protons (3) for two hours in the cyclotron at Harwell. The target was flown to Bombay. The Ba fraction of the bombarded target gave us a strong $^{128}Ba \to ^{128}Cs$ source and the Cs fraction contained, along with ^{132}Cs, a good amount of 30 hour ^{129}Cs. The study of the radiations of ^{132}Cs was started a few days later, by which time the contribution of ^{129}Cs had become much smaller. The ^{132}Cs source was finally purified in an ion-exchange column.

3. – Scintillation spectrometer studies.

The scintillation spectrometer used for the study of γ-rays from ^{132}Cs consisted of a NaI(Tl) crystal, 3 in. in diameter, 3 in. high, with a well $\frac{1}{4}$ in. in diameter, $1\frac{1}{2}$ in. deep, mounted on a 6363 DuMont photomultiplier, the integral assembly supplied by Harshaw and Co., and a single-channel analyser. The source was kept at a distance of 12 cm. The spectrum of γ-rays is reproduced in Fig. 1. The spectrum was analysed with the help of standard sources, placed

TABLE I.

Energy of the γ-rays in keV	Relative intensity
670	100
1040 ± 20	0.23 ± 0.03
1140 ± 20	0.55 ± 0.06
1320 ± 20	0.75 ± 0.08
1700 ± 30	0.01 ± 0.005
1800 ± 30	0.02 ± 0.005
1980 ± 30	0.04 ± 0.01

(5) B. SARAF: *Phys. Rev.*, **94**, 642 (1954).

2380

in identical geometry. Starting from the highest energy end of the spectrum, the contribution of each γ-ray was subtracted from the composite spectrum. The result of the analysis giving the energy and the intensity of the individual γ-rays is given in Table I.

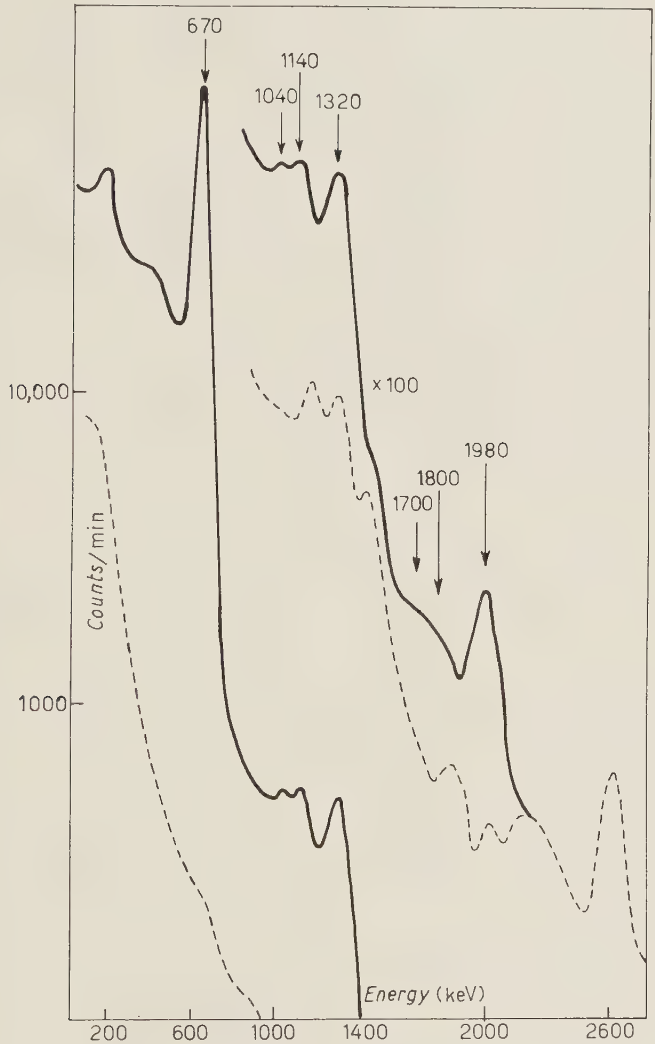

Fig. 1. – The γ-ray spectrum of ^{132}Cs in 3 in. × 3 in. NaI(Tl) crystal, source distance 12 cm. The dotted line shows the spectrum of background radiation.

A much weaker source in a glass tube was placed inside the well of the scintillation crystal. The spectrum of the γ-rays in this almost 4π geometry is reproduced in Fig. 2.

The full line in this figure indicates the composite spectrum of the γ-rays from ^{132}Cs and the background radiation; and the dotted line gives the back-

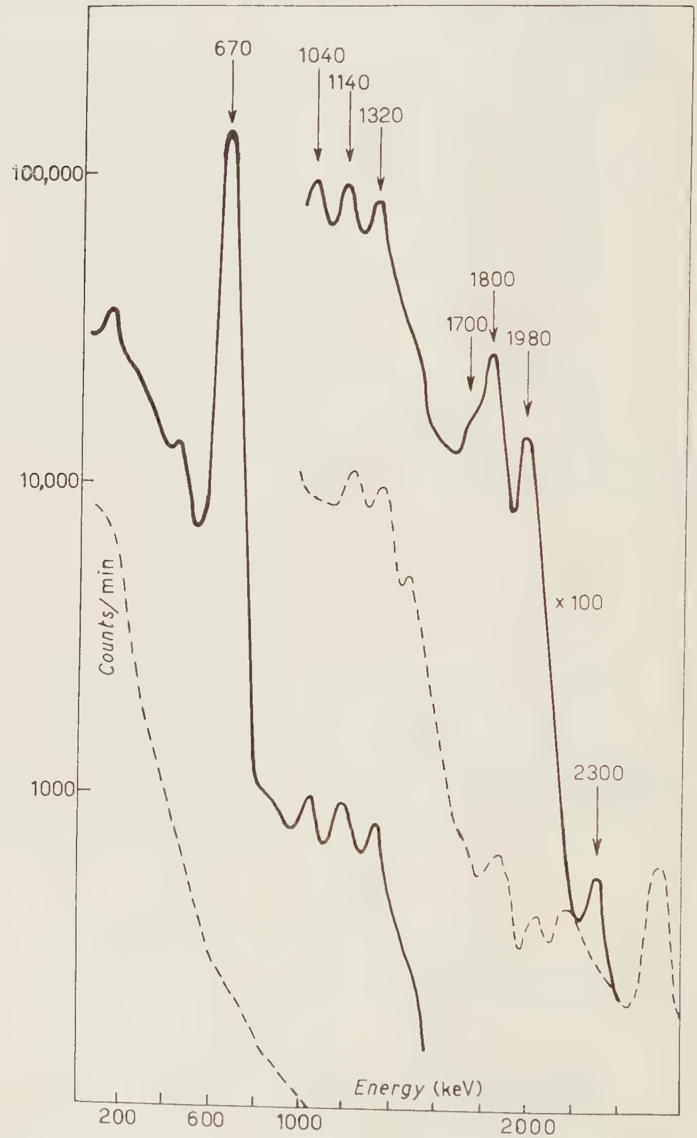

Fig. 2. – The spectrum of γ-rays of ^{132}Cs in 3 in. × 3 in. NaI(Tl) crystal with the source inside the well of the crystal. The dotted line is the contribution of the background radiation (*).

(*) *Note added in proof.* – It was inferred from half-life and chemical separation experiments that the 2300 keV peak shown in the figure and not discussed in the text belongs to some impurity in the ^{132}Cs source.

2382

ground alone. One can see peaks at 670 kV, 1040 keV, 1140 keV, 1320 keV, 1700 keV, 1800 keV and 1980 keV. The comparison of the spectra taken inside and outside shows that the peaks at 1040 keV, 1140 keV, 1700 keV, 1800 keV and 1980 keV are relatively larger in intensity in the spectrum taken with the source inside the crystal. It is also clear that the increase in the intensities of the 1700 keV and 1800 keV sum-peaks is larger than that of the 1980 keV sum-peak. In order to ascertain if the increase in these peaks was due to double or multiple summing, a spectrum was taken with the source on the top of the crystal (spectrum not reproduced). It is obvious that the probability of multiple summing goes down much faster with the decreasing solid angle than does the double summing. With this consideration, the spectrum of the γ-rays with the source on top of the crystal showed that the sum-peaks at 1700 keV and 1800 keV are contributed to from multiple summing also, while the sum-peak at 1980 keV is almost entirely due to double summing. The sum-peak at 1040 is completely absent in the spectrum with the source at the top of the crystal. From the coincidence experiment to be described hereafter, the presence of annihilation radiation was inferred. In this light, the sum-peak at about 1040 keV in Fig. 2 has been interpreted as arising from the simultaneous detection of two annihilation quanta inside the

TABLE II.

Energy in keV of γ-ray photopeaks	Possible origin
670	Single
1040	Single 1040 keV and summing of 510 and 510 keV annihilation radiation
1140	Single 1140 keV and summing of 510 keV and 670 keV
1320	Single 1320 keV and summing of 670 keV and possibly 650 keV (*)
1700	single 1700 keV, double summing of 1040 keV and 670 keV and multiple summing of 670 keV and possibly 650 keV (*) and 330 keV (*)
1800	Single 1800 keV, double summing of 670 keV and 1140 keV, and multiple summing of 670 keV, 650 keV (*) and 480 keV (*)
1980	Single 1980 keV and almost entirely a double summing of 670 keV and 1320 keV

(*) Cf. results of coincidence experiments.

crystal. From the comparison of the spectrum of γ-rays of ^{132}Cs taken with the source at about 12 cm., the source on the face of the crystal and the source in the well of the crystal, the possible origin of the peaks in Fig. 2 is given in Table II.

4. – Coincidence experiments.

A rather extensive coincidence study was carried out with the help of two NaI(Tl) crystals, $1\frac{1}{2}$ in. in diameter 2 in. high, and single-channel analysers. The resolving time of the coincidence unit was $2\cdot10^{-7}$ s. Fig. 3 shows the spectrum of γ-rays (lower energy region) in coincidence with the 670 keV γ-ray. Although the statistics are not good, one can see that perhaps there are peaks due to 510 keV, 480 keV, 380 keV, 280 keV, 180 keV and 100 keV γ-rays. These γ-rays are completely swamped by the Compton continuum of the intense 670 keV γ-ray in the single spectrum of Fig. 1. It was found that the region of 510 keV showed a strong peak in coincidence when the crystal and multiplier units were in a straight line at 180° to each other. This 510 keV peak dwindled very much in intensity when the coincidence was observed at 90°. It was, therefore, concluded that ^{132}Cs decays by positron emission also. The fact that 510 keV and 670 keV γ-rays were observed in coincidence with each other indicated that the positron decay of ^{132}Cs leads to the 670 keV level of ^{132}Xe. From the coincidence experiment, the intensity of the positron branching was estimated to be about

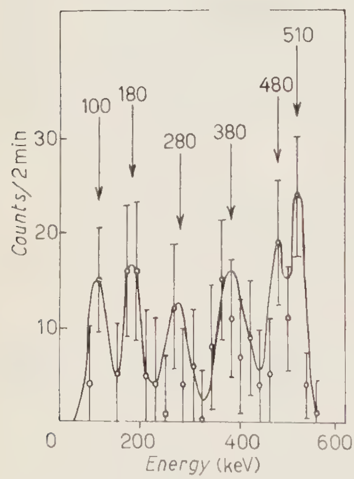

Fig. 3. – The spectrum of low energy γ-rays in coincidence with the 670 keV γ-ray.

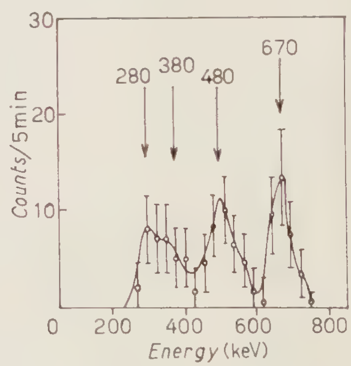

Fig. 4. – The spectrum of γ-rays in coincidence with the 1320 keV γ-ray.

(1.2 ± .4) %. Fig. 4 gives the spectrum of γ-rays in coincidence with the 1320 keV γ-ray taken with a single-channel analyser. One can see from the figure that in coincidence with the 1320 keV γ-ray one gets 670 keV, 480 keV, 380 keV and 280 keV γ-rays. Lastly, the region between 500 keV and 1400 keV was scanned in coincidence with the 670 keV γ-ray with the help of a 20-channel pulse-height analyser. The γ-spectrum obtained is reproduced in Fig. 5. The results of the coincidence studies are given in Table III.

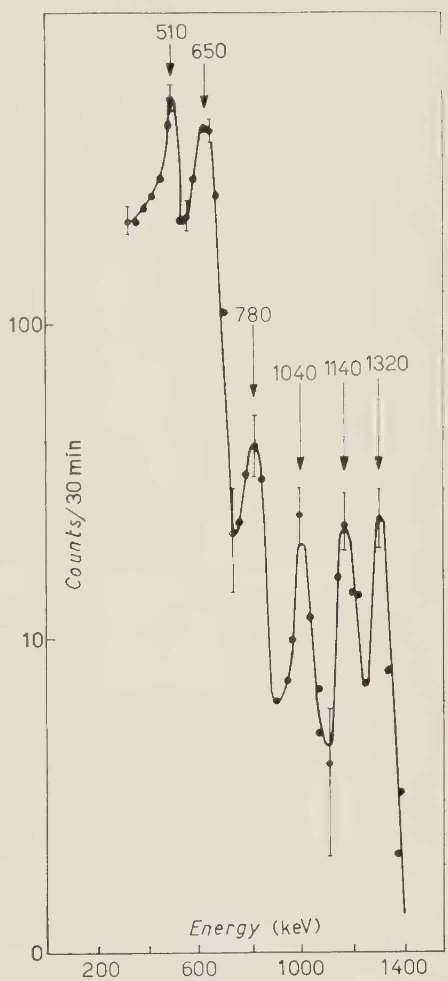

Fig. 5. – The spectrum of γ-rays in coincidence with the 670 keV γ-ray taken in a 20-channel pulse-height analyser.

TABLE III.

	The energy in keV of the γ-ray in the gate	Energy in keV of the γ-rays found in coincidence
1.	510	510, 670
2.	670	100, 180, 280, 380, 480, 510, 650, 780, 1040, 1140 and 1320
3.	1320	670, 480, 380, 280

5. – The spectrum of β-rays.

The spectrum of β-particles from ^{132}Cs was studied in an anthracene crystal, but due to the presence of the conversion lines of the 670 keV γ-ray, no clear-cut evidence was obtained. In order to establish a β^--branching in ^{132}Cs decay, a search was made for a possible 470 keV γ-ray from the first excited state of ^{132}Ba [1]. In the normal spectrum, no definite evidence could be gathered because of the presence of the 480 keV γ-ray associated with the electron-capture branching found in coincidence experiments, and because of large intensity Compton continuum of the 670 keV γ-ray. From a spectrum taken inside the well of the crystal, where the intensity of the continuum is smaller and the major portion of the 480 keV γ-ray, accompanying electron-capture, gets summed up, it was concluded that the possible β^--branching of ^{132}Cs is less than 3 %. The conclusion is made uncertain particularly because of the inherent difficulty of analysing summed-up γ-ray contributions.

6. – Decay scheme.

From the studies described above, as well as from earlier studies, it is clear that the decay of ^{132}Cs takes place predominantly through orbital electron-captures to the 670 keV states of ^{132}Xe. The fact that the presence of annihilation radiation in coincidence with the 670 keV γ-ray has been established shows that ^{132}Cs decays to the 670 keV state of ^{132}Xe with a small branching (about 1 %) by the emission of positrons. From the coincidence of the 670 keV and 1320 keV γ-rays and from the occurrence of a 1980 keV γ-ray, one can conclude that a level in ^{132}Xe at 1980 keV is fed in the electron-capture decay. From the area of the sum-peak at 1980 keV and from the knowledge of the possible modes of de-excitation of this level, the intensity of the electron-capture branching to the 1980 keV state is estimated [4] to be about 0.6 %. This analysis also shows that only about 70 % of the total 1320 keV γ-ray can be accounted for as arising from the cascade de-excitation of the 1980 keV state; the rest ($\approx$ 30 %) must be originating elsewhere. This fact, the occurrence of a 650 keV γ-ray in coincidence with the 670 keV γ-ray, and the occurrence of 480 keV and 380 keV γ-rays in coincidence with both 670 keV and 1320 keV γ-rays indicate that there is a level at 1320 keV fed by the electron-capture in ^{132}Cs.

The fact that there are sum-peaks at 1700 keV and 1800 keV and the fact that in coincidence with the 670 keV γ-ray one gets 1040 keV and 1140 keV γ-rays show that there are levels in ^{132}Xe at 1700 keV and 1800 keV which de-excite to the ground and also by cascade emission through the

670 keV state. From the relative areas of the sum peaks and the knowledge of the decay modes of these levels, the electron capture branching to these levels have been estimated to be about 1.2 % and 0.6 % respectively.

There is a slight hump in the spectrum with the source inside the crystal at 1450 keV (Fig. 2); and in the spectrum of γ-rays in coincidence with the 670 keV γ-ray, there is a peak at about 780 keV (Fig. 5). From these observations, it is suspected that the level in ^{132}Xe at 1450 keV, well known in the β^--decay $^{132}_{53}$I-^{132}Xe (6,7), is fed also in the electron-capture decay of ^{132}Cs.

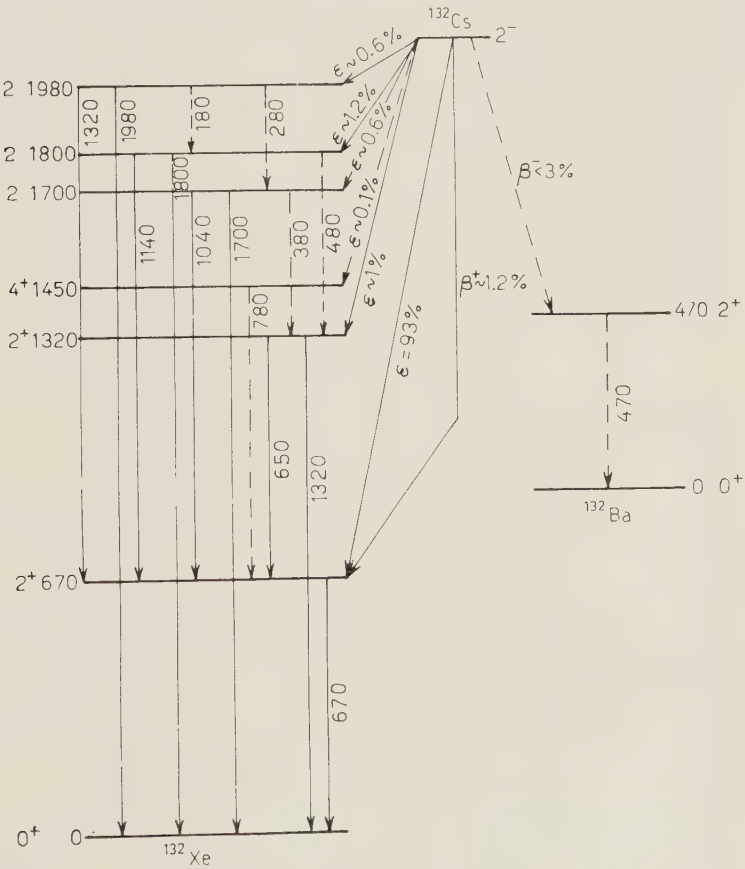

Fig. 6.

Based on these considerations, a decay-scheme of ^{132}Cs has been drawn, which is shown in Fig. 6 and log *ft* values for capture branches to different

(6) H. L. Finston and W. Bernstein: *Phys. Rev.*, **96**, 71 (1954).
(7) H. G. Devare: to be published.

2387

levels are given in Table IV. In this decay scheme, the transitions, which are suspected but for which enough evidence could not be provided, have been shown with a dotted line. To this class belongs the β^--decay of ^{132}Cs.

TABLE IV.

Electron-capture branching to the level	Decay energy in keV	Intensity %	log *ft*
670 keV	1430	93	6.6
1320 keV	780	1	8.0
1450 keV	650	0.1	8.8
1700 keV	400	0.6	8.0
1800 keV	300	1.2	7.1
1980 keV	120	0.6	7.3

7. – Discussion.

The decay scheme given in Fig. 6 differs essentially from the one proposed earlier. There were two faults in the earlier work. The resolution of the scintillation crystal and photomultiplier assembly was rather bad, ($\approx 15\%$ for the 661 keV ^{137}Cs γ-ray), so that the peaks were not well-resolved. The energy calibration was in error partly for want of a high energy γ-ray calibration source and partly also because of the change in the pulse height of the DuMont photomultiplier due to a large counting rate.

The highest level of ^{132}Xe which is now claimed to be populated in the decay of ^{132}Cs is at 1980 keV. The β-decay systematics ([8]) give the decay-energy of ^{132}Cs–^{132}Xe at about 2100 keV. This decay-energy has been estimated also from the mass data of JOHNSON *et al.* ([9]). EVERLING *et al.* ([10]) give the decay-energy values as (1817 ± 147) keV. From our studies of the decay of ^{132}Cs, it seems to us that the decay-energy should be about 2100 keV.

The spin of ^{132}Cs is measured ([1]) to be 2. It is stated that the parity is

([8]) K. WAY and M. WOOD: *Phys. Rev.*, **94**, 119 (1954).

([9]) W. H. JOHNSON jr. and A. O. NIER: *Phys. Rev.*, **105**, 1014 (1957).

([10]) F. EVERLING, L. A. KONIG, J. H. E. MATTAUCH and A. H. WAPSTRA: *Nucl. Phys.*, **18**, 529 (1960).

even. The log *ft* for electron-capture to the 670 keV state is 6.8. The spin and parity of the 670 keV state should be 2^+. The 1450 keV state of ^{132}Xe is fed in the β-decay of ^{132}I (spin 4) (1) and the β-spectrum has a straight Fermi plot, indicating that the 1450 keV state is presumably the 4^+ member of the triplet second vibrational state of ^{132}Xe. If the parity of ^{132}Cs were even, the log *ft* for the positron decay and electron-capture decay to the the 670 keV state would have been less than 6, and no detectable decay to the 1450 keV state would be predicted. On the other hand, the log *ft* for the decay to the 670 keV and 1450 keV states can be understood if ^{132}Cs has odd parity. As a matter of fact, the parities of all the neighbouring isotopes whose spins are different from 1 are odd: ^{122}Sb(2^-) (1), ^{124}Sb(3^-) (1), ^{124}I(2^-) (1), ^{126}I(2^-) (1), ^{128}I(1^+) (1), ^{130}I(5^-) (11), ^{132}I(4^+) (1), ^{136}I(2^-) (12), ^{126}Cs(1^+) (1), ^{128}Cs(1^+) (1), ^{130}Cs(1^+)(1), ^{134}Cs(4^+)(1) and ^{138}Cs(3^-) (13). The only exceptions are ^{132}I and ^{134}Cs. It seems to us unlikely that the parity of ^{132}I is even. It is being investigated in this laboratory from the study of β-γ angular correlation of ^{132}I. The even parity of ^{134}Cs seems to have been carried down in the literature from the original assignment of SUNYAR *et al.* (14).

There is some evidence for the existence of the level at 1320 keV in the β-decay of ^{132}I also (7). Unless one postulates that β-decay and electron capture decay of ^{132}I and ^{132}Cs to this level of ^{132}Xe is abnormal, the most plausible hypothesis seems to be that the 1320 keV level is 2^+. The 1320 keV (2^+)and the 1450 keV (4^+) levels could thus be two members of the triplet second vibrational state of ^{132}Xe. It may be pointed out that the log *ft* for the electron capture decay to the 1320 keV level, though somewhat uncertain, seems to be rather high for the $2^- \to 2^+$ type of decay.

The levels at 1700 keV, 1800 keV and 1980 keV all have spin and parity presumably of 2^+. We are ruling out the spin and parity $0^\pm$ on the ground that the feeding of such a level from the 2^- ^{132}Cs ground state would be very much smaller. We are ruling out the spin and parity $1^\pm$ because this will make the transition to the ground state much stronger than it is.

* * *

This work was greatly helped by the careful chemical separation done by Mr. K. S. BHATKI, Mr. K. P. GOPINATHAN and Mr. A. T. RANE. Our thanks are due to Dr. B. SARAF for lending us his 20-channel pulse-height analyser for this work.

---

(11) W. G. SMITH, P. H. STELSON and F. K. McGOWAN: *Phys. Rev.*, **114**, 1435 (1960).
(12) N. R. JOHNSON and G. D. O'KELLEY: *Phys. Rev.*, **114**, 279 (1959).
(13) M. E. BUNKER, R. B. DUFFIELD, J. P. MIZE and J. W. STARNER: *Phys. Rev.*, **103**, 1417 (1956).
(14) A. W. SUNYAR, J. W. MIHELICH and M. GOLDHABER: *Phys. Rev.*, **95**, 570 (1954).

2389

RIASSUNTO (*)

Abbiamo preparato del ^{132}Cs (vita media 6.48 d) irradiando con neutroni il Ba naturale e separando chimicamente il Cs dal Ba, bombardando poi il Cs con protoni di 90 MeV. Abbiamo osservato con uno spettrometro a scintillazione i seguenti raggi γ: 670 keV (100), (1040 ± 20) keV (0.25 ± 0.03), (1140 ± 20) keV (0.55 ± 0.05), (1320 ± 20) keV (0.75 ± 0.08), (1700 ± 30) keV (0.01 ± 0.005), (1800 ± 30) keV (0.02 ± 0.005) e (1980 ± 30) keV (0.04 ± 0.01). Mediante studi con la tecnica convenzionale di coincidenza e somma, deduciamo l'alimentazione dei seguenti livelli nel ^{132}Xe: 670 keV (93%), 1320 keV (1%), 1450 keV (0.1%), 1700 keV (0.6%), 1800 keV (1.2%) e 1980 keV (0.6%). Questi livelli forse hanno rispettivamente spin e parità 2^+, 2^+, 4^+, 2, 2 e 2. Il branching del positone allo stato di 670 keV è di circa l'1.2%. Il decadimento β allo stato di 470 keV è inferiore al 3%. Desumiamo che l'energia di decadimento del ^{132}Cs è di circa 2100 keV. Suggeriamo uno schema di decadimento.

(*) *Traduzione a cura della Redazione.*

IL NUOVO CIMENTO Vol. XX, N. 6 16 Giugno 1961

Dimensionless Quantities, Spacelike Intervals and Proper Time in General Relativity.

A. Finzi

Istituto di Fisica dell'Università - Roma
Israel Institute of Technology - Haifa

(ricevuto il 9 Febbraio 1961)

Summary. — It is shown that metric measurements, which are essential to the theory of general relativity, are those based only on strong and electromagnetic interactions. Strong and electromagnetic interactions must not vary throughout the four-dimensional world, if general relativity is to remain a meaningful theory. The implications of these remarks on cosmology are discussed.

1. – Dimensionless quantities in physics.

The geometrical conception of physics, which is characteristic of general relativity, originates from the observation (principle of equivalence) that for any infinitesimal region of space-time it is possible to choose a system of reference in such a way that the gravitational forces are eliminated. For such a system, we can define the distance $\mathrm{d}s$ between two points belonging to the infinitesimal region, by means of the equation

$$\mathrm{d}s^2 = -(\mathrm{d}x^1)^2 - (\mathrm{d}x^2)^2 - (\mathrm{d}x^3)^2 + (\mathrm{d}x^4)^2 .$$

The distance can be determined experimentally by using a clock and a rod.

In a similar way, in the theory of surfaces, which served as a model to general relativity, it is always possible to choose, for an infinitesimal region of a surface, a system of co-ordinates so that the square of the distance between two points is expressed by the form $(\mathrm{d}x^1)^2+(\mathrm{d}x^2)^2$. This possibility corresponds to the fact that any two infinitesimal regions of the surface are essentially equivalent, and equivalent to an infinitesimal region of a plane.

From this last point of view, however, the situation is different in the case of physical reality. There exist a certain number of dimensionless quantities which can be determined by experiments performed in laboratories at rest in inertial systems at different points of the world. In particular we shall consider the fine structure constant $e^2/\hbar$ $(c=1)$ and the ratio

$$\frac{km^2}{e^2} \simeq 2.4 \cdot 10^{-43} ,$$

of the newtonian to the electrostatic force acting between two electrons. (It must be clear, of course, that it always makes sense to compare the values which e^2/h takes at two distant points. It would be, however, meaningless to compare the values taken by a dimensional quantity like, for instance, the radius of Bohr, before we introduce, in the four-dimensional world, the metrics of EINSTEIN $g_{ik}\,\mathrm{d}x^i\,\mathrm{d}x^k$.)

If the dimensionless quantities do not take the same values everywhere, the neighbourhoods of two points are really not equivalent, and in this sense one cannot consider the geometrical conception as giving a complete picture of physical reality (*). As a matter of fact, however, the consistency of general relativity requires, as we shall show, that at least some of these quantities should not vary.

2. – Physical meaning of Einstein's metrics.

Let us now introduce Einstein's metrics

$$\mathrm{d}s^2 = g_{ik}\,\mathrm{d}x^i\,\mathrm{d}x^k ;$$

it is possible to deduce some relevant indications about the behaviour of some of the dimensionless quantities from the study of the physical meaning of the metrics. The operational definition of the metrics is not always given very clearly; the reason for this is, probably, the following: in most problems of general relativity one first considers the distribution of masses, which are the

(*) Strictly speaking, the geometrical equivalence subsists, of course, only for the neighbourhoods of the first and second order of the two points. It is, however, rather doubtful that the laws of physics at a point P may depend on the second or higher order derivatives of the g_{ik}. In any case, the only invariant, which is linear in the second order derivatives of the g_{ik}, is the invariant of curvature R. Because of the equations $R \quad \chi T$, which follows immediately from Einstein's equations, one can easily rule out the possibility that the laws of physics at P may depend on R.

sources of the gravitational field, and one uses Einstein's equations

$$G_{ik} = -\chi T_{ik} \tag{1}$$

to deduce the metrics from the tensor T_{ik}. From the metrics, using the geodesic theorem, one determines the motion of test bodies. In such a procedure it is not obvious (and it is not even immediately relevant) what is the physical meaning of the metrics.

On the other hand the metrics gives the square of the distance between two points. It can be experimentally determined by using a clock and a rod. We must, therefore, see how to ensure the following things.

First, the metrics must be independent of the choice of the clock, chosen out of a large class of possible clocks, and of the unity-measuring rod.

Secondly, the metrics so obtained must coincide with the metrics determined by Einstein's equations.

Let us first discuss the measurement of time-like intervals. Though the classical concept of time has gone through two profound critical analyses represented by special and general relativity, the following idea does not seem to have been affected: *every* kind of clock is suitable to indicate the proper time correctly when only care is taken to eliminate errors, which are conceptionally unessential. This would imply the following: let us suppose that two clocks, based on different physical principles, are going at the same rate when placed together at a given point of the world, at rest in the same inertial system. They will still go at the same rate when they are placed together at another point of the world, also at rest in an inertial system.

This assumption, which probably represents a survival of the classical idea of absolute time, may perhaps be a too general and stringent one. We shall, however, ensure *the equivalence* of a very large class of clocks, namely *of all clocks based exclusively on strong and electromagnetic interactions.*

We shall ensure this by requiring that the fine structure constant, and all other possible dimensionless quantities, which can be defined by means of strong and electromagnetic interactions and the structure of the elementary particles (*), *do not vary* throughout the four-dimensional world.

In fact, should two of our clocks not be equivalent, the ratio between their rates would represent a *variable* dimensionless quantity, defined by means of strong and electromagnetic interactions and the structure of elementary particles, in contradiction with what we have just assumed.

(*) We do not know, of course, how many independent quantities of this kind exist, since we have no satisfactory theory of strong interactions, and almost no theory of elementary particles at all. We can be fairly sure, however, that, in any case, their number must be very small.

Let us mention some of the clocks included in our class.

A mechanical clock regulated by a balance (not by a pendulum).

Clocks based on the rate of decay of an α or γ radioactive element.

Atomic clocks. It is a common feature of these clocks that quantal systems, having two sharply defined energy levels, act as the balance of the clock.

More generally, it seems there is no conceptual difficulty in assuming the existence of a clock based on any quantal system (a molecule, an atom, a nucleus) having two sharply defined energy levels, whenever the system can jump from one state to the other by emitting or absorbing a photon.

The main reason for the requirement made above is the fact that under a less stringent requirement (*e.g.* the constancy of e^2/h alone) perhaps not even two of the clocks mentioned above would be exactly equivalent, and so the theory of general relativity would loose most of its physical content. That it is so, is probably obvious in the case of clocks based on the rate of α or γ-decay, or on the existence of two sharp energy levels of a nucleus, because a change in the strong interactions would bring about a change in the energy levels of the nucleus. In the other cases, the change in the rate of the clock would depend mainly on the fact that the mass defects and the magnetic moments of the nuclei would vary. We must admit that, in the case of a clock based on the energy levels of an atom, the change in its rate, because of the variation of the mass and the magnetic moment of the nucleus, would really be very small.

Considering now space-like intervals, we could, perhaps, assume as an unit of length the classical radius of the electron, or the radius of Bohr, or the wave length of a definite spectral line. *A priori* these units would seem to define three different metrics; one easily sees, however, that the three metrics become essentially equivalent when one only postulates the constancy of e^2/h.

Usually one defines the unit of length by means of a rod. It is easily seen that this definition is equivalent to the previous ones under the assumption that strong and electromagnetic interactions should not vary. In fact, should the ratio between the length of a given rod and the radius of Bohr vary, this ratio would represent a *variable* dimensionless quantity, defined exclusively by means of strong and electromagnetic interactions and the structure of elementary particles, in contradiction to the assumption made above.

We have still to show that the metrics defined through measurements based on strong and electromagnetic interactions coincides with the metrics determined by Einstein's equations.

The displacement towards the red of the spectral lines of the light coming from a deep gravitational potential, which is satisfactorily explained by the theory of general relativity, shows that a clock based on the energy levels of an atom measures the proper time correctly. The gravitational red shift has recently been detected in the γ-rays originating from the decay of an excited

level of the nucleus of ^{57}Fe using the Mössbauer effect (1-3); the experiment amounts to showing that a clock based on the two levels of ^{57}Fe would also measure the proper time correctly.

There are plans at present to place an atomic clock on a satellite. If the behaviour of the clock should appear to conform to the theory, this would viceversa be equivalent to having detected the gravitational red shift in the rays emitted by the quantal system, on which the atomic clock is based.

We have to show now that rods measure space-like intervals according to Einstein's metrics. We can correctly define the unit of time as the time a light signal takes to travel from one end to the other of a given rod. In fact, this is a time-measuring device exclusively based on strong and electromagnetic interactions. Then we can also correctly define the unit of length by means of the rod itself ($c = 1$).

At the end of this paper we shall give a more direct demonstration of the fact that the length of the radius of Bohr according to Einstein's metrics does not vary throughout the world, so that we can legitimately take the radius of Bohr as unit.

We conclude that the measurements of space-like and time-like intervals, which are essential to the theory of the general relativity, are those based only on strong and electromagnetic interactions. We can say that Einstein's metrics is determined by the equations of gravitation, but is operationally defined by strong and electromagnetic interactions. This represents a fundamental connection between atomic physics and general relativity.

3. – Clocks based on gravitation or on weak interaction.

We have still to consider clocks based on gravitational forces or on weak interaction.

A gravitational clock may consist of a free falling body of mass M and of a test body, subject only to the newtonian attraction of the body of mass M, and rotating on a circular orbit of radius R.

Another gravitational clock, essentially equivalent to the first one, may consist of a free falling rigid body and of a pendulum, suspended to a point rigidly connected with the body, and free to oscillate under the attraction of the body in a plane through the center of gravity.

Gravitational clocks form a class clearly separate from the much more important class, which we considered in the second section, and we are not

(1) R. V. Pound *et al.*: *Phys. Rev. Lett.*, **3**, 554 (1959).
(2) T. E. Granshaw *et al.*: *Phys. Rev. Lett.*, **4**, 163 (1960).
(3) Mössbauer effect: Univ. of Illinois. Summary Report (1961).

able to see any profound reason for the equivalence of the time they define with the proper time. However, as we shall show in the third section, such an equivalence seems to be an inescapable consequence of the equations of general relativity, in the form they were given by EINSTEIN.

The introduction of gravitation adds *one* new independent dimensionless quantity, km^2/e^2, to the set of dimensionless quantities defined through strong and electromagnetic interactions. Then, the above statement about gravitational clocks just means that km^2/e^2 must not vary.

As regards clocks based on β-decay, the situation is again different. Neither the equivalence of these clocks with clocks based only on strong and electromagnetic interactions seems to be essential to the consistency of general relativity, nor can one, at present, postulate their behaviour on the basis of some other theoretical argument. This seems to offer one of the most impressive demonstrations of the fact, that the present connection between atomic physics and general relativity is still not adequate.

In conclusion, the use of clocks based on weak interaction to define the proper time does not seem justified in the present situation of physics. Accordingly, one can not rule out the possibility that dimensionless numbers characterizing weak interaction may vary throughout the world.

4. – Cosmological theories.

Our line of argument in the second section can be summarized as follows: we can be confident that general relativity is valid, to a very high degree of approximation, at least for regions of the four-dimensional world in which newtonian mechanics has been previously successfully used (regions whose dimensions are very small in comparison with the dimensions of the universe). Then the logical consistency of general relativity requires that strong and electromagnetic interactions should not vary throughout these four-dimensional regions.

The situation is quite different in the field of cosmology. Here we have not very strong arguments which could assure us, *a priori*, that general relativity is valid. Therefore, we cannot completely rule out the possibility that strong and electromagnetic interactions may vary *on a cosmological scale.* In this case the very concept of geometry of the universe, on which present day cosmological theories are based, would become meaningless.

The question of whether or not these interactions vary throughout the universe, should probably be answered by experimental methods. There are at least two experiments which could, in principle, help in answering the question.

The radioactive dating of a rock can sometimes be performed by two independent methods, by considering the products of the decay of two radioactive

elements [4]. The consistency of the results in the case of a very old rock would indicate that strong interaction did not vary.

A second experiment could be based on the study of the light curves of distant supernovae. There is a phase in the evolution of supernovae where the light curve is an exponential, and the energy is probably provided chiefly by some radioactive element (fissionable ^{254}Cf?) decaying through strong and electromagnetic interactions. The study of the light curve should, therefore, be equivalent to the observation of a half life. The observation of such an elementary process in a distant region of the universe would certainly be a very remarkable thing; it should be noticed, however, that the interpretation of the results would not be immediate. In fact, the experiment would amount to the comparison between a clock placed on the supernova and an earthly clock, while only the comparison between two different clocks placed on the supernova could directly answer our question. Also, the exact determination of the slope of the exponential for very distant supernovae is not possible with present day equipment [5].

5. – Dimensional quantities in general relativity.

Let us go back to general relativity.

We have pointed out in the first section that, *a priori*, only for a *dimensionless* quantity the comparison between the values taken at two distant points P_1 and P_2 is meaningful. The comparison becomes, however, possible also for a *dimensional* quantity, after we have endowed the four-dimensional world with a metrics.

That must be obvious when the dimensional quantity is an (infinitesimal) time-like or space-like interval, since the metrics itself offers the possibility of comparing the length of a vector at P_1 with that of a vector at P_2.

We shall also be able, however, to compare a mass at P_1 with a mass at P_2 (and finally, therefore, any dimensional quantity at P_1 with a quantity of the same dimensions at P_2) after we have introduced a definition of the unit of mass, which remains meaningful throughout the four-dimensional world.

We define the unit of (gravitational) mass as the mass which creates, at a distance r, a newtonian potential $-(\chi/8\pi)(1/r)$ $(c=1;$ χ is the numerical constant, which appears in (1), and which need to be chosen only once for all). The reason for using Newton's law to arrive at the definition of the unit of mass, instead of taking the mass of an elementary particle as a unit, lies in

(4) L. H. Ahrens: *Rep. Progr. Phys.*, **19**, 80 (1956).

(5) A. Finzi: *Ann. d'Astrophys.*, **24**, 68 (1961).

2307

the fact that Newton's law, *with the coefficient* $\chi/8\pi$, can be shown to follow from Einstein's equations, when a small mass is placed in a (previously) inertial system of reference; we must therefore make sure that the unit of mass always creates the same potential, when placed at different points. The two methods of defining the unit will be shown, however, in a moment, to be equivalent.

As is well known, one can define the operation of parallel displacement of an infinitesimal vector along a line; such a displacement preserves the length of the vector. Quite similarly, it follows from Einstein's equations that the (gravitational) mass of a test body does not vary, as the body moves freely along a (geodesic) line: $\mathrm{d}m/\mathrm{d}s = 0$. We shall demonstrate this result in the next section; and we shall look here at some of the consequences.

Let f be the ratio between the inertial masses of two small bodies placed at P_1. Owing to the proportionality between the inertial and gravitational mass of bodies placed at the same point, the ratio between the gravitational masses will also, of course, equal f. Because of the above result, this last ratio will not vary when we move the two bodies together to P_2 along a geodesic. Finally, the ratio between the inertial masses at P_2 will also equal f.

This shows, first of all, that the existence of well defined ratios between the (inertial) masses of the elementary particles is consistent with general relativity. If we take, on the other hand, the two bodies to be a proton and a nucleus, we see that the mass defect does not vary. The constancy of the mass defects of many hundreds of different nuclei, which seems therefore to be required by general relativity, is only consistent with the hypothesis that strong and electromagnetic interactions do not vary.

We have already used this last argument in the second section; there, however, the constancy of the mass defects was deduced from the requirement of the equivalence of certain clocks, while here it is shown to be a consequence of Einstein's equations. We are therefore justified in considering the deduction of this section as independent evidence of the fact that general relativity requires the constancy of strong and electromagnetic interactions.

6. – Demonstration of the geodesic theorem.

We shall prove that $\mathrm{d}m/\mathrm{d}s = 0$ and at the same time demonstrate the geodesic theorem, closely following the simple line of argument due to EDDINGTON and WEYL [6-9]. Let us consider a test body moving in the gravi-

(6) H. WEYL: *Raum-Zeit-Materie*, 5th Ed, (Berlin, 1923) § 38.
(7) A. S. EDDINGTON: *The Mathematical Theory of Relativity*, (London, 1923) § 56.
(8) A. EINSTEIN and J. GROMMER: *Sitz. Preuss. Akad. Wiss.*, **1**, 2 (1927).
(9) L. INFELD and A. SCHILD: *Rev. Mod. Phys.*, **24**, 408 (1949).

tational field due to a system of external bodies. In order to account for the test body in Einstein's equations we shall put

$$T^{\mu\nu} = \sigma \frac{\mathrm{d}x^\mu}{\mathrm{d}s} \frac{\mathrm{d}x^\nu}{\mathrm{d}s},$$

in the narrow world-tube described by the test body. σ gives the amount of (gravitational) matter per unit of three-dimensional volume, the volume being calculated, by means of Einstein's metrics, in a system of co-ordinates moving with the body. Put

$$\mathrm{d}\tau = \iiiint \mathrm{d}x^1\,\mathrm{d}x^2\,\mathrm{d}x^3\,\mathrm{d}x^4,$$

the integral being extended to a thin filament of the tube; we have $\sqrt{-g}\,\mathrm{d}\tau = \mathrm{d}v\,\mathrm{d}s$, where $\mathrm{d}v$ is the three-dimensional volume of the section of the filament, calculated by means of Einstein's metrics, in a system of co-ordinates moving with the test body. Then

$$\iiiint \sigma\sqrt{-g}\,\mathrm{d}\tau = \int \mathrm{d}s \iiint \sigma\,\mathrm{d}v = m\int \mathrm{d}s, \tag{2}$$

here m is the total (gravitational) mass of the test body.

Let us consider a parallelepiped defined by the hyperplans $x^i = x^i_0$, $x^i = x^i_0 + \Delta x^i$, and let us suppose that the world-line of the test body enters the parallelepiped through the face $x^1 = x^1_0$ and comes out through the face $x^1 = x^1_0 + \Delta x^1$. Let us further suppose that the world-lines of all other bodies do not cross the parallelepiped.

From Einstein's eq. (1) we deduce, for the tensor density $\sqrt{-g}\,T^{\mu\nu}$, the relations

$$\frac{\partial}{\partial x^\mu}(\sqrt{-g}\,T^{\mu\nu}) = -\begin{Bmatrix}\alpha\ \nu\\ \mu\end{Bmatrix}\sqrt{-g}\,T^{\alpha\nu}.$$

Integrate these relations over the parallelepiped. The left-hand side can be integrated once. On the boundary, however, $T^{\mu\nu}$ vanishes everywhere except on the two small regions cut by the world-tube; therefore we find a result different from zero only when we integrate with respect to x^1. We get

$$\left[\iiint \sigma\sqrt{-g}\,\frac{\mathrm{d}x^\mu}{\mathrm{d}s}\frac{\mathrm{d}x^1}{\mathrm{d}s}\,\mathrm{d}x^2\,\mathrm{d}x^3\,\mathrm{d}x^4\right]_{x^1_0}^{x^1_0+\Delta x^1} =$$

$$= -\iiiint \begin{Bmatrix}\alpha\ \nu\\ \mu\end{Bmatrix}\frac{\mathrm{d}x^\alpha}{\mathrm{d}s}\frac{\mathrm{d}x^\nu}{\mathrm{d}s}\,\sigma\sqrt{-g}\,\mathrm{d}x^1\,\mathrm{d}x^2\,\mathrm{d}x^3\,\mathrm{d}x^4,$$

or, remembering (2),

$$\left[m\,\frac{\mathrm{d}x^\mu}{\mathrm{d}s}\right]_{x_0^1}^{x_0^1+\Delta x^1} = -\int \left\{\begin{matrix}\alpha\ \nu\\ \mu\end{matrix}\right\} \frac{\mathrm{d}x^\alpha}{\mathrm{d}s}\,\frac{\mathrm{d}x^\nu}{\mathrm{d}s}\, m\,\mathrm{d}s\,.$$

For $\Delta x^1 \to 0$ this gives

$$\frac{\mathrm{d}}{\mathrm{d}s}\left(m\,\frac{\mathrm{d}x^\mu}{\mathrm{d}s}\right) = -\,m \left\{\begin{matrix}\alpha\ \nu\\ \mu\end{matrix}\right\} \frac{\mathrm{d}x^\alpha}{\mathrm{d}s}\,\frac{\mathrm{d}x^\nu}{\mathrm{d}s}\,. \tag{3}$$

These are the equations of a geodesic, provided m is constant. To prove this, multiply (3) by $mg_{\mu\beta}(\mathrm{d}x_\beta/\mathrm{d}s)$ and sum with respect to the index μ,

$$mg_{\mu\beta}\,\frac{\mathrm{d}x^\beta}{\mathrm{d}s}\,\frac{\mathrm{d}}{\mathrm{d}s}\left(m\,\frac{\mathrm{d}x^\mu}{\mathrm{d}s}\right) = -\,m^2 \begin{bmatrix}\alpha\ \nu\\ \beta\end{bmatrix} \frac{\mathrm{d}x^\beta}{\mathrm{d}s}\,\frac{\mathrm{d}x^\alpha}{\mathrm{d}s}\,\frac{\mathrm{d}x^\nu}{\mathrm{d}s} =$$

$$= -\frac{1}{2}\,m^2\,\frac{\partial g_{\alpha\beta}}{\partial x^\nu}\,\frac{\mathrm{d}x^\nu}{\mathrm{d}s}\,\frac{\mathrm{d}x^\alpha}{\mathrm{d}s}\,\frac{\mathrm{d}x^\beta}{\mathrm{d}s} = -\frac{1}{2}\,m^2\,\frac{\partial g_{\alpha\beta}}{\mathrm{d}s}\,\frac{\mathrm{d}x^\alpha}{\mathrm{d}s}\,\frac{\mathrm{d}x^\beta}{\mathrm{d}s}\,.$$

Changing on the left-side μ into α and adding the same equation with α and β interchanged, we get

$$g_{\alpha\beta}m\,\frac{\mathrm{d}x^\beta}{\mathrm{d}s}\,\frac{\mathrm{d}}{\mathrm{d}s}\left(m\,\frac{\mathrm{d}x^\alpha}{\mathrm{d}s}\right) + g_{\alpha\beta}\,m\,\frac{\mathrm{d}x^\alpha}{\mathrm{d}s}\,\frac{\mathrm{d}}{\mathrm{d}s}\left(m\,\frac{\mathrm{d}x^\beta}{\mathrm{d}s}\right) + m\,\frac{\mathrm{d}x^\alpha}{\mathrm{d}s}\,m\,\frac{\mathrm{d}x^\beta}{\mathrm{d}s}\,\frac{\mathrm{d}g_{\alpha\beta}}{\mathrm{d}s} = 0\,,$$

or

$$\frac{\mathrm{d}}{\mathrm{d}s}\left(g_{\alpha\beta}m\,\frac{\mathrm{d}x^\beta}{\mathrm{d}s}\,m\,\frac{\mathrm{d}x^\alpha}{\mathrm{d}s}\right) = \frac{\mathrm{d}m^2}{\mathrm{d}s} = 0\,. \tag{1}$$

We notice that the proof is not absolutely above criticism. It requires, in fact, the existence of a solution of the gravitational equations, corresponding to the presence of the test body and of the external bodies, which tends continuously to the solution corresponding to the presence of the external bodies alone, as the mass of the test body tends to zero. As a matter of fact, however, not even the existence of a rigorous solution for the two body problem has ever been demonstrated.

7. – Consistency of the gravitational clocks and of the unit defined by the radius of Bohr with Einstein's metrics.

A direct consequence of the above theorem is the fact, already mentioned in the third section, that gravitational clocks indicate the proper time. Let us consider the first of the gravitational clocks described there. As the clock

moves freely throughout the four-dimensional continuum, the gravitational mass M of the attracting body does not vary. In an inertial system of co-ordinates moving with the body, this mass creates a weak constant gravitational field. The period of rotation of the test body moving in a circular orbit of radius R is then uniquely defined by the geodesic theorem; the clock seems therefore to give the proper time correctly.

Lastly let us prove the statement made in the second section, that the length of the radius of Bohr does not vary throughout the four-dimensional world. Let us suppose that the test body considered at the sixth section carries an electric charge. Integrating the equation of continuity

$$\frac{\partial(\sqrt{-g}\,\boldsymbol{s}^i)}{\partial x^i} = 0\,,$$

over the parallelepiped one finds that the charge entering through the face $x^1 = x^1_0$ is equal to the charge coming out through the face $x^1 = x^1_0 + \Delta x^1$. This enables us to state, quite generally, that the elementary charge never varies when expressed in a system of units consistent with general relativity.

Since the mass m of an electron, and its charge e, do not vary, the same thing must be true for the classical electronic radius e^2/m. Finally, from the constancy of $e^2/\hbar$, we conclude that also the radius of Bohr $\hbar^2/me^2$ does not vary.

* * *

I wish to thank Professors E. AMALDI, L. MEZZETTI and E. PERSICO for having read the manuscript and for a number of fruitful discussions.

RIASSUNTO

Si fa vedere che le misure di intervalli spaziali e temporali, che sono essenziali per la teoria della relatività generale, sono quelle basate esclusivamente sulle interazioni forte e elettromagnetica. La consistenza logica della relatività generale richiede che le interazioni forte e elettromagnetica non variino nello spazio-tempo. Le consequenze di queste osservazioni in cosmologia sono prese in esame.

IL NUOVO CIMENTO VOL. XX, N. 6 16 Giugno 1961

A Covariant Formulation of Quantum Mechanics - I.

G. SZAMOSI (*)

Israel Atomic Energy Comission, Department of Physics - Rehovoth

(ricevuto il 10 Febbraio 1961)

Summary. — An attempt is made to introduce explicitly the concept of an invariant time parameter (proper-time) into the relativistic one particle quantum mechanics. A compact unified formulation of the free scalar and spin $\frac{1}{2}$ particles is presented. Covariant equations of motion, including the covariant « Zitterbewegungen », are derived. The quantum equations of motion are compared to the classical ones and their relationship is discussed briefly.

Introduction.

In this paper we propose a new formulation and treatment of the relativstic elementary (one-particle) quantum-mechanics. The essentially new point here is the explicit use of an invariant time parameter (proper-time). This will enable us first to derive well-known results of the theory from the new formulation in a completely covariant way. We shall further obtain some new results concerning the covariant equations of motion of physical operators and also simple equations for the time dependence of bilinear expressions. The most remarkable characteristic of the whole formulation is that it can be only carried out in relativistic theory and has no parallel in the non-relativistic quantum theory.

In the section **1** we briefly summarize the relativistic canonical method for a free particle. Turning to the Hamilton-Jacobi equation we shall observe that it may be written as a very simple total differential equation (eq. (7)). This will be used for the transition to the quantum theory.

(*) Present adress: National Research Council of Canada, Division of Pure Physics, Ottawa, Ont.

Many years ago FOCK [1] had proposed an interesting way for the introduction of the proper time into quantum mechanics and his work was developed and applied later by NAMBU [2]. Our quantization method is basically different fron that of FOCK and NAMBU, since ours leads directly *either* to the scalar or to Dirac's equation and no use is made of the connection between the two. We propose in Section **2** to write the relativistic equation, describing the behaviour of a free particle in the form of a very simple total differential equation. Then the scalar equation and the Dirac equation will appear as special cases. No simple formulation has, however, been found for other relativistic equations for stable particles in the proposed scheme. (Since our formulation is valid for stable particles with finite rest-mass only this restriction is not necessarily a disadvantage.)

In Section **3** of this paper we develop the covariant equations of motion for the physical operators of a free Dirac particle. These operator equations have close resemblence to the classical equations of motion of a spinning particle. The operators of the four space-time co-ordinates perform covariant « Zitterbewegungen » with respect to the invariant proper time.

In the last section very simple total differential equations are given for the time development of the bilinear expressions formed from Dirac operators and four-spinors. These equations are again entirely without parallel in the non-relativistic quantum mechanics.

1. – Classical preliminaries.

Consider the motion of a free particle in classical physics. Suppose that the particle has no intrinsic angular momentum (pole-particle). Then the motion may be described by means of the Lorentz invariant Lagrangian having the form (1):

$$\mathscr{L} = \frac{1}{2} m_0 \dot{x}_\nu \dot{x}_\nu - \frac{m_0}{2}\,. \tag{1}$$

(We use the usual notations: $x_4 = it$; $c = 1$ and the summation convention.) Here m_0 is the rest mass of the particle and the dot denotes derivation with respect to the invariant proper time. The variational principle

$$\delta S = \delta \int \mathscr{L}\, \mathrm{d}s = 0\,,$$

([1]) V. FOCK: *Phys. Zeit. Sov. Un.*, **12**, 404 (1937).

([2]) Y. NAMBU: *Prog. Theor. Phys.*, **5**, 82 (1950).

2403

with the usual conditions gives the equations of motion

$$m_0 \ddot{x}_\nu = 0 \,.$$

The particular form of the Lagrangian in eq. (1) has the consequence that the Hamiltonian

$$\mathscr{H} = \dot{x}_\nu \frac{\partial \mathscr{L}}{\partial \dot{x}_\nu} - \mathscr{L} \equiv \dot{x}_\nu p_\nu - \mathscr{L} = - m_0 \,,$$

numerically equal to the (negative) total rest-energy of the particle (note that $\dot{x}_\nu \dot{x}_\nu = -1$). The canonical equations are

$$\dot{p}_\nu = 0 \,; \qquad \dot{x}_\nu = \frac{1}{m_0} p_\nu \,. \tag{3}$$

Turning to the Hamilton-Jacobi equation one gets formally:

$$\frac{\partial S}{\partial s} + \mathscr{H}\left(x_\nu ; \frac{\partial S}{\partial x}\right) = 0 \,; \qquad \left(p_\nu = \frac{\partial S}{\partial x_\nu}\right), \tag{4}$$

or making use of (2) and writing for S

$$S(x_\nu, s) = m_0 s + S_0(x_\nu) \tag{5}$$

the more simple equation

$$\mathscr{H} = \frac{1}{2m_0}\left(\frac{\partial S_0}{\partial x_\nu}\right)^2 - \frac{m_0}{2} = - m_0 \tag{6}$$

results.

Now one observes that with the help of (3) the right-hand side of eq. (6) may be written as

$$\left(\dot{x}_\nu \frac{\partial S_0(x_\nu)}{\partial x_\nu} \equiv\right), \qquad \frac{\mathrm{d}S_0}{\mathrm{d}s} = - m_0 \,, \tag{7a}$$

or again with the help of (5)

$$\left(\frac{\partial S}{\partial s} + \dot{x}_\nu \frac{\partial S}{\partial x_\nu} \equiv\right), \qquad \frac{\mathrm{d}S(x_\nu, s)}{\mathrm{d}s} = 0 \,. \tag{7b}$$

The possibility of rewriting eq. (6) and (4) into the simple and compact forms (7a) and (7b) seems in general to have been overlooked. One observes that in the non-relativistic dynamics there is absolutely no possibility of having

the Hamilton-Jacobi equation in the form of a total differential equation. The reason for this difference in behaviour of the action function lies obviously in the fact that in non-relativistic dynamics the energy of the particle is arbitrary up to a constant. In relativistic dynamics, however, the four components of the momenta completely determine the rest-energy of the particle, and it is this fact which gives the possibility of contracting the eq. (4) and (6) to the simple forms (*7a*) and (*7b*). We also made use of the particular form of the Lagrangian given by (1). This restriction will, however, be proven as useful.

These features of the formulation will be reflected in the quantum region too. In our *c*-number treatment the « eigenvalue » of the relativistic Hamiltonian is given (*i.e.* no mass-quantization). Thus if one wishes to make use of the framework of quantum theory to calculate the probabilities of the results of actual measurements, one has to decompose the compact relativistic formulation into the usual space-time picture. This should always be kept in mind when considering the equations presented below.

Although eq. (7) are equivalent to eq. (4) and (6) their form is *not* the Hamiltonian one. For example, (*7b*) cannot be used to determine the form of the Hamiltonian function, since $\dot{x}_\nu\,(\partial S_0/\partial x_\nu)$ is *not* the Hamiltonian and its use would contradict the canonical eq. (3). After quantization, however, eq. (7) may also be considered as the Hamilton-Jacobi equation (see below).

The differential eq. (7) will be used to go over to the quantum theory of the free particle.

2. – Quantization.

The transition to quantum theory may be done in the very usual way using the relativistic Hamiltonian of the free particle. Corresponding to eq. (5) we may put for the wave function

$$\Psi(x_\nu, s) = \exp\left[\frac{i}{\hbar}\, m_0 s\right] \psi(x_\nu)\,. \tag{8}$$

Applying the correspondence principle and thus making the Hamiltonian (2) into an operator one obtains the scalar wave equation as is well known.

But, instead of doing this, we would like to use the proper time explicitly and for this purpose we should start from eq. (7). The suggestion is now that the relativistic wave equation of a free particle should have the form

$$\frac{\hbar}{i}\,\frac{\mathrm{d}\Psi(x_\nu, s)}{\mathrm{d}s} = 0\,, \tag{9}$$

corresponding to (*7b*).

2405

With the help of (8) eq. (9) becomes

$$\left(m_0 + \frac{\hbar}{i}\frac{\mathrm{d}}{\mathrm{d}s}\right)\psi(x_\nu) = 0, \tag{10}$$

corresponding to eq. (7*a*).

The quantization now proceeds as follows. We suppose the validity of the canonical commutation relations:

$$[p_\mu, x_\nu] = \frac{\hbar}{i}\delta_{\mu\nu}\,, \tag{11a}$$

$$[p_\mu, p_\nu] = [x_\mu, x_\nu] = 0\,. \tag{11b}$$

Differentiating the commutation relation (11*a*) with respect to the proper time one gets

$$[\dot p_\mu, x_\nu] + [p_\mu, \dot x_\nu] = 0\,. \tag{12}$$

We shall require that (for a free particle)

$$\dot p_\nu = 0\,. \tag{13}$$

The relation (12) then gives

$$[p_\nu, \dot x_\mu] = 0\,. \tag{14}$$

(This is a trivial relation only if we suppose *a priori* a connection between velocity and momentum.)

From (11*a*) and (14) we may now write eq. (10) as

$$(m_0 + \dot x_\nu p_\nu)\,\psi(x_\nu) = 0\,, \tag{15}$$

where $p_\nu = -i\hbar\,(\partial/\partial x_\nu)$. The $\dot x_\nu$ velocity operator is as yet unknown. Making different assumptions for it we shall get different physical theories. The most simple assumption is the « classical » one, that is, velocity and momentum are proportional

$$\dot x_\mu = \frac{1}{m_0}\,p_\mu\,. \tag{16}$$

By this assumption (14) is satisfied while (15) again gives the scalar wave equation

$$(p_\nu^2 + m_0^2)\,\psi_\nu(x) = 0\,.$$

The situation is now completely parallel to that of the preceding point. Eq. (15) together with eq. (16) is equivalent to the scalar wave equation but this does not have the Hamiltonian form.

Now we ask if there is a possibility, in quantum theory, of choosing a velocity operator in such a way that eq. (15) has the Hamiltonian form: in other words, whether we could find a canonical formalism in which

$$\mathscr{H} \to \frac{\hbar}{i}\,\frac{\mathrm{d}}{\mathrm{d}s} = \dot{x}_\nu p_\nu\,. \tag{17}$$

This correspondence is actually satisfied in Dirac's theory. Instead of showing this directly by supposing the well known commutation relations for the $\dot{x}_\nu$'s (*i.e.* for the γ_ν's) we shall proceed in a more didactical way by « deriving » those commutation relations. The direct physical meaning of these might become clearer in this way.

Using (17) we may write obviously

$$\dot{x}_\nu = \frac{i}{\hbar}\,[\mathscr{H}, x_\nu]\,, \tag{18}$$

and hence

$$(\dot{x}_\varrho x_\nu - x_\nu \dot{x}_\varrho)p_\varrho = 0\,. \tag{19}$$

(We shall see later that this is satisfied by $[\dot{x}_\varrho, x_\nu] = 0$ but now we shall use only (19).) Eq. (19) shows that eq. (16) cannot be valid anymore, since it would violate (11*b*). The invalidity of (16) shows further that the actual motion is more complex than that of a scalar particle. We may, however, suppose that there exists a kind of « centre of mass » co-ordinate the velocity of which is parallel to the momentum. The definition of this « centre of mass » co-ordinate is quite unique. For if we apply the Hamiltonian to any solution of eq. (15) it will give the value of the rest mass and so the definition of the « centre of mass » co-ordinate reads

$$X_\nu = -\frac{1}{2m_0}\,(\mathscr{H}x_\nu + x_\nu\mathscr{H})\,. \tag{20}$$

If now the actual velocity $\dot{x}_\nu$ is not proportional to the momentum, the velocity of the « centre of mass » still could be

$$\dot{X}_\nu = -\frac{1}{2m_0}\,(\mathscr{H}\dot{x}_\nu + \dot{x}_\nu\mathscr{H}) = \frac{1}{m_0}\,p_\nu \;(^*)\,. \tag{21}$$

(*) Note that:

$$\overset{(n)}{X}_\nu = \frac{i}{\hbar}\,[\mathscr{H}, \overset{(n-1)}{X}_\nu] = -\frac{1}{2m_0}\,(\mathscr{H}\overset{(n)}{x}_\nu + \overset{(n)}{x}_\nu\mathscr{H})\,.$$

2407

This now leads immediately to the commutation relations:

$$\dot{x}_\mu \dot{x}_\nu + \dot{x}_\nu \dot{x}_\mu = -2\delta_{\mu\nu} \tag{22}$$

so we have Dirac's theory ($\dot{x}_\nu \to i\gamma_\nu$) without using the scalar wave equation. *We have actually both in eq.* (15) with the velocity operator (16) or (22) (*).

The X_ν co-ordinate operator has the following simple meaning if it applies to any solution of eq. (15):

$$X_\nu = x_\nu + i\lambda_0 \dot{x}_\nu \,, \tag{23}$$

where $\lambda_0 = \hbar/2m_0$ is half the Compton wave length of the particle (**).

The commutation relation

$$[p_\nu, X_\mu] = -\frac{i\hbar}{m_0}\mathscr{L}\mathscr{H}\delta_{\mu\nu} \,,$$

shows that p_ν and X_μ are canonically conjugate if the commutator applies to any solution of (15). The general relation

$$\dot{X}_\mu \dot{X}_\nu = -1$$

shows the role of $\dot{X}_\nu$ as representative of the ordinary four-velocity.

For the sake of completeness we remark that the six-vector of the total angular momentum

$$\mathscr{F}_{\mu\nu} = L_{\mu\nu} + S_{\mu\nu} = x_\mu p_\nu - x_\nu p_\mu + \frac{i\hbar}{4}(\dot{x}_\mu \dot{x}_\nu - \dot{x}_\nu \dot{x}_\mu) \,,$$

is a constant of the motion

$$\frac{\mathrm{d}\mathscr{F}_{\mu\nu}}{\mathrm{d}s} = 0 \,. \tag{24}$$

(*) It may be mentioned in this connection that eqs. (20) (21) have meaning also in the case of a scalar particle. If the scalar Hamiltonian is used, then it turns out that $\dot{X}_\nu = \dot{x}_\nu$ and so from (15) the eq. (21) will be valid. (22) will, of course, not follow from (21) but in what follows almost all of the equations will be valid for a scalar particle too. Many of them, however, would just be empty identities (*e.g.* (26)) since the motion here is more simple than that of the Dirac particles.

(**) This co-ordinate has, already, been introduced by many authors in different connection.

There is another constant six-vector in the theory, namely the orbital angular momentum of the « centre of mass »

$$\bar{\mathscr{F}}_{\mu\nu} = X_\mu p_\nu - X_\nu p_\mu = \text{const} .$$

3. – Covariant equations of motion.

We shall now make use of the formalism just developed for obtaining covariant equations of motion. From (21) one gets for the motion of the « centre of mass »

$$\ddot{X}_\nu = 0 . \tag{25}$$

This equation can be expressed in terms of the actual co-ordinates with the help of (23). This yields

$$\ddot{x}_\nu + i\lambda_0 \ddot{x}_\nu = 0 . \tag{26}$$

These are the equations for the covariant « Zitterbewegungen ». The formal solution of the equations of motion gives for the position operator if it applies to any solution of (15):

$$X_\nu(s) = -\, \lambda_0^2 \ddot{x}_\nu(0) \, \exp\left[\frac{i}{\lambda_0}\, s\right] + \dot{X}_\nu(0) s . \tag{27}$$

It is remarkable that the fourth component, the time-co-ordinate, performs « Zitterbewegungen » too. This means that the actual motion of the particle is confined into a four-dimensional tube having a diameter of the Compton-wave length of the particle.

As a consequence of (27) and (26) one can derive equations of motion for the basic quantities of the Dirac algebra. These operator equations are, of course, valid only if we apply them to any solution of (15). Denoting the element of the Dirac algebra by $\sigma_{\mu\nu}(\equiv \dot{x}_\mu \dot{x}_\nu)$, $\sigma_{\mu\nu\lambda}(\equiv \dot{x}_\mu \dot{x}_\nu \dot{x}_\lambda)$ and γ_5 one gets easily the following eleven equations in addition to (26):

$$\ddot{\sigma}_{\mu\nu} + i\lambda_0 \ddot{\sigma}_{\mu\nu} = 0 , \tag{27a}$$

$$\ddot{\sigma}_{\mu\nu\lambda} + i\lambda_0 \ddot{\sigma}_{\mu\nu\lambda} = 0 , \tag{27b}$$

$$\dot{\gamma}_5 = \frac{i}{\lambda_0} \gamma_5 . \tag{27c}$$

(The last equation is particularly simple. It gives γ_5 as a pure periodic function of the (proper) time:

$$\gamma_5(s) = \gamma_5(0) \exp\left[\frac{i}{\lambda_0} s\right].$$

There is no comparable simple expression for the time dependence of the γ_5 operator in the usual, non-relativistic Hamiltonian method.)

As a consequence of eq. (27) the following general theorem is valid. Let Γ be any operator which acts only on the spinor part of the solutions of (15) and let us denote $\dot{\Gamma} = G$. Then any solution of (15) will satisfy the pure harmonic operator equation

$$\ddot{G} + (\lambda_0)^{-2} G = 0 .$$

(If Γ commutes with the Hamiltonian, then this equation reduces to an empty identity.)

Further equations connecting the basic dynamical quantities can be easily derived. The operator equation

$$\ddot{x}_\mu p_\mu = 0$$

shows that the acceleration operator is perpendicular to the four-momentum, and the classically well-known orthogonality of the four-velocity and four-acceleration is reflected in the equation

$$\ddot{x}_\mu \dot{x}_\mu + \dot{x}_\mu \ddot{x}_\mu = 0 .$$

which is a simple consequence of (22).

The covariant way of writing the time dependence of the dynamical variables enables us also to compare directly the basic dynamical equations of the quantum-theory with those of the classical dynamics of spinning particles. The latter was studied in a number of papers very recently (see *e.g.* (3)).

The classical equations for a spinning free particle contain first the conservation of momentum and angular momentum,

$$\dot{p}_\nu = 0 , \tag{30}$$

$$S^{(\mathrm{cl})}_{\mu\nu} = \dot{x}_\nu p_\mu - \dot{x}_\mu p_\nu , \tag{31}$$

where $S^{(\mathrm{cl})}_{\mu\nu}$ denotes the classical spin tensor. This set of equations is, however, not complete. In order to have a full description of the classical motion, one supplements them with three additional conditions. The choice of these should be guided by physical considerations. The most « popular » choice have been

the conditions:

$$S^{(\mathrm{cl})}_{\mu\nu}\dot{x}_\mu = 0 \,. \tag{32}$$

These were first introduced by THOMAS and FRENKEL and were extensively used later by WEYSENHOFF. These conditions are considered to express covariantly that the particle has no « electric »-like moment in its own rest system. Occasionally, for various purposes, other supplementary conditions have also been considered. The conditions

$$S^{\mathrm{cl}}_{\mu\nu}p_\nu = 0 \,, \tag{33}$$

were used by NAKANO [3] and very recently the conditions

$$\ddot{x}_\mu \sim S^{(\mathrm{cl})}_{\mu\nu}\dot{x}_\nu \,, \tag{34}$$

were introduced by D. BOHM *et al.* [4].

In Dirac's theory the eq. (30) and (31) clearly have their quantized counterparts in (13) and (24). There are no explicit supplementary conditions. Their place are taken by the commutation relations (22) for the velocities. There are however identities which are consequences of these commutation relations and which might be considered as quantum representatives of the classical supplementary conditions. The identity (from (22) and (24))

$$S_{\mu\nu}\dot{x}_\nu + \dot{x}_\nu S_{\mu\nu} \equiv 0 \tag{35}$$

is clearly the quantum « picture » of the condition (32). The usual physical considerations which are attached to (32) do not, however, seem to be valid for (35) since there is no system in which $\dot{x}_\nu = 0$.

Another quantum identity connects the acceleration with the momentum:

$$\ddot{x}_\mu \equiv \left(\frac{2}{\hbar}\right)^2 \cdot S_{\nu\mu}p_\nu \,. \tag{36}$$

Classically (36) is a consequence of (38) if the latter is considered as a classical identity [5]. In quantum theory both are consequences of the (22) commutation relations.

Another remark may be added on the connection between momentum and

---

[3] T. NAKANO: *Prog. Theor. Phys.*, **15**, 333 (1956).

[4] D. BOHM, P. HILLION, T. TAKABAYASI and J. P. VIGIER: *Prog. Theor. Phys.*, **23**, 496 (1960).

[5] S. SHANMUGADASHAN: *Can. Journ. Phys.*, **31**, 1 (1953).

velocity. In classical theory one gets for p_ν from (31)

$$p_\mu = M\dot{x}_\mu - \dot{S}_{\mu\nu}\dot{x} , \tag{37}$$

where $M = -\dot{x}_\nu p_\nu$ the invariant rest-energy of the particle. (Classically distinction should be made between M and the constant $m_0 = (-p_\nu^2)^{\frac{1}{2}}$. In Dirac's theory the two are obviously identical by (22)). In quantum theory the equation corresponding to (37) is the following:

$$p_\mu = -\tfrac{1}{6}(\dot{S}_{\mu\nu}\dot{x}_\nu + \dot{x}_\nu\dot{S}_{\mu\nu}) .$$

4. – Bilinear forms.

We shall now briefly consider the application of the covariant proper time formalism to bilinear forms. First we observe that introducing $\overline{\psi} = -i\psi^+\dot{x}_4$ it will satisfy the equation:

$$\dot{\overline{\psi}} - \frac{i}{2\lambda_0}\overline{\psi} = 0 .$$

Hence we get with the help of (15) the compact form:

$$\frac{\mathrm{d}\overline{\psi}\psi}{\mathrm{d}s} = 0 , \tag{38}$$

of the continuity equation. (38) can, however, also be considered as a special case of a more general equation. Let O be any quantum mechanical operator. Then it follows from (15) and (37) that if φ and ψ are solutions of them, the bilinear expression $\overline{\varphi}O\psi$ satisfies the equation

$$\frac{\mathrm{d}}{\mathrm{d}s}(\overline{\varphi}O\psi) = \overline{\varphi}\frac{\mathrm{d}O}{\mathrm{d}s}\psi . \tag{39}$$

There are obviously no comparable equations in the non-relativistic quantum dynamics.

Examples of (39) have already been given in the previous section. The following further relations may be of interest. Consider eq. (39) with $O = x_\nu$ and $\varphi = \psi$. Write the corresponding equation in the form

$$\overline{\psi}x_\nu\psi = \int \overline{\psi}\dot{x}_\nu\psi \, \mathrm{d}s .$$

Then this equation can be verified by explicit calculation. The current vector $j_\mu = \psi \dot{x}_\mu \psi$ provides another example. By (26) it satisfies the following simple equation

$$\dot{j}_\mu + i\lambda_0 \ddot{j}_\mu = 0 .$$

Hence one gets the relation

$$\ddot{j}_\mu + \lambda_0^{-1} \dot{j}_\mu = \frac{4m_0}{\hbar^2} \mathscr{F}_\mu ,$$

where

$$\mathscr{F}_\mu = \frac{1}{m_0} \left(\psi (p_\nu \psi) - (p_\nu \bar{\psi}) \psi \right) .$$

The equation

$$\bar{\psi} S_{\mu\nu} \psi = \frac{\hbar}{i} \int \left(\frac{\partial j_\nu}{\partial x_\mu} - \frac{\partial j_\mu}{\partial x_\nu} \right) \mathrm{d}s ,$$

may also have some interest since it connects the spin tensor with the rotation of the four current.

In a forthcoming paper we shall consider the dynamical equations in the presence of an external field.

* * *

The author wishes to thank Prof. N. Rosen (Haifa) for interesting discussions.

RIASSUNTO (*)

Si tenta di introdurre esplicitamente il concetto di parametro temporale invariante (tempo proprio) nella meccanica quantistica relativistica di una particella. Si presenta una formulazione unificata compatta delle particelle libere scalari e di spin $\frac{1}{2}$. Si derivano equazioni covarianti del moto, comprese le « Zitterbewegungen » covarianti. Si confrontano le equazioni quantistiche del moto con quelle classiche e si discutono brevemente i loro rapporti.

(*) *Traduzione a cura della Redazione.*

Direct Electronic Decay of Three π^0's Emitted from an Antineutron Annihilation Star.

TSAI-CHÜ and C. SIMONIN-HAUDECOEUR

Laboratoire de Physique Enseignement, Faculté des Sciences - Paris

(ricevuto il 10 Febbraio 1961)

Summary. — Continuous search for antineutron annihilation events in an antiproton stack leads to the discovery of a star of $10+15\bar{n}$. Of the fifteen shower particles of this star, twelve are identified as electrons and three as pions. A negative pion among the three comes to rest. The ten heavy prongs contain only evaporation protons. All the protons come to rest in the emulsion and each proton has a kinetic energy less than 15 MeV. Dividing the twelve electrons into three groups and assuming each group as the decay of $\pi^0 \to e^+ + e^- + e^+ + e^-$, we can evaluate the masses of the three π^0's respectively as (136 ± 14), (135 ± 14) and (136 ± 13) MeV. The probability for the simultaneous decay of three ordinary π^0's is only $4 \cdot 10^{-14}$. This event suggests the possibility of a new process for the production of electrons, *e.g.* the existence of a second π^0. Considering the high multiplicity, the wide angular distribution and the right average energy of the pions as well as the total energy of the star, we conclude that this event is the result of an annihilation between an antineutron and a nucleon. A small-cell technique is proposed for the measurement of the multiple scattering of the inclined minimum-ionizing tracks.

1. – Introduction.

In a stack of K-5 emulsions exposed to the enriched antiproton beam of a momentum of 740 MeV/c, we have found five stars showing the characteristics of an antineutron annihilation star. One of these stars which is associated with an antiproton stop has already been reported in a previous article (1).

(1) TSAI-CHÜ, M. MORAND, G. BOURLET, C. SIMONIN and D. SCHUNE: *Nuovo Cimento*, **17**, 259 (1960).

The present star contains ten black prongs and fifteen shower particles. The shower particles spread uniformly over a projection angle of 150°; thirteen of them are minimum-ionizing tracks. Among the latter, two tracks forming a small angle reveal the familiar characteristics of an electron-positron pair. Six other minimum-ionizing tracks can also be easily identified as electrons because of their very low energy. These facts establish at once the presence of a large number of electrons. As the tracks have large dips, a special method has to be proposed to eliminate the distortion of the emulsion and to deduce the precise value of their energy from multiple scattering. Scattering measurements by small cells and the c.g. method are found quite satisfactory for inclined tracks with large dips and for particles having intermediate energy.

From the detailed measurements, we can calculate the energy of all the shower particles. Twelve of the minimum-ionizing tracks can be identified as electrons by ionization and multiple scattering. The only rapid process known for the production of electrons is the decay of $\pi^0 \rightarrow e^+ + e^- + e^+ + e^-$. Considering the twelve electrons as the decay of three π^0's, we have eventually obtained their respective values of mass in excellent agreement with that of a π^0. But the probability of decay of even a single π^0 is already very small. In fact, from more than six thousand antiproton annihilations studied, no example of electronic decay of π^0 has yet been observed up to the present. The presence of three π^0 decays in this event should indicate a significant difference between antiproton and antineutron annihilation events. It is possible that the π^0's observed here have different properties from the usual ones.

2. – Identification of shower particles. Electrons and pions.

Among the 15 shower particles of the star, track 1 (Fig. 1 and Table I) has a small dip and an ionization of $g/g_0 = 2.74 \pm 0.11$ at emission, where g is the blob density of the track, and g_0 the plateau value of the blob density of minimum-ionizing tracks. It comes to rest in the same plate. Observing the σ-star after a range of 9.36 mm, we identify particle 1 as a negative pion of 22.5 MeV. Particle 6 is another flat track and has an ionization of 1.03 ± 0.02 and a scattering angle of (0.0260 ± 0.0020) degree for a 100 μm cell. The latter is measured by basic cells of 50 μm and calculated by quadruple cells of 200 μm. So particle 6 is not a proton and is compatible with a pion of (812 ± 74) MeV. All the other shower particles have inclined tracks, four of which have dips even as large as 60°. The energy of these tracks cannot be deduced correctly from multiple scattering due to the distortion of the emulsion. The third difference is usually employed to eliminate the distortion. This method is efficient where the distortion produces a constant curvature of the trajectory. In this case, the second difference of multiple scattering is

then increased by a constant term which can be eliminated by the third difference. This is only true for tracks having a moderate dip and showing a

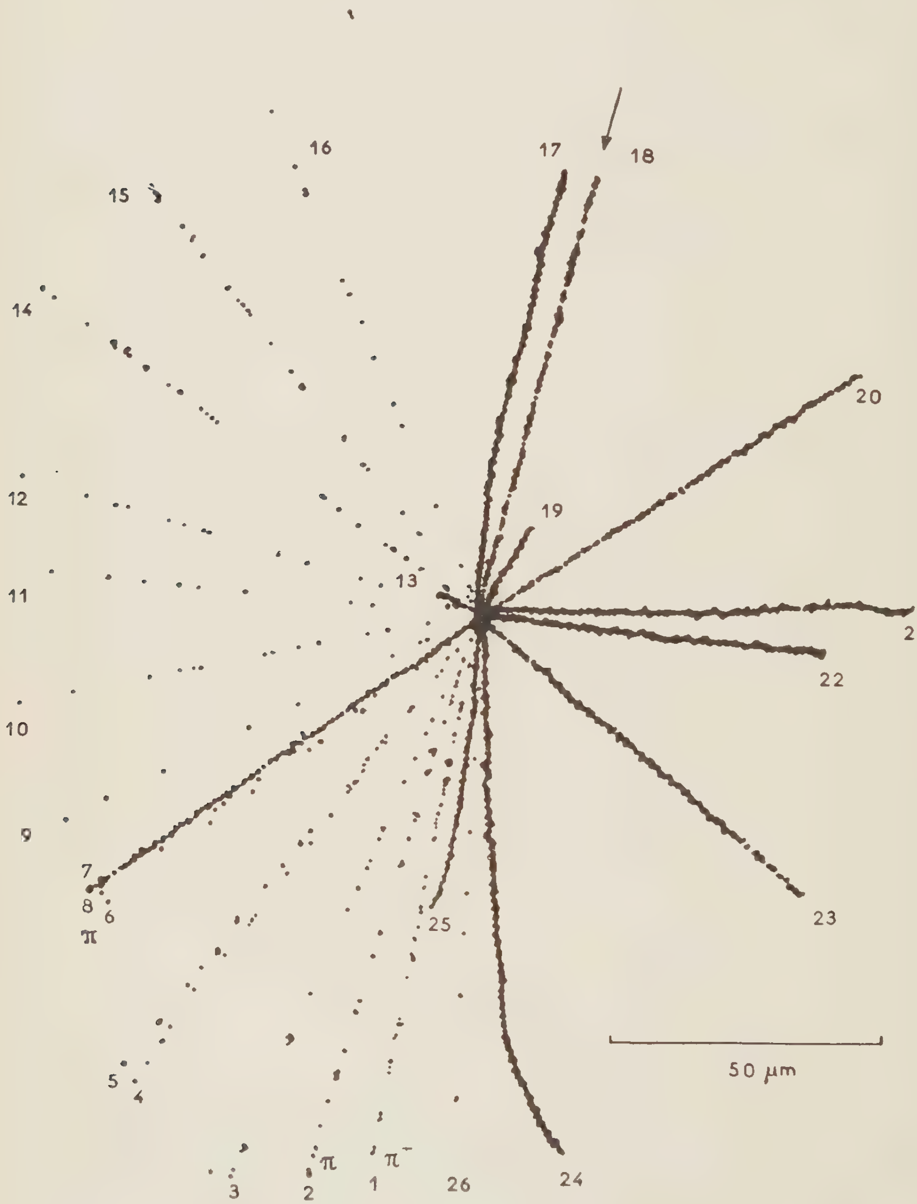

Fig. 1. – The emission of twelve electrons in an antineutron annihilation star.

regular C-type distortion. The detailed study of these inclined tracks enable us to determine the distortion of the emulsion, its variation with the direction

and depth in the emulsion and finally to propose a method for measuring the multiple scattering of inclined tracks.

TABLE I. – *Results of measurement of the fifteen shower particles.*

Track no.	Proejction in degrees	Dip in degrees	Ionization g/g_0	Nature	Energy (MeV)
1	20.2	6° 10′	2.74 ± 0.11	π^-	22.5
2	24.4	60° 40′	1.55 ± 0.12	π	46.6 ± 8.1
3	32.6	54° 25′	0.97 ± 0.08	e	26.1 ± 5.6
4	44.6	61° 40′	1.00 ± 0.09	e	53 ± 13
5	45.8	62° 5′	0.94 ± 0.08	e	73 ± 18
6	62.0	5° 40′	1.03 ± 0.02	π	812 ± 74
8	62.6	45°	1.08 ± 0.06	e	20.0 ± 2.5
9	72.2	53° 15′	0.90 ± 0.06	e	36.9 ± 7.8
10	88.7	39° 10′	1.08 ± 0.06	e	25.3 ± 3.5
11	104.8	46° 55′	1.11 ± 0.09	e	38.4 ± 7.4
12	115.9	33° 30′	0.96 ± 0.05	e	136 ± 22
14	136.2	61° 30′	0.97 ± 0.06	e	120 ± 40
15	152.2	61° 20′	1.10 ± 0.07	e	42.3 ± 6.3
16	167.0	34° 15′	1.04 ± 0.05	e	109 ± 16
26	12.0	21° 25′	1.00 ± 0.03	e	178 ± 26

a) *Distortion vectors.* The deformation of an emulsion can be measured in terms of distortion vectors of the first and second order. They can be (2) deduced from scattering measurements made on inclined tracks. Let $\Delta^2 y$ be the second difference of the ordinate of the distorted track, $\Delta^2 y_0$ the second difference of the undistorted track, and $K_2 \sin\alpha_2$ one of the components of the second order vector, we have (2)

$$\Delta^2 y = \Delta^2 y_0 + \frac{2n(\Delta z)^2 K_2 \sin\alpha_2}{t^2}\,, \qquad \text{with } \Delta^2 y_0 = 0\,, \tag{1}$$

where n is the number of second differences, t the thickness of the emulsions Δz the thickness of a cell. Eq. (1) is true when Δz is assumed to be constant along the track throughout the emulsion. The component $K_2 \sin\alpha_2$ is perpendicular to the track and parallel to the surface of the emulsion. It is the major cause for errors in multiple scattering. The projection angle from tracks 26 to 16 increases to about 150° and $K_2 \sin\alpha_2$ calculated from (1) changes from a positive to a negative sign. The star is in the middle of plate 105. All

(2) TSAI-CHÜ: *Nuovo Cimento*, 5, 1128 (1957).

the shower particles traverse from air to glass across the following plates 104, 103 and so on. The average magnitude of $K_2 \sin\alpha_2$ over all the inclined minimum-ionizing tracks is 10 and 6 μm respectively for plates 105 and 103 and is 45 μm for 104. Fig. 2 shows the variation of $K_2 \sin\alpha_2$ with the depth of the emulsion and with the dips of tracks. The abscissa represents the depth measured from the air in units of 100 μm, whilst the ordinate indicates the magnitude of $K_2 \sin\alpha_2$ in arbitrary units for plate 104. $K_2 \sin\alpha_2$ starts from a small value near the air and it increases rapidly with the depth for steeper tracks.

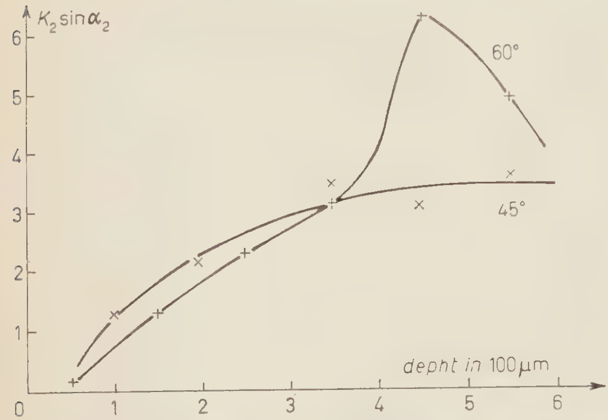

Fig. 2. – The variation of the $K_2 \sin\alpha_2$ with the depth of the emulsion for different dips.

b) Small-cell technique. The $K_2 \sin\alpha_2$ component of each track is calculated by eq. (1). Wherever its variation with depth (Fig. 2) becomes important, different values of $K_2 \sin\alpha_2$ are calculated for different layers in the emulsion. The second difference $\Delta^2 y_0$ of the undistorted tracks is obtained by subtracting a correction term from the measured $\Delta^2 y$, *i.e.*

$$\Delta^2 y_0 = \Delta^2 y - \frac{2(\Delta z)^2 K_2 \sin\alpha_2}{t} . \tag{2}$$

The multiple scattering of each track is afterwards deduced from the corrected $\Delta^2 y_0$ values. The correction term in (2) increases with the square of a cell length; so for big cells, it becomes more important than the multiple scattering. In fact, for small cells of 5 to 10 μm, the correction is practically negligible for tracks in plates 105 and 103. But for steeper tracks in plate 104, one-third of the $\Delta^2 y$ values near the glass has to be eliminated because of its abnormally big magnitude. Since most of the tracks are anticipated to be electrons, it is often necessary to apply a bremsstrahlung correction whenever the track length observed in emulsion is comparable with the radiation length of electrons. In order to avoid this correction, we measure the energy of electrons by considering a track length as short as possible. A few millimeters of each track are measured by the Koritska R 4 microscope in constant cells of 5 or 10 μm. The ordinate of each cell is estimated by the grain nearest to the extremity of the cell. The average noise in the measurements is below

2418

0.1 μm and the signal to noise ratio is kept at a level higher than 1.5. The constant of multiple scattering is slightly diminished by the smoothing effect during the measurement. The statistical error is increased by the small signal-to-noise ratio. For particles of higher energy, multiple scattering of the track becomes small compared with the noise level; sometimes it may be completely drowned out by the fluctuation of the noise. This situation is remedied by the c.g. method [3]. Each basic cell is divided into several subcells, the c.g. of the ordinates of the subcells replaces the ordinate of a basic cell in calculating the second difference. For a cell containing n subcells, the noise of the combined cell [4] is reduced by a factor $1/\sqrt{n}$. For a cell with two subcells, we have [4]

$$\overline{D(2)}^2 = \frac{55}{8}\,k^2s^3 + \frac{e^2}{2}\,, \tag{3}$$

and

$$\bar{d}^2 = k^2s^3 + e^2\,, \tag{4}$$

where $D(2)$ is the mean second difference of the c.g. of the ordinates of two subcells, d the second difference of the ordinate of a subcells, k^2s^3 the multiple scattering for the subcell s, and e the noise of the measurement. By eliminating e^2 between (3) and (4), we have

$$k^2s^3 = \frac{4[2\overline{D(2)}^2 - d^2]}{51}\,. \tag{5}$$

Similarly,

$$\overline{D(4)}^2 = \frac{853}{16}\,k^2s^3 + \frac{e^2}{4}\,, \tag{6}$$

$D(4)$ is the second difference of the c.g. of the ordinate with four subcells, we have, by eliminating the noise between (6) and (4),

$$k^2s^3 = \frac{4[4\overline{D(4)}^2 - d^2]}{819}\,. \tag{7}$$

The noise level is reduced by increasing the number of subcells, but the precision of scattering measurement decreases with the number of combined cells. There should be a compromise between these two requirements.

([3]) TSAI-CHÜ: *Nuovo Cimento*, **10**, 435 (1958).

([4]) B. DÉPAUX and TSAI-CHÜ: *Compt. Rend.*, **249**, 2187 (1959).

c) Identification of shower particles. Table I gives the results of each shower particle with respect to the projection angle, dip, ionization, energy and nature. The energy of each particle is deduced from the multiple scattering which is measured and calculated by the proposed method. All the inclined tracks except track 2 have a minimum ionization. Particle 2 has a $g/g_0 = 1.55 \pm 0.12$ and a scattering angle of (0.295 ± 0.084) degree for a 100 μm cell. It has a mass of $(230 \pm 64)\,m_e$ and is identified as a pion. The energy of the electrons in Table I assumes the value of the product of momentum (p) and velocity (v). Each pv value of tracks 3, 8, 9, 11 and 15 by scattering is below 50 MeV. If these tracks were pions, they should have a g/g_0 value higher than 2. Track 26 has the highest pv value, but its ionization $g/g_0 = 1.00 \pm 0.03$ is two standard deviations lower than that of a pion. The ionization of the other tracks is more than three standard deviations lower. These results prove without doubt that the twelve inclined minimum ionization particles are all electrons. The last portion of track 10 in plate 103 shows an evident loss of energy and it has not been taken into account because of a possible bremsstrahlung. As for particle 2, the results obtained by the proposed method give a reasonable value of mass. This method is further confirmed by the average ratio, (pv) plate $104/(pv)$ plate 105 and 103, of all the inclined tracks. The value of the ratio 1.01 ± 0.02 signifies that the correction made on the big distortion in plate 104 is exact. Finally, the excellent values of mass of the three π^0's furnish another support of this method.

3. – Salient features of the star. Direct electronic decay of three π^0's.

One of the salient feature of the star is the presence of a large number of electrons. Whatever its origin may be, there has not yet been observed a star which ejects more than four electrons. The presence of low energy electrons directly at the centre of the star and their wide angular distribution exclude the electro-magnetic or cascade origin of an electronic shower. Consequently, it is most probable to consider them as the decay of one or several short-lived particles. The π^0 has the shortest lifetime among the known elementary particles. About one in 30 000 decays into four electrons [5,6]. Other salient features of this star are the prevalent emissions of pions and evaporation protons with the absence of any knock-on nucleon. As nearly all the energy of the primary is transformed into visible energy, it is therefore not difficult to determine the nature of the reaction which produces the star.

(5) N. Kroll and W. Wada: *Phys. Rev.*, **98**, 1355 (1955).
(6) N. P. Samios: *Nuovo Cimento*, **18**, 154 (1960).

a) Combination of electrons into π^0's. The most ideal case is to consider the electrons as the simultaneous decay of three π^0's. Then, it will be seen that there is only a unique good combination among the 12 electrons. Accordingly, we divide the electrons into three groups and consider each group as the decay of a π^0. Let p_1c, p_2c, p_3c and p_4c be the momenta of the four electrons, pc and U their resultant momentum and total energy, and m_1c^2 the rest mass of the π^0, all in MeV units, we have

$$U = p_1c + p_2c + p_3c + p_4c\,,$$

$$(pc)^2 = \Big[\sum_1^4 (p_ic)_x\Big]^2 + \Big[\sum_1^4 (p_ic)_y\Big]^2 + \Big[\sum_1^4 (p_ic)_z\Big]^2$$

and

$$m_0c^2 = \sqrt{U^2 - (pc)^2}\,,$$

with an error

$$\Delta m_0c^2 = \frac{1}{m_0c^2}\sqrt{\sum_1^4 (\Delta p_ic)^2[U - pc\cos(\boldsymbol{p}\cdot\boldsymbol{p}_i)]^2}\,.$$

The error in mass, Δm_0c^2, is not very sensitive to the momentum errors, because each Δp_ic is multiplied by a factor involving the difference between the total energy and momentum. Since the electrons of each π^0 do not assemble in isolated and distinct groups, the electrons of one π^0 are mixed with those of the other two π^0's. To sort them out for each π^0, we have to try $^{12}_{4}\mathrm{C} = 495$ combinations with no *a priori* knowledge about their groupement in advance Fortunately, the electron pair 4, 5 (Fig. 2, Table I) belong certainly to the same π^0; the other pairs like 3, 9; 8, 11; 12, 16 and 14, 15 with nearly the same dip could belong respectively to the one and the same π^0. With the electron pair 4, 5, the number of combinations is reduced to 255, instead of 495 Fortyfive combinations with the pair 4, 5 and any two of the other ten electrons have been calculated; 84 combinations with electron 26 and any three of the other nine electrons, and so on. The result of the best combination is found when the electrons are divided into the following groups in Table II. Here, each group gives an excellent value of mass close to that of a π^0. The

TABLE II. – *Total energy and resultant momentum of the electrons composing the* π^0. *Direction of the momentum and mass of* π^0.

Electrons	U	pc	projection	dip	m_0c^2
4, 5, 12, 15	304 ± 32	272 ± 22	99° 30′	55° 10′	136 ± 14
3, 9, 14, 16	292 ± 44	259 ± 30	140° 55′	57°	135 ± 14
8, 10, 11, 26	262 ± 27	224 ± 19	29° 35′	33° 25′	136 ± 13

form an average angle of 40° with the resultant momentum, so that the average transversal momentum of a pion is 65 % of the average longitudinal momentum parallel to their resultant momentum. These results are consistent with the annihilation of a nucleon by an antineutron, because the energy liberated in this event does not have a big forward momentum. From the estimated total energy of 2.49 GeV and the momentum of 1.29 GeV/c, we can calculate the velocity in the c.m. system of the antineutron and nucleon as $\beta_c^2 = 1.29/2.49 = = 0.519 \pm 0.016$ and the rest mass of the two particles as $2.49(1-\beta_c^2) = = (1823 \pm 66)$ MeV. Therefore the mass of the antineutron or nucleon is (912 ± 33) MeV. It is only the errors of the pion momenta that contribute to the error of the mass.

From a total energy of (2.49 ± 0.10) GeV of the primary, we deduce the kinetic energy of the antineutron as (617 ± 100) MeV and its momentum (1.24 ± 0.12) GeV/c. The latter is in good agreement with the estimated momomentum of the primary, *i.e.* 1.29 GeV/c. This antineutron has a momentum higher than that of the antiproton beam, so it must be produced outside the stack. The antiproton beam is first deflected by a 60-inch magnet and then by three 8-inch magnetic quadrupoles and three other magnets. It passes through a beryllium absorbant of 20 g/cm² and another absorbant of ¼-inch lead. The beam is deflected 103°. The maximum momentum of antiprotons is 855 MeV/c at production and it is slowed down to 740 MeV/c on arriving at the edge of the stack. The antiprotons enter the stack with a projection angle indicated by the arrow in Fig. 1 and with a dip nearly zero. The star is found in the 15-th emulsion sheet counted from the most exterior one. It is located at 17 cm from the edge where the antiprotons enter into the stack. The plane of the emulsions is faced toward the target. It is therefore very probable for antineutrons which are produced either by primary protons at the target or by high energy antiprotons to have a chance to penetrate into the stack. The density of this kind of stars is of the order of one tenth of that of the antiproton stars in the stack.

4. – Conclusion.

The star reported in our previous article (1) ejects four electrons, whilst twelve are ejected by this star. Another star under study also emits electrons. The prevalent emission of electrons forms a special characteristic of these stars. The electrons must be produced by a new process which has never been observed. Indeed, up to now, only one event (8) involving four electrons from a π^0 decay

(8) A. L. HODSON, J. BALLAM, W. H. ARNOLD, D. R. HARRIS, R. R. RAU, G. T. REYNOLDS and S. B. TREIMAN: *Phys. Rev.*, 96, 1089 (1954).

has been observed in a cosmic-ray event. The electrons in our first star were considered as two pairs, each of them being produced respectively by the decay of a π^0. The twelve electrons of the present star are demonstrated as resulting from the direct electronic decay of three π^0's. However, from statistics made on a large number of π^0 decays (6,7), it was found that a π^0 decays essentially into two photons, only one in eighty decays into an electron pair and a photon; and one in 30 000 decays into four electrons. Therefore, if the electrons in our stars were produced by the same ordinary π^0's, then the probability to observe four electrons is $1.4 \cdot 10^{-4}$ and the probability to observe twelve is $4 \cdot 10^{-14}$. Such small probabilities would exclude any possibility to interpret our events in terms of any existing phenomena.

In addition to the five stars (1) mentioned before, a number of others are found, by scanning in volume, in the same stack. Each star contains at least two shower particles. All of them are produced by a neutral primary and each star shows the emission of low energy pions. The proportion of K-mesons is higher than that observed in neutron-nucleus interactions. Furthermore, the total visible energy of these stars is of the order of one GeV. Therefore the stars observed are considered as antineutron annihilation stars, especially the present star, for the mass of the antineutron estimated agrees very well with that of a nucleon. However, there are only a few electron pairs among three hundred antiproton annihilation events found in our stack. These results are confirmed by more than six thousand antiproton annihilations studied by other groups. The observation of a larger proportion of electrons should indicate a special characteristic of antineutrons.

Theoretical studies (9) favors the existence of a second π^0 with isotopic spin zero. Experiments (10,11) are made with an attempt to search for this second π^0. The results so far obtained are not yet decisive. The π^0's observed in our stars may suggest a second π^0 which has a shorter lifetime than the ordinary ones and a higher probability of decaying into electrons. The angle formed by the electron pair may be less prominant in small values. There were also theoretical arguments (12) and experimental search (13) for a ρ^0-meson which has also a zero isotopic spin and decays instantly into pions. If the three π^0's were produced by the decay of a ρ^0-meson, the mass of this one would be (552 ± 83) MeV.

---

(9) A. M. BALDIN and P. K. KABIR: *Nuovo Cimento*, **9**, 547 (1958).

(10) M. GETTNER, L. HOLLOWAY, D. KRAUSS, K. LANDE, E. LEBOY, W. SELOVE and R. SIEGEL: *Phys. Rev. Lett.*, **2**, 471 (1959).

(11) N. BOOTH, O. CHAMBERLAIN and E. ROGERS: *Bull. Am. Phys. Soc.*, **4**, 446 (1959).

(12) S. N. GUPTA: *Phys. Rev.*, **111**, 1436, 1698 (1958).

(13) C. BERNARDINI, R. QUERZOLI, G. SALVINI, A. SILVERMAN and G. STOPPINI: *Nuovo Cimento*, **14**, 268 (1959).

* * *

We wish to express our sincere thanks to Professor M. MORAND, director of this laboratory for the facilities of his laboratory and his constant interest in our work. One of us (TSAI) wants to thank the French Centre National de la Recherche Scientifique for the research fellowship.

RIASSUNTO (*)

La continua ricerca di eventi di annichilazione in una pila di lastre esposte ad antiprotoni ci ha portato alla scoperta di una stella di $10+15\pi$. Delle quindici particelle dello sciame di questa stella, dodici le identifichiamo con elettroni e tre con pioni. Un pione negativo fra i tre si arresta. Tutti i protoni si arrestano nell'emulsione ed ogni protone ha un'energia cinetica inferiore a 15 MeV. Dividendo i dodici elettroni in tre gruppi e supponendo che ogni gruppo provenga dal decadimento $\pi^0 \to e^+ + e^- + e^+ + e^-$, possiamo valutare le masse dei tre π rispettivamente in (136 ± 14), (135 ± 14) e (136 ± 13) MeV. La probabilità per il decadimento di tre π^0 ordinari è $4 \cdot 10^{-14}$. Questo evento suggerisce la possibilità di un nuovo processo per la produzione di elettroni, cioè l'esistenza di un secondo π^0. In considerazione dell'alta molteplicità, dell'ampia distribuzione angolare, della giusta energia media dei pioni e dell'energia totale della stella, concludiamo che questo evento è il risultato dell'annichilazione di un protone ed un nucleone. Si propone la tecnica delle piccole celle per la misura dello scattering multiplo delle tracce con ionizzazione minima.

(*) *Traduzione a cura della Redazione.*

2426

Internal Pairs from π^--Proton Interactions at Rest (*) (**).

H. Kobrak (*.*)

The Enrico Fermi Institute for Nuclear Studies
The Physics Department, The University of Chicago - Chicago, Ill.

(ricevuto l'11 Febbraio 1961)

Summary. — 7741 examples of internal pair production in pion-proton interactions at rest were recorded in hydrogen bubble chamber photographs. These pairs originate in the reaction $\pi^-+p\to n+e^++e^-$ and in the decay $\pi^0\to\gamma+e^++e^-$. These events were analysed to find the experimental distribution in the mass of the pair and another variable related to the energy partition between the members of the pair. These distributions were compared with a theory which includes corrections due to nucleon form factors and radiative corrections. The experimental results are in good agreement with this theory. Longitudinal virtual photon contributions are necessary to properly describe the experimental results for radiative capture pairs and as predicted theoretically are not visible for π^0 pairs. In accord with present theory, the form factor effects are found to be small for both reactions.

1. – Introduction.

If a negative pion is brought to «rest» ($\beta<10^{-2}$) in hydrogen, it will, with high probability, be captured and form a π-mesic hydrogen atom. Such

---

(*) Research supported by a joint program of the Office of Naval Research and the U.S. Atomic Energy Commission.

(**) A thesis submitted to the Department of Physics, the University of Chicago, in partial fulfillement of the requirements for the Ph. D. degree.

(*.*) Now at Sloan Laboratory of Physics, California Institute of Technology, Pasadena, California.

an atom will rapidly interact in one of the following channels:

$$\pi^- + p \rightarrow n + \gamma\,, \tag{1}$$

$$\pi^- + p \rightarrow n + \pi^0\,, \tag{2}$$

$$\pi^- + p \rightarrow n + e^+ + e^-\,. \tag{3}$$

The neutral pion formed in the charge-exchange reaction (2) will decay with a lifetime $\tau \approx 3 \cdot 10^{-16}$ s via the channels:

$$\pi^0 \rightarrow \gamma + \gamma\,, \tag{4}$$

$$\pi^0 \rightarrow \gamma + e^+ + e^-\,, \tag{5}$$

$$\pi^0 \rightarrow e^+ + e^- + e^+ + e^-\,, \tag{6}$$

The process (3) is customarily referred to as internal conversion of the photon from reaction (1), and similarly reactions (5) and (6) are considered as internal conversion of the photons from reaction (4). Quantum electrodynamics predicts the relative probabilities for the occurrence of reactions (3) and (1) and for reactions (5) or (6) and (4). A complete verification of these predictions is only possible if the relative frequency of reactions (2) and (1) (Panofsky ratio) is known. Even without the knowledge of this ratio, which makes the determination of absolute conversion coefficients impossible, the theory can be tested in its other details. This paper describes an experimental study of the characteristics of 7741 pairs produced in reactions (3) and (5) as observed in a hydrogen bubble chamber. Such a pair can be seen in Fig. 1. A detailed discussion of the measurement of the Panofsky ratio via internal conversion reactions will be presented elsewhere (1).

2. – Theory.

Electron-positron pairs from internal conversion in the π^0-decay were first predicted by DALITZ (2). With the simplest phenomenological treatment of the interaction responsible for this decay, he derived the conversion coefficient between reactions (4) and (5) and some of the detailed structure of the pairs. KROLL and WADA (3) made a general analysis, to first order in α, of internal pair production and applied it to the problem outlined in the Introduction.

---

(1) H. KOBRAK and S. C. WRIGHT (to be published).
(2) R. H. DALITZ: *Proc. Phys. Soc. (London)*, A **64**, 667 (1951).
(3) N. KROLL and W. WADA: *Phys. Rev.*, **98**, 1355 (1955).

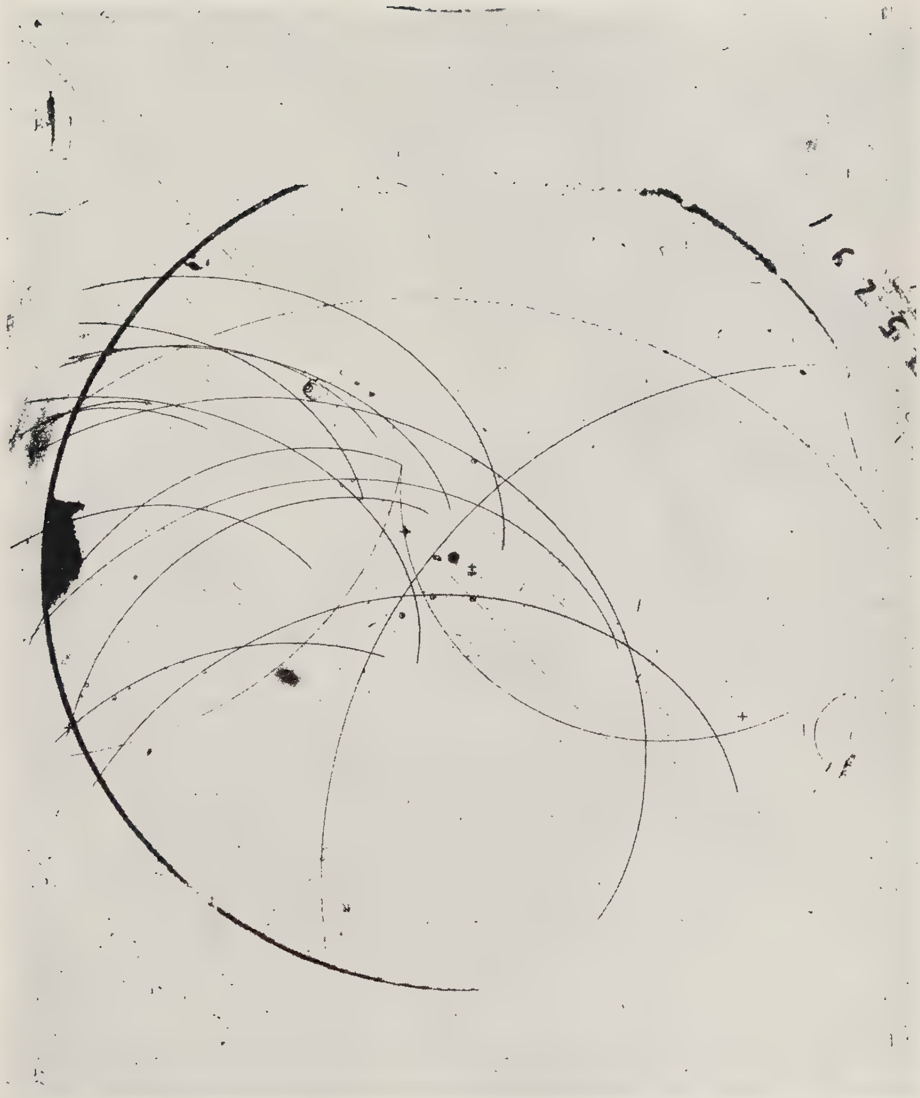

Fig. 1. – Photograph showing twelve π^- stops reacting via channel 1 or 2 and one reacting via channel 3 or 5.

Effects due to the electromagnetic structure of the nucleon and to terms of second order in α were not included in their treatment. These effects were computed by ROCKMORE and TAYLOR [4] and JOSEPH [5].

The results of these papers can be summarized as follows. A pair is conveniently described by two variables. One is its relativistically invariant « mass » x ($x^2 = E_T^2 - P_T^2$) (*). If x^2 is scaled in terms of its maximum possible value, it will hereafter be referred to as ξ ($\xi \leqslant 1$). The other is the angle θ between the electron-positron momentum vector in the center of mass of the pair and the momentum vector of the pair in the rest frame of the original system. This variable appears in the combination

$$y^2 = \cos^2\theta \left[1 - \frac{4m^2}{x^2}\right], \qquad (m = \text{electron mass}).$$

y has a simple physical interpretation. It is the component of the electron velocity in the pair center-of-mass system along the total momentum vector of the pair in the rest frame of the decaying system. Other variables describe polarization effects and do not lend themselves to experimental study with bubble chamber techniques. In terms of the diagrams in Fig. 2, x is also the « mass » of the intermediate virtual photon.

The theory gives us the ratio between the probability density in x and y for the reaction going via the pair channel (3) or (5) and the probability of the reaction going via the corresponding photon channel (1) or (4). Each of these expressions involves the ratio of the matrix elements of the hamiltonian of the electromagnetic interaction between initial and final states. They will be functions of the nucleon parts of the corresponding current operator matrix elements. It is the lack of knowledge of these current operators which complicates the theoretical treatment. In the expressions for the transition probability densities, these current operators appear in the form

$$R(P_T) = \frac{|\boldsymbol{J}(\boldsymbol{P}_T)|^2}{|\boldsymbol{J}(\boldsymbol{P}_\nu)|^2}, \tag{7}$$

where $\boldsymbol{P}_T$ is the vector momentum of the pair, $\boldsymbol{P}_\nu$ is the vector momentum of the corresponding real photon and $\boldsymbol{J}$ the current operator matrix element in question.

(*) We use units where $c=1$ and a notation where the subscripts mean: $+$, $-$, T, quantities associated with the positron, electron and pair as a whole, respectively.

(4) R. ROCKMORE and J. G. TAYLOR: *Phys. Rev.*, **112**, 992 (1958).

(5) D. JOSEPH: *Nuovo Cimento*, **16**, 997 (1960).

Real photons must be transversally polarized due to their vanishing mass $(J_3(\boldsymbol{P}_\nu)=0)$ (*). No such limitation exists for pairs, *i.e.* « virtual photons » may be longitudinal polarized.

As in other interactions between nucleons, pions and electrons, the electromagnetic structure of the nucleon may contribute appreciably to the operator $\boldsymbol{J}$. The diagrams shown (Fig. 2) only represent the interaction to lowest order in α. Contributions from higher order diagrams may be important.

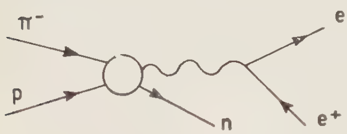

$\pi^- + p \to n + e^+ + e^-$

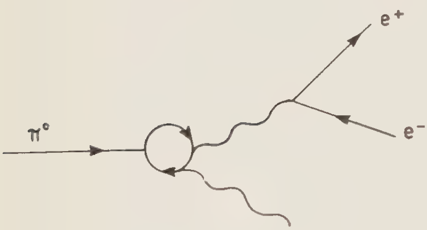

$\pi^\circ \to e^+ + e^- + \gamma$

Fig. 2. – First order diagrams for processes (3) and (5).

Applying these considerations to the present problem, the following conclusions were reached. For the process involving the radiative capture reactions (1) and (3), results from meson physics were used. The procedures outlined by KROLL and RUDERMAN [6] were employed to obtain the main part of $R(P_T)$. The effects due to electromagnetic structure were obtained from the treatment by FUBINI *et al.* [7] of the process

$$e^- + p \to e^- + n + \pi^+$$

which can be considered as photo-pion production by a virtual photon of imaginary mass ($x^2 < 0$) emitted by the incident electron. In the present case, the p-π^- system emits a neutron and a virtual photon of real mass ($x^2 > 0$) which then creates a pair. For further details, see references [4] and [5]. JOSEPH [5] shows that in the structure contribution, magnetic moment and size effects almost cancel each other, so that the net structure effect is not noticeable in the present experiment. He further applied the calculations of KÄLLÉN and SABRY [8] to compute corrections to the conversion probability density in x^2 to second order in α. The end result is that the normalized distri-

(*) Here we follow the notation: J_3 is the component of the current parallel to the momentum of the photon, J_1 and J_2 are the components of the current perpendicular to the momentum of the photon.

(6) N. KROLL and M. RUDERMAN: *Phys. Rev.*, **93**, 233 (1954).

(7) S. FUBINI, Y. NAMBU and V. WATAGHIN: *Phys. Rev.*, **111**, 329 (1958).

(8) G. KÄLLÉN and A. SABRY: *Dan. Mat. Fys. Med.*, **29**, No. 17 (1955).

2430

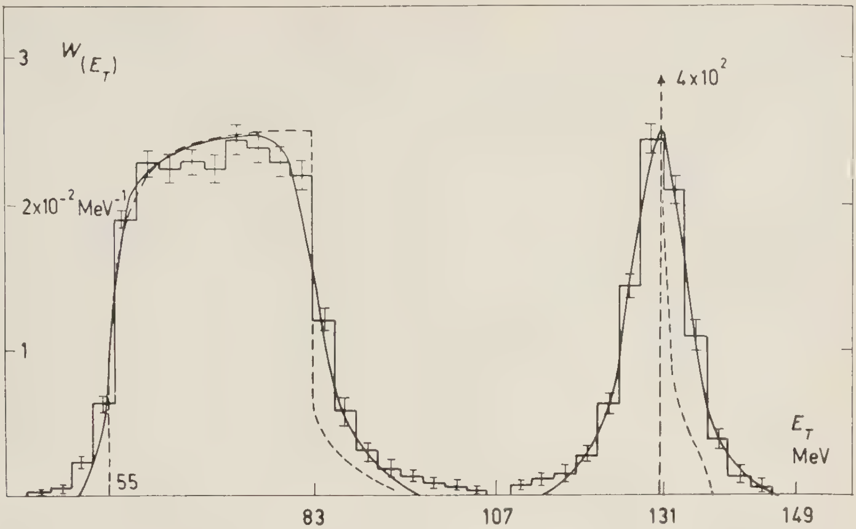

Fig. 3. – Energy distribution of all pairs. The broken curve is given by the theory. The full curve includes a 3% energy resolution. The histogram represents the data.

bution in x^2 can be written as the sum of five terms,

$$W(x^2) = .972\, W_{TO}(x^2) + .020\, W_{LO}(x^2) + .009\, W_R(x^2) + .008\, W_{TS}(x^2) - .009\, W_{TM}(x^2)\,.$$

Here all the $W(x^2)$ functions are individually normalized. W_{TO} is the first order contribution due to transverse photons without structure corrections. W_{TS} and W_{TM} are these corrections due to size and magnetic moment effects, respectively. W_{LO} is the contribution due to longitudinal photons and W_R that from radiative corrections. The functional forms of W_{TO} and W_R are similar and strongly peaked

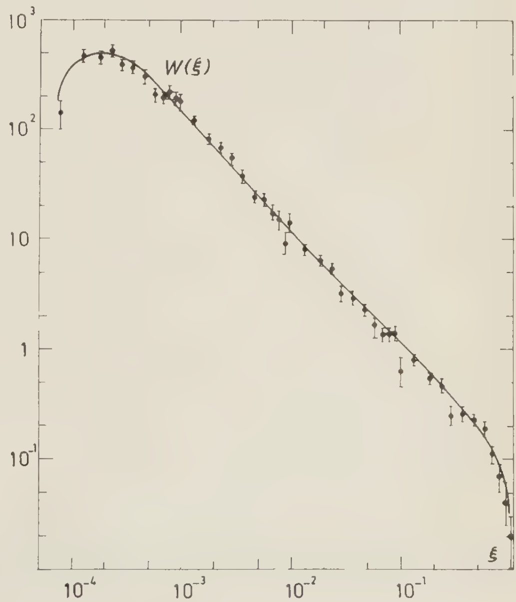

Fig. 4. – Mass distribution $W(\xi)$ for the pairs from the reaction $\pi^-+p\to n+e^++e^-$ including a 3% energy resolution and 0.7° angle resolution

$$\xi = \frac{E_T^2 - |P_T|^2}{(M_p + M_{\pi^-} - M_n)^2}\,.$$

2431

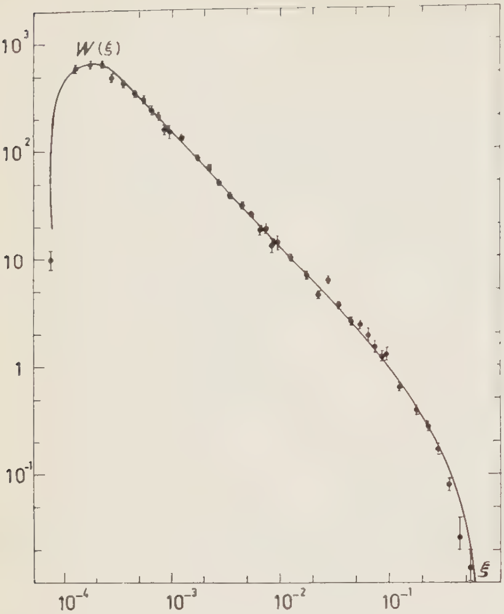

Fig. 5. – Mass distribution $W(\xi)$ for the reaction $\pi^0 \to e^+ + e^- + \gamma$ including a 3% energy resolution and a 0.7° angle resolution.

at low x^2. W_{TS} and W_{TM} approximate the form $x^2 W_{TO}$. W_{LO} follows W_{TM} at low x^2 but rises faster at high x^2. The precise form of these distributions can be seen in JOSEPH's (5) paper. If the contributions of W_{TM}, W_{TS} and W_{LO} are to be detected, experiment and theory should be compared at high values of x^2 where W_{TO} is no longer overwhelming. Fig. 4 shows $W(x^2)$ modified, as discussed later, to include the resolution of this experiment.

For the decay processes of the π^0 involving reactions (4) and (5), invariance arguments (3) show that the transverse contribution to $R(P_T)$ is given by $|\boldsymbol{P}_T|/|\boldsymbol{P}_\nu|$. Due to the presence of a real photon in reaction (5), there is no longitudinal contribution. The structure effects due to the strong interaction vertex of Fig. 2 are small, and radiative corrections are similar to those for the previous case (5). Fig. 5 shows the distribution in x^2 for π^0 pairs modified again to include the experimental resolution.

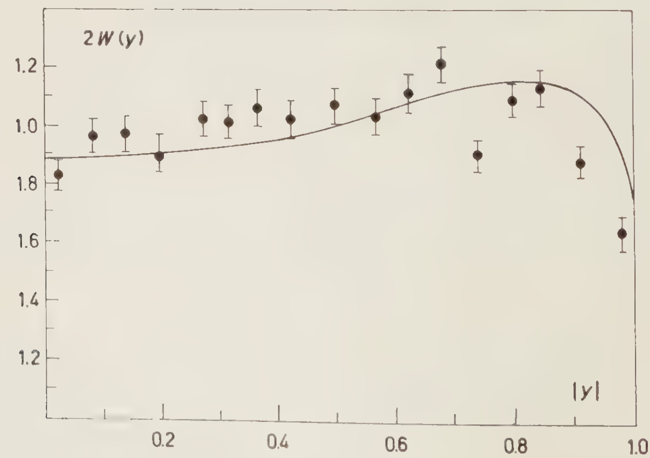

Fig. 6. – Distribution $W(y)$ in $y = (E_+ - E_-)/|P_T| = \cos\theta\sqrt{1-(2m/x)^2}$, for the reaction $\pi^0 \to \gamma + e^+ + e^-$.

Distributions in y for both types of pairs are obtained in references (2) and (4) and are shown in Fig. 6 and 7. JOSEPH (5) points out that it follows from invariance arguments that for pairs with $x^2 \gg (2m)^2$ the ratio between the transverse and longitudinal parts of the conversion probability density in y is as $(1+y^2)$ to $(1-y^2)$.

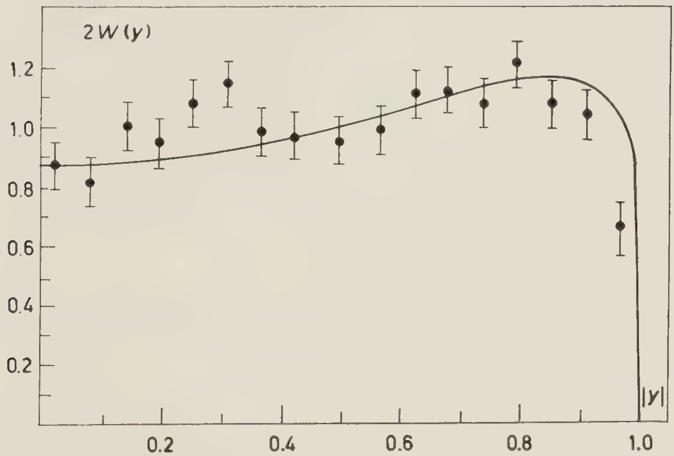

Fig. 7. – Distribution $W(y)$ in $y=(E_+-E_-)/|P_T| = \cos\theta\sqrt{1-(2m/x)^2}$, for the reaction $\pi^-+p \to n+e^++e^-$.

Further form factor effects on the matrix elements (7) can be expected from resonant pion-pion interactions at the strong interaction vertices of the diagrams in Fig. 2. If such effects are small, they change the function $R(P_T)$ by a factor $(1+a\xi)$, where ξ is x^2 divided by its maximum possible value.

3. – Equipment.

A beam of 68 MeV negative pions was brought to rest in the central part of a cylindrical liquid hydrogen bubble chamber 23 cm in diameter and 14.5 cm deep. This chamber was located in a magnetic field of $2.47\cdot10^4$ G oriented along the axis of the chamber and uniform to 0.5% over the useful part of the chamber. Efficient detection of interesting events requires a maximum ratio of tracks of pions stopping in the chamber to tracks of other particles. This ratio was kept to approximately $3\div4$ to 1 for an average of twelve « stops » per picture. Fig. 1 represents an example of such a picture. The chamber was illuminated approximately 1.2 ms after the passage of the pions through a monitoring counter. The photographs were taken through three lenses placed 120° apart with a common principal plane. After the chamber

reached a stationary state, this plane was adjusted to be parallel to the inside of the chamber front window, and the lens system was made coaxial and in phase with a pattern of fiducial marks on the inside surface of this window. These marks can be seen on Fig. 1. At regular intervals during the cyclotron run, the precise alignment of the lens system with respect to the system of fiducial marks was checked. The excitation function of the magnet was reproducible to better than 0.1 %, and the variations in the magnet current were kept to below 0.05 %. Approximately $1.8 \cdot 10^5$ photographs were taken, and the results from about 10^5 of them are reported here.

The developed film was then processed (*) using the following equipment:

1) Events were located by scanning each frame at least twice on Recordak (9) microfilm readers, modified to fulfill the requirements of the experiment.

2) The vector momenta of the electrons of the events found were measured by determining on each stereo view the co-ordinates of four points on each track and of two fiducial marks. This was done by means of a cross hair which is free to move on the screen onto which the view is projected and whose motion is linked to two digitized linear-to-angular displacement converters. The numerical information thus obtained, plus the necessary logical information, is simultaneously printed out and punched into paper tape in a standard six bit code with parity check.

The four points where co-ordinates are measured are the origin of the pair and three points which divide the available length of the track into three nearly equal sections. The data on the paper tape were then fed into the GEORGE digital computer at Argonne National Laboratory who was asked to fit them by a minimization procedure (made possible by the over-determination of the measurement) to the track expected from an electron with a given initial vector momentum in liquid hydrogen and in a magnetic field with the properties of the one used in this experiment. The computer, after ascertaining that certain rough matching criteria were fulfilled, yields the following information:

1) Scalar momentum and three direction cosines of each electron and of the pair. The total energy, x^2 and y^2 of the pair.

2) A goodness of fit parameter of the origin of the pair and a parameter for the goodness of fit of the measured points to the theoretical shape of the track.

(*) Processing of the film refers to the retrieval of the information contained in it, not the chemical development.

(9) Recordak Corp., Kingsport, Tenn., U.S.A.

3) Location of the origin in the chamber and arc length of each track.

4) Information about the agreement with certain conservation laws (see next section).

5) Information identifying the event.

All these data were put on tabulating cards and the subsequent data processing was done on standard tabulating equipment. Considerable care was taken to be certain that the transmission of information from the bubble chamber to the recorded results was free from distortions. Initially, the different components were submitted to individual checks by measuring points of known location and by presenting artificial « tracks » to the computer. Checks on the overall freedom from distortions and on the more sensitive components (encoders, programmer, tape punch, etc.) were made routinely.

4. – Data analysis.

In order to make a meaningful comparison between the information on the tabulating cards and the corresponding theoretical predictions, the following steps must be taken: identification of the electron pairs as to their originating reaction, correlation between detection efficiency and structure of the pair and analysis of the measurement resolution for x^2, y^2 and E_T.

Since both reactions (3) and (5) can be considered as two-body decays into a « virtual photon » and a recoil particle, the total energy of the pair (or « virtual photon ») in the center of mass of the decaying system will be a linear function of x^2, the square of the « mass » of the pair. If the decaying system is moving in the frame in which the observer is at rest, the energy spectrum for pairs of a given mass will be Doppler broadened. This is the case in the decay of the π^0 formed

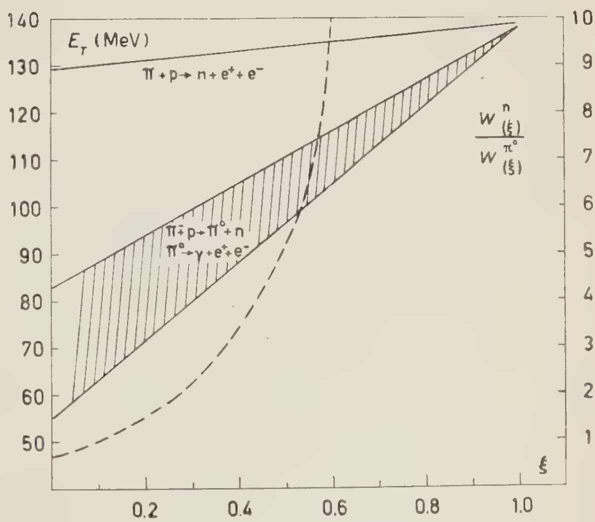

Fig. 8. – Regions in the E_T-ξ plane to which the two types of pairs should be confined (full lines) and ratio of the probability density $\overset{N*}{W}(\xi)$ for the radiative capture reaction to the probability density $\overset{\pi^0}{W}(\xi)$ for the decay of the π^0 (broken line).

in reaction (2) with a laboratory velocity of about $0.2c$. Since the π^0-decay is isotropic in its center of mass, this spectrum is uniform over the allowed range of E_T. This is illustrated in Fig. 8 where the allowed region for π^0 pairs is the shaded area and that for the pairs from the direct decay of the π-mesic atom is the upper line. For comparison purposes, the dashed line shows the ratio of the probability densities in x^2 for the occurrence of both types of pairs. In the region where the two distributions are close by, the radiative capture pairs greatly predominate. Therefore, the ability to separate the two types of pairs is limited only by the experimental resolution.

Of the 7 741 events analyzed, 27 are in a region where a clear cut separation as to originating reaction is not possible. The separation was done along the locus of equal probability for reactions (3) and (5) in the x^2-E_T plane.

Included in this sample are about 28 internal pairs from the decay of neutral pions produced by the reaction

$$\pi^- + \mathrm{p} \rightarrow \mathrm{n} + \pi^0 \tag{8}$$

in flight, and about 10 pairs externally produced by real photons from reactions (1) and (4) at a distance of less than 0.5 mm from the end of the pion track. There are no further events which interfere with the experiment.

Each photograph was scanned either two or three times. 12 % of the events found on film scanned twice were missed once and 1.1 % of the events found on film scanned three times were missed twice. This is interpreted as an overall detection efficiency of 98.5 %. Of the 925 events which were missed once, 235 had a value of $y > 0.94$. This was an expected inefficiency in the detection of pairs with a high value of y (where one electron has a very low energy). No correlation between detection deficiency and x^2 or E_T has been found other than that inherent in the correlation with y.

As stated in the previous section, the vector momentum of an electron is determined by fitting measurements of a projected track to the curve expected for the track of an electron under the conditions of the experiment. Included in this treatment are interactions of the electron with the medium whose occurrence has a large probability. The «single processes» whose effects on the results cannot be treated on a statistical basis are: large angle scattering of the electron from protons and orbital electrons of the medium and bremsstrahlung. Electron-electron collisions are recognized by the recoil electrons (δ-rays). Elastic and radiative electron-proton collision do not produce charged recoils of detectable range. In elastic collisions the main change occurs in the transverse momentum (angular deflection), while in the radiative ones, the energy is principally affected (change in curvature). As the length of track used for the measurement increases, the effects due to the interaction of the electrons with the medium increase and the effects due to finite instrumental

resolution decrease. The arc length of track used was chosen so as to optimize the overall resolution and was (except in the case of detectable interactions) one radian. The above effects on angular and energy measurements (except those involving an actual loss of energy) are symmetric to first order in the errors and will affect only the resolution without introducing systematic shifts in the results. Single interactions involving a large momentum transfer if undetected are very likely (though not certain) to appear as anomalously bad fits to theoretical electron tracks and be in disagreement with results from conservation laws. The resolution and systematic errors introduced by the equipment used to record and study the events will also affect the measurements. Checks on the absence of distortion in the optical and measuring equipment and on the calibration and monitoring of the magnetic field were described in the previous section. Measurements on electron tracks in a field free chamber indicate that mechanical turbulence and buoyancy (displacement of the bubbles during the time between the passage of the electron and the photographic recording) produce no noticeable effect on this experiment. Effects due to optical turbulence (large local gradients in the index of refraction) have been minimized by restricting measurements to the non-turbulent portions of the tracks. The measurements are further affected by the combined resolution of the recording and projecting equipment and the skill of the person handling the measuring equipment. Carefully repeated measurements of selected tracks and fiducial marks have shown that the dispersion of routine measurements is less than 50 % wider than the best attainable resolution which is about 10 % of the inherent resolution of the experiment. Analysis of the preceding considerations leads to a symmetrical resolution function of a single track with a σ of 4 % in the energy and 0.014 radians in the angle.

The measurements just discussed refer to single electron momenta while the quantities which enter most directly into the theory are x^2, y and E_T. The resolution function for these latter quantities can be obtained from that for the former. Those for E_T and y are symmetrical and their second moments are respectively

$$\sqrt{\left\langle\left(\frac{\delta E_T}{E_T}\right)^2\right\rangle} = \sqrt{\frac{1}{2}\left\langle\left(\frac{\delta E_\pm}{E_\pm}\right)^2\right\rangle} = 3\,\%\,,$$

and

$$\langle(\delta y)^2\rangle = (1-y^2)^2\left\langle\left(\frac{\delta E_T}{E_T}\right)^2\right\rangle .$$

The expression for $\langle(\delta y)^2\rangle$ follows from the relation

(9) $$y = \frac{E_+ - E_-}{|P_T|}\,,$$

which is valid in the rest frame of the decaying system. Since the π^0 is formed in reaction (2) with a velocity of $0.2c$, (9) is no longer correct. In the Appendix it is shown that by transforming the expression

$$\frac{E_+ - E_-}{P_T},$$

from the rest frame of the π^0 to the laboratory frame, the first moment of its distribution is displaced from the value of y in the π^0 rest frame by a fraction of the order of $P_0^3 x^2/M_0^5$ (P_0: momentum of the π^0 in the laboratory; M_0: mass of the π^0) which for all but 10 of the 5600 pairs of this type is less (usually much less) than $4 \cdot 10^{-3}$. It is further shown that the range of the distribution is correspondingly small. Thus the motion of the π^0 does not affect the analysis of the distribution in y.

Since

$$x^2 = 4E_+E_- \sin^2 \Theta/2 + (2m)^2$$

in the approximation that $P_\pm \gg m$ and where Θ is the angle between positron and electron in the laboratory frame, the resolution function in this variable is symmetric only at angles where $\delta\Theta \ll \Theta$. In this case

$$\left\langle \left(\frac{\delta\xi}{\xi}\right)^2 \right\rangle \approx 4 \left\langle \left(\frac{\delta E_T}{E_T}\right)^2 \right\rangle + a \left(\frac{\delta\theta}{\xi}\right)^2.$$

At smaller angles

$$(\delta\xi)^2 \approx a \left[\frac{3}{8} (\delta\theta)^4 + \xi(\delta\theta)^2\right].$$

In this case the first moment is not longer zero. It is

$$\langle\delta\xi\rangle = \frac{a}{2} (\delta\theta)^2 ,$$

ξ is x^2 in units of the square of the total available energy ($\xi < 1$) and

$$a = 1 \quad \text{for reaction (3)},$$

$$a = \tfrac{1}{4} \quad \text{for reaction (5)}.$$

Fig. 4 through 7 show the distribution in x^2 and y for both types of pairs after these resolution functions have been folded into the theoretical expressions. Fig. 3 is a similar distribution for the total energy of the pairs.

2438

For the charge exchange reaction (3) 50% of the pairs should be within a 0.08 MeV and 90% within a 0.8 MeV span (dashed curve on the high energy part of Fig. 3). The fit of the data to this curve after folding in the energy resolution confirms the error estimates made in this section.

Similarly, the low mass and of the distributions on Fig. 4 and 5 depends strongly on the resolution function derived from the estimated angular accuracy. These estimates are confirmed by the good fit of the data to the expected distribution.

5. – Comparison between experiment and theory.

5·1. *Mass distribution.* – In the analysis all the data were fitted to the distribution expected from Joseph's [5] theory after folding in the experimental resolution function. These result are presented in Table I. It is seen that the fit is good for both types of pairs. It is also seen, in the radiative capture reaction, that if the longitudinal contribution is omitted the fit is quite unacceptable. This is one confirmation that such a term is necessary. In the $W(x^2)$ distribution W_{TO}, W_{LO}, and W_R are more firmly founded theoretically than the terms W_{TM} and W_{TS} which involve nucleon form factors. Since the main x^2-dependence of all form factor contributions to $W(x^2)$ is of the type:

$$ax^2 W_{TO} ,$$

this experiment will put limits on allowable values of « a ». As W_{TO} is very highly peaked at small x^2, the limits on « a » will be determined by an analysis of the high x^2 end of the mass distribution. The results of such an analysis for the range $0.1 \leqslant \xi \leqslant 1$ are given in Table II. The values of the form factor

TABLE I. – *Mass distribution. First order effects.*

Distribution	Reaction	χ^2	$\langle\chi^2\rangle$	$\sqrt{\langle(\chi^2-\langle\chi^2\rangle)^2\rangle}$
$W(\xi)$ for $\xi_0 \leqslant \xi \leqslant 1$	$\pi^- + p \to n + e^+ + e^-$	54	46	9
$W(\xi) - W_{LO}'(\xi)$ for $0.1 \leqslant \xi \leqslant 1$	$\pi^- + p \to n + e^+ + e^-$	33	10	4
$W(\xi)$ for $\xi_0 \leqslant \xi \leqslant 1$	$\pi^0 \to \gamma + e^+ + e^-$	48	43	9

TABLE II. - *Mass distribution. Form factor effects.*

Distribution	Reaction	a
$\dfrac{W(\xi)(1+a\xi)}{N}$ for $0.1 \leqslant \xi \leqslant 1$	$\pi^- + p \to n + e^+ + e^-$	-0.1 ± 0.2
	$\pi^0 \to \gamma + e^+ + e^-$	-0.3 ± 0.2

2439

parameters « a » were determined by least squares. The corresponding limits on these estimates refer to « a » values which increase χ^2 by a factor two from its minimum value. It is seen that this experiment shows the form factor effects to be small.

5'2. « y » *distribution*. – The y distribution presents two interesting features. First, the predominant part due to transverse photons and second the small longitudinal part. In Section 2 it was mentioned that these two contributions are comparable for high x^2. Accordingly, two fits made were.

1) The data were fitted to the distributions shown in Fig. 6 and 7. It was pointed out in Section 3 that an expected low scanning efficiency was found for high values of y. The low values of the experimental points in this region of the distributions for both types of pairs is attributed to this inefficiency. To avoid uncertain efficiency corrections, the span $0.9 < y \leqslant 1$ was excluded from the analysis. The results of the fit are presented in Table III, where it is seen that this experiment is in good agreement with Joseph's ([5]) theory.

TABLE III. – *y Distribution. First order effects.*

Distribution	Reaction	χ^2	$\langle\chi^2\rangle$	$\sqrt{\langle(\chi^2-\langle\chi^2\rangle)^2\rangle}$
$W(y)$ for $0 \leqslant \lvert y\rvert \leqslant 0.9$, $\xi_0 \leqslant \xi \leqslant 1$	$\pi^- + p \to n + e^+ + e^-$	11	15	5.5
$W(y)$ for $0 \leqslant \lvert y\rvert \leqslant 0.9$, $\xi_0 \leqslant \xi \leqslant 1$	$\pi_0 \to \gamma + e^+ + e^-$	20	15	5.5

2) To bring out the effect of virtual longitudinal photons, the events with $0.1 \leqslant \xi \leqslant 1$ and $0 \leqslant |y| \leqslant 0.84$ were compared to the distribution

$$W(y) = A(1 + y^2) + B(1 - y^2) .$$

For given B, A is fixed by normalization. B was determined by least squares for both types of pairs and the corresponding limits refer to B values which increase χ^2 a factor two above its minimum value. The results, together with their theoretical expectations, are presented in Table IV. For the charge exchange reaction, the value of $B = .23 \pm .07$ corresponds to a $(2.6 \pm .8)\%$

TABLE IV. – *y distribution. High mass part.*

Distribution	Reaction	B_{exp}	B_{theor}
$A(1 + y^2) + B(1 - y^2)$	$\pi^- + p \to n + e^+ + e^-$	$.23 \pm .07$	.19
$A(1 + y^2) + B(1 - y^2)$	$\pi^0 \to \gamma + e^+ + e^-$	$.003 \pm .03$	0

2440

longitudinal contribution in $W(\xi)$ as compared to an expected 2.0 %. For the π^0-decay reaction, the longitudinal contribution is $(0 \pm 0.3)\%$ as compared to an expected 0 %. Therefore, the distributions in y agree with the theoretical predictions and disclose the presence of longitudinal photons in the charge exchange reaction.

5'3. *Energy distribution.* – The energy distribution of all the pairs is shown in Fig. 3. Attention is called to the shape and position of the energy spectrum for

$$\pi^- + p \to n + e^+ + e^- .$$

The position of the centroid of this spectrum depends only very weakly on the theory and in terms of accepted particle masses should lie at 129.55 MeV. The mean value of the experimental distribution is 129.8 MeV showing the absence of systematic errors in the momentum measurements. Moreover, the fit of the data to the whole spectrum supports the treatment of the energy resolution presented in Section **3**.

Besides two early experiments ([10,11]) with a limited number of events, two other experiments ([12,13]) investigating the same processes by the same general method have been performed lately. While their number of events is smaller and the resolution much wider than in this experiment, the results are not in disagreement with those presented here.

7. – Conclusions.

This experiment is in good agreement with the theoretical treatment of internal pair production. The extent of this agreement is embodied in Tables I, II, III and IV. These data show that the overall fit is good. Longitudinal virtual photon contributions are necessary to properly describe the experimental results in the x^2 and y distributions of the radiative capture pairs. As predicted, there is no visible longitudinal effect for π^0 pairs. Form factor effects are shown to be small. For the radiative capture pairs, they are in accord with the present theory. For the π^0-decay where no form factor effects

---

([10]) B. M. ANAND: *Proc. Phys. Soc.* (*London*), A **220**, 183 (1953).

([11]) C. P. SARGENT, R. CORNELIUS, M. RINEHART, L. M. LEDERMAN and K. ROGERS: *Phys. Rev.*, **98**, 1349 (1955).

([12]) M. DERRICK, J. G. FETKOVITCH, T. H. FIELDS and J. DEAHL: *Phys. Rev.* **120**, 1022 (1960).

([13]) N. P. SAMIOS: *Phys. Rev.*, **121**, 275 (1961).

are expected if two pion resonant interactions are ignored, the experiment indicates a small negative values of « a ». However, the range of the estimate does not rule out a zero value.

* * *

The author wishes to express his appreciation to S. C. WRIGHT, who suggested this problem, for his constant encouragement and his continued help in the preparation and execution of the experiment and in the evaluation and interpretation of the data. The experiment was performed with a hydrogen bubble chamber designed by R. H. HILDEBRAND, whose work in operating the chamber along with M. PYKA during the cyclotron runs was essential to the success of the experiment. R. BIZZARI made substantial contributions during early stages of the chamber construction.

J. BERRYHILL, E. PRUSA, B. BRENNAN, V. ZAVITKOVSKY and S. CHENG performed the tedious task of finding and measuring the events. The results of these measurements were converted into meaningful data by procedures developed by M. SCHIFF of this Institute and S. D. WARSHAW and B. GARBOW of the Argonne National Laboratory. L. SEEFELDT built and serviced the scanning and measuring equipment. Much of the insight into the theoretical aspects of the problem was gained from discussions with R. H. DALITZ, Y. NAMBU and D. JOSEPH. P. K. KLOEPPEL and R. HANDLER contributed many months of work to set up and operate the experimental equipment. To all these and the many others who made this experiment possible go my sincere thanks.

APPENDIX

Transformation of the expression $(E_+ - E_-)/|\boldsymbol{P}_T|$ from the π^0 rest frame to the laboratory frame.

Notation. $+$, $-$, T, 0 subscripts refer to quantities associated with the positron, electron, pair as a whole and π^0 respectively. Symbols with a bar above them refer to the π^0 rest frame; those without bars refer to the laboratory frame.

$\bar{\boldsymbol{k}}$ momentum of the π^0 decay photon ($\pi^0 \to e^+ + e^- + \gamma$) in the π^0 rest frame.

$\mu_\pm = \cos(\boldsymbol{P}_0, \bar{\boldsymbol{P}}_\pm)$;

$\nu_\pm = \cos(\bar{\boldsymbol{P}}_\pm, \bar{\boldsymbol{P}}_T)$;

$\alpha = \cos(\bar{\boldsymbol{P}}_T, \boldsymbol{P}_0)$;

2442

φ angle between the $\boldsymbol{P}_0$, $\overline{\boldsymbol{P}}_T$ plane and the $\overline{\boldsymbol{P}}_+$, $\overline{\boldsymbol{P}}_-$ plane;

Γ, H energy and momentum of the π^0 in the laboratory frame in units of the π^0 rest mass;

M π^0 rest mass;

ξ $\dfrac{E_T^2 - |\boldsymbol{P}_T|^2}{M^2}$.

Auxiliary formulas. $\mu_\pm$ is related to $\nu_\pm$, α and φ by

$$\mu_\pm = \nu_\pm \alpha \pm \sqrt{1-\nu_\pm^2}\sqrt{1-\alpha^2}\cos\varphi\,.$$

From energy and momentum conservation

$$|\bar{k}| = |\overline{P}_T| = \frac{M}{2}(1-\xi)\,,$$

$$\bar{E}_T = \frac{M}{2}(1+\xi)\,,$$

$$\overline{P}_\pm \nu_\pm = \tfrac{1}{2}(\bar{k} \pm \bar{E}_T \bar{y})\,.$$

Transformation of $(\bar{E}_+ - \bar{E}_-)/|\overline{P}_T| = \bar{y}$ *into* $(E_+ - E_-)/|P_T| = y$. The Lorentz transformation from the π^0 rest frame to the laboratory frame yields

$$|P_T|^2 = (\Gamma\bar{k}\alpha + H\bar{E}_T)^2 + \bar{k}^2(1-\alpha^2) = \bar{k}^2\left[H^2\left(\alpha^2 + \left\{\frac{1+\xi}{1-\xi}\right\}^2\right) + 2\Gamma H\frac{1+\xi}{1-\xi}\alpha + 1\right],$$

$$E_+ - E_- = \Gamma(\bar{E}_+ - \bar{E}_-) + H(|\overline{P}_+|\mu_+ - |\overline{P}_-|\mu_-) =$$
$$= \Gamma\bar{k}\bar{y} + H\alpha\bar{E}_T\bar{y} + H\sqrt{1-\alpha^2}\cos\varphi(|P_+|\sqrt{1-\nu_+^2} + |P_-|\sqrt{1-\nu_-^2}\,.$$

From which it follows that

$$y = \frac{\bar{y}\left(\Gamma + H\alpha\dfrac{1+\xi}{1-\xi}\right) + 2H\sqrt{1-\alpha^2}\cos\varphi\,\dfrac{|P_+|\sqrt{1-\nu_+^2} + |P_-|\sqrt{1-\nu_-^2}}{M(1-\xi)}}{\sqrt{H^2\alpha^2 + 2\Gamma H\dfrac{1+\xi}{1-\xi}\alpha + 1 + H^2\left(\dfrac{1+\xi}{1-\xi}\right)^2}}\,.$$

First moment of the y distribution for a given $\bar{y}$. Integrating the above expression over α and φ and dividing by the appropriate normalizing factors

$$\langle y\rangle = \bar{y}\left\{\left(\frac{1+\xi}{1-\xi}\right)^2\left(1 - \frac{\Gamma}{H}\ln(\Gamma+H)\right) + \frac{\Gamma}{H}\ln(\Gamma+H)\right\}.$$

In the present case $H = 0.2$.

Expanding in H/Γ and keeping terms up to third order

$$\langle y \rangle \approx \bar{y}\left[1 - \frac{2\xi H^3}{(1-\xi)^2}\right],$$

for values of $\xi \leqslant 0.5$.

This shows that $\langle y \rangle$ is displaced from $\bar{y}$ by a fraction

$$\frac{2\xi H^3}{(1-\xi)^2} \approx \frac{2P_0^3 x^2}{M^5},$$

a very small number for practically all pairs.

RIASSUNTO (*)

7 741 esempi di produzione interna di coppie nelle interazioni pione-protone a riposo, furono registrate su fotografie di una camera a bolle ad idrogeno. Queste coppie si generano nella reazione $\pi^- + p \to n + e^+ + e^-$ e nel decadimento $\pi^0 \to \gamma + e^+ + e^-$. Tali eventi vennero analizzati per cercare la distribuzione sperimentale nella massa della coppia ed un'altra variabile collegata alla ripartizione dell'energia fra i membri della coppia. Queste distribuzioni furono confrontate con una teoria che comprende correzioni dovute a fattori di forma del nucleone e correzioni radiative. I risultati sperimentali sono in buon accordo con la teoria. I contributi longitudinali del fotone virtuale sono necessari per ben descrivere i risultati sperimentali per le coppia da cattura radiativa e, come predetto teoricamente, non sono visibili per le coppie di π^0. In concordanza con questa teoria, si trova che gli effetti dei fattori di forma sono piccoli per entrambe le reazioni.

(*) *Traduzione a cura della Redazione.*

IL NUOVO CIMENTO Vol. XX, N. 6 16 Giugno 1961

An Investigation of Possible Bound Σ-Hyperon-Nucleon Systems and Their Decay.

A. K. Common

Department of Physics University College - London

(ricevuto il 17 Febbraio 1961)

Summary. — The binding of Σ-hyperons to nucleons is investigated using potentials suggested by field theory. Special attention is paid to the possibility that the Σ^--hyperon can bind to a neutron while the Σ^+-hyperon and proton are unbound. Tables are given showing the effect of changes in the coupling constants. The lifetime of this hypothetical bound (Σ^-, n) system is calculated, and it is shown that, for certain forms of the weak Hamiltonian responsible for the decay, the interaction in the final state between the two nucleons can be neglected. It is also found that the effect of the Pauli principle in the final state is appreciable even if the (Σ^-, n) system is assumed to have a binding energy less than 1 MeV.

1. – Introduction.

The possibility that a Σ-hyperon may be bound with a nucleon has been suggested by several authors [1,2]. The only two systems that can exist as uniquely defined states are (Σ^+, p) and (Σ^-, n), for any other is connected by strong interactions to a corresponding (Λ, nucleon) system. Some evidence was suggested for the existence of a bound (Σ^-, n) system [3], but this has been withdrawn. Baldo-Ceolin *et al.* [4] have reported an event as possible evi-

---

(1) F. Ferrari and L. Fonda: *Nuovo Cimento*, **6**, 1027 (1957).

(2) G. Snow: *Phys. Rev.*, **110**, 1192 (1958).

(3) E. Gandolfi, J. Heughebaert and E. Quercigh: *Nuovo Cimento*, **13**, 864 (1959).

(4) M. Baldo-Ceolin, W. F. Fry, W. D. B. Greening, H. Huzita and S. Limentani: *Nuovo Cimento*, **6**, 144 (1957).

dence for a bound (Σ^+, p) system, but there are alternative interpretations which the authors discuss. A systematic search for a bound (Σ^+, p) system has been made by R. C. KUMAR and F. R. STANNARD (5), but this was unsuccessful. At the present time no event indicating a bound (Σ-hyperon-nucleon) system has been observed.

The bound (Σ^+, p) system, if it existed, would decay into two charged particles and a neutral one, whilst the bound (Σ^-, n) system would decay into one charged and two neutral particles. Therefore it would be more difficult to attribute an event to the decay of a (Σ^-, n) system than to attribute a corresponding event to the decay of a (Σ^+, p) system. It may be the case that the bound (Σ^-, n) system does exist, but because of this comparative difficulty has not been observed, whilst the bound (Σ^+, p) system, which would be observed more easily, does not exist. The purpose of this paper is to investigate this situation and see what deductions can be made from the assumption of field theoretical potentials for the Σ-hyperon nucleon forces. Assuming a possible bound (Σ^-, n) system, the rate of its decay through the reaction

$$(\Sigma^-, n) \to n + n + \pi^-$$

is also calculated.

FERRARI and FONDA (1) have considered the binding of hyperons to nucleons using field theoretical potentials, but further attention is paid here to the situation suggested above. The assumption that the (Σ^+, p) is not bound will put an upper limit on the binding energy of the (Σ^-, n) system, as has been suggested previously (2).

. – The two-body bound state problem.

2·1. *The form of the potential.* – We make the assumptions that the parity of the Σ-hyperon is positive and that of the K-meson negative. This follows the evidence of GELL-MANN (6), although this assignment is not yet completely definite. As in (1), the interaction Lagrangian for the pion-hyperon-nucleon field is given by

$$\mathscr{L}_\pi = ig_{n\pi}\bar{n}\gamma_5(\boldsymbol{\tau}\cdot\boldsymbol{\pi})n + g_{\Lambda\pi}(i\bar{\Lambda}\gamma_5\cdot\boldsymbol{\pi}\cdot\boldsymbol{\Sigma} + \text{h.c.}) + g_{\Sigma\pi}(\bar{\boldsymbol{\Sigma}}\gamma_5\times\boldsymbol{\Sigma})\cdot\boldsymbol{\pi}\,,$$

where $g_{n\pi}$, $g_{\Lambda\pi}$, and $g_{\Sigma\pi}$ are respectively the pion-nucleon, the pion-Λ-hyperon and the pion-Σ-hyperon coupling constants. The Lagrangian for Σ-hyperon–K-meson coupling is given by

$$\mathscr{L}_{\Sigma K} = ig_{\Sigma K}\bar{n}\gamma_5\boldsymbol{\tau}\cdot\boldsymbol{\Sigma}K\,,$$

(5) R. C. KUMAR and F. R. STANNARD: *Nuovo Cimento*, **14**, 250 (1959).
(6) M. GELL-MANN: *Phys. Rev.*, **106**, 1296 (1957).

2446

where $g_{\Sigma K}$ is the K-meson–Σ-hyperon coupling constant. Only the parts of the potential due to one and two-π-meson exchange and one-K-meson exchange will be taken into account. Working from now on in units where $\hbar = c = 1$, the potential for one and two-π-meson exchange is given by

$$(1)\qquad V_\pi = \frac{-g_{n\pi}}{2M_n}\frac{g_{\Sigma\pi}}{2M_\Sigma}\frac{1}{(2\pi)^3}\int d^3\boldsymbol{k}(\boldsymbol{\sigma}_1\cdot\boldsymbol{k})(\boldsymbol{\sigma}_2\cdot\boldsymbol{k})\exp[i\boldsymbol{k}\cdot\boldsymbol{r}]/\omega^2 -$$

$$-\left(\frac{g_{n\pi}}{2M_n}\right)^2\frac{1}{(2\pi)^6}\iint d^3\boldsymbol{k}\, d^3\boldsymbol{k}'\exp[i(\boldsymbol{k}+\boldsymbol{k}')\cdot\boldsymbol{r}]\cdot$$

$$\cdot\left\{(\boldsymbol{k}\cdot\boldsymbol{k}')^2\left[\left(\frac{g_{\Lambda\pi}}{M_\Sigma+M_\Lambda}\right)^2\left(\frac{1}{\omega+\omega'}+\frac{1}{\omega'}\right)+\left(\frac{g_{\Sigma\pi}}{2M_\Sigma}\right)^2\left(\frac{1}{\omega+\omega'}+\frac{2}{\omega'}\right)\right]+\right.$$

$$\left.+\boldsymbol{\sigma}_1\cdot(\boldsymbol{k}\times\boldsymbol{k}')\boldsymbol{\sigma}_2\cdot(\boldsymbol{k}\times\boldsymbol{k}')\left[\left(\frac{g_{\Lambda\pi}}{M_\Sigma+M_\Lambda}\right)^2\left(\frac{1}{\omega+\omega'}+\frac{1}{\omega'}\right)+\left(\frac{g_{\Sigma\pi}}{2M_\Sigma}\right)^2\left(\frac{2}{\omega+\omega'}+\frac{1}{\omega'}\right)\right]\right\},$$

where M_n and M_Σ are respectively the masses of the nucleon and the Σ-hyperon in the bound (Σ-hyperon, nucleon) system, and M_Λ is the mass of the Λ-hyperon.

$\omega = (\mu^2 + k^2)^{\frac{1}{2}}$, where μ is the mass of the π-meson. The potential for one-K-meson exchange is

$$(2)\qquad V_K = -\frac{1}{3}\frac{(g_{\Sigma K})^2}{2\pi}\mu_K\left(\frac{\mu_K}{2M_n}\right)^2 P_x P_\sigma\left\{\boldsymbol{\sigma}_1\cdot\boldsymbol{\sigma}_2+\frac{3+3\mu_K r+\mu_K^2 r^2}{(\mu_K r)^3}S_{12}\right\}\cdot\frac{\exp[-\mu_K r]}{\mu_K r},$$

where μ_K is the mass of the K-meson and $P_\sigma = 1$ for parallel and -1 for antiparallel spins. $P_x = 1$ for even states.

It is reasonable to assume that if the (Σ-hyperon, nucleon) system is bound, it is in the singlet S state. For in the triplet S state, the central part of the one pion exchange potential is repulsive, in contrast to the situation for the nucleon-nucleon interaction.

In the singlet case

$$(3)\qquad V_\pi = -\frac{\mu^3}{4M_n M_\Sigma}\frac{g_{n\pi}g_{\Sigma\pi}}{4\pi}\frac{\exp[-\mu r]}{r} -$$

$$-\frac{1}{4}\left(\frac{g_{n\pi}}{2M_n}\right)^2\frac{\mu^5}{(2\pi)^3}\left\{2\left(\frac{g_{\Lambda\pi}}{M_\Lambda+M_\Sigma}\right)^2\left[K_0(2\mu r)\left(\frac{47}{\mu^3 r^3}+\frac{4}{\mu r}\right)+K_1(2\mu r)\left(\frac{47}{\mu^4 r^4}+\frac{28}{\mu^2 r^2}\right)\right]+\right.$$

$$+\left(\frac{g_{\Sigma\pi}}{2M_\Sigma}\right)^2\left[K_0(2\mu r)\left(\frac{142}{\mu^3 r^3}+\frac{8}{\mu r}\right)+K_1(2\mu r)\left(\frac{142}{\mu^4 r^4}+\frac{88}{\mu^2 r^2}\right)\right]+$$

$$\left.+\frac{4}{\mu r}\exp[-\mu r]\left(\frac{g_{\Sigma\pi}}{2M_\Sigma}\right)^2\left[K_0(\mu r)-\frac{1}{\mu r}K_1(\mu r)\right]\right\},$$

2447

and

$$V_\text{K} = -\frac{(g_{\Sigma\text{K}})^2}{2\pi}\,\mu_\text{K}\left(\frac{\mu_\text{K}}{2M_\text{n}}\right)^2 \frac{\exp[-\mu_\text{K} r]}{\mu_\text{K} r}\,. \tag{4}$$

The sum of these potentials $V = V_\pi + V_\text{K}$ gives rise to the Σ-hyperon-nucleon force at distances $\geqslant 1/\mu_\text{K}$. At closer distances of approach many meson forces and velocity dependent effects will be appreciable. It is also impossible to solve the Schrödinger equation with the high singularity in the two pion exchange potential at the origin, if V is taken to represent the forces at very small distances. As is well known, for the Schrödinger equation to be soluble, $V \sim r^{-s}$ as $r \to 0$ with $s < 2$. In the singlet case, both, the part of V corresponding to one-π-meson exchange and that corresponding to one-K-meson exchange satisfy this requirement, but the part of V corresponding to two-pion exchange does not. So V has to be cut off in some manner for small values of r, even if we ignore the many-meson and other effects at short range.

Let V_1 be the sum of the one-π-meson and one-K-meson exchange parts of V, and V_2 be the two-π-meson exchange part of V. Two methods of cutting off V were used:

1) V_1 and V_2 were cut off at a given radius $r = r_c$ and the physical effect of the unknown short range forces was simulated by a hard core, *i.e.* $V = \infty$ for $0 \leqslant r \leqslant r_c$.

2) V_2 alone was cut off at a given radius $r = r_c'$ and V taken equal to V_1 for $0 \leqslant r \leqslant r_c'$.

In the expression for the potentials the π meson-baryon coupling constants have been taken equal, *i.e.*, $g_{\text{n}\pi} = g_{\Lambda\pi} = g_{\Sigma\pi}$. This leaves two parameters to work with, $g_{\Sigma\text{K}}$ and r_c. The most recent experimental evidence for $g^2_{\Sigma\text{K}}$ gives a value in the region of $\frac{1}{3}g^2_{\text{n}\pi}$, so a range of values for $g^2_{\Sigma\text{K}}$ has been taken about this point.

2'2. *Calculation of the binding energy.* – The method developed by BLATT and JACKSON in their discussion of nucleon-nucleon binding is used (7). This method is a good way of introducing the effect of the Coulomb force which can cause the (Σ^+, p) system to be unbound whilst the corresponding (Σ^-, n) system is bound.

The first step is to solve the zero energy Schrödinger equation for the relative motion of the (Σ-hyperon, nucleon) system in a potential V. Putting the wave function $\psi(r) = u(r)/r$, this equation becomes

$$-\frac{\mathrm{d}^2 u}{\mathrm{d}r^2} = W(r)\,u, \qquad \text{where} \qquad W(r) = -\frac{2M_\text{n}M_\Sigma}{M_\text{n} + M_\Sigma}\,V(r)\,.$$

(7) J. BLATT and J. JACKSON: *Rev. Mod. Phys.*, **22**, 77 (1950).

There are two sets of boundary conditions corresponding to the two different methods of cutting off V for small values of r:

1) Using the first method, the boundary conditions are $u(r)=0$ for $0 \leqslant r \leqslant r_c$ and $u(r) \sim 1-\alpha r$ as $r \to \infty$.

2) Using the second method, the boundary conditions are $u(r)=0$ for $r=0$ and $u(r) \sim 1-\alpha r$ as $r \to \infty$.

When the value of α has been found, two cases have to be considered.

i) (Σ^-, n) system. This system will be bound if there exists a $K>0$ such that $K=\alpha+\frac{1}{2}r_0K^2$, where r_0 is the effective range.

It can be seen from this equation that the condition for binding is $\alpha>0$, and then the binding energy B is given by

$$B=\frac{K^2}{M}, \qquad \text{where} \qquad M=\frac{M_\Sigma M_\mathrm{n}}{M_\Sigma+M_\mathrm{n}}\,.$$

ii) (Σ^+, p) system. In this case the Coulomb potential is first neglected and α calculated as in i). This potential is then introduced as a perturbation and a correction factor added to α. Let the corrected value of α be α_c, then as shown by BLATT and JACKSON [7]

$$\alpha_c=\alpha+\frac{1}{R}\left\{\ln\left(\frac{r_0}{R}\right)+2\gamma\right\}-\frac{1}{Ru^2(r_0)}\int_0^{r_0}\frac{u^2(r)}{r}\,\mathrm{d}r\,, \tag{5}$$

where $R=2(M_\Sigma+M_\mathrm{n})/e^2M_\Sigma M_\mathrm{n}$ and γ is Euler's constant. $u(r)$ is the zero-energy wave function for the system when the Coulomb potential is neglected and r_0 is the corresponding effective range. Following BLATT and JACKSON, an approximation to the term

$$\frac{1}{u^2(r_0)}\int_0^{r_0}\frac{u^2(r)}{r}\,\mathrm{d}r\,,$$

is obtained by putting $u(r)=\sin(\pi r/2r_0)$ and then

$$\frac{1}{u^2(r_0)}\int_0^{r_0}\frac{u^2(r)}{r}\,\mathrm{d}r=0.824\,.$$

The expression for α_c then becomes,

$$\alpha_c=\alpha+\frac{1}{R}\left\{\ln\left(\frac{r_0}{R}\right)+0.330\right\}.$$

Various calculations were made to check the above approximation and it was found to be good enough for the accuracy required in this paper.

As in the case of the (Σ^-, n) system, the (Σ^+, p) system will be bound if $\alpha_c > 0$ and the binding energy B is given by

$$B = \frac{K^2}{M},$$

where K and M are defined as before, with α replaced by α_c.

Trial calculations were made to find the ranges for r_c and r_c', which include the region where one system is bound and the other not bound. The range of parameters was chosen accordingly, and the following tables of results obtained (*), where λ is the ratio of $g^2_{\Sigma K}$ to $g^2_{n\pi}$.

TABLE I. – *First type of cut-off (hard core).* Table of values for α in the case of the (Σ^-, n) system and for α_c in the case of the (Σ^+, p) system.

r_c \ λ	0.2	0.3	0.4
0.30	0.3671 0.2354	0.4163 0.2815	0.4634 0.3259
0.31	0.1968 0.0782	0.2491 0.1272	0.2985 0.1720
0.32	0.0397 −0.0638	0.0958 −0.0129	0.1485 0.0350
0.33	−0.1116 −0.2008	−0.0050 −0.1453	0.0023 −0.0936
0.34	−0.2592 −0.3344	−0.1925 −0.2738	−0.1305 −0.2175

For each set of values for the parameters r_c and λ, two numbers are given in the table. The upper number is the corresponding value of α and the lower number is the corresponding value of α_c.

If the assumption is made that the (Σ^+, p) system is not bound, the binding energy of the (Σ^-, n) system will always be smaller than its value in the case when the binding energy of the (Σ^+, p) system is zero. From Table I, for values of r_c and λ which give $\alpha_c = 0$, $\alpha \simeq 0.11$. Also it has been calculated that for these same values $r_0 \simeq 1.4$ and then the binding energy of the (Σ^-, n) system

(*) Distances are given in units of the pion Compton wavelength $= 1/\mu$.

is 0.25 MeV. So with the first type of cut-off in the potential, the maximum value of the binding energy of the (Σ^-, n) system when the (Σ^+, p) system is unbound, is 0.25 MeV.

Similarly from Table II, when $\alpha_c = 0$, $\alpha \simeq 0.13$ and $r_0 = 1.18$. Then the binding energy of the (Σ^-, n) system is 0.36 MeV. So with the second type of cut-off in the potential, the maximum value of the binding energy of the (Σ^-, n) system when the (Σ^+, p) system is unbound, is 0.36 MeV.

TABLE II. – *Second type of cut-off (V_2 only cut off).* Table of values for α in the case of the (Σ^-, n) system and for α_c in the case of the (Σ^+, p) system.

r'_c \ λ	0.2	0.3	0.4
0.6	0.2827 0.1425	0.4450 0.2908	0.6470 0.4831
0.7	0.0644 −0.0258	0.2544 0.1140	0.4833 0.3227
0.8	−0.0715 −0.1867	0.1387 0.0080	0.3976 0.2405
0.9	−0.1836 −0.2832	0.0608 −0.0635	0.3468 0.1949
1.0	−0.2620 −0.3556	0.0070 −0.1132	0.3146 0.1611

For each set of values for the parameters r'_c and λ, the numbers given are as in Table I.

3. – The decay of the bound (Σ^-, n) system.

The following decay mode has been studied using methods similar to those developed by other authors [8,9] for hyperfragments known to exist in nature,

$$(\Sigma^-, n) \rightarrow n + n + \pi^- .$$

3·1. *Calculation of the transition matrix for the decay.* – Treating the decay interaction in first order perturbation theory, the transition matrix element for the decay is given by

$$T = \sum \langle \Psi_f | \boldsymbol{k}_1, \boldsymbol{k}_2, \boldsymbol{k}_\pi \rangle \langle \boldsymbol{k}_2, \boldsymbol{k}_\pi | H | \boldsymbol{k}_\Sigma \rangle \langle \boldsymbol{k}_\Sigma, \boldsymbol{k}_1 | \Psi i \rangle ,$$

(8) N. BYERS and W. N. COTTINGHAM: *Nucl. Phys.*, **11**, 554 (1959).
(9) R. H. DALITZ: *Phys. Rev.*, **112**, 605 (1958).

where the sum is taken over momentum and spin variables of intermediate states.

$\boldsymbol{k}_1$, $\boldsymbol{k}_2$, $\boldsymbol{k}_\pi$, and $\boldsymbol{k}_\Sigma$ are respectively the momentum of the spectator neutron, the decay neutron (*), the decay pion, and the bound Σ^--hyperon in the intermediate states. Ψ_f and Ψ_i are wave functions of, respectively, the final state of two neutrons and one pion, and the initial (Σ^-, n) bound state. The spin dependence of these equations is taken to be understood.

$\langle \boldsymbol{k}_\Sigma, \boldsymbol{k}_1 | \Psi_i \rangle$ and $\langle \boldsymbol{k}_1, \boldsymbol{k}_2, \boldsymbol{k}_\pi | \Psi_f \rangle$ are the Fourier transforms of these wave functions.

$\langle \boldsymbol{k}_2, \boldsymbol{k}_\pi | H | \boldsymbol{k}_\Sigma \rangle$ is the matrix element for the decay of a free Σ^--hyperon with momentum $\boldsymbol{k}_\Sigma$, into a pion with momentum $\boldsymbol{k}_\pi$ and a neutron with momentum $\boldsymbol{k}_2$. Allowing for parity non-conservation, the most general decay hamiltonian in the non-relativistic approximation is (**)

$$\langle \boldsymbol{k}_2, \boldsymbol{k}_\pi | H | \boldsymbol{k}_\Sigma \rangle = (2\pi)^2 \left(\frac{1+\mu}{\omega_\pi}\right)^{\frac{1}{2}} (s + p\boldsymbol{\sigma}\cdot\boldsymbol{q})\, \delta(\boldsymbol{k}_\Sigma - \boldsymbol{k}_2 - \boldsymbol{k}_\pi) \left(\frac{2\pi}{V}\right)^{\frac{3}{2}}, \tag{6}$$

where $\boldsymbol{q} = (\boldsymbol{k}_\pi - \mu\boldsymbol{k}_2)/(1+\mu)$, μ now being defined as the ratio of pion to neutron mass. V is the volume of normalization and the components of σ are the Pauli spin matrices and ω_π is the total energy of the π-meson.

Working in the rest frame of the (Σ^-, n) system,

$$\Psi_i = \frac{1}{V^{\frac{1}{2}}}\, \psi_i(\boldsymbol{r}_1 - \boldsymbol{r}_\Sigma)\,,$$

where $\boldsymbol{r}_1$ and $\boldsymbol{r}_\Sigma$ are the position vectors of the neutron and Σ^--hyperon in the initial state, and $\psi_i(\boldsymbol{r}_1 - \boldsymbol{r}_\Sigma)$ is the wave function for the relative motion of the two particles in the (Σ^-, n) bound system. Then

$$\langle \boldsymbol{k}_\Sigma, \boldsymbol{k}_1 | \boldsymbol{\Psi}_i \rangle = \frac{(2\pi)^3}{V^{\frac{1}{2}}}\, \delta(\boldsymbol{k}_\Sigma + \boldsymbol{k}_1) \int \exp\left[-i\boldsymbol{r}\cdot\left(\frac{1}{1+M_\Sigma}\boldsymbol{k}_\Sigma - \frac{M_\Sigma}{1+M_\Sigma}\right)\right] \psi_i(\boldsymbol{r})\,\mathrm{d}\boldsymbol{r}, \tag{7}$$

where $\boldsymbol{r} = \boldsymbol{r}_\Sigma - \boldsymbol{r}_1$.

As previously [8,9], the interaction of the pion with the neutrons in the final state is neglected. In this case

$$\boldsymbol{\Psi}_f = \frac{1}{V^{\frac{3}{2}}} \exp[i\boldsymbol{K}_\pi\cdot\boldsymbol{r}_\pi] \exp\left[\frac{i}{2}(\boldsymbol{K}_1 + \boldsymbol{K}_2)\cdot(\boldsymbol{r}_1' + \boldsymbol{r}_2)\right] \psi_f(\boldsymbol{r}')\,, \tag{8}$$

(*) The expression « spectator neutron » is used to denote the neutron originally bound to the Σ^--hyperon, whilst « decay neutron » is used to denote the neutron coming from the decay of the Σ^--hyperon.

(**) It is now more convenient to work with units where $\hbar = c =$ mass of neutron $= 1$.

2452

where $\boldsymbol{r}_1'$, $\boldsymbol{r}_2$, $\boldsymbol{r}_\pi$ are respectively the position vectors of the spectator neutron, decay neutron, and pion in the final state. $\boldsymbol{K}_1$, $\boldsymbol{K}_2$, and $\boldsymbol{K}_\pi$ are the momentum vectors of these particles in the asymptotic region of the final state. $\psi(\boldsymbol{r}')$ is the wave function for the relative motion of the two neutrons in the final state and $\boldsymbol{r}' = \boldsymbol{r}_2 - \boldsymbol{r}_1'$.

The set of co-ordinates $\boldsymbol{R}$, $\boldsymbol{\rho}$, and $\boldsymbol{r}'$ is now used for the final state, where

$$\boldsymbol{R} = \tfrac{1}{3}(\boldsymbol{r}_2' + \boldsymbol{r}_2 + \boldsymbol{r}_\pi); \qquad \boldsymbol{\rho} = \boldsymbol{r}_\pi - \tfrac{1}{2}(\boldsymbol{r}_2 + \boldsymbol{r}_1') .$$

From (8), it follows that

$$(9) \qquad \langle \boldsymbol{k}_1, \boldsymbol{k}_2, \boldsymbol{k}_\pi \rangle |\Psi_f\rangle = \frac{1}{V^3}\iiint \exp\left[i\boldsymbol{R}\cdot[(\boldsymbol{K}_1 + \boldsymbol{K}_2 + \boldsymbol{K}_\pi) - (\boldsymbol{k}_1 + \boldsymbol{k}_2 + \boldsymbol{k}_\pi)] + \right.$$

$$\left. + (i\boldsymbol{r}'/2)\cdot(\boldsymbol{k}_1 + \boldsymbol{k}_2) + i\boldsymbol{\rho}\cdot\left[\boldsymbol{K}_\pi - \frac{2}{2+\mu}\,\boldsymbol{k}_\pi + (\boldsymbol{k}_1 + \boldsymbol{k}_2)\,\frac{\mu}{2+\mu}\right]\right] \psi_f(\boldsymbol{r}')\,\mathrm{d}\boldsymbol{R}\,\mathrm{d}\boldsymbol{\rho}\,\mathrm{d}\boldsymbol{r}' .$$

Using (6), (7), and (9), the transition element is

$$(10) \quad T = (2\pi)^{-11/2}\left(\frac{1+\mu}{\omega_\pi}\right)^{\frac{1}{2}} \frac{1}{V^2}\int \psi_f^*(\boldsymbol{r}')(s + p\boldsymbol{\sigma}\cdot\boldsymbol{q})\,\delta(\boldsymbol{k}_\Sigma - \boldsymbol{k}_2 - \boldsymbol{k}_\pi)\,\psi_i(\boldsymbol{r})\,\delta(\boldsymbol{k}_\Sigma + \boldsymbol{k}_1)\cdot$$

$$\cdot\exp\left[- i\boldsymbol{R}\cdot[\boldsymbol{K}_1 + \boldsymbol{K}_2 + \boldsymbol{K}_\pi - (\boldsymbol{k}_1 + \boldsymbol{k}_2 + \boldsymbol{k}_\pi)] - \frac{i}{2}\,\boldsymbol{r}'\cdot(\boldsymbol{k}_1 - \boldsymbol{k}_2) - \right.$$

$$\left. - i\boldsymbol{\rho}\cdot\left[\boldsymbol{K}_\pi - \frac{2}{1+\mu}\,\boldsymbol{k}_\pi + (\boldsymbol{k}_1 + \boldsymbol{k}_2)\,\frac{\mu}{1+\mu}\right] - i\boldsymbol{r}\cdot\left[\frac{1}{1+M_\Sigma}\,\boldsymbol{k}_\Sigma - \frac{M_\Sigma}{1+M_\Sigma}\,\boldsymbol{k}_1\right]\right]\cdot$$

$$\cdot\,\mathrm{d}\boldsymbol{r}\,\mathrm{d}\boldsymbol{r}'\,\mathrm{d}\boldsymbol{R}\,\mathrm{d}\boldsymbol{\rho}\,\mathrm{d}\boldsymbol{k}_\Sigma\,\mathrm{d}\boldsymbol{k}_\pi\,\mathrm{d}\boldsymbol{k}_1\,\mathrm{d}\boldsymbol{k}_2 ,$$

where all spin indices have been suppressed.

3·2. *Spin dependence, the exclusion principle and final state wave functions.* – As in the final state there are two neutrons and a pion, the total spin S can only take on the values $S = 1$ and 0. In the former case the spin wave function of the final state is symmetrical with respect to the interchange of the two neutrons, whilst in the latter case it is antisymmetrical. The total wave function representing the relative motion of the two neutrons must be antisymmetrical to satisfy the Pauli exclusion principle, and so $\psi_f(\boldsymbol{r})$ must satisfy the following conditions:

a) For $S = 0$, $\psi_f(\boldsymbol{r})$ is symmetrical and is denoted by $\psi_{fS}(\boldsymbol{r})$.

b) For $S = 1$, $\psi_f(\boldsymbol{r})$ is antisymmetrical and is denoted by $\psi_{fT}(\boldsymbol{r})$.

It has been suggested earlier in this paper that if the bound (Σ^-, n) system exists, then it will be in a spin singlet state and then it is easy to show that,

averaging over initial and summing over final spin states,

$$\sum_{\text{spins}} |T|^2 = |s|^2 |M_1|^2 + |p|^2 |\boldsymbol{M}_2|^2 , \tag{11}$$

where M_1 is the coefficient of s in the expression for T above and $\boldsymbol{M}_2$ is that vector which scalarly multiplies $p\sigma$ in this same expression. The form of ψ_f to be substitutted in M_1 is ψ_{fS}, while on the other hand in $\boldsymbol{M}_2$, it is ψ_{fT}.

The momentum K received by the neutron from the decay of a Σ^- hyperon at rest is 192 MeV/c. Taking the radius of the nucleon-nucleon interaction, a, to be equal to the π-meson Compton wave length, then for all integers l greater than zero,

$$\tfrac{1}{2} aK < \sqrt{l(l+1)} ,$$

so it is a good approximation to consider only the s-wave scattering for the relative motion of the two final state neutrons. The two different final spin states are now considered.

a) Triplet spin state. The space part of the final state wave function $\psi_{fT}(\boldsymbol{r})$ is antisymmetric and contains no scattered waves. Since the two neutrons have to be considered as identical particles, $\psi_{fT}(\boldsymbol{r})$ has to be normalized to two particles per unit volume and so has the form

$$\psi_{fT}(\boldsymbol{r}) = \exp[i\boldsymbol{k}_f\cdot\boldsymbol{r}] - \exp[-i\boldsymbol{k}_f\cdot\boldsymbol{r}] , \tag{12}$$

where $\boldsymbol{k}_f = \frac{1}{2}(\boldsymbol{K}_2 - \boldsymbol{K}_1)$.

b) The space part of the final state wave function $\psi_{fS}(\boldsymbol{r})$ is antisymmetric and contains a scattered s wave. However to simplify the calculations, final state interaction is omitted and then

$$\psi_{fS}(\boldsymbol{r}) = \exp[i\boldsymbol{k}_f\cdot\boldsymbol{r}] + \exp[-i\boldsymbol{k}_f\cdot\boldsymbol{r}] . \tag{13}$$

As only M_1 contains ψ_{fS}, it can be seen from (6) that, if s is small compared with p, the error in neglecting the final state interaction will also be small.

The expression for M_1 is easily reduced to the form

$$M_1 = \frac{(2\pi)^{7/2}}{V^2}\left(\frac{1+\mu}{\omega_\pi}\right)^{\frac{1}{2}} \delta(\boldsymbol{K}_\pi + \boldsymbol{K}_1 + \boldsymbol{K}_2)\int \exp[-(i/2)\boldsymbol{K}_\pi\cdot\boldsymbol{r}]\,\psi^*_{fS}(\boldsymbol{r})\,\psi_i(\boldsymbol{r})\,\mathrm{d}\boldsymbol{r} .$$

In the general case $\boldsymbol{M}_2$ is more difficult to evaluate, but with the forms for $\psi_{fS}(\boldsymbol{r})$ and $\psi_{fT}(\boldsymbol{r})$ defined above in (12) and (13), the following is obtained.

$$M_1 = \frac{(2\pi)^{7/2}}{V^2}\left(\frac{1+\mu}{\omega_\pi}\right)^{\frac{1}{2}} \delta(\boldsymbol{K}_\pi + \boldsymbol{K}_1 + \boldsymbol{K}_2)\{g(\boldsymbol{K}_1) + g(\boldsymbol{K}_2)\} , \tag{14}$$

where

$$g(\boldsymbol{K}) = \int \exp\,[i\boldsymbol{K}\cdot\boldsymbol{r}]\,\psi_i(\boldsymbol{r})\,\mathrm{d}\boldsymbol{r}\,,$$

$$(15)\qquad M_2 = \frac{(2\pi)^{7/2}}{V^2}\left(\frac{1+\mu}{\omega_\pi}\right)^{\frac{1}{2}}\delta(\boldsymbol{K}_\pi+\boldsymbol{K}_1+\boldsymbol{K}_2)\left\{[g(\boldsymbol{K}_1)-g(\boldsymbol{K}_2)]\left[\frac{\boldsymbol{K}_\pi-\mu\boldsymbol{K}_2}{1+\mu}\right]-\right.$$
$$\left.-\frac{g(\boldsymbol{K}_2)\mu}{1+\mu}\,[\boldsymbol{K}_2-\boldsymbol{K}_1]\right\}.$$

3'3. *The wave function of the initial state.* – The form for $\psi_i(\boldsymbol{r})$ is similar to that used by SNOW [2]. The (Σ^-, n) system is assumed to be bound by a square well potential with range b_1 and depth V_1.

The correctly normalized wave function is given by

$$(16)\qquad \begin{cases} r\psi_i(\boldsymbol{r}) = \dfrac{1}{(4\pi)^{\frac{1}{2}}}\left(\dfrac{2\gamma_1}{1+\gamma_1 b_1}\right)^{\frac{1}{2}}\sin d_1 r\,, & 0 < r < b_1\,,\\[2ex] \qquad = \dfrac{d_1}{K_1}\,\dfrac{1}{(4\pi)^{\frac{1}{2}}}\left(\dfrac{2\gamma_1}{1+\gamma_1 b_1}\right)^{\frac{1}{2}}\exp\,[-\gamma_1(r-b_1)]\,, & b_1 < r\,, \end{cases}$$

where ε is the binding energy, $\gamma_1 = [(2M_\Sigma/(1+M_\Sigma))\varepsilon]^{\frac{1}{2}}$, d_1 is the root of the equation $d_2 \operatorname{ctg} d_1 b_1 = -\gamma_1$, and $K_1^2 = d_1^2 + \gamma_1^2$. With this form for $\psi_i(\boldsymbol{r})$, one obtains

$$(17)\qquad g(\boldsymbol{K}) = 2\left(\frac{2\pi\gamma_1}{1+\gamma_1 b_1}\right)^{\frac{1}{2}}\left\{\frac{\sin d_1 b_1}{d_1^2-K^2}+\frac{d_1}{K_1}\,\frac{1}{\gamma^2+K^2}\right\}\{\gamma_1 \sin b_1 K + K\cos b_1 K\}\,.$$

3'4. *The phase space factor of the transition probability.* – The energy released in the decay of the Σ^--hyperon is greater than the mass of the pion and so it is necessary to treat this particle in the final state relativistically. As the total momentum of the system is conserved, variables which designate the final state in the decay

$$(\Sigma^-, \mathrm{n}) \to \mathrm{n} + \mathrm{n} + \pi^-\,,$$

are $\boldsymbol{k}_f$, the momentum conjugate to the relative displacement of the two neutrons, and $\boldsymbol{K}_\pi$, the momentum of the pion. The transition probability per unit time, ω, is given by

$$\omega = 2\pi \sum_{\text{spins}} |T|^2 \varrho(E)\,,$$

where $\varrho(E)\,\mathrm{d}E = \frac{1}{2}\mathrm{d}\boldsymbol{k}\,\mathrm{d}\boldsymbol{K}_\pi$ (*), E being the energy of the final state. As energy

(*) As the two neutrons in the final state are identical, the phase space into which the (Σ^-, n) system decays is multiplied by a factor $\frac{1}{2}$.

2455

as well as momentum is conserved, ω depends on two independent kinematic variables which are chosen to be k and θ, where θ is the angle between $\boldsymbol{k}_f$ and $\boldsymbol{K}_\pi$. It is given by (*)

$$\omega(k_f, \cos\theta) = \frac{2\pi}{2}\left[\frac{V}{(2\pi)^3}\right]^4 K_\pi^2 \frac{\mathrm{d}K_\pi}{\mathrm{d}E} k_f^2 \mathrm{d}k_f \,\mathrm{d}\cos\theta\, 8\pi^2 \sum_{\text{spins}} |T|^2 . \tag{18}$$

The energy equation is

$$E = 2 + \frac{K_\pi^2}{4} + k_f^2 + \sqrt{\mu^2 + K_\pi^2}\,, \tag{19}$$

and then

$$K_\pi \frac{\mathrm{d}K_\pi}{\mathrm{d}E} = \frac{2\omega_\pi}{\omega_\pi + 2}\,, \tag{20}$$

where

$$\omega_\pi^2 = \mu^2 + K_\pi^2 .$$

From eq. (20), (18), (11), and substituting K_1 for $\cos\theta$,

$$\omega(k_f, K_1) = \frac{1}{\pi^2}\frac{1+\mu}{2+\omega_\pi}\{|s|^2|I_S|^2 + |p|^2|\boldsymbol{I}_T|^2\} K_1 k_f \,\mathrm{d}K_1\, \mathrm{d}k_f\,, \tag{21}$$

where

$$I_S = \{g(\boldsymbol{K}_1) + g(\boldsymbol{K}_2)\}; \qquad \boldsymbol{I}_T = \{g(\boldsymbol{K}_1) - g(\boldsymbol{K}_2)\}\left(\frac{\boldsymbol{K}_\pi - \mu\boldsymbol{K}_2}{1+\mu}\right) - \frac{g(\boldsymbol{K}_2)\mu}{1+\mu}(\boldsymbol{K}_2 - \boldsymbol{K}_1)\,.$$

3.5. *The total transition rate.* – The total transition rate, ω, is obtained by integrating $\omega(k_f, K_1)$ over k_f and K_1. For a given K_1, k_f ranges over these values satisfying the inequalities

$$K_\pi + 2k_f \geqslant 2K_1 \geqslant |K_\pi - 2k_f|\,.$$

The range of integration of K_1 then lies between zero and some maximum value determined by the energy equation.

ω was calculated in the case when $s = 0$, for then the effect of the final state interaction is small, and this situation also has some theoretical support ([10]). $|p|^2$ is then given in terms of τ the lifetime of the free Σ^--hyperon by the equation,

$$|p|^2 = \frac{1}{2q_{\text{free}}}\frac{\omega_{\text{free}}^3 + 1}{\mu + 1}\,,$$

(*) The δ function has been removed from T in this expression.

([10]) B. D'ESPAGNAT and J. PRENTKI: *Phys. Rev.*, **114**, 1366 (1959).

where q_{free} is the relative momenutm of the two particles in the final state and $\omega_{\text{free}}^2 = q_{\text{free}}^2 + \mu^2$.

Then

$$\omega = \frac{2\pi^2}{1} \iint \frac{\omega_\pi + 2}{\omega_{\text{free}}^3 + 1} \frac{1}{\tau q_{\text{free}}} |I_T|^2 K_1 k_f \, dK_1 \, dk_f .$$

The calculations were carried out for different values of the binding energy ε and square well radius b_1, and $1/\omega$, the lifetime of the (Σ^-, n) system is given in Table III, where ε is measured in MeV, b_1 in 10^{-13} cm and $1/\omega$ in 10^{-10} s.

TABLE III.

b_1 \ ε	.25	.5	.75
1	2.19	2.45	2.66
2	2.04	2.21	2.34

These values compare with $1.74 \cdot 10^{-10}$ s, the lifetime of the free Σ^- hyperon. As there are no accurate experimental values for s and p, it seems desirable to calculate the lifetime for the case when $p = 0$. Using the form for ψ_{fs} given by (13), it was found that for $\varepsilon = .25$ MeV and $b_1 = 10^{-13}$ cm, the lifetime was equal to $1.55 \cdot 10^{-10}$ s.

In Fig. 1 the distribution of values of K_1 is plotted for the case where ε

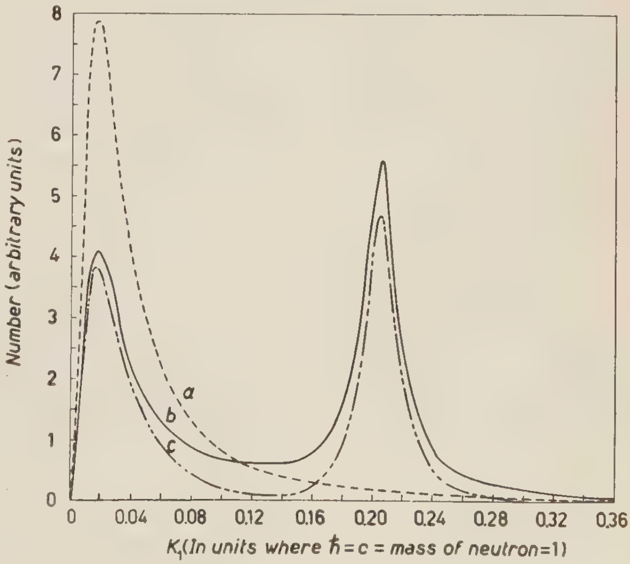

Fig. 1. – The momentum distribution of the recoil neutron from the decay of a (Σ^-, n) hyperfragment in those cases where, a) the exclusion principle has been ignored and $p = 0$, (the corresponding distribution where $s = 0$ is very close to that shown by a),) b) the exclusion principle has been taken into account and $p = 0$, and c) the exclusion principle has been taken into account and $s = 0$.

2457

and b_1 have the values given above. Two curves are shown to represent the extreme cases where 1) $s = 0$ and 2) $p = 0$. These are compared in the same figure with those obtained by ignoring the effect of the exclusion principle in the final state. In this case of course, the wave function for the relative motion of the two neutrons is

$$\psi_f = \exp\left[i\boldsymbol{k}_f \cdot \boldsymbol{r}\right].$$

When $s = 0$, the lifetime is equal to $1.9 \cdot 10^{-10}$ s and when $p = 0$, it is equal to $1.79 \cdot 10^{-10}$ s.

4. – Conclusions.

From Table I it can be seen that, where an infinite hard core has been assumed, the values of r_c for which the (Σ^-, n) system is bound and the (Σ^+, p) system is not bound, lie in the range 0.31 to 0.33 π-meson Compton wave lengths, for the values of λ considered here. The situation is therefore very sensitive to the value of r_c. However JASTROW, in a paper on nucleon-nucleon forces [11], used an infinite hard core in the singlet state and found that, for consistency with experiment, its radius has the value 0.42 π-meson Compton wave lengths. It is interesting to see that if r_c is given this value, then for all values of λ used, both the (Σ^-, n) system and the (Σ^+, p) system will be unbound.

In the case of the second type of cut-off, with no hard core, it will be seen from Table II that, for the (Σ^+, p) system to be unbound, r_c has to be greater than 0.6 π-meson Compton wave lengths. This means that the two-π-meson exchange potential has to be cut off to zero for most of the values of r for which it is appreciable, and leads to a potential which is not very realistic.

The maximum values that the binding energy of the (Σ^-, n) system can have, when the (Σ^+, p) system is not bound, are rather smaller than those suggested by SNOW [2].

It has been shown that, for small values of s compared with p the interaction between the two neutrons in the final state will have little effect on the lifetime of the bound (Σ, n) system. However, even for such lightly bound systems, there is an effect due to the exclusion principle. For $s = 0$, the lifetime is increased from $1.90 \cdot 10^{-10}$ s, when the exclusion principle is ignored, to $2.19 \cdot 10^{-10}$ s when it is included, for a particular choice of potential. Si-

---

([11]) R. JASTROW: *Phys. Rev.*, **81**, 165 (1951).

milarly for $p = 0$, the inclusion of the exclusion principle decreases the lifetime from $1.79 \cdot 10^{-10}$ s to $1.55 \cdot 10^{-10}$ s.

It will be seen from Fig. 1 that two maxima occur for those cases where the exclusion principle has been taken into account. As is expected, the first maximum is close to that of the distribution of the momentum of the bound neutron, whilst the second is close to the value of the momentum which the neutron receives from the decay of a Σ^--hyperon at rest.

* * *

It is a pleasure to thank Professor E. H. S. Burhop and Dr. E. A. Power for many discussions and Dr. R. Kumar for initiating interest in the possible existence of the (Σ^-, n) system. I wish also to thank the D.S.I.R. for a Research Studentship and the University of London Computer Unit for the use of their facilities.

RIASSUNTO (*)

Si analizza il legame degli iperoni Σ ai nucleoni, facendo uso dei potenziali suggeriti dalla teoria di campo. Si dedica una speciale attenzione alla possibilità che l'iperone Σ^- possa legarsi ad un neutrone mentre l'iperone Σ^- ed il protone non sono legati. Si danno delle tabelle che mostrano gli effetti delle variazioni delle costanti di accoppiamento. Si calcola la vita media di questo ipotetico sistema legato (Σ^-, n), e si mostra che, per alcune forme dell'Hamiltoniano debole responsabile del decadimento si può trascurare l'interazione nello stato finale fra i due nucleoni. Si trova che l'effetto del principio di Pauli sullo stato finale è apprezzabile anche se si suppone che il sistema (Σ^-, n) abbia una energia di legame inferiore ad 1 MeV.

(*) *Traduzione a cura della Redazione.*

On the Electron Paramagnetic Resonace Spectra of V^{3+} in Corundum (Al_2O_3).

D. K. Ray (*)

Institut Fourier - Grenoble

(ricevuto il 18 Febbraio 1961)

Summary. — Detailed investigations of the e.p.r. spectra of V^{3+} in Corundum have been made taking into account the effect of excited ^3P state, trigonal field mixing, and also covalent bonding. Trigonal splitting comes out to be of the order of 400 cm^{-1}. Second-order g-factors arising from the effect of higher orbital states through spin-orbit interaction are shown to have very significant effect on the evaluation of the covalent bonding factors.

Introduction.

An investigation (1) on the e.p.r. spectra of V^{3+} in Al_2O_3 has recently been made on the basis of the data given by Zverev and Prokhorov (2). In that analysis the effect of spin-orbit interaction only among the lowest three orbital states were considered. Moreover, as the magnitude of the trigonal field parameter came out to be of the order ot 400 cm^{-1}, the mixing of states due to this field was neglected. Also, no consideration was taken of the nearby excited ^3P level. Recently, Foner and Low (3), using pulsed magnetic field technique, give a value of the splitting between the lowest singlet spin state and the upper doublet spin states (in the language of spin-Hamiltonian) as (7.85 ± 0.4) cm^{-1} compared to the value given by Zverev and Prokhorov as (7.0 ± 0.3) cm^{-1}. Foner and Low also report about an absorption line

(*) On leave of absence from Saha Institute of Nuclear Physics, Calcutta.
(1) D. K. Ray: *Žurn. Ėksp. Theor. Phys.* (to be published).
(2) G. M. Zverev and A. M. Prokhorov: *Žurn. Ėksp. Theor. Phys.* (to be published).
(3) S. Foner and W. Low: *Phys. Rev.*, **120**, 1585 (1960).

near about 800 cm^{-1} which they correlate with the trigonal splitting Δ. It will be of interest to see, whether such a value of Δ is compatible with the g-values reported by ZVEREV and PROKHOROV and also to see how much effect does the second-order g-factors have on the covalent bonding factors as has recently been done for the case of a single $3d$ electron [4].

1. – Evaluation of crystal field orbital states and second-order g-factors.

The energy levels of V^{3+} in Al_2O_3 were evaluated earlier by PRYCE and RUNCIMAN [5] on the assumption of the trigonal splitting of the lowest orbital triplet to be 1200 cm^{-1}. So, for our purpose, we cannot take straightway the values of their energy levels. Our previous analysis on the basis of first-order g-factors gave Δ to be around 400 cm^{-1}. If we take D to be 7.85 cm^{-1} as reported by FONER and LOW, the value of Δ does not change appreciably. Some possible values of Δ on the basis of $D = 7.85$ cm^{-1}, taking first order g-values and following the procedure of reference [1], are given in Table I

TABLE I.

α^0	γ	λ_1	θ	Δ from D of ref. [2] (in cm^{-1})	Δ from D of ref. [3] (in cm^{-1})
1.6	8° 50′	1.34	10° 20′	428.3	480.5
1.5	9° 2′	1.27	10° 32′	420.5	471.8
1.4	9° 10′	1.24	10° 42′	391.4	439.1
1.2	9° 23′	1.2	10° 54′	361.4	405.3
1	9° 41′	1.16	11° 36′	352.8	396

here. The significance of the parameters α, β, λ^{α_1}, λ^{β_1} are given in reference [1] as well as in eq. (10) here. It can be shown that if we neglect the effect of trigonal field mixing and the excited ^3P-state, then $\alpha_1 = \beta_1 = \frac{3}{2}K$ and $\lambda^{\alpha_1} = \lambda^{\beta_1} = \frac{3}{2}\lambda R$. So for such a case $\alpha_1/\beta_1 = \lambda^{\alpha_1}/\lambda^{\beta_1} = 1$. From the table it is seen that this happens when $\alpha_1 \rightleftarrows 1.2$ and Δ for this case is 361 cm^{-1} and 405 cm^{-1} for the two D-values. So we can safely use Δ as 400 cm^{-1} for the evaluation of the energy levels and eigenstates which we require for second-order calculations. Instead of following the procedure used by PRYCE and RUNCIMAN, we shall use throughout Racah's formalism [6] in the evaluation of matrix elements the of crystal field and we get the following determinants to be solved [7]:

(4) D. K. RAY: *Nuovo Cimento* (to appear).
(5) M. H. L. PRYCE and W. A. RUNCIMAN: *Dis. Farad. Soc.*, **26**, 34 (1958).
(6) G. RACAH: *Phys. Rev.*, **62**, 438 (1942).
(7) D. K. RAY: *Žurn. Èksp. Theor. Phys.* (to be published).

2461

$$
(1)\qquad
\begin{array}{ccc}
|30\rangle & \frac{1}{\sqrt{2}}(|33\rangle - |3-3\rangle) & |10\rangle \\
\hline
-\sqrt{\frac{4}{15}}\,A_1 + \sqrt{\frac{2}{11}}\,B_1 & -\sqrt{\frac{7}{11}}\,C_1 & 3\sqrt{\frac{1}{35}}\,A_3 - \sqrt{\frac{4}{21}}\,B_3 \\
-\sqrt{\frac{7}{11}}\,C_1 & \sqrt{\frac{5}{12}}\,A_1 + \sqrt{\frac{1}{22}}\,B_1 & -\sqrt{\frac{1}{6}}\,C_3 \\
3\sqrt{\frac{1}{35}}\,A_3 - \sqrt{\frac{4}{21}}\,B_3 & -\sqrt{\frac{1}{6}}\,C_3 & -\sqrt{\frac{2}{5}}\,A_2 + E_p
\end{array}
$$

and

$$
(2)\qquad
\begin{array}{ccc}
|31\rangle & |3-2\rangle & |11\rangle \\
\hline
-\sqrt{\frac{3}{20}}\,A^0 + \frac{1}{3}\sqrt{\frac{1}{22}}\,B_1 & \sqrt{\frac{7}{99}}\,C_1 & \sqrt{\frac{6}{35}}\,A_3 + \sqrt{\frac{1}{14}}\,B_3 \\
\sqrt{\frac{7}{99}}\,C_1 & -\frac{7}{3}\sqrt{\frac{1}{22}}\,B_1 & -\frac{1}{2}\,C_3 \\
\sqrt{\frac{6}{35}}\,A_3 + \sqrt{\frac{1}{14}}\,B_3 & -\frac{1}{2}\,C_3 & \sqrt{\frac{1}{10}}\,A_2 - E_p\,.
\end{array}
$$

Here the states are described in the $|LM_L\rangle$ scheme and the cubic and trigonal potential is used in the form:

$$
(3)\qquad V = A_0^2 r^2 Y_0^2 + A_0^4 r^4 \left[Y_0^4 + \sqrt{\frac{10}{7}}\,(Y_3^4 - Y_{-3}^4) \right],
$$

and also,

$$
(4)\qquad
\left\{
\begin{aligned}
A_1 &= \frac{A_0^2 \overline{r^2}}{\sqrt{7}} \langle 3 \| Y^{(2)} \| 3 \rangle = -\frac{1}{7}\sqrt{\frac{3}{\pi}}\,\overline{r^2} A_0^2\,, \\
B_1 &= \frac{A_0^4 \overline{r^4}}{\sqrt{7}} \langle 3 \| Y^{(4)} \| 3 \rangle = -\frac{3}{7}\sqrt{\frac{11}{2\pi}}\,\overline{r^4} A_0^4\,, \\
C_1 &= \sqrt{\frac{10}{7}}\,B_1 = -\frac{3}{7}\sqrt{\frac{55}{7\pi}}\,\overline{r^4} A_0^4\,, \\
A_2 &= \frac{A_0^2 \overline{r^2}}{\sqrt{3}} \langle 1 \| Y^{(2)} \| 1 \rangle = \sqrt{\frac{1}{2\pi}}\,\overline{r^2} A_0^2\,, \\
A_3 &= \frac{A_0^2 \overline{r^2}}{\sqrt{3}} \langle 1 \| Y^{(2)} \| 3 \rangle = 2\sqrt{\frac{1}{7\pi}}\,\overline{r^2} A_0^2\,, \\
B_3 &= \frac{A_0^4 \overline{r^4}}{\sqrt{3}} \langle 1 \| Y^{(4)} \| 3 \rangle = -\sqrt{\frac{3}{7\pi}}\,\overline{r^4} A_0^4\,, \\
C_3 &= -\sqrt{\frac{30}{49\pi}}\,\overline{r^4} A_0^4\,.
\end{aligned}
\right.
$$

2462

We should mention here also that the axis of quantization is along the trigonal field direction.

The solutions of determinants (1) and (2) give the positions of $^3A_2$ and ^3E levels respectively. From the values of the constants given in eq. (4), it is evident that ultimately there are three unknown parameters in these determinants A_1, B_1 and E_p because the other constants can be expressed in terms of B_1 and A_1. We have at first adjusted the values of B_1 and E_p such that the positions of levels approximately coincide with those reported by PRYCE and RUNCIMAN and then adjusted the values of A_1 so that the separation between the lowest $^3A_2$ and ^3E is nearly 400 cm^{-1}. The results with $B_1 = 1.6 \cdot 10^4$ cm^{-1} and $E = 8 \cdot 10^3$ cm^{-1} and $A_1 = 8 \cdot 10^2$ cm^{-1} are as follows:

$$(5)\quad \begin{cases} {}^3A_2 \textit{ levels}: & -1.278\,073 \cdot 10^4\,(W_0)\,, \quad 1.201\,821 \cdot 10^4\,(W_5)\,, \quad 2.054\,535 \cdot 10^4\,(W_4)\,, \\ E \quad \textit{levels}: & -1.237\,756 \cdot 10^4\,(W_1)\,, \quad 0.302\,334 \cdot 10^4\,(W_3)\,, \quad 0.949\,899 \cdot 10^4\,(W_5)\,. \end{cases}$$

All the values are in cm^{-1} and the W's indicate the nomenclature used in Table II, where we have given all the states and the energy levels. The eigenstates which follow from these energy levels can be determined in the straightforward method and the coefficients of mixing are given by:

$$(6)\quad \begin{cases} \varepsilon_1' = 0.646\,57\,; & \varepsilon_2' = -0.707\,05\,; & \varepsilon_3' = 0.154\,49\,; \\ \varphi_1' = 0.487\,63\,; & \varphi_2' = 0.465\,95\,; & \varphi_3' = 0.212\,34\,; \\ \tau_1' = 0.326\,15\,; & \tau_2' = 0.087\,75\,; & \tau_3' = -0.941\,24\,; \\ \varepsilon_1 = 0.389\,00\,; & \varepsilon_2 = -0.919\,79\,; & \varepsilon_3 = -0.005\,33\,; \\ \varphi_1 = 0.867\,90\,; & \varphi_2 = 0.392\,13\,; & \varphi_3 = 0.337\,36\,; \\ \tau_1 = -0.309\,92\,; & \tau_2 = -0.014\,63\,; & \tau_3 = 0.941\,35\,. \end{cases}$$

Besides these levels, there is another one of representation $^3A_1$ whose position is given by,

$$W_2 = \sqrt{\frac{5}{12}}\,A_1 + \sqrt{\frac{1}{22}}\,B_1 = 0.392\,76 \cdot 10^4 \text{ cm}^{-1}\,.$$

Without going into details of covalent bonding, it is evident from the value of E_p that it has been considerably reduced due to such a cause from its free-spin value. Now if we want to consider the effect of covalent bonding explicitely, we must consider to reductions of orbital angular momentum and spin-

orbit interaction in the following forms:

$$(7)\qquad \begin{cases} \langle\psi_m|\ \boldsymbol{L}|\psi_n\rangle = K_{mn}\langle\psi^d_m|\ \boldsymbol{L}|\psi^d_n\rangle \\ \langle\psi_m|\lambda\boldsymbol{L}|\psi_n\rangle = R_{mn}\langle\psi^d_m|\lambda\boldsymbol{L}|\psi^d_n\rangle\,. \end{cases}$$

TABLE II.

Designation of the state				State	Energy
Term	Cubic	Trig	No		
^{3}P	^{3}T$_1$	^{3}E	$\|6\rangle$ $\|6^*\rangle$	$\left.\begin{array}{l} -\varepsilon_3\|31\rangle+\varrho_3\|3-2\rangle-\tau_3\|11\rangle \\ \varepsilon_3\|3-1\rangle+\varrho_3\|32\rangle+\tau_3\|1-1\rangle \end{array}\right\}$	W_6
		^{3}A$_2$	$\|5\rangle$	$\varepsilon'_3\|30\rangle+\varrho'_3(\|33\rangle-\|3-3\rangle)+\tau'_3\|10\rangle$	W_5
^{3}F	^{3}A$_2$	^{3}A$_2$	$\|4\rangle$	$\varepsilon'_2\|30\rangle+\varrho'_2(\|33\rangle-\|3-3\rangle)+\tau'_2\|10\rangle$	W_4
	^{3}T$_2$	^{3}E	$\|3\rangle$ $\|3^*\rangle$	$\left.\begin{array}{l} -\varepsilon_2\|31\rangle+\varrho_2\|3-2\rangle-\tau_2\|11\rangle \\ \varepsilon_2\|3-1\rangle+\varrho_2\|32\rangle+\tau_2\|1-1\rangle \end{array}\right\}$	W_3
		^{3}A$_1$	$\|2\rangle$	$\frac{1}{\sqrt{2}}(\|33\rangle+\|3-3\rangle)$	W_2
	^{3}T$_1$	^{3}E	$\|1\rangle$ $\|1^*\rangle$	$\left.\begin{array}{l} -\varepsilon_1\|31\rangle+\varrho_1\|3-2\rangle-\tau_1\|11\rangle \\ \varepsilon_1\|3-1\rangle+\varrho_1\|32\rangle+\tau_1\|1-1\rangle \end{array}\right\}$	W_1
		^{3}A$_2$	$\|0\rangle$	$\varepsilon'_1\|30\rangle+\varrho'_1(\|33\rangle-\|3-3\rangle)+\tau'_1\|10\rangle$	W_0

In the above we have taken different reductions for angular momentum and spin-orbit interaction as first suggested by TINKHAM ([8]), but instead of taking the reduction of $\lambda\boldsymbol{L}$ as simply the product of normalization constants N_n and N_m of covalently bonded wave-functions ψ_n and ψ_m, it is better to take another independent parameter R_{mn} for it, because we do not know actually how far the wave-functions around the central nucleus might contribute to spin-orbit interaction. The states given in eq. (7) are individual electron states expressed in a cubic system of axes as covalent bonding takes place mainly by p-electrons of oxygen arranged in an octahedral manner, the deviation from this symmetry being small. So it is necessary to express our states of $(3d)^2$ configuration in terms of individual electron states expressed in cubic axis system. But if we take $K_{\pi\pi}=K_{\pi\sigma}=K$, and $R_{\pi\pi}=R_{\pi\sigma}\equiv R$, then from the invariance of matrix elements of observables to co-ordinate rotations, we can straightway write the matrix elements of $\boldsymbol{L}$ and $\lambda\boldsymbol{L}$ reduced by the K and R respectively. The non-vanishing matrix elements among the lowest three

([8]) M. TINKHAM: *Proc. Roy. Soc.*, A **236**, 549 (1956).

orbital states are given by:

$$\tag{8} \begin{cases} \langle 1 | L_z | 1 \rangle = - \langle 1^* | L_z | 1^* \rangle = - \alpha_1 \\ \langle 1 | L_x | 0 \rangle = - \langle 1^* | L_x | 0 \rangle \ = - \beta_1 / \sqrt{2} \\ \langle 1 | L_y | 0 \rangle = - \langle 1^* | L_y | 0 \rangle \ = \quad i\beta_1 / \sqrt{2} \end{cases}$$

and

$$\tag{9} \begin{cases} \langle 1 | \lambda L_z | 1 \rangle = - \langle 1^* | \lambda L_z | 1^* \rangle = - \lambda^{\alpha_1} \\ \langle 1 | \lambda L_x | 0 \rangle = - \langle 1^* | \lambda L_x | 0 \rangle \ = - \lambda^{\beta_1} / \sqrt{2} \\ \langle 1 | \lambda L_y | 0 \rangle = \quad \langle 1^* | \lambda L_y | 0 \rangle \ = \quad i\lambda^{\beta_1} / \sqrt{2} \end{cases}$$

where,

$$\tag{10} \begin{cases} \alpha_1 \ = (-\varepsilon_1^2 + 2\varrho_1^2 - \tau_1^2) K , \\ \beta_1 \ = (\sqrt{6}\, \varepsilon_1 \varepsilon_1^1 + 3\, \varrho_1 \varrho_1^1 + \tau_1 \tau_1^1) K , \\ \lambda^{\alpha_1} = (-\varepsilon_1^2 + 2\varrho_1^2 - \tau_1^2) \lambda\, R , \\ \lambda^{\beta_1} = (\sqrt{6}\, \varepsilon_1 \varepsilon_1^1 + \sqrt{3}\, \varrho_1 \varrho_1^1 + \tau_1 \tau_1^1 (\lambda R . \end{cases}$$

Using these matrix elements, we can now calculate the energies and states of the Hamiltonian:

$$\tag{11} \mathscr{H} = V + \lambda \boldsymbol{L} \cdot \boldsymbol{S} .$$

On the assumption that the orbital singlet lies lowest, the g-factors, which are first-order in the sense that we have considered mixing due to spin-orbit interaction only among the lowest three orbital levels, are given by:

$$\tag{12} \begin{cases} g_{\parallel}^{(1)} = 2 \cos^2 \gamma - \alpha_1 \sin^2 \gamma , \\ g_{\perp}^{(2)} = \sqrt{2} \sin \theta \sin \gamma + 2 \cos \theta \cos \gamma - \dfrac{1}{\sqrt{2}} \sin \theta \cos \gamma \beta_1 - \cos \theta \sin \gamma \beta_1 , \end{cases}$$

where,

$$\tag{13} \begin{cases} \operatorname{tg} \gamma = \dfrac{-\Delta + (\Delta^2 + 4 \lambda^{\beta_1 2})^{\frac{1}{2}}}{2 \lambda^{\beta_1}} , \\ \operatorname{tg} \theta = \dfrac{-\Delta - \lambda^{\alpha_1} + \{ (\Delta + \lambda^{\alpha_1})^2 + 8 \lambda^{\beta_1 2} \}^{\frac{1}{2}}}{2 \sqrt{2} \lambda^{\beta_1}} . \end{cases}$$

Now if we consider the first-order perturbation of the lowest orbital triplet due to the higher orbital states through spin-orbit interaction we can easily

calculate the second-order g-factors. These come out for this case as:

$$
(14) \quad \begin{cases}
g_{\parallel}^{(2)} = -\cos^2\gamma\left(\dfrac{\lambda^q q}{W_2 - W_0}\right) - \\
\qquad\qquad - 2\sin\gamma\cos\gamma\left(\dfrac{\lambda^{\beta_2}\alpha_2}{W_3 - W_0} + \dfrac{\lambda^{\beta_3}\alpha_3}{W_6 - W_0} + \dfrac{\lambda^{f_1} q}{W_2 - W_1}\right), \\[2ex]
g_{\perp}^{(2)} = -\dfrac{\sin\theta\sin\gamma}{\sqrt{2}}\left(\dfrac{3\lambda^{g_1} g_2}{W_4 - W_1} + \dfrac{3\lambda^{h_1} h_1}{W_5 - W_1} - \dfrac{\lambda^{f_1} f_1}{W_2 - W_1}\right) - \\
\qquad\qquad + \dfrac{\sin\theta\cos\gamma}{\sqrt{2}}\left(\dfrac{\lambda^q f_1}{W_2 - W_0} + \dfrac{\lambda^{\alpha_2}\beta_2}{W_3 - W_1} + \dfrac{\lambda^{\alpha_3}\beta_3}{W_6 - W_1}\right) - \\
\qquad\qquad - 2\cos\theta\cos\gamma\left(\dfrac{\lambda^{\beta_2}\beta_2}{W_3 - W_0} + \dfrac{\lambda^{\beta_3}\beta_3}{W_6 - W_0}\right),
\end{cases}
$$

where,

$$
(15) \quad \begin{cases}
\alpha_2 = (-\varepsilon_1\varepsilon_2 + 2\varrho_1\varrho_2 - \tau_1\tau_2)K\,, \\
\alpha_3 = (-\varepsilon_1\varepsilon_3 + 2\varrho_1\varrho_3 - \tau_1\tau_3)K\,, \\
q \ = 3\sqrt{2}\,\varrho_1' K\,, \\
\beta_2 = (\sqrt{6}\,\varepsilon_2\varepsilon_1' + \sqrt{3}\,\varrho_2\varrho_1' + \tau_2\tau_1')K\,, \\
\beta_3 = (\sqrt{6}\,\varepsilon_3\varepsilon_1' + \sqrt{3}\,\varrho_3\varrho_1' + \tau_3\tau_1')K\,, \\
f_1 = \sqrt{\tfrac{3}{2}}\,\varrho_1 K\,, \\
g_1 = (\sqrt{6}\,\varepsilon_1\varepsilon_2' + \sqrt{3}\,\varrho_1\varrho_2' + \tau_1\tau_2')K\,, \\
h_1 = (\sqrt{6}\,\varepsilon_1\varepsilon_3' + \sqrt{3}\,\varrho_1\varrho_3' + \tau_1\tau_3')K
\end{cases}
$$

and the corresponding matrix elements of $\lambda \boldsymbol{L}$ are given by a proper prefix on λ.

2. – Analysis of experimental g-values.

The spin hamiltonian constants given by ZVEREV and PROKHOROV are:

$$
\begin{cases}
g_{\parallel} \ = 1.915 \pm 0.002\,, \\
g_{\perp} \ = 1.63 \pm 0.05\,, \\
D \ = (7.0 \pm 0.3)\ \text{cm}^{-1}\,, \\
|A| = (0.959 \pm 0.005)\cdot 10^{-2}\ \text{cm}^{-1}\,, \\
|E| < 10^{-2}\ \text{cm}^{-1}\,.
\end{cases}
$$

2466

As the rhombic field is very small, we have analysed the above data on the basis of the first-order g-factors and using the expression of D, which is given by:

$$D = -\tfrac{1}{2}\lambda^{\alpha_1} + \tfrac{1}{2}\{(\Delta + \lambda^{\alpha_1})^2 + 8\lambda^{\beta_1^2}\}^{\frac{1}{2}} - \tfrac{1}{2}\{\Delta^2 + 4\lambda^{\beta_1^2}\}^{\frac{1}{2}} . \tag{16}$$

In our approximation $\alpha_1/\beta_1 = \lambda^{\alpha_1}/\lambda^{\beta_1}$, so corresponding to each value of α_1 and β_1, we have θ and γ fixed up from a comparison of theoretical expressions for first order g-values and the experimental data. Then the value of D fixes up Δ, λ^{α_1}, λ^{β_1}. If we do not evaluate the coefficients ε_1, etc., then there are various possible values of Δ as shown in Table I. But taking the values of coefficients ε_1, etc., into account we get,

$$\alpha_1 = 1.259\,73\,K$$

$$\beta_1 = 1.248\,36\,K$$

and so

$$\begin{cases} \lambda^{\alpha_1} = 1.259\,74\,\lambda R\,, \\ \lambda^{\beta_1} = 1.248\,36\,\lambda R \end{cases} \tag{17}$$

Consequently

$$\frac{\alpha_1}{\beta_1} = \frac{\lambda^{\alpha_1}}{\lambda^{\beta_1}} = 1.009\,. \tag{18}$$

As seen from Table I, this occurs only near about $\alpha_1 = \beta_1 = 1.2$ in which case the Δ's are 361.4 cm^{-1} and 405 cm^{-1} for the two D-values. The values of the covalent bonding factors come out as $K = 0.95$ and $R = 0.47$. The magnitude of R has increased considerably from the value which we obtained previously.

Now we calculate the contribution of second-order g-factors using the values of energy levels and states obtained earlier. These are given by:

$$\begin{cases} g_{\parallel}^{(2)} = -\,(0.026\,64)\,RK\cos^2\gamma - (0.017\,46)\,RK\sin\gamma\cos\gamma\,, \\ g_{\perp}^{(2)} = -\,(0.00\,12)\,RK\sin\theta\sin\gamma + (0.005\,8)\,RK\sin\theta\cos\gamma) - \\ \qquad\qquad - (0.19\,99)\,RK\cos\theta\cos\gamma\,. \end{cases} \tag{19}$$

We now use the values of R and K obtained above and add these g-factors to the first-order ones. But in this case the effect of the second-order terms becomes so much pronounced that it becomes impossible to get proper values of θ and γ so that $\alpha_1/\beta_1 = \lambda^{\beta_1}/\beta^{\alpha_1} = 1.00\ \theta$. So it is seen though the absolute magnitude of second-order terms is not large, but as the covalent factors depend

very sensitively on the deviations of the g's from the free spin value, so even this small second-order terms have profound effect on the magnitudes of K and R. The failure in our case to find values of K and R when second-order g-factors are taken into account may be due to a number of causes. First, our approximation of taking $K_{\pi\pi} = K_{\pi\sigma} = K$ and $R_{\pi\pi} = R_{\pi\sigma} = R$ is not correct as the contribution of π-bonding should not be as large as that of σ-bonding. But if we take into account two separate parameters for these bondings, it is not possible to find out these two parameters separately from the experimental values of the g's. Moreover, the calculations in the case of trigonal field become much more involved. Secondly, we have neglected the rhombic field effect. But in a precise calculation, one must take account of this also. This requires more calculations and so has not been attempted here. Thirdly, we have neglected the spin-spin interaction in the above analysis. If we take a value of 0.36 cm^{-1} for its contributions to D, then Δ for the two cases 1 and 2 becomes 383 and 424 cm^{-1}. So there is not any appreciable change in the value of the trigonal field splitting parameter.

3. – Conclusion.

Though it was not possible to find the effect of the second-order g-factors on the magnitude of Δ, but Δ should not be much different from the value of 400 cm^{-1}. This is smaller than that reported by FONER and LOW by a factor of 2. In order to clarify the position, we propose to undertake susceptibility measurements in the near future.

* * *

In conclusion, the author expresses his gratitude to Prof. M. SOUTIF for his interest in the work and to M. GASTINEL for arranging machine calculations.

RIASSUNTO (*)

Tenendo conto dell'effetto dello stato eccitato ^3P, della miscela trigonale del campo e anche del legame covalente, si sono eseguite analisi dettagliate degli spettri di risonanza parametrica degli elettroni della V^{3+} nel corindone. Risulta che la frattura trigonale è dell'ordine di 400 cm^{-1}. Si mostra che i fattori g del secondo ordine, provenienti dall'effetto degli stati orbitali superiori tramite interazioni spin-orbita, hanno un effetto molto significativo sulla valutazione dei fattori covalenti di legame.

(*) *Traduzione a cura della Redazione.*

IL NUOVO CIMENTO Vol. XX, N. 6 16 Giugno 1961

Primary Cosmic Ray α-Particles - II.

A. Engler (*), F. Foster, T. L. Green and J. Mulvey
The Clarendon Laboratory, University of Oxford - Oxford

(ricevuto l'8 Marzo 1961)

Summary. — Results of our investigation of the flux and energy spectrum of cosmic ray α-particles in August 1958 at a geomagnetic latitude of 61 °N are presented. The modulation mechanism recently proposed by Elliot is shown to provide a good description of the change in the energy spectrum between times of minimum and maximum solar activity.

Introduction.

In this paper we discuss observations of the fluxes and differential energy spectra of α-particles at a geomagnetic latitude 61° N. This region is of particular interest, since early studies ([1]) indicated the existence of a latitude « knee », *i.e.* a conspicuous lack of low energy particles. Later measurements, in particular those of Fowler *et al.* ([2]), contradicted the earlier findings, and were in fact among the first clues to our present picture of the correlation between primary cosmic ray intensities and the solar cycle.

Since the experimental procedure has been dealt with in detail in the first paper of this series, Engler *et al.* ([3]) which will be referred to as I, only the main points of the present experiment will be given. The results will then be compared with other data obtained at these latitudes and finally a discussion of the low energy part of the differential energy spectrum will be given.

(*) Now at Duke University, N. C.

([1]) S. F. Singer: *Prog. in Elementary Particle and Cosmic Ray Physics*, (Amsterdam, 1958), vol. 4, p. 286.

([2]) P. H. Fowler, C. J. Waddington, P. S. Freier, J. Naugle and E. P. Ney: *Phil. Mag.*, **2**, 157 (1957).

([3]) A. Engler, M. F. Kaplon, A. Kernan, J. Klarmann, C. E. Fichtel and M. W. Friedlander: *Nuovo Cimento*, **19**, 1090 (1961).

1. – Experimental details.

On August 3, 1958, a stack of 150 Ilford G-5 stripped emulsions 12 in. × × 8 in. × 600 μm, was flown from Neepawa, Man., Canada (*). The time-altitude

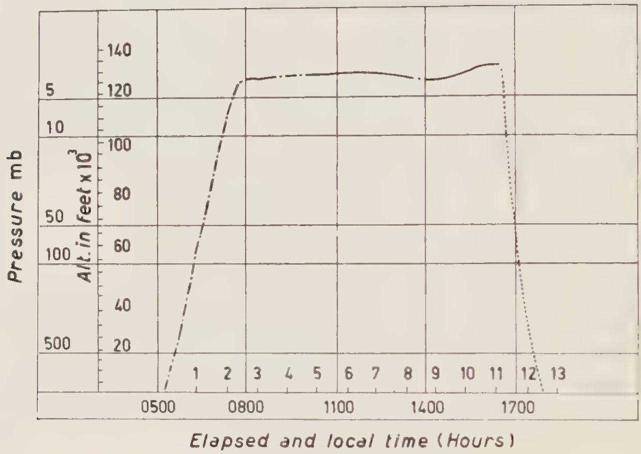

Fig. 1. – Time-altitude curve.

curve and flight trajectory are given in Fig. 1 and 2. A mechanism for rotating the emulsions at ceiling altitude, as described in I, was used. The total amount

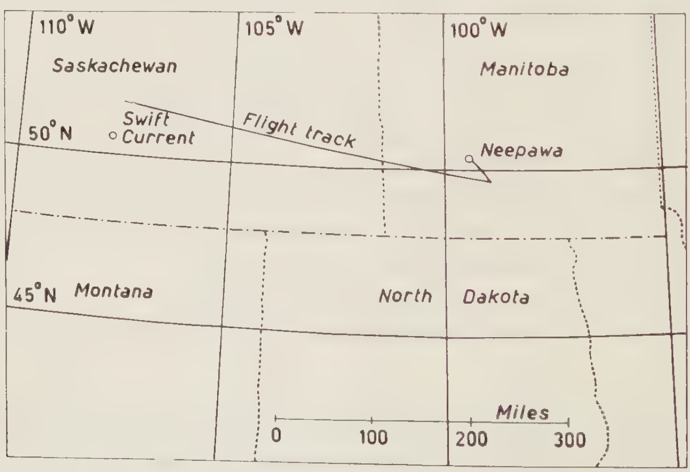

Fig. 2. – Flight track.

(*) A simultaineous flight was made from Moberly, Mo., U.S.A. and the results of this investigation will be presented in the next paper of this series.

2470

of matter above the stack was 3.8 g/cm², and the effective exposure time 8.5 hours.

The emulsion pellicles were slightly bent near the top of the stack and so the scanning for α-particle tracks was performed in two-stages. The first scan, to find α-particles with an energy greater than 120 MeV/nucleon at the top of the atmosphere, was carried out on a line 3 cm below the top edge where the effects of the bend would not influence the estimation of energy by the measurement of multiple scattering. In order to find less energetic α-particles, where the energy determination could be made by measurements of ionization alone, a second scan was made 0.5 cm below the top; in this case the lower energy limit for detection was ≈ 80 MeV/nucleon at the top of the atmosphere.

i) *Scan I.* Tracks crossing a line 3 cm below the top edge were selected according to the following criteria:

a) projected length per plate, $l \geqslant 7$ mm,

b) projected zenith angle, $\theta \leqslant 45°$,

c) grain density, $g \geqslant 34/100$ μm,
(the plateau grain density for α-particles, g^0_α, was 44/100 μm),

1014 tracks were found in this way and all were then followed through the stack. At this stage tracks which could be identified as due to protons by ionization and range measurement were removed from the sample. Finally only tracks with $l \geqslant 1$ cm and $\theta \leqslant 40°$ were accepted for further study.

ii) *Scan II.* The initial criteria for this scan, made at a depth of 0.5 cm, were:

a) $l \geqslant 5$ mm,

b) $\theta \leqslant 45°$,

c) grain density $\geqslant 68/100$ μm $(1.5 g^0_\alpha)$

and for inclusion in the energy measurements the final selection was of tracks with $l \geqslant 7$ mm and $\theta \leqslant 40°$. In order that the application of the scanning criterion on grain density should not lead to inefficiency, an upper limit of 275 MeV/nucleon $(g \approx 1.75 g^0_\alpha)$ was subsequently set in counting the contribution of the second scan to the total flux and differential energy spectrum (this corresponds to an energy ≈ 300 MeV/nucleon at the top of the atmosphere).

The overall scanning efficiency in both scans was 96 % and the flux values contain this correction.

Ionization and multiple scattering measurements, including correction for C shaped distortion and spurious scattering, were made as described in I. The error in the ionization parameter g^* was 8 % which gives an error in energy of $\lessapprox 15$ % for α-particles with energy less than 300 MeV/nucleon. In the determination of energy by measurement of multiple scattering enough readings were taken to ensure that the error, when calculated as in I (Appendix A), was always < 26 %.

2. – Results.

In the first scan a total of 239 α-particles were found, in the second 35. From this the flux of α-particles at the top of the atmosphere can be obtained in the same manner as in I. The original emulsion thickness had been measured prior to the flight and for the plates scanned the mean was 617 μm. In the present experiment an interaction mean free path for α-particles in emulsion of $\lambda = (24 \pm 2)$ cm was obtained. The value used in the calculation of the flux was $\lambda = 22$ cm (*) (the mean between our value and $\lambda = 20$ cm as given by WADDINGTON (4)). The flux value obtained is given in Table I, together with other data obtained at high altitudes.

TABLE I.

Location	Date of flight	Residual matter above detector (g/cm^2)	Zenith angle cut-off	$E_{\min}$ (MeV)	Flux (particles/m^2·srs)	Reference
Saskatoon, Can.	18 June 1954	10.6	45°	124	290 ± 20	(2)
Prince Albert, Can.	11 Sept. 1957	7.6	30°	100	137 ± 11	(5) Pt. IV
Neepawa, Can.	3 Aug. 1958	3.8	40°	80	135 ± 8	Present work

All flights were confined very nearly to $\lambda = 61°$, and the detectors emulsions.

(*) The change in flux due to a change in λ of 2 cm is of the order of 2%.

(4) V. Y. ROJOPADHYE and C. J. WADDINGTON: *Phil. Mag.*, **3**, 19 (1958).

(5) H. AIZU, Y. FUJIMOTO, S. HASEGAWA, M. KOSHIBA, I. MITO, J. NISHIMURA, K. YOKOI and M. SCHEIN: *Phys. Rev.*, **116**, 436 (1959) and *Proc. Moscow Cosmic Ray Conf.*, (1959), vol. 3.

Our data are in excellent agreement with those obtained at Prince Albert [5] one year earlier and show a decrease in the total flux of α-particles from the period of solar minimum of 55 %. Comparison with the data obtained at $\lambda = 55°$ (see I) shows that within experimental accuracy the fluxes at both latitudes are the same, *i.e.*, the additional flux in the energy range (90 ÷ 145) MeV (the cut-off values predicted by QUENBY and WEBBER at geomagnetic latitudes 61° and 55° N respectively [6]) is negligible. This is borne out by the rapid fall in intensity in the energy interval shown by the differential energy spectra, which are shown in Fig. 3. These results are also not inconsistent with a cut-off energy of 90 MeV/nucleon for α-particles at geomagnetic latitude 61° N [6].

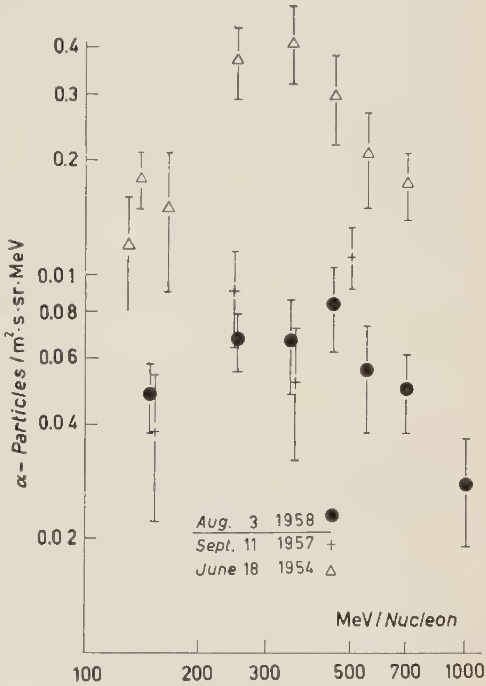

Fig. 3. – Differential energy spectra at solar maximum (1957-1958) compared with data at solar minimum (1954).

3. – Discussion.

From measurements of α-particle fluxes and differential energy spectra at $\lambda = 55°$ and higher latitudes with emulsions and counters during the period 1950-1958 as summarized in I, and the present paper, the following main features emerge:

a) The energy spectra during the period of low solar activity (1950-1956) are quite similar (apart from small variations which may be partly due to short time variations) in that they show a broad maximum around 350 MeV/nucleon kinetic energy with no noticeable increase in total flux with lower cut-off energy.

The « knee » previously observed is thus easily explained. At higher energies above about 600 MeV/nucleon the spectrum approaches asymptotically

---

([6]) J. J. QUENBY and W. R. WEBBER: *Phil. Mag.*, 4, 90 (1959).

2473

a power spectrum of the form

$$J(E) = K/(1+E)^y\,, \qquad y \approx 2.5.$$

b) During the subsequent period of high solar activity (from 1957 onwards) the total fluxes have decreased to about 55% of this previous value, the decrease being most pronounced at low energies while the maximum in the differential energy spectrum seems to have shifted to about 500 MeV/nucleon.

In addition the work of MACDONALD and WEBBER [7,8] has shown that protons and α-particles have very similar rigidity spectra during both periods of solar activity. There is also similar evidence [5] from studies of the heavy component of the primary cosmic radiation (particles with $Z \geq 3$) although less conclusive.

A number of models have been proposed to account not only for the long term variation of cosmic ray intensity but also to explain other phenomena such as Forbush decreases etc. In the model proposed by NAGASHIMA [9] it is assumed that during the period of increased solar activity particles of the cosmic radiation encounter a uniformly decelerating electric field as they approach the solar system. While the form of the rigidity spectrum predicted by this «electric» modulation mechanism accounts quite well for the change of the differential rigidity spectrum with time, it predicts a difference in this change for protons and α-particles at low rigidities due to the different charge-to-mass ratio of these particles, contrary to recent experimental evidence [7].

PARKER [10] has postulated that there exists a heliocentric shell of disordered magnetic field through which cosmic ray particles have to diffuse to reach the earth. If during times of high solar activity the sun were to emit ionized gas moving with relatively high velocity ((500 ÷ 1500) m/s) this «solar wind» would carry the magnetic field irregularities of the shell outwards and so reduce the intensity of cosmic rays inside the shell. However, the change in the rigidity spectrum predicted by this model is not in agreement with experiment [11]. Moreover the modulation is predicted to be different for protons and α-particles, again in contradiction to experiment.

The last model to be discussed here has recently been proposed by ELLIOT [12] who suggests that there exists a current system in the solar corona

(7) F. B. McDONALD: *Phys. Rev.*, **116**, 462 (1959).

(8) F. B. McDONALD and W. R. WEBBER: *Phys. Rev.*, **115**, 194 (1959).

(9) K. NAGASHIMA: *Journ. of Geomag. and Geoelect.*, **5**, 141 (1953).

(10) E. N. PARKER: *Phys. Rev.*, **110**, 1445 (1958).

(11) H. ELLIOT, R. J. HYNDS, J. J. QUENBY and G. J. WENK: *I.U.P.A.P. Cosmic Ray Conference* (Moscow, 1959) Vol. **3**.

(12) H. ELLIOT: *Phil. Mag.*, **5**, 601 (1960).

which generates an interplanetary magnetic dipole field. The effect of this field is modified by the presence of ionized gas clouds emitted by the sun and carrying magnetic fields which act as « scattering centres »; this provides a mechanism for particles of low rigidity, which might otherwise be excluded by the simple dipole fields, to diffuse into the solar region. Absorption by the sun, which competes with this process of diffusion, prevents the intensity within the solar system rising to equal the incident, galactic, intensity. The observed time variations in cosmic ray intensity are thus to be correlated with changes in the properties of the coronal ring currents and in the emission of ionized gas clouds.

ELLIOT finds the following expression relating the observed cosmic ray flux at the earth φ_E to the unmodulated galactic flux φ_∞:

$$\varphi_E = \varphi_\infty \left(\frac{45 M_s}{r_e^2 p}\right)^Y ,$$

where

$Y = \frac{1}{4}\left[1 - \{1 + 4\alpha K[(P_0 + P)/P]^2\}^{\frac{1}{2}}\right]$,

$M_s =$ the effective dipole moment of the coronal current system,

$r_e = 1.5 \cdot 10^{13}$ cm the distance between sun and earth,

$P =$ particle rigidity,

and K and P_0 are parameters related to the absorption probability and the scale and strength of the magnetic inhomogeneities respectively.

The above modulation mechanism is a function of rigidity only and thus protons and α-particles will be affected in a similar way, in agreement with experiment.

Following ELLIOT, we compare the differential energy spectra at the two epochs of solar activity under two assumptions:

a) The spectrum observed during solar minimum represents the actual galactic spectrum. For α-particles this has been shown ([13]) to be well represented by the relation:

$$J(E) = \frac{1.5 \cdot 415}{(1+E)^{2.5}}\,(1 - \exp[-80E^3]) ,$$

where E is the kinetic energy per nucleon.

([13]) F. B. MCDONALD: *Phys. Rev.*, **109**, 1367 (1958).

b) The galactic spectrum is actually a power spectrum

$$J(E) = 1.5\cdot 415/(1+E)^{2.5}\,,$$

and some modulation exists even at times of solar minimum. Under these assumptions we have calculated the spectra to be expected during the solar

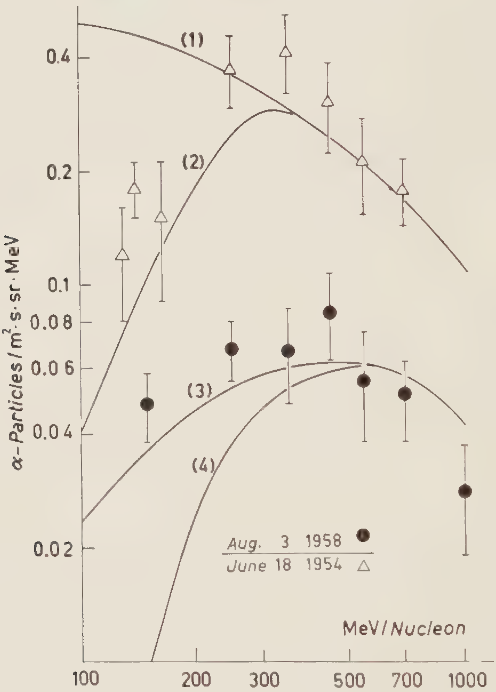

Fig. 4. – Upper curves (1), (2), show the theoretical spectra

$$J(E) = \frac{1.5\cdot 415}{(1+E)^{2.5}} \qquad \text{and} \qquad J(E) = \frac{1.5\cdot 415}{(1+E)^{2.5}}\left(1-\exp\left[-80E^3\right]\right).$$

The lower curves (3), (4), are obtained by applying the Elliot modulation function to (1) and (2) respectively.

maximum using the parameters suggested by ELLIOT, *i.e.*, $M = 3\cdot 10^{35}$ (*), $\alpha K = 0.5$ and $P_0 = 1.5$. The results are shown in Fig. 4 and it is seen that the agreement is quite good, especially under assumption *b*).

(*) During the recent Pioneer V flight a steady component of the magnetic field was observed with a value $2.7\cdot 10^{-5}$ G [14]; this corresponds to an effective solar dipole field of moment $\approx 10^{35}$ G cm³. Perturbations of this field were also found consistent in scale with those postulated in the Elliot model.

[14] P. J. COLEMAN jr., L. DAVIES and C. P. SONETT: *Phys. Rev. Lett.*, **5**, 43 (1960).

2476

Before any conclusions can be drawn about the correctness of this picture it is clearly necessary to have more accurate data regarding the very low energy end of the differential energy spectrum ($E < 250$ MeV/nucleon). Furthermore, measurements will have to be made during many intervals of the solar cycle to establish the range of variation of the parameters in the Elliot model.

* * *

The authors wish to thank Prof. WILKINSON and all members of the Oxford Emulsion group for helpful discussions; the Raven Industries Inc., South Dakota, for a successful balloon flight; F. F. and T. L. G. wish to thank the D.S.I.R. and the Shell Company respectively for maintenance grants.

We are most grateful to Mrs. BARBARA FOLEY, Miss JULIA PETTS, Mrs. ROMA VINCENT and Miss JOAN WALLER for carrying out the exacting task of scanning the plates.

RIASSUNTO (*)

Presentiamo i risultati del nostro studio sul flusso e sullo spettro di energia delle particelle α dei raggi cosmici nell'Agosto 1958 alla latitudine geomagnetica di 61° N. Mostriamo che il meccanismo di modulazione proposto recentemente da ELLIOT dà una buona descrizione del cambiamento dello spettro di energia fra le epoche di minima e di massima attività solare.

(*) *Traduzione a cura della Redazione.*

IL NUOVO CIMENTO Vol. XX, N. 6 16 Giugno 1961

Associated Production of Strange Particles.

M. Gourdin

Faculté des Sciences - Orsay (*)
Faculté des Sciences - Bordeaux (**)

M. Rimpault

Faculté des Sciences - Bordeaux (**)

(ricevuto il 22 Marzo 1961)

Résumé. – On se propose, dans cet article, de présenter un modèle pour le calcul de la production associée des particules étranges. Nous montrons que la complexité de la condition d'unitarité rend très difficile et probablement sans succès la technique des relations de dispersions. On envisage alors de considérer l'amplitude de réaction comme une somme de termes dûs d'une part à l'approximation de Born, d'autre part, à des resonances (pion-nucléon, pion-hypéron, pion-méson K). Les différentes possibilités pour les parités intrinsèques encore mal connues devront être considérées. Une confrontation du modèle avec les résultats expérimentaux est actuellement en cours mais les données expérimentales extrêmement imprécises et incomplètes rendent difficiles des conclusions nettes et des réponses précises aux problèmes que nous nous posons.

1. – Introduction.

The associated production of strange particles is of great importance in the elementary-particle physics. The simultaneous production of hyperons and K-mesons by pion-nucleon collisions at high energy is at the origin of the

(*) Postal adress: Laboratorie de Physique Théorique et Hautes Energies B.P. 12, Orsay (Seine et Oise).

(**) Postal address: Laboratoire de Physique Théorique, 351 Cours de la Libération, Talence (Gironde).

strangeness concept which led Gell-Mann and Nishijima to the famous scheme, mathematically understood later by D'ESPAGNAT and PRENTKI.

The problem of the theoretical calculation of the associated production amplitude from a quantum field theory is not yet resolved. The theory of perturbations is not satisfactory and cannot give a satisfactory explanation of the experimental results.

In this paper, we consider only the Λ and Σ hyperon of strangeness -1. The following reactions have been observed:

$$\pi^- + p \to \Lambda^0 + K^0$$

$$\pi^- + p \to \Sigma^- + K^+$$

$$\pi^- + p \to \Sigma^0 + K^0$$

$$\pi^+ + p \to \Sigma^+ + K^+ .$$

Under the assumption of charge independence, the three Σ production amplitudes $T^{(-)}$, $T^{(0)}$, $T^{(+)}$ are related to each other by

$$T^{(+)} - T^{(-)} = \sqrt{2}\, T^{(0)} .$$

It follows the existence of triangular inequalities for the three square roots of the differential and total cross-sections. The prediction seems, at present, to be experimentally verified (1).

The small mass difference between Λ and Σ suggests the possibility of some symmetries in the coupling of Λ and Σ with π-mesons, K-mesons, nucleons. By two different ways GELL-MANN (2) and SCHWINGER (3) assume the existence of a global symmetry where all baryons have the same interaction with π-mesons and cannot be distinguished. One can also postulate a symmetrical interaction of Λ and Σ with π-mesons and K-mesons: the restricted symmetry. Unfortunately, global and restricted symmetries lead to theoretical predictions uncompatible with experimental results on associated production.

PAIS (4) has suggested a possibility of reconciling experiments with the restricted symmetry: a K^+K^0 opposite parity. The fundamental symmetry is broken down at once by the $\Lambda\Sigma$ mass difference and the possibility of a direct $K^+K^0\pi$ parity conserving interaction with a strength similar to the electromagnetic interaction. But several theoretical difficulties remain as the K^+K^0 mass difference or the $N\Xi$ mass difference. We will not retain here this possibility.

---

(1) M. SCHWARTZ: *Report at the Rochester Conference* (1960).
(2) M. GELL MANN: *Phys. Rev.*, **10**, 1297 (1957).
(3) J. SCHWINGER: *Ann. Phys.*, **2**, 407 (1957).
(4) A. PAIS: *Phys. Rev.*, **110**, 1480 (1958).

If the relative $\Lambda\Sigma$ parity is odd, the concept of fundamental symmetry in the coupling of Λ and Σ with other particles loses any justification. We have no, at present, definitive experimental evidence about this problem. Nevertheless, the observed cusp in the Λ^0 production at the Σ threshold [5-7], is an indication, supported by some Λ and Σ photoproduction results [8] for an odd relative parity.

Another very important problem is the determination of the K intrinsic parity with respect to the Λ or the Σ. It has been shown that if the spin of the hyperfragment ${}^4\mathrm{He}_\Lambda$ is zero, the reaction:

$$\mathrm{K}^- + {}^4\mathrm{He} \to {}^4\mathrm{He}_\Lambda + \pi^-$$

is a selection rule for a pseudoscalar K-meson odd relative KΛ parity. This reaction has been observed [9]; unfortunately the spin of the ${}^4\mathrm{He}_\Lambda$ ground state is not at present unambiguously defined and the question is still open.

A very interesting feature of the associated production is the strong backward peaking of the angular distribution, in the center of mass system for the Λ^0 and Σ^0. On the other hand, in the Σ^+ production, no backward peaking has been observed and in the Σ^- production there seems to be some forward peaking at high energy. But the data, especially for the Σ production, are particularly meager.

The aim of this paper is to suggest a model to understand, in terms of poles, the associated production that can be valid only at low energy. We try to see how the π-Λ resonance and the π-K resonance can affect the associated production and if it is possible to obtain some information on the relative K, Λ, Σ intrinsic parities. We show that the use of a dispersion relation approach is very difficult and, in our opinion, not feasible.

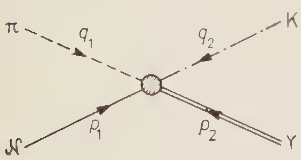

Fig. 1.

2. – Lorentz invariance.

2·1. *Kinematics.* – The ingoing energy-momentum four-vectors are labelled by q_i for the mesons and p_f for the baryons as indicated on Fig. 1. The symbol Y represents the Λ or Σ-hyperon.

(5) A. I. BAR and L. B. OKUN: *Žurn. Ėksp. Theor. Fiz.*, **35**, 757 (1958).
(6) R. ADAIR: *Phys. Rev.*, **111**, 632 (1958).
(7) M. H. ALSTON, J. A. ANDERSON, P. G. BURKE, D. D. CARMONY, F. S. CRAWFORD, N. SCHMITZ and S. E. WOLF: *Proceedings of the Rochester Conference* (1960).
(8) F. TURKOT: *Report at the Rochester Conference* (1960).
(9) M. M. BLOCK, E. B. BRUCKER, I. S. HUGHES, T. K. KUCHI, C. MELTGER, F. ANDERSON, A. PEVSNER, E. M. HARTH, J. LEITNER and H. O. COHN: *Phys. Rev. Lett.*, **3**, 291 (1959).

We introduce as usual three scalar quantities

$$\begin{cases} s = -(p_1+q_1)^2 = -(p_2+q_2)^2\,, \\ t = -(p_1+p_2)^2 = -(q_1+q_2)^2\,, \\ u = -(p_1+q_2)^2 = -(p_2+q_1)^2\,. \end{cases}$$

Channel I describes the associated production of strange particles.

Channel II is the nucleon-antihyperon pair production from the pion-kaon system.

Channel III corresponds to the hyperon production by K-meson absorption in nucleons.

We have the following conservation rules:

$$\begin{cases} p_1+p_2+q_1+q_2=0\,, \\ s+t+u = M_{\mathcal{N}}^2+M_{\text{Y}}^2+\mu^2+\varkappa^2=\sum m^2\,, \end{cases}$$

where $M_{\mathcal{N}}$, M_{Y}, μ, $\varkappa$ are respectively the nucleon, hyperon, π-meson and K-meson masses.

2'2. *S-matrix element.* – We disregard, for a moment, the problem of invariance, in the isotopic spin space. With a convenient choice of normalization factors, the S-matrix element can be written as:

$$S_{fi} = \delta_{fi} - i(2\pi)^4\delta_4(p_1+p_2+q_1+q_2)\,\frac{1}{(2\pi)^6}\,\frac{\sqrt{M_{\mathcal{N}}M_{\text{Y}}}}{2(p_1^0p_2^0q_1^0q_2^0)^{\frac{1}{2}}}\,\mathcal{T}_{fi}\,. \tag{3}$$

We now consider the general process where a boson of spin zero collides a fermion of spin $\frac{1}{2}$ producing a boson of spin zero and a fermion of spin $\frac{1}{2}$. The problem of intrinsic parities is very crucial and we introduce the quantity ε_{Y} defined as the intrinsic parity for the system KY$\mathcal{N}$.

From Lorentz invariance, the general form for the $\mathcal{T}$ matrix is well known. For $\varepsilon_{\text{Y}}=+1$ we have:

$$\mathcal{T}_{fi} = \bar{u}_{\text{Y}}(-p_2)\left[i\gamma_5 A(s,t,u) + B(s,t,u)\gamma_5\gamma_\mu\,\frac{(q_1-q_2)}{2}\,\mu\right]u_{\mathcal{N}}(p_1)\,, \tag{4}$$

and for $\varepsilon_{\text{Y}}=-1$

$$\mathcal{T}_{fi} = \bar{u}_{\text{Y}}(-p_2)\left[-A(s,t,u) + iB(s,t,u)\gamma_\mu\,\frac{(q_1-q_2)}{2}\,\mu\right]u_{\mathcal{N}}(p_1)\,, \tag{5}$$

where $u_{\mathrm{Y}}(-p_2)$ and $u_{\mathcal{N}}(p_1)$ are the free Dirac spinors describing respectively the hyperon and the nucleon.

The two functions A and B are spin independent.

2'3. *Center-of-mass system.* – We introduce the center-of-mass variables for the channel I by the following definitions:

$$p_1 = (-\boldsymbol{k}_1, E_1)\,, \qquad q_1 = (+\boldsymbol{k}_1, \omega_1)\,,$$
$$p_2 = (-\boldsymbol{k}_2, -E_2)\,, \quad q_2 = (+\boldsymbol{k}_2, -\omega_2)\,,$$

with

$$E_1 = \sqrt{k_1^2 + M_{\mathcal{N}}^2}\,, \qquad \omega_1 = \sqrt{k_1^2 + \mu^2}\,,$$
$$E_2 = \sqrt{k_2^2 + M_{\mathrm{Y}}^2}\,, \qquad \omega_2 = \sqrt{k_2^2 + \varkappa^2}\,.$$

We immediately deduce

$$\left|\begin{array}{l} s = W^2 = (E_1 + \omega_1)^2 = (E_2 + \omega_2)^2\,, \\ t = (\omega_1 - \omega_2)^2 - (\boldsymbol{k}_1 + \boldsymbol{k}_2)^2 = \mu^2 + \varkappa^2 - 2\omega_2\omega_1 - 2k_1k_2\cos\theta\,, \\ u = (E_1 - \omega_2)^2 - (\boldsymbol{k}_1 - \boldsymbol{k}_2)^2 = M_{\mathcal{N}}^2 + \varkappa_2 - 2\omega_2 E_1 + 2k_1k_2\cos\theta\,, \end{array}\right.$$

θ is the center-of-mass angle between the incident pion and the outgoing hyperon, defined by

$$\boldsymbol{k}_1\cdot\boldsymbol{k}_2 = k_1k_2\cos\theta\,.$$

It is then easy to obtain the differential cross-section

$$\frac{\mathrm{d}\sigma}{\mathrm{d}\Omega} = \frac{k_1}{k_2}\left(\frac{1}{8\pi W}\right)^2 |\langle\chi_{\mathrm{Y}}|T|\theta\chi_{\mathcal{N}}\rangle|^2\,, \tag{6}$$

where χ_{Y} and $\chi_{\mathcal{N}}$ are two Pauli spinors describing the fermion spin states and T a 2×2 matrix in the spin space one can easily compute from the $\mathcal{T}$ matrix previously introduced.

The general form for the T matrix depends of the parity ε_{Y}. We introduce two scalar functions f_1 and f_2 by the definitions:

$$T = i(\boldsymbol{\sigma}\cdot\hat{k}_2)f_1 - i(\boldsymbol{\sigma}\cdot\hat{k}_1)f_2\,, \qquad \text{for } \varepsilon_{\mathrm{Y}} = +1\,, \tag{7}$$

and

$$T = f_1 - (\boldsymbol{\sigma}\cdot\hat{k}_2)(\boldsymbol{\sigma}\cdot\hat{k}_1)f_2\,, \qquad \text{for } \varepsilon_{\mathrm{Y}} = -1\,,$$

$\hat{k}_1$ and $\hat{k}_2$ are unit vectors for initial and final c.m. momenta.

The functions f_1 and f_2 are given in terms of A and B defined in eq. (4) or (5) by:

$$(9)\quad \begin{cases} f_1 = \sqrt{(E_1 + M_{\mathcal{N}})(E_2 - M_Y)}\left[A + B\left(W + \dfrac{M_Y - M_{\mathcal{N}}}{2}\right)\right], \\ f_2 = -\sqrt{(E_1 - M_{\mathcal{N}})(E_2 + M_Y)}\left[A - B\left(W - \dfrac{M_Y - M_{\mathcal{N}}}{2}\right)\right], \end{cases} \quad \text{for } \varepsilon_Y = +1 ,$$

and (*)

$$(10)\quad \begin{cases} f_1 = \sqrt{(E_1 + M_{\mathcal{N}})(E_2 + M_Y)}\left[A + B\left(W - \dfrac{M_Y + M_{\mathcal{N}}}{2}\right)\right], \\ f_2 = -\sqrt{(E_1 - M_{\mathcal{N}})(E_2 - M_Y)}\left[A - B\left(W + \dfrac{M_Y + M_{\mathcal{N}}}{2}\right)\right], \end{cases} \quad \text{for } \varepsilon_Y = -1 .$$

2'4. *Eigenstates of total angular momentum J and parity ω.* – Conservation of total angular momentum J and parity ω gives some selection rules for the orbital angular momentum l.

If $\varepsilon_Y = -1$, the orbital angular momentum is a good quantum number and we have $l_f = l_i = l$; $J = l \pm \frac{1}{2}$.

If $\varepsilon_Y = +1$ the orbital angular momentum changes by one unit and more precisely:

$$J = l_i \pm \tfrac{1}{2} = l_f \mp \tfrac{1}{2}, \qquad l_f = l_i \pm 1 .$$

We now expand the T matrix in eigenstates of angular momentum J and parity ω. For a given value of the orbital angular momentum l for the initial M-N system, we have:

$$\begin{cases} J = l + \frac{1}{2} \quad \omega = (-1)^{l+1} \Rightarrow \begin{cases} l_f = l & \varepsilon_Y = -1 \\ l_f = l + 1 & \varepsilon_Y = +1 \end{cases} \\[2ex] J = l - \frac{1}{2} \quad \omega = (-1)^{l} \Rightarrow \begin{cases} l_f = l & \varepsilon_Y = -1 \\ l_f = l - 1 & \varepsilon_Y = +1 . \end{cases} \end{cases}$$

The knowledge of J and l permits us in the two cases $\varepsilon_Y = \pm 1$, to precise the final orbital momentum for the KY system. This leads us to introduce so reduced matrix elements, $f_l^{\pm}$, the sign $\pm$ corresponding to the values of $J = l \pm \frac{1}{2}$. By using straightforward methods [10] we expand T in eigenstates

(*) With the definitions (4), (5), (7), (8), we remark that the trick to go from the case $\varepsilon_Y = +1$ to the case $\varepsilon_Y = -1$ is simply the change of M_Y into $-M_Y$.

[10] See for example R. STORA: *Seminar given in Istituto di Fisica* (Bologna, 1960).

of J and ω in the following manner:

$$T=\sum_l (2l+1)[f_l^+P_l^+ + f_l^-P_l^-]P_l(\cos\theta)\,, \qquad \text{if } \varepsilon_Y=-1\,,$$

and

$$T=i(\boldsymbol{\sigma}\cdot\hat{k}_2)\sum_l (2l+1)[f_l^+P_l^+ + f_l^-P_l^-]P_l(\cos\theta)\,, \qquad \text{if } \varepsilon_Y=+1\,.$$

The projection operators $P_l^\pm$ are defined as usual by

$$P_l^+=\frac{l+1+\boldsymbol{\sigma}\cdot\boldsymbol{l}}{2l+1}\,, \qquad P_l^-=\frac{l-\boldsymbol{\sigma}\cdot\boldsymbol{l}}{2l+1}\,,$$

where $\boldsymbol{l}$ is the orbital angular momentum defined in a diagonal representation by

$$\boldsymbol{l}=\frac{1}{i}\hat{k}_2\cdot\nabla_{\hat{k}_2}\,.$$

with the following property

$$\boldsymbol{l}P_l(\cos\theta)=\frac{1}{i}(\hat{k}_2\times\hat{k}_1)P_l'(\cos\theta)\,.$$

We are now able to obtain the development of f_1 and f_2 in partial matrix elements f_l^+ and f_l^-. The formulas are the same in the two cases $\varepsilon_Y=\pm1$:

$$f_1=\sum_l (f_{l-1}^+ - f_{l+1}^-)P_l'(\cos\theta)\,,$$

$$f_2=\sum_l (f_l^+ - f_l^-)P_l'(\cos\theta)\,.$$

By inverting these formulas we can obtain the expression of $f_l^\pm$ in terms of f_1 and f_2

$$f_l^+=\frac{1}{2}\int_{-1}^{+1}[f_1P_l(\cos\theta)-f_2P_{l+1}(\cos\theta)]\,\mathrm{d}\cos\theta\,,$$

$$f_l^-=\frac{1}{2}\int_{-1}^{+1}[f_1P_l(\cos\theta)-f_2P_{l-1}(\cos\theta)]\,\mathrm{d}\cos\theta\,.$$

3. – Isospin and Born terms.

1) For the process

$$\pi_\alpha+\mathcal{N}\to\mathrm{K}+\Lambda$$

2484

one has only one isospin state $I=\frac{1}{2}$. The amplitude T_α for a π incident meson of isospin index α has the simple form:

$$T_\alpha = (\tau_\alpha)\, T\,,$$

where T is now independent of isospin.

2) In the case of Σ associated production

$$\pi_\alpha + \mathcal{N} \rightarrow \mathrm{K} + \Sigma_\beta$$

we have two isospin states $I=\frac{1}{2}$ and $I=\frac{3}{2}$, as in the $\pi\mathcal{N}$ scattering case. It becomes then very evident that the $T_{\beta\alpha}$ amplitude can be written as:

$$T_{\beta\alpha} = \delta_{\beta\alpha} T^{(0)} + \tfrac{1}{2}[\tau_\beta\,, \tau_\alpha]\, T^{(1)}\,,$$

where the Pauli matrices act on the nucleon.

3) The first Born term, in channel I consists in one nucleon intermediate state:

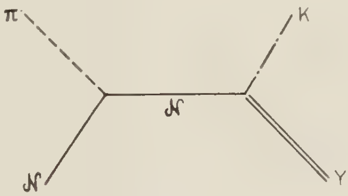

Fig. 2.

One has a pole at $s = M^2_{\mathcal{N}}$ and the value of the residue for A and B depends on the parity ε_Y. The results are given in Table I:

TABLE I.

	A	B
$\varepsilon_\mathrm{Y} = 1$	$-\dfrac{M_\mathrm{Y} + M_{\mathcal{N}}}{2}$	1
$\varepsilon_\mathrm{Y} = -1$	$\dfrac{M_\mathrm{Y} - M_{\mathcal{N}}}{2}$	1

with the common factor for A and B:

$$\left|\begin{array}{ll} g_{\pi\mathcal{N}\mathcal{N}}g_{K\Lambda\mathcal{N}}\dfrac{\tau_\alpha}{M_{\mathcal{N}}^2-s}, & \text{for the } \Lambda \text{ production,} \\ g_{\pi\mathcal{N}\mathcal{N}}g_{K\Sigma\mathcal{N}}\dfrac{\tau_\beta\,\tau_\alpha}{M_{\mathcal{N}}^2-s}, & \text{for the } \Sigma \text{ production.}\end{array}\right.$$

4) The second Born term corresponds to a pole in the channel III:

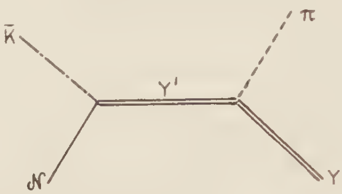

Fig. 3.

The intermediate hyperon Y′ must be a Σ if Y is a Λ and can be a Σ or a Λ if Y is a Σ. The relative parity ΣΛ, quoted as ε ($\varepsilon = \varepsilon_\Lambda \varepsilon_\Sigma$) plays a very important role in this diagram.

We give the results in Table II, with the common factor for A and B

TABLE II.

	A	B
$\varepsilon_{Y'} = 1$, $\varepsilon = 1$	$-M_{Y'} + \dfrac{M_Y - M_{\mathcal{N}}}{2}$	1
$\varepsilon_{Y'} = -1$, $\varepsilon = 1$	$-M_{Y'} + \dfrac{M_Y + M_{\mathcal{N}}}{2}$	-1
$\varepsilon_{Y'} = 1$, $\varepsilon = -1$	$M_{Y'} + \dfrac{M_Y + M_{\mathcal{N}}}{2}$	-1
$\varepsilon_{Y'} = -1$, $\varepsilon = -1$	$-M_{Y'} - \dfrac{M_Y - M_{\mathcal{N}}}{2}$	-1

$$\left|\begin{array}{ll} g_{K\Sigma\mathcal{N}}g_{\pi\Sigma\Lambda}\dfrac{\tau_\alpha}{M_\Sigma^2-u}, & \text{for the } \Lambda \text{ production,} \\ g_{K\Sigma\mathcal{N}}g_{\pi\Sigma\Sigma}\dfrac{\frac{1}{2}[\tau_\beta,\tau_\alpha]}{M_\Sigma^2-u}, & \text{for the } \Sigma \text{ production with an intermediate } \Sigma, \\ g_{K\Lambda\mathcal{N}}g_{\pi\Sigma\Lambda}\dfrac{\delta_{\alpha\beta}}{M_\Lambda^2-u}, & \text{for the } \Sigma \text{ production with an intermediate } \Lambda.\end{array}\right.$$

4. – Unitarity condition and associated production channel.

The study of the various intermediate states contributing to the dispersion integrals for the three channels has been made in a previous paper ([11]). We now try to see if these results can be applied in a practical way to determine the associated production amplitude.

1) In channel I, the dispersion integrals with respect to the energy variable S begin at $(M_{\mathcal{N}}+\mu)^2$, corresponding to the one nucleon-one pion state, while the physical threshold for the associated production of strange particles is $(M_Y+\varkappa)^2$. We then have an anomalous cut from $(M_{\mathcal{N}}+\mu)^2$ to $(M_Y+\varkappa)^2$ which is very large ([12]). In Fig. 4, we reproduce the various cuts, in the complex S plane corresponding to the pole and the various multipole pions production thresholds:

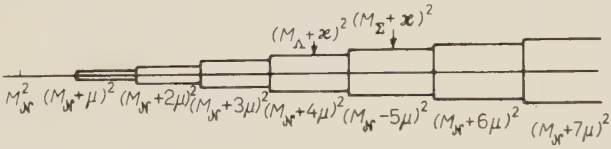

Fig. 4.

If we retain only the one nucleon-n pion states, the unitarity condition takes the following symbolic form:

$$\operatorname{Im}\langle YK|T|\mathcal{N},\pi\rangle = \sum_n \langle YK|T|\mathcal{N}, n\pi\rangle\langle\mathcal{N}, n\pi|T|\mathcal{N},\pi\rangle^* .$$

The spectral function on the anomalous cut is the analytic continuation of this unitarity condition ([13]) obtained by simple analytic continuation of the $Y+K \to \mathcal{N}+n\pi$ transition amplitude.

For example, in the range $(M_{\mathcal{N}}+\mu)^2 < s < (M_{\mathcal{N}}+2\mu)^2$, the unitarity condition can be continuated in the simple form:

$$\operatorname{Im} f_l^{\pm} = f_l^{\pm} \exp[-i\delta_l^{\pm}] \sin\delta_l^{\pm} ,$$

where $\delta_l^{\pm}$ is the pion-nucleon scattering phase shift in the state of orbital

([11]) M. Gourdin et M. Rimpault: *Production associée de particules, étranges* (Bordeaux, 1959).

([12]) For a systematical study of the kinematic for problems involving strange particles see: J. Trotin: *Thesis* (Bordeaux, 1960).

([13]) S. Mandelstam: *Phys. Rev. Lett.*, **4**, 84 (1960).

angular momentum l and total angular momentum $j=l\pm\frac{1}{2}$. Such a form for the spectral function leads to an Omnès-Mushkelishvili integral equation, one can solve in terms of contributions from channels II and III [14]. Unfortunately we are interested by the associated production amplitude in the physical range $s>(M_Y+\varkappa)^2$. By inspection of Fig. 4, we immediately see that the present situation is the same as for the multiple pion production amplitude

$$\pi+\mathcal{N}\to n\pi+\mathcal{N}$$

with n of the order of 5 or 6.
In follows that, in the dispersion integrals it is a complete non-sense to use the approximate spectral function calculated, as before, with only the one nucleon-one pion intermediate state. It is not possible to neglect the inelastic processes in this range of energy. On the other hand, we do not know the analytic properties for the transition amplitudes corresponding to multiple pion production. There is then no manner to take into account such intermediate states which are certainly very important.

The technique of dispersion relations cannot be used for the associated production process, just as for the multiple pion production, without some drastic approximations.

2) In this paper we shall not use this very difficult and probably unsuccessful approach. We only try to construct a phenomenological model for the associated production at low energy, more refined than the Born approximation unable to reproduce the experimental data. In the spirit of dispersion relations, we consider simultaneously all three channels and try to replace the cuts on the variables, s, t and u, by some appropriate poles in order to reproduce the effects of resonant states in the three channels.

It is not difficult to understand why such an approximation, applied to channels II and III is legitimate, so long as we are interested by the associated production amplitude of channel I.

For the π-$\mathcal{N}$ resonances, the situation appears evidently as more difficult. We essentially know three π-$\mathcal{N}$ resonances:

a) The famous $I=\frac{3}{2}$, $J=\frac{3}{2}$, $L=1$ resonance at 190 MeV (kinetic energy of the incident π-meson in the laboratory system).

b) The second resonance at 605 MeV, probably in the states:

$$I=\tfrac{1}{2}\,,\qquad J=\tfrac{3}{2}\,,\qquad L=2\,.$$

(14) See for example: Appendix III in M. GOURDIN and A. MARTIN: *Nuovo Cimento*, **17**, 224 (1960).

c) The third resonance at 890 MeV with the probable quantum numbers:

$$I = \tfrac{1}{2}\,, \qquad J = \tfrac{5}{2}\,, \qquad L = 3\,.$$

For the second and third resonance, the resonant states are not perfectly defined; the results quoted here are those given by a polarization analysis of a π^0 photoproduction experiment ([15]).

We associate in the s-plane, a pole to each resonance and we reproduce, in Fig. 5, the position of the three resonances with respect to the production thresholds:

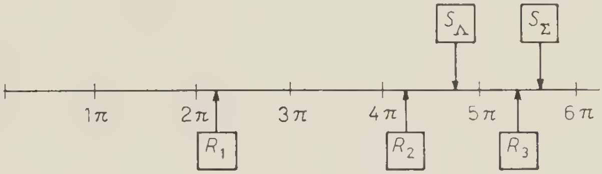

Fig. 5.

In order to understand the multiple π-meson production mechanism, as far as the associated production process we certainly must take into account the existence of the π-$\mathcal{N}$ resonances ([16]), in a phenomenological way. We shall construct a model which possesses some similitudes with an isobaric model and we add to the π-$\mathcal{N}$ terms some contributions given by channels II and III.

5. – Contributions from channels II and III.

The first intermediate state, in channel II is a π-K state and, in channel III, a π-Y state. In both cases a resonance has been observed experimentally. For the associated production amplitude, we shall retain only these resonant contributions and replace the cut over the variables t and u by some poles located at the resonance energies.

5·1. *Channel II.* – By measuring the momentum distribution of the outgoing proton in the reaction:

$$K^- + p \to \overline{K}^0 + \pi^- + p\,.$$

([15]) R. Querzoli, G. Salvini and A. Silvestrini: *Nuovo Cimento*, **19**, 53 (1961).

([16]) R. F. Peierls: *Lectures given in the Corsica Summer School* (1960); *Phys. Rev.*, **118**, 325 (1960).

Good interprets the deviation of the spectrum from the statistical phase space distribution as a π-K resonance (17). The position of this resonance appears as well defined: $E_k = (880 \div 900)$ MeV and it seems to be very sharp $\Gamma \simeq 10$ MeV. On the other hand, some theoretical speculations (18) permit to predict the existence of a $J = 0$, $I = \frac{1}{2}$ πK resonance, labelling the K′ particle, with an odd K′K relative parity in order to allow a parity conserving KK′π coupling. Unfortunately, at present the quantum numbers J and I of this π-K resonance are yet experimentally very bad known.

The K′ particle gives a contribution of the form:

$$\frac{\lambda}{t - t_R}, \quad \text{where } t_R = E_R^2 = M_{K'}^2,$$

and this corresponds, in the $\cos\theta$ plane, to a pole, in the unphysical region for $\cos\theta < -1$ provided that t_R is sufficiently large. The estimations given by Tiomno with a one pole model for associated $\Lambda^0 K^0$ production leads to a value $M_{k'} \simeq \varkappa + \mu$ for the K′ particles mass.

The isospin assignment of the resonance is particularly important. In the case of Λ^0 and Σ^0 production, a strong backward peaking has been observed (19) and can be explained by the K′ pole (20) if $I = \frac{1}{2}$ and $J = 0$. One immediately sees that with such an assumption, the K′ mechanism is not available for Σ^- production where some forward peaking has been experimentally observed. In the alternative of a $I = \frac{3}{2}$ isospin for the π-K resonance the situation is inverted: we have no contribution in Λ^0 production and contribution in Σ^- production; and the situation is more confusing.

5·2. *Channel III.* – A π-hyperon resonance has been found in the reactions

$$K^- + p \rightarrow \Lambda^0 + \pi^- + \pi^+ \qquad (21)$$

$$K^- + {}^4\mathrm{He} \rightarrow \Lambda^0 + \pi^- + {}^3\mathrm{He} \qquad (22)$$

by using the same method as for the π-K resonance.

The peak in the π^+ momentum distribution in the first experiment, and

(17) M. L. Good: *Report in the Rochester Conference* (1960).

(18) J. Bernstein and S. Weinberg: *Phys. Rev. Lett.*, **5**, 481 (1960).

(19) See *e.g.* J. Steinberger: *Proceedings of the Geneva Conference* (1958).

(20) For the role of such a pole in associated production process, see J. G. Taylor: *Nucl. Phys.*, **9**, 357 (1959).

(21) M. Alston, L. W. Alvarez, P. Eberhard, M. L. Good, W. Graziano, H. K. Ticho and S. G. Wojcicki: *Phys. Rev. Lett.*, **5**, 520 (1960); M. Ferro-Luzzi, J. P. Berge, J. Kirz, J. M. Murray, A. H. Rosenfeld and M. Watson: *Bull. Am. Phys. Soc.*, **5**, 509 (1960).

in the ^{3}He momentum distribution for the second reaction can be explained by a Λ^0-π^- resonance labelling the Y* state at the energy $E_R = (1380 \pm 30)$ MeV. The isospin is well defined because the Λ-π system can be only in the $I = 1$ state. For the total angular momentum J and the intrinsic parity ξ_{Y^*} the experimental situation is not yet so clear.

Preliminary results on polarization experiments seem to indicate the value $J = \frac{1}{2}$ for the total angular momentum of the state Y*. On the other hand, we have observed an S-decay $Y^* \to \Lambda + \pi$ and no decay $Y^* \to \Sigma + \pi$. These results can be explained if one assumes a $\xi_{Y^*} = -1$ intrinsic parity ([23]) which permits the S wave for the $\Lambda + \pi$ system and a $\xi_\Sigma = -1$ intrinsic parity which forbids the S wave for the $\Sigma + \pi$ system. But it is not the unique way to understand the experimental results.

The existence of some other $\pi\Sigma$ resonances in the $I = 0$ or $I = 2$ isospin states has been predicted in some theoretical models ([24]). We have no experimental evidence for such resonances at least up to 1600 MeV. This energy is sufficiently large to permit us to neglect these other possible resonances in our problem.

The Y* state gives a contribution of the form:

$$\frac{\lambda}{u - u_R}, \quad \text{where } u_R = E_R^2 = M_{Y^*}^2,$$

In the complex $\cos\theta$ plane, this corresponds to a pole in the unphysical region for channel I, more precisely for $\cos\theta > +1$. This pole can produce a forward peaking in the angular distribution but the effect is more difficult to understand, because we have a competition with the Born terms and the total result cannot be predicted *a priori*.

6. – Model and programme of calculations.

We represent the associated production amplitude as a sum over three types of terms classified according to the channels whence they come.

1) *Channel I.* We have the Born term, given in Fig. 2 with a one nucleon intermediate state and the π-$\mathcal{N}$ resonance pole terms. The corres-

---

([22]) A. STANGHELLINI: private communication.

([23]) For the particles of strangeness $s = \pm 1$, we can choose arbitrarily an intrinsic parity as reference; by convention we put $\varepsilon_Y = +1$.

([24]) D. AMATI, A. STANGHELLINI and B. VITALE: *Nuovo Cimento*, **13**, 1143 (1959); *Phys. Rev. Lett.*, **5**, 524 (1960).

ponding contributions to the scalar functions A and B are of the general form:

$$\frac{\lambda_{\text{I}}}{s - s_R}.$$

and depend evidently on the isospin states.

2) *Channel II.* We retain only the K′ particle contribution

$$\frac{\lambda_{\text{II}}}{t - t_R}, \quad \text{with } t_R = M^2_{\text{K}'}.$$

3) *Channel III.* We have here, the Born terms given in Fig. 3 with a one hyperon intermediate state and the πY resonance simulated by the Y* particle

$$\frac{\lambda_{\text{III}}}{u - u_R}.$$

The quantities λ_{I}, λ_{II}, λ_{III} are closely related to the quantum numbers J, L and I of the one particle or metastable particle intermediate state.

The parameters entering in the transition amplitude are of two types:

1) *The coupling constants.* π meson-baryon and K meson-baryon which, at present, are yet bad known. In particular the knowledge of the relative $\Lambda\Sigma$ intrinsic parity is very important. If $\varepsilon(\Lambda\Sigma) = -1$ the notion of global or restricted symmetry is meaningless and it becomes very difficult to estimate an order of magnitude for the $g_{\Sigma\Lambda\pi}$ and $g_{\Sigma\Sigma\pi}$ coupling constants.

2) *The residues λ for the resonance terms.* One can interpret in terms of coupling constants between the Y* or K′ particles with pions, kaons and baryons. In principle, the same constants occur in some other phenomena where the Y* and K′ particles play a part, as K-nucleon scattering, K absorption by nucleons, hyperon-nucleon scattering, strange particle associated photoproduction, etc. At least in principle, it is possible to relate these processes to each other in order to obtain some indications on the values of the results. Unfortunately the experimental results are so poor that no valid information can be obtained at present in this manner.

For the π-$\mathcal{N}$ resonances, the problem is lightly different because we have more experimental information on the π-meson multiple production. As an example, the consideration of the $\frac{3}{2}$ $\frac{3}{2}$ isobar is a fruitful concept not only for a qualitative description of some experimental features but also for a quantitative explanation of the data as the second π-$\mathcal{N}$ resonance.

Our programme of computations is to try to reproduce the experimental results for Λ, Σ^+, Σ^- production at low energy, differential and total cross-sections, in order to obtain an answer to the following questions:

1) Domain of validity, in energy, of the model.

2) Relative importance of the various contributions.

3) Determination of the best set of intrinsic parities.

Identical considerations can be used for the photoproduction of strange particles. We introduce beside the Born terms, the Y^* and K' intermediate states and we take into account the $\pi\mathcal{N}$ resonances in the photoproduction channel. Some parameters occuring in this model are the same as in the associated production model and we hope to improve the knowledge of the parameters by considering simultaneously the two types of reactions.

7. – Conclusions.

Some numerical calculations are in progress in order to obtain some information on the associated production problem.

In the first approach, we can neglect the Y^* contribution because the corresponding pole is very far from the physical domain. The situation is not exactly the same for the K' particle but it remains difficult to understand why one can neglect the πK cut, from $(\mu+\varkappa)$ to the resonance energy. Nevertheless it seems possible to explain the backward peaking in the Λ^0 and Σ^0 production with a πK $I=\frac{1}{2}$ resonance. But one can hold for certain that it cannot be the only explanation for the features exhibited by the associated production amplitudes. For the π-$\mathcal{N}$ terms, one uses a Breit-Wigner formula to evaluate the residues from experimental data (resonance energy and width); but in the physical range of associated production, we can neglect the width in a preliminary calculation.

RIASSUNTO (*)

Ci proponiamo in questo articolo di presentare un modello per il calcolo della produzione associata delle particelle strane. Mostriamo che la complessità della condizione di unitarietà rende molto difficile e probabilmente priva di successo la tecnica delle relazioni di dispersione. Si propone allora di considerare l'ampiezza di reazione come una somma di poli dovuti da una parte a termini di Born, d'altra parte a risonanze (pione-nucleone, pione-iperone, pione-mesone K). Si dovrebbero prendere in considerazione le differenti possibilità per le parità intrinseche, ancora mal note. Un confronto del modello con i risultati sperimentali è attualmente in corso, ma i dati sperimentali estremamente imprecisi e incompleti rendono difficile giungere a delle conclusioni nette e dare delle risposte esatte ai problemi che ci poniamo.

(*) *Traduzione a cura della Redazione.*

IL NUOVO CIMENTO   Vol. XX, N. 6   16 Giugno 1961

On the Uniqueness of a Potential Fitting a Scattering Amplitude at a Given Energy.

A. Martin and Gy. Targonski

CERN - Geneva

(ricevuto il 22 Marzo 1961)

Summary. — It is shown that when a scattering amplitude is known to be produced by a superposition of Yukawa potentials, the exact knowledge of the scattering amplitude at a given energy determines in a unique way the potential. This is established in two steps: i) by proving that, once the physical scattering amplitude is known, the discontinuity across the cut in the complex plane of the momentum transfer is uniquely defined; ii) by establishing the rigorous connection between this discontinuity and the potential. In order to be fitted by a superposition of Yukawa potentials at a given energy a scattering amplitude has to satisfy certain conditions which are investigated. The treatment can be modified in order to include the case of exchange forces.

1. – Introduction.

The problem of the determination of a potential fitting a given partial wave amplitude has been considered some time ago by various authors (1). Up to now the only work on the construction of a potential from the knowledge of the scattering amplitude at all angles, for a given energy, is that of Regge (2), who makes use of complex angular momenta. Regge shows that once the possible interpolating phase shifts for non-integral values of the angular momentum are known, a unique potential corresponds to a given interpolation. Here we want to use another approach to this problem. We shall be mainly

(1) R. Jost and W. Kohn: *Phys. Rev.*, **87**, 979 (1952) (this contains reference to previous work).

(2) T. Regge: *Nuovo Cimento*, **14**, 591 (1959).

interested by scattering amplitudes which can be produced by a potential of the type

$$\int_{\mu}^{\infty} C(\alpha)\,\frac{\exp[-\alpha r]}{r}\,\mathrm{d}\alpha\,. \tag{1}$$

In this special case we prove that the analytic continuation of the scattering amplitude for complex angles is unique; the discontinuity across the cut in the $\cos\theta$ plane is unique, and from it one can construct the potential. We also look at the necessary conditions which must be fulfilled by a scattering amplitude to be produced by a potential of family (1); these conditions are obtained by making a conformal mapping of the regularity domain of the scattering amplitude on a circle. Our treatment can be extended to the case of exchange forces.

2. – Uniqueness of the continuation of the scattering amplitude for complex angles.

Let us define $t=-2k^2(1-\cos\theta)$, where k is the momentum and θ the scattering angle . The physical region for the scattering amplitude $T(t)$ (*) is $-4k^2\leqslant t\leqslant 0$. This is the region where $T(t)$ is supposed to be known.

Let us now make the assumption that the potential $V(r)$ which produces this scattering amplitude is exponentially decreasing, *i.e.* that there exist μ such that

$$\lim_{r\to\infty} \exp[+\mu r]V(r) = \text{finite}\,. \tag{2}$$

Then it is known (3) that $T(t)$ has an analytic continuation which is regular inside the ellipse with foci $t=0$, $t=-4k^2$, and which cuts the real axis at $t=\mu^2$ and $t=-4k^2-\mu^2$. When $f(t)$ is known in the physical domain the analytic continuation inside the ellipse is unique, because of the well-known theorem that when two functions coincide on a line inside a common regularity domain they coincide everywhere inside the regularity domain. If the continuation of $T(t)$ can be made in the whole complex plane (with possible singularities: cuts, poles, essential singularities, etc.) the continuation is unique for the same reason.

Let us now make the more specific assumption that *one* of the potentials (if it exists) fitting, in the physical range, $T(t)$, has the form

$$V(r)=\int_{\mu}^{\infty}\frac{C(\alpha)\exp[-\alpha r]\,\mathrm{d}\alpha}{r}\,, \tag{3}$$

with $\int|C(\alpha)|\,\mathrm{d}\alpha$ finite, $\mu>0$.

(*) We drop the energy variable, which is kept fixed in the whole problem.

(3) See for instance J. BOWCOCK and A. MARTIN: *Nuovo Cimento*, 14, 516 (1959).

Then the analytic properties of $T(t)$ are known to be very simple [3,4]: it is regular in the whole complex plane, except along a cut on the real axis from $t=\mu^2$ to $t=+\infty$ (Fig. 1). Then $T(t)$ can be continued in a unique way in the whole complex t plane, because this is so in an arbitrarily large finite domain avoiding the cut. In particular, the discontinuity of $T(t)$ across the cut is uniquely defined when $T(t)$ is known in the physical region. As it will appear clearly in the next section when a potential of family (1) is used, the discontinuity is finite if $C(\alpha)$ is a finite function. It is a distribution if $C(\alpha)$ is a distribution.

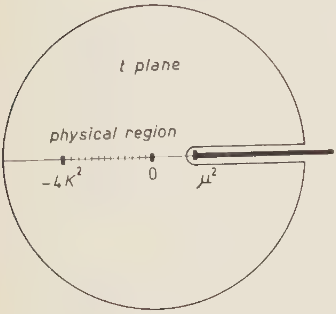

Fig. 1.

We see that if the analytic continuation of $T(t)$ is as indicated on Fig. 1 (the conditions for this will be investigated in Section **4**) the discontinuity of $T(t)$ across the cut is uniquely defined and, particularly μ itself is determined from the knowledge of $T(t)$ in the physical region.

A practical way of obtaining this discontinuity $2i\pi D(t)$ would be to try to solve the following first kind Fredholm equations:

$$T(t)=\int\limits_{\mu^2}^{\infty}\frac{D(t')\,\mathrm{d}t'}{t'-t}\,, \qquad \text{with } -4k^2\leqslant t\leqslant 0\,, \tag{4}$$

$$T(t)=a_0+a_1t+\ldots+a_{n-1}t^{n-1}+t^n\int\limits_{\mu^2}^{\infty}\frac{D(t')\,\mathrm{d}t'}{(t'-t)t'^n}\,, \qquad -4k^2\leqslant t\leqslant 0\,, \tag{5}$$

where n has to be finite according to REGGE's work [2]. From what we said, at most one of these equations has a solution, or, more precisely, if one equation has a solution, those with larger number of subtractions give exactly the same solution. Here it is obvious that one needs to know $T(t)$ with *infinite accuracy* to draw such a conclusion. Otherwise a fit by a polynomial in t, with $D(t)=0$, is always possible when only n values of $T(t)$ are known.

3. – Determination of the potential from the discontinuity along the cut in the t plane.

We have seen, in the preceding section, that when $T(t)$ is known in the physical region, and when the potential belongs to family (1) the discontinuity across the unphysical cut is uniquely determined. Let us now show in an explicit way how to get the potential from the discontinuity. The connection

(4) R. BLANKENBECLER, M. GOLDBERGER, N. KHURI and S. TREIMAN: *Ann. of Phys.*, **10**, 62 (1960); A. KLEIN: *Journ. Math. Phys.*, **1**, 41 (1960).

between potential and discontinuity in the t variable has been already established for low t values ($t < 9\mu^2$) by CHARAP and FUBINI [5], but we wish to give here a general proof.

Let us write the scattering amplitude as

$$T = T_1 + \dots + T_n + R_n\,, \tag{6}$$

where T_n is the n-th Born term. It has a cut starting at $t = n^2\mu^2$. On the other hand, by writing $R_n = T_{n+1} + \dots + T_N + R_N$ and taking N large enough one can show that R_n is regular inside an ellipse with foci, 0, $-4k^2$, cutting the real axis at $t = (n+1)^2\mu^2$ [6]. Therefore to compute the discontinuity across the cut in the region $\mu^2 < t < (n+1)^2\mu^2$ it is sufficient to consider the n first Born terms.

Let us split the potential in various parts:

$$V = V_1 + V_2 + \dots + V_n + V_{n+1}\,, \tag{7}$$

where

$$\left|\begin{aligned} &V_l = \int\limits_{l\mu}^{(l+1)\mu} \frac{C(\alpha)\exp[-\alpha r]\,\mathrm{d}\alpha}{r}\,, \qquad\qquad l \leqslant n\,, \\ &\text{and} \\ &V_{n+1} = \int\limits_{(n+1)\mu}^{\infty} \frac{C(\alpha)\exp[-\alpha r]\,\mathrm{d}\alpha}{r}\,. \end{aligned}\right. \tag{8}$$

A typical contribution to the i-th Born term will be

$$V_{n_1} G_0 V_{n_2} G_0 \dots G_0 V_{n_i}\,, \tag{9}$$

where G_0 is the free Green's function.

From previous work (see for instance ref. [4]) it is known that this contribution will have a cut in the t plane starting at $t = (n_1 + n_2 + \dots n_i)^2\mu^2$. So in the region $\mu^2 < t < (n+1)^2\mu^2$:

i) V_{n+1} will never contribute to the discontinuity;

ii) V_n will contribute to the discontinuity through the first Born term T_1 and nowhere else. More precisely, since

$$T_1(t) = \int \frac{C(\alpha)\,\mathrm{d}\alpha}{t-\alpha^2}\,, \qquad T_1(t+i\varepsilon) - T_1(t-i\varepsilon) = 2i\pi\cdot\frac{C(\sqrt{t})}{2\sqrt{t}}\,. \tag{10}$$

[5] J. CHARAP and S. FUBINI: *Nuovo Cimento*, **14**, 540 (1959) and **15**, 73 (1960).
[6] See for instance A. MARTIN: *Nuovo Cimento*, **19**, 344 (1961), Appendix.

2497

These remarks lead us to use an iterative procedure to determine $C(\alpha)$ from the discontinuity of T across that cut.

Assume that $C(\alpha)$ is known from $\alpha=\mu$ to $\alpha=n\mu$ then $V_1 \dots V_{n-1}$ are known; then in the region $n^2\mu^2 < t < (n+1)^2\mu^2$ we have:

$$2\pi i\,\frac{C(\sqrt{t})}{2\sqrt{t}} = 2\pi i D(t) - \text{discontinuity of } (T_2 + \dots + T_n)\,: \tag{11}$$

the discontinuity of $T_2 + \dots + T_n$ is known in terms of $V_1 \dots V_{n-1}$. Hence V_n is known and the iterative procedure can go on.

We have now completed the proof that a given scattering amplitude at a given energy can be fitted by at most one potential which is a superposition of Yukawa potentials. However, the scattering amplitude in the physical region must fulfil certain requirements in order to ensure the existence of one solution. These will be investigated in the next section.

4. – Necessary conditions on the scattering amplitude.

We shall now investigate the conditions to impose on the scattering amplitude in the physical region to make it have the analytic properties indicated in Section 2. This is obviously necessary (but not necessarily sufficient) to make it possible to reproduce the scattering amplitude by a superposition of Yukawa potentials. In the first place, we have to check that the starting point of the cut is $t=\mu^2$. This means that inside an ellipse with foci $-4k^2$, 0 cutting the real axis at $t=\mu^2$ a Legendre expansion of T is convergent and that outside the ellipse this expansion diverges. This means [6]:

$$\lim_{l\to\infty}\left|\int_{-4k^2}^{0} T(t)\,P_l\left(1+\frac{t}{2k^2}\right)\frac{dt}{2k^2}\right|^{1/l} = h\,, \tag{12}$$

where h is a number such that

$$\frac{1}{2}\left(h+\frac{1}{h}\right) = 1 + \frac{\mu^2}{2k^2}\,, \qquad 0 < h < 1. \tag{13}$$

Eq. (13) fixes μ. Let us now check that the whole analytic behaviour is correct. For this we shall make a conformal mapping of the regularity domain

inside the unit circle (*). A possible mapping is

$$t = \frac{4\mu^2 Z}{(Z+1)^2} \quad \text{(see Fig. 2)}. \tag{14}$$

The upper (lower) half of the circle corresponds to the upper (lower) lip of the cut. $Z=1$ corresponds to $t=\mu^2$; $Z=-1$ corresponds to $t=\infty$. The physical domain lies on the real Z axis from

$$Z_{\min} = -\left(1+\frac{\mu^2}{2k^2}\right) + \sqrt{\left(1+\frac{\mu^2}{2k^2}\right)^2 - 1} \qquad (t=-4k^2) \text{ to } Z=0\ (t=0).$$

Then the condition to impose on $T((4\mu^2 Z)/(Z+1)^2)$ is that the power series expansion of T around $Z=0$ has a radius of convergence $|Z|=1$, namely, with

$$T = \sum a_n Z^n, \qquad \overline{\lim}\,(a_n)^{1/n} = 1. \tag{15}$$

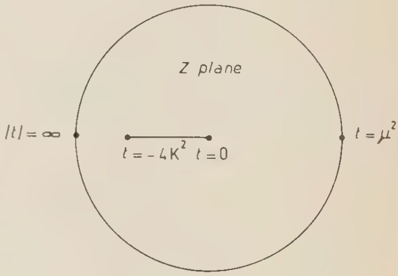

Fig. 2.

Of course this power series expansion must fit the values of T in the whole physical region.

These conditions are necessary but not sufficient. For instance, nothing has been said about the fact that $T(t)$ should not increase stronger than a polynomial at infinity. Even so it is not obvious that the iterative procedure for the construction of $C(\alpha)$ will give an acceptable potential. It might happen that $C(\alpha)$ increases too fast as $\alpha \to \infty$.

5. – Extension to exchange forces.

When exchange forces are present, with the same minimum range μ, T for fixed energy has two cuts. Using the variable $\cos\theta$ instead of t we get two symmetrical cuts starting at

$$\cos\theta = \pm\left(1+\frac{\mu^2}{2k^2}\right);$$

(*) A similar operation has been suggested independently by W. FRAZER in a different connection ([7]).

([7]) W. FRAZER: *Bulletin of the American Physical Society*, 6, 81 (1961).

it is useful to introduce variables

$$(16) \qquad \left\{ \begin{array}{l} t = -2k^2(1 - \cos\theta) \\ \text{and} \\ \bar{t} = -2k^2(1 + \cos\theta) . \end{array} \right.$$

The right hand cut starts at $t = \mu^2$, while the left hand cut starts at $\bar{t} = \mu^2$ [3]. Extending our preceding reasoning to this case we see that the knowledge of $T(\cos\theta)$ in the physical domain determines uniquely both discontinuities across the two cuts for potentials of the type

$$\int_{\mu}^{\infty} \frac{[C_D(\alpha) + PC_E(\alpha)] \exp[-\alpha r] \, d\alpha}{r}$$

(P = Majorana exchange operator).

One can write T as [3-8]:

$$(17) \qquad T = \sum_{i=1}^{n} \left(T_{iD}(t) + T_{iE}(\bar{t})\right) + R_n ,$$

where the exchange potential appears an even (odd) number of times in T_{iD} (T_{iE}). T_{iD} as a function of t has a single cut from $t = i^2\mu^2$ to $t = \infty$. T_{iE} has the same properties provided one replaces t by $\bar{t}$. Again, one can show that R_n is regular inside an ellipse with foci $\cos\theta = \pm 1$ cutting the real axis at

$$\cos\theta = \pm \left[1 + \frac{(n+1)^2\mu^2}{2k^2}\right].$$

The argument concerning the additivity of the inverses of the ranges of the potentials entering in a matrix element of the Born series still holds. Then if the contribution to the potential

$$\int_{\mu}^{n\mu} \frac{[C_D(\alpha) + PC_E(\alpha)] \exp[-\alpha r]}{r} \, d\alpha$$

is known, the discontinuity in the region

$$1 + \frac{n^2\mu^2}{2k^2} < \cos\theta < 1 + \frac{(n+1)^2\mu^2}{2k^2}$$

(8) J. Hamilton: *Phys. Rev.*, **114**, 1170 (1959).

consists of known terms plus the contribution of

$$\int_{n\mu}^{(n+1)\mu} \frac{C_D(\alpha)\exp[-\alpha r]\,\mathrm{d}\alpha}{r}\,,$$

to the first Born approximation; in the region

$$-\left[1+\frac{(n+1)^2\mu^2}{2k^2}\right] < \cos\theta < -\left[1+\frac{n^2\mu^2}{2k^2}\right],$$

the discontinuity also consists of known terms plus the contribution of

$$P\int_{n\mu}^{(n+1)\mu} \frac{C_E(\alpha)\exp[-\alpha r]\,\mathrm{d}\alpha}{r}\,,$$

to the first Born approximation. So the iteration procedure to determine $C_D(\alpha)$ and $C_E(\alpha)$ still works.

To look at the necessary conditions to impose on the scattering amplitude one can make the mapping of the cut plane on the unit circle

$$\frac{\cos\theta}{1+\mu^2/2k^2} = \frac{2Z}{Z^2+1}\,. \tag{18}$$

Here the branch points correspond to $Z=\pm 1$, the physical domain becomes a symmetrical segment on the real Z axis, and $t=\infty$ (with $\mathrm{Im}\, t \gtrless 0$) corresponds to $Z=\pm i$.

6. – Concluding remarks.

We have solved the problem « *in principle* » of determining the potential from the scattering amplitude at a given energy when it is known that this potential (with or without exchange forces) is a superposition of Yukawa potentials. The statement that the discontinuity across the cuts is determined by the scattering amplitude is only valid when the scattering amplitude is known with infinite accuracy; to make this statement useful in practical cases one has to have some *a priori* idea of the maximum number of subtractions in the integral representation of the scattering amplitude. A systematic procedure to get the potential from the discontinuity of the scattering amplitude for fixed energy has been given. This is in a sense a generalization of the treatment of FUBINI and CHARAP (5) which was restricted to low values of t;

but from another point of view our treatment is much less deep then the one of CHARAP and FUBINI who show, on a field theoretical basis, the energy-independence of the potential obtained in this way.

One might be tempted to apply our remarks to other objects having the same analytic properties as scattering amplitudes. This is assumed to be the case for the electromagnetic form factors of the nucleon. One then gets the curious result that knowing exactly a form factor in a limited range of values of the momentum transfer one knows it for any value of the momentum transfer. Unfortunately this statement is almost useless because of the limited accuracy of the experiments.

Note added in proof.

Reality of the potential. – If, at the energy under consideration, there is not any other open channel than scattering, one may ask whether the potential one obtains is real or not. In the general case the only condition due to unitarity is

$$\int \mathrm{d}^3\boldsymbol{x}\, \psi^*_{\boldsymbol{k}'}(\boldsymbol{x})\, [\operatorname{Im} V(\boldsymbol{x})]\, \psi_{\boldsymbol{k}}(\boldsymbol{x}) = \varphi(t, k) = 0\,,$$

for all $\boldsymbol{k}$ and $\boldsymbol{k}'$ such that $|\boldsymbol{k}| = |\boldsymbol{k}'| = k$. This is not sufficient in general to ensure that $\operatorname{Im} V(x) = 0$. However, when one considers superpositions of Yukawa potentials only $\varphi(t, k)$ has the same kind of analytic properties in t as the scattering amplitude itself, and since it vanishes in the physical range of values of t it vanishes everywhere in the t complex plane. From this point it is not difficult to prove that $\operatorname{Im} V(x)$ must vanish. We prefer this direct proof to the careful examination of the step by step procedure of construction of the potential.

RIASSUNTO (*)

Dimostriamo che quando si sa che un'ampiezza di scattering è prodotta dalla sovrapposizione di potenziali di Yukawa, la conoscenza esatta dell'ampiezza di scattering a una data energia determina univocamente il potenziale. Questo viene dimostrato in due passaggi successivi: 1) dando la prova che, quando è nota l'ampiezza fisica di scattering, la discontinuità sul taglio nel piano complesso del trasferimento dell'impulso è univocamente definita; 2) determinando la rigida connessione fra la discontinuità ed il potenziale. Per essere approssimata da una sovrapposizione di potenziali di Yukawa ad una data energia, l'ampiezza di scattering deve soddisfare ad alcune condizioni che vengono ricercate. Il procedimento può essere modificato in modo da includere il caso delle forze di scambio.

(*) *Traduzione a cura della Redazione.*

Magnetic Dispersion Corrections to Elastic Electron Scattering (*).

A. GOLDBERG (**)

Institute of Theoretical Physics, Department of Physics, Stanford University - Stanford, Cal.

(ricevuto il 23 Marzo 1961)

Summary. — The second-order dispersive corrections to the cross section for elastic scattering of high energy electrons by ^{4}He are estimated. The nuclear currents are the convection and spin currents of each nucleon. A closure approximation is used to evaluate the amplitude. The spin effects are calculated explicitly assuming an independent particle nuclear model for two different charge form factors. These are found to be less than four percent of the first-order cross section. It is shown how the convection current contribution may be evaluated within the restrictions of gauge invariance. Only part of the convection terms are calculated; these are found to be much smaller than the correction due to the pure Coulomb interaction. It is concluded that the dominant contribution to the second-order correction is due to the Coulomb potential, and that this is true in general, not only for ^{4}He. Lastly, the relevance of these corrections to experiments measuring the electron's electric and magnetic dipole moment form factors is mentioned.

1. – The cross-section for scattering of electrons by light nuclei is usually calculated in first Born approximation only. Since the expansion parameter is $Z/137$ (Z = atomic number), one would expect that higher order corrections are of this order, *i.e.*, several percent. If the Born approximation is valid, it can be shown that the cross-section for elastic scattering of unpolarized electrons is given in terms of two invariant functions of the momentum transfer q(1)

$$\frac{\mathrm{d}\sigma}{\mathrm{d}\Omega} = \sigma_M \left\{A(q^2) + B(q^2)\,\mathrm{tg}^2\frac{\theta}{2}\right\}, \tag{1}$$

(*) Supported in part by the U.S. Air Force through the Air Force Office of Scientific Research.

(**) Present address: Institute for Theoretical Physics, Blegdamsvej 17, Copenhagen.

(1) J. D. BJORKEN and J. FUJITA: (Stanford University) to be published.

where σ_M is the Mott cross-section

$$\sigma_M = \frac{e^4}{4k^2} \frac{\cos^2 \frac{1}{2}\theta}{\sin^4 \frac{1}{2}\theta}\,.$$

k is the electron energy. (The mass of the nucleus M_T is taken as infinite.) $A(q^2)$ and $B(q^2)$ contain all the pertinent information about the specific target nucleus. If the electron current is the Dirac matrix γ^μ, $A(q^2)$ and $B(q^2)$ represent the nuclear non-spin flip and spin flip transition probabilities, respectively. If the nuclear spin is zero, *e.g.*, ^{4}He, $B(q^2)$ is necessarily zero, and the cross-section is

$$\frac{\mathrm{d}\sigma}{\mathrm{d}\Omega} = \sigma_M F^2(q^2)\,, \tag{2}$$

with $F(q^2)$ the charge form factor.

It has been proposed (²) that measurement of the cross-section for elastic scattering by ^{4}He be used as a sensitive test of quantum electrodynamics. The presence of non-vanishing electron electric or anomalous magnetic dipole moment form factors $\lambda(q^2)$ and $\mu(q^2)$ (in Bohr magnetons) would lead to large back-angle scattering through the cross-section

$$\frac{\mathrm{d}\sigma}{\mathrm{d}\Omega} = \sigma_M F^2(q^2)\left\{1 - \frac{q^2}{m^2}\left(1 + \mathrm{tg}^2\frac{\theta}{2}\right)\left[\lambda^2(q^2) + \mu^2(q^2)\right]\right\}. \tag{3}$$

By measuring the angular variation of $\mathrm{d}\sigma/\mathrm{d}\Omega$ for given q^2, accurate limits on λ and μ may be fixed. Measurements of this type have been made by BURLESON and KENDALL (³). Within the range $q = 1$ to $2.25 \cdot 10^{13}\ \mathrm{cm}^{-1}$ ($q/m \sim 10^3$), they have set the limits on the moments (⁴)

$$\left.\begin{matrix}\lambda(q^2)\\ \mu(q^2)\end{matrix}\right\} \leqslant 2 \cdot 10^{-4}\,.$$

It is essential to the interpretation of this experiment in terms of electron dipole moments that the first Born approximation be valid. Since $Z = 2$ this should be the case. However, since the first-order scattering is entirely due to the nuclear charge and decreases rapidly at back angles, it is possible that second-order virtual nuclear transitions through magnetic interactions could produce relatively strong angular variations in the cross-section. These might tend to cancel or mask the effect of any electron moments. It is our

(²) B. MARGOLIS, S. ROSENDORFF and A. SIRLIN: *Phys. Rev.*, **114**, 1530 (1959); G. V. AVAKOV and K. A. TER-MARTIROSYAN: *Nucl. Phys.*, **13**, 685 (1959).

purpose here to estimate the effect of these second-order transitions. We ignore second-order charge scattering, for reasons indicated below.

We shall picture these transitions as proceeding through the nuclear absorption of two photons emitted by the electron. The first photon excites the nucleus to a virtual level, from which it is de-excited back to the ground state by the second photon. The second-order amplitude is the sum of these transitions weighted with the energy denominator encountered in perturbation theory. This sum will be performed with a closure approximation, replacing the nuclear Hamiltonian with an average excitation energy. The integrals over the photon momenta will then be evaluated approximately.

We expect that these second-order effects are small. We shall therefore assume that the nucleus can be treated non-relativistically. Relativistic effects should not strongly change the results. If the results prove appreciable, the calculation is not valid in any case. The nuclear currents are then the charge, convection and Pauli spin terms for each nucleon.

The second Born approximation for high energy electron scattering has been evaluated thus far only for pure electrostatic interactions. DALITZ [5] first gave a correct relativistic treatment for electrons scattering from a stationary point charge. LEWIS [6] extended this to charge distributions, in particular Gaussian, Yukawa, and exponential distributions. In the range of momentum transfer for which measurements have been made, the second-order corrections are several percent of the first-order cross-section.

Second-order processes involving nuclear excitation through the Coulomb potential have been considered by SCHIFF [7] and LEWIS [8]. They also performed the sum over nuclear levels with the closure approximation. KRALL and SALPETER [9] attempted to improve on this procedure with a numerical evaluation of the amplitude. Their expression for the matrix elements, however, appears to be incorrect, thus invalidating their results [10]. The major problem in calculation of the second-order amplitude arises from the effects of proton correlation within the nucleus, entering when the two scatterings involve different protons. Assuming an independent particle nuclear model,

---

(3) G. R. BURLESON and H. W. KENDALL: *Nuclear Phys.*, **19**, 68 (1960).

(4) The electron does have an anomalous magnetic moment which at $q^2=0$ is $\mu(0)=e^2/2\pi$. However, at large momentum transfers this does not contribute to the cross-section since here the moment varies as $\mu(q^2)=(e^2/2\pi)(m^2/q^2)\log(q^2/m^2)$, *e.g.* S. D. DRELL and F. ZACHARIASEN: *Phys. Rev.*, **111**, 1727 (1958).

(5) R. H. DALITZ: *Proc. Roy. Soc.* (*London*), A **206**, 509 (1951).

(6) R. R. LEWIS: *Phys. Rev.*, **102**, 537 (1956).

(7) L. I. SCHIFF: *Phys. Rev.*, **98**, 756 (1955).

(8) R. R. LEWIS: *Phys. Rev.*, **102**, 544 (1956).

(9) N. A. KRALL and E. E. SALPETER: *Phys. Rev.*, **115**, 457 (1959).

(10) In their eq. (1) the factor $1/(E_n - E_0 + p_\mu \gamma^\mu - m)$ should be replaced by $1/[E_n - E_0 + \boldsymbol{\alpha}\cdot(\boldsymbol{p} - \boldsymbol{p}_i)]$.

2505

LEWIS calculated these virtual excitation effects—the so-called dispersive contribution—as several percent of the first order cross-section ([11]). We may also mention an optical potential analysis of the dispersive effects by GOTTFRIED ([12]). While he is led to evaluation of the same types of quantities as in the previous works, GOTTFRIED was able to conclude that the Coulomb corrections are of order 1/137, independently of the atomic number.

Below, we shall extend these calculations to include, in addition to the Coulomb interaction, the effects of the nucleon convection and spin currents. We expect that these are of order q^2/M^2 compared wtih the Coulomb effects. We are interested in the range $q/M \sim 0.5$, and we are mainly concerned with the possibility that strong angular dependences may lead to relatively large back-angle scattering. The results will be valid only at large angles.

2. – *a*) The energy transferred in elastic scattering to a nucleus with mass M_T is

$$q_0 = -\frac{q^2}{2M_T}\,,$$

where q is the momentum transfer, $q^2 = -4k_i k_f \sin^2 \frac{1}{2}\theta$. Since $|q/2M_T| \ll 1$, $q_0 \ll |q|$ and we shall assume $q_0 = 0$. The first-order scattering is then due only to the charge and the matrix element is

$$S_{fi}^{(1)} = 4\pi i \frac{(2\pi)^4}{V} \frac{m}{k} e^2 (\overline{U}_f, \gamma_0 U_i) \frac{F(q^2)}{q^2} \delta(\boldsymbol{P}_f - \boldsymbol{q}) \delta(q_0)\,. \tag{4}$$

k is the electron energy and m its mass, $k \gg m$. e^2 is the fine structure constant. $(\overline{U}_f, \gamma_0 U_i)$ is the Dirac matrix between initial and final spinors with all plane wave functions normalized to volume V. Lastly $\boldsymbol{P}_f$ is the final momentum of the nucleus, and $F(q^2)$ the charge form factor.

Let $T_{\nu\mu}(q_2, q_1)$ be the amplitude for nuclear absorption of two photons of momenta and polarizations q_1, μ and q_2, ν. The second order S-matrix is ([13])

$$S_{fi}^{(2)} = -\frac{(4\pi)^2}{V^2} e^4 \frac{m}{k} \delta(q_0) \delta(\boldsymbol{P}_f - \boldsymbol{q}) \int \mathrm{d}^4 q_1 t_{\lambda\sigma} \frac{g^{\lambda\nu}}{q_2^2 + i\alpha} \frac{g^{\sigma\mu}}{q_1^2 + i\beta} T_{\nu\mu}\,, \tag{5}$$

([11]) As pointed out by LEWIS, one of the approximations in Schiff's calculation of these two-particle effects is invalid. A specific non-independent particle model has also been treated by B. DOWNS: *Phys. Rev.*, **101**, 820 (1956).

([12]) K. GOTTFRIED: *Nucl. Phys.*, **15**, 92 (1960).

([13]) S. S. SCHWEBER, H. A. BETHE and F. DE HOFFMANN: *Mesons and Fields*, Vol. I, (Evanston, Ill., 1955).

where $q_2 = q - q_1$, and

$$t_{\lambda\sigma} = \frac{1}{2}\left\{\left[\bar{U}_f, \gamma_\lambda \frac{1}{k_i\gamma - q_1\gamma + i\delta}\gamma_\sigma U_i\right] + \left[\bar{U}_f, \gamma_\lambda \frac{1}{k_f\gamma + q_1\gamma + i\delta}\gamma_\sigma U_i\right]\right\}.$$

$t_{\lambda\sigma}$ is in symmetrized form here, but in the actual integrations it may be replaced by

$$t_{\lambda\sigma} = \left[\bar{U}_f, \gamma_\lambda \frac{1}{k_i\gamma - q_1\gamma + i\delta}\gamma_\sigma U_i\right].$$

$T_{\nu\mu}$ includes two terms, the first in which the photon emitted first is absorbed first (uncrossed diagram), and the second in which it is absorbed last (crossed diagram). The nuclear interaction with a photon (q_1, μ) is

$$\tfrac{1}{2}\sum_{i=1}^{A}\{J_{\mu i}, \exp[i\,\boldsymbol{q}_1\cdot\boldsymbol{R}_i]\},$$

the bracket denoting the anti-commutator, and $J_{\mu i}$ the i-th nucleon's current vector at position $\boldsymbol{R}_i$, referred to the nuclear center-of-mass. Finally we need the Green function $G(t_2, t_1)$ propagating the nucleus from time t_1 to a later time t_2. This is

$$G(t_2, t_1) = \sum_n \theta(t_2 - t_1)\,|n\rangle\langle n|\exp[-i\varepsilon_n(t_2 - t_1)],$$

with $\theta(t_2 - t_1)$ the unit step function. $|n\rangle$ is the n-th nuclear state with energy ε_n, $H_0|n\rangle = \varepsilon_n|n\rangle$. The absorption amplitude is then

$$T_{\nu\mu} = \langle 0|\frac{1}{2}\sum_{i=1}^{A}\{J_{\nu i}, \exp[i\boldsymbol{q}_2\cdot\boldsymbol{R}_i]\}\frac{1}{H_0 - q_{10} - i\eta}\,\frac{1}{2}\sum_{j=1}^{A}\{J_{\mu j}, \exp[i\boldsymbol{q}_1\cdot\boldsymbol{R}_j]\} + \frac{R}{H_0 + q_{10} - i\eta}|0\rangle. \tag{6}$$

R in the second term means that the two anti-commutators are interchanged. (We have set the ground state energy equal to zero.) The cross-section is obtained from $|S_{fi}^{(1)} + S_{fi}^{(2)}|^2$. Since we want only the leading correction to the first-order cross-section, $|S_{fi}^{(1)}|^2$, we shall include only the interference term $2\,\mathrm{Re}\,S_{fi}^{(1)*}S_{fi}^{(2)}$. After the final state sums and the initial state averages are performed in the usual manner, the cross-section is

$$\frac{\mathrm{d}\sigma}{\mathrm{d}\Omega} = \sigma_M F^2(q^2)\{1 + C(\boldsymbol{q})\}. \tag{7}$$

$C(\boldsymbol{q})$ is the fractional dispersion correction,

$$C(\boldsymbol{q}) = -\frac{e^2}{F(q^2)}\,\frac{\operatorname{tg}^2\theta/2}{4\pi^3}\,\operatorname{Re} i\int \mathrm{d}^4 q_1\,\frac{\operatorname{Tr}\gamma^0 \boldsymbol{k}_f\gamma\gamma^\nu(\boldsymbol{k}_i\gamma - q_1\gamma)\gamma^\mu \boldsymbol{k}_i\gamma}{(q_1^2+i\alpha)(q_2^2+i\beta)\,[(k_i-q_1)^2+i\delta]}\,T_{\nu\mu}\,. \tag{8}$$

b) We shall first calculate the effects due to the nucleon spin. The current operator absorbing a photon (q_1, μ) is $(\mu_i/2M)(\boldsymbol{\sigma}_i\times\boldsymbol{q}_1)$: ($\mu_i$ = magnetic moment) and

$$\tfrac{1}{2}\sum_{i=1}^{A}\{J_{\mu i}, \exp[i\boldsymbol{q}_1\cdot\boldsymbol{R}_i]\} = \sum_{i=1}^{A}\mu_i(\boldsymbol{\sigma}_i\times\boldsymbol{q}_1)_\mu\exp[i\boldsymbol{q}_1\cdot\boldsymbol{R}_i]\,.$$

We make the closure approximation, replacing H_0 in $T_{\nu\mu}$ by an average excitation energy ε. Hopefully, the numerical results are not strongly dependent on the value of ε.

The correction due to the spins, $C^{(s)}(\boldsymbol{q})$, contains two types of terms, those in which both interacting nucleons are the same (single-particle terms), and those in which they are different (two-particle terms). With the recognition that any component of $\boldsymbol{\sigma}_i$ averages to zero, the single-particle correction, after evaluation of the traces, is

$$C_1^{(s)}(\boldsymbol{q}) = -\frac{e^2}{\pi^3}\operatorname{tg}^2\frac{\theta}{2}\sum_{i=1}^{A}\frac{\mu_i^2}{4M^2}\,\frac{\langle 0|\exp[i\boldsymbol{q}\cdot\boldsymbol{R}_i]|0\rangle}{F(q^2)}\,,$$

$$\int \mathrm{d}^4 q_1\,\frac{1}{q_1^2+i\alpha}\,\frac{1}{q_2^2+i\beta}\,\frac{1}{(k_i-q_1)^2+i\delta}\left\{\frac{1}{\varepsilon-q_{10}-i\eta}+\frac{1}{\varepsilon+q_{10}-i\eta}\right\}\cdot$$

$$\cdot\left\{2\boldsymbol{q}_1\cdot\boldsymbol{q}_2\left[kp\cdot(k_i-q_1)+\frac{q^2}{2}(k-q_{10})\right]+2k\boldsymbol{p}\cdot\boldsymbol{q}_1\,\boldsymbol{k}_f\cdot\boldsymbol{q}_1+\right.$$

$$\left.+\,k\boldsymbol{p}^2\,\boldsymbol{q}_1\cdot\boldsymbol{q}_2 - k\boldsymbol{p}\cdot\boldsymbol{q}_1\,\boldsymbol{q}\cdot(\boldsymbol{k}_i-\boldsymbol{q}_1)+\frac{\boldsymbol{q}^2}{2}(k-q_{10})\right\},$$

$$p = k_i + k_f\,,\qquad p\cdot q = \boldsymbol{p}\cdot\boldsymbol{q} = 0\,,\qquad \boldsymbol{p}^2 = 4k^2\cos^2\frac{\theta}{2}\,.$$

The factor $\sum_{i=1}^{A}\mu_i^2\langle 0|\exp[i\boldsymbol{q}\cdot\boldsymbol{R}_i]|0\rangle$ involves a sum over protons and over neutrons. Outside of effects due to the Coulomb repulsion between protons, these are equal, each giving the charge form factor

$$\sum_{i=1}^{A}\frac{\mu_i^2}{4M^2}\langle 0|\exp[i\boldsymbol{q}\cdot\boldsymbol{R}_i]|0\rangle = \frac{\mu_P^2+\mu_N^2}{4M^2}\,F(q^2)\,.$$

The factor $1/(\varepsilon - q_{10})$ arises from the uncrossed diagram, $1/(\varepsilon+q_{10})$ from the crossed. It is more convenient to integrate each diagram separately rather

than add them immediately. While their sum converges, each is logarithmically divergent. Accordingly a convergence procedure is used, whereby the nuclear denominators are replaced by

$$\frac{1}{\varepsilon - q_{10} - i\eta} \rightarrow \frac{2\mathscr{M}}{(P - q_1)^2 - (\mathscr{M} - \varepsilon)^2 - i\eta}\,,$$

$$\frac{1}{\varepsilon + q_{10} - i\eta} \rightarrow \frac{2\mathscr{M}}{(P - q_2)^2 - (\mathscr{M} - \varepsilon)^2 - i\eta}\,,$$

with P a pure timelike vector, $P = (\mathscr{M}, 0)$. After all integrations we take $\mathscr{M} \rightarrow \infty$. The integrations over q_1 are then straightforward and may be done via the Feynman parametrization method. The resulting expression is quite lengthy, and numerical results are given below. To give an idea of the order of magnitude of the results, in the static limit, $\varepsilon \rightarrow 0$, the single particle spin correction is

$$C_1^{(s)}(\boldsymbol{q}) = \frac{e^2}{2\pi}(\mu_P^2 + \mu_N^2)\frac{\boldsymbol{q}^2}{4M^2}\left\{-2 + \frac{1 + \sin^2\theta/2}{\sin\theta/2}\left[R\left(\frac{\sin\theta/2 - 2\,\mathrm{tg}^2\,\theta/2}{\sin\theta/2 + 2\,\mathrm{tg}^2\,\theta/2}\right) - R\left(\frac{\sin\theta/2 + 2\,\mathrm{tg}^2\,\theta/2}{\sin\theta/2 - 2\,\mathrm{tg}^2\,\theta/2}\right)\right]\right\}.$$

The function $R(x)$ is defined by

$$R(x) = \int_0^x \frac{\mathrm{d}t}{t}\log(1 + t)\,,$$

and has been tabulated by MITCHELL [14].

The two-particle correction $C_2^{(s)}(\boldsymbol{q})$ requires further assumptions, since the oscillating phase factors enter into the q_1 integration. The simplest assumption about the ^{4}He nucleus is that all nucleons are in pure S-states, the total wave function being a product of functions for each nucleon. Since the total spin is zero, the pair of protons and pair of neutrons each have zero spin. Those parts of $C_2^{(s)}(\boldsymbol{q})$ in which a proton absorbs one photon and the other photon is absorbed by one neutron cancel with those in which the other neutron absorbs the second photon. We need then consider only terms in which the nucleons are either both protons or both neutrons, and for which $\boldsymbol{\sigma}_i = -\boldsymbol{\sigma}_j$. Hence the factor arising from the spin matrices differs from that in $C_1^{(s)}(\boldsymbol{q})$ only in sign. Lastly, under the independent particle assumption, the phase

([14]) K. MITCHELL: *Phil. Mag.*, **40**, 351 (1949).

2509

factors become

$$\sum_{\substack{i,j\\ i\neq j}} \frac{\mu_i \mu_j}{4M^2} \langle 0|\exp\left[i(\boldsymbol{q}_1\cdot\boldsymbol{R}_i + \boldsymbol{q}_2\cdot\boldsymbol{R}_j)\right]|0\rangle = \frac{\mu_P^2 + \mu_N^2}{4M^2} F(\boldsymbol{q}_1^2)F(\boldsymbol{q}_2^2)\,.$$

The integrand of $C_2^{(s)}(\boldsymbol{q})$ is then identical with that in $C_1^{(s)}(\boldsymbol{q})$ except for an overall sign and the form factors $F(\boldsymbol{q}_1^2)F(\boldsymbol{q}_2^2)$.

We take two extreme form factors, the slowly varying Yukawa function

$$F_Y(\boldsymbol{q}^2) = \frac{Za^2}{a^2 + \boldsymbol{q}^2}\,,$$

and the very rapidly decreasing Gaussian function

$$F_G(\boldsymbol{q}^2) = Z\exp\left[-a^2\boldsymbol{q}^2\right]\,.$$

Each corresponds to a charge distribution with a mean square radius $6a^2$. These two functions should straddle the results for other form factors, setting limits on the two-particle correction.

The integration over q_{10} may be performed with Cauchy's theorem, the imaginary terms in the denominators defining the contours of integration. With Yukawa form factors the integration over the direction of $\boldsymbol{q}_1$ is straightforward leaving one remaining integral over the magnitude of $\boldsymbol{q}_1$. This is rather complicated and, while it could be done numerically, we have made two approximations. First, we expect the nuclear energy ε to be much smaller than the electron energy k, and expansions in ε/k are rapidly convergent. We therefore keep terms only to order ε/k in the integrals. (This is not a power series expansion, since quantities of the form $\log \varepsilon/k$ appear.) Secondly, we are interested in the large angle behavior of the correction, and only terms vanishing more slowly than $\cos^4\frac{1}{2}\theta$ at $\theta \to 180°$ are retained. The integration may then be done, and numerical results are given below.

Using Gaussian form factors, the product $F_G(\boldsymbol{q}_1^2)\,F_G(\boldsymbol{q}_2^2)$ is

$$F_G(\boldsymbol{q}_1^2)\,F_G(\boldsymbol{q}_2^2) = Z^2\exp\left[-a^2\boldsymbol{q}^2/2\right]\exp\left[-2a^2\left(\boldsymbol{q}_1 - \frac{\boldsymbol{q}}{2}\right)^2\right].$$

This peaks very sharply at $\boldsymbol{q}_1 = \boldsymbol{q}/2$. Where possible (*i.e.* where it does not lead to infinities) $\boldsymbol{q}_1$ is then replaced by $\boldsymbol{q}/2$. When the integrand is expanded to second order in $\cos^2\frac{1}{2}\theta$, the integration over $\boldsymbol{q}_1$ is possible, although the result is quite lengthy. Numerical results appear below.

In computing $C_1^{(s)}(\boldsymbol{q})$ and $C_2^{(s)}(\boldsymbol{q})$ we shall use two values for the excitation energy ε. The separation energy of a nucleon in ^{4}He is about 20 MeV. For

the range of momentum transfers to be considered, we do not expect that ε can differ from this very strongly. Accordingly a set of computations is given with $\varepsilon = 20$ MeV. A second choice can be made through consideration of the form of the matrix element, eq. (5). At $\boldsymbol{q}_1 = \boldsymbol{q}/2$, the two photon propagators coalesce into into a single second order pole, rather than two distinct first order poles. We then take as the likeliest momentum transfer leading to spin transitions, $\boldsymbol{q}_1 = \boldsymbol{q}/2$. Calculation of the ^{4}He electrodisintegration cross-section ([15]) indicates that the dominant process is the ejection of a single nucleon and all energy goes into that particle's kinetic energy. Hence we shall take as a second choice

$$\varepsilon = \frac{\boldsymbol{q}_1^2}{2M} = \frac{\boldsymbol{q}^2}{8M}\,.$$

As in the Burleson-Kendall experiment ([3]) we want the deviation $C(\boldsymbol{q})$ from eq. (2) as a function of θ for given q^2. We have computed $C_1^{(s)}(\boldsymbol{q})$ and $C_2^{(s)}(\boldsymbol{q})$ for three values of $|\boldsymbol{q}|$; $|\boldsymbol{q}| = 1.0$, 1.5, and $2.0 \cdot 10^{13}$ cm^{-1}, the region in which the measurements were made. Table I gives the single particle correction $C_1^{(s)}(\boldsymbol{q})$; I-*a* that with $\varepsilon = 20$ MeV and I-*b* that with $\varepsilon = \boldsymbol{q}^2/8M$. In all cases the correction is less than 1 %, and is generally much smaller. $C_2^{(s)}(\boldsymbol{q})$ has been computed for these values of $|\boldsymbol{q}|$ using the Yukawa and Gaussian form factors. The parameter a is determined from the nuclear r.m.s. charge radius $R = \sqrt{6}\,a$, which the measurements ([3]) indicate to be $R = 1.68 \cdot 10^{-13}$ cm. The results in Tables II and III are for the Yukawa and Gaussian function respectively. Since $C_2^{(s)}(\boldsymbol{q})$ involves a $\cos^2 \frac{1}{2}\theta$ expansion, computations were made only for $\theta \geqslant 90°$, those for $\theta = 90°$ being least reliable. Table II gives the correction as being at best about 1 % for these q-values. The Gaussian function gives rise to a larger correction, Table III, about 4 %, due to the

TABLE I. – *Percentage correction due to single-particle spin effects.*
a) $\varepsilon = 20$ MeV; *b*) $\varepsilon = \boldsymbol{q}^2/8M$.

	a			*b*		
q	1.0×10^{13} cm^{-1}	1.5	2.0	1.0	1.5	2.0
θ	$C_1^{(s)}(\boldsymbol{q})$	$C_1^{(s)}(\boldsymbol{q})$	$C_1^{(s)}(\boldsymbol{q})$	$C_1^{(s)}(\boldsymbol{q})$	$C_1^{(s)}(\boldsymbol{q})$	$C_1^{(s)}(\boldsymbol{q})$
60°	−0.05	−0.07	−0.06	−0.08	−0.16	−0.24
90°	−0.10	−0.13	−0.08	−0.13	−0.28	−0.44
120°	−0.03	−0.04	−0.06	−0.09	−0.17	−0.25
150°	+0.08	0.46	0.94	−0.09	−0.06	−0.03

([15]) T. MUTO and T. SEBE: *Prog. Theor. Phys.* (*Kyoto*), **18**, 621 (1957).

TABLE II. – *Percentage correction due to two-particle spin effects with Yukawa form factors,* $\sqrt{6}a = 1.68 \cdot 10^{-13}$ cm. *a*) $\varepsilon = 20$ MeV, *b*) $\varepsilon = \boldsymbol{q}^2/8M$.

	a			*b*		
q	$1.0 \cdot 10^{13}\ \text{cm}^{-1}$	1.5	2.0	1.0	1.5	2.0
θ	$C_2^{(s)}(\boldsymbol{q})$	$C_2^{(s)}(\boldsymbol{q})$	$C_2^{(s)}(\boldsymbol{q})$	$C_2^{(s)}(\boldsymbol{q})$	$C_2^{(s)}(\boldsymbol{q})$	$C_2^{(s)}(\boldsymbol{q})$
90°	0	0.14	−1.00	−0.03	0.13	−1.00
120°	−0.35	−0.42	−0.80	−0.36	−0.03	−0.80
150°	−0.84	−0.26	−0.54	−0.85	−0.28	−0.54

TABLE III. – *Percentage correction due to two-particle spin effects with Gaussian form factors,* $\sqrt{6}a = 1.68 \cdot 10^{-13}$ cm. *a*) $\varepsilon = 20$ MeV, *b*) $\varepsilon = \boldsymbol{q}^2/8M$.

	a			*b*		
q	$1.0 \cdot 10^{13}\ \text{cm}^{-1}$	1.5	2.0	1.0	1.2	2.0
θ	$C_2^{(s)}(\boldsymbol{q})$	$C_2^{(s)}(\boldsymbol{q})$	$C_2^{(s)}(\boldsymbol{q})$	$C_2^{(s)}(\boldsymbol{q})$	$C_2^{(s)}(\boldsymbol{q})$	$C_2^{(s)}(\boldsymbol{q})$
90°	−0.70	−1.16	2.21	−0.42	−0.38	−0.58
120°	−0.24	−0.76	−3.47	−0.21	−0.44	−1.42
150°	−0.17	−0.34	−1.40	−0.13	−0.23	−1.09

factor $(\exp[-a^2\boldsymbol{q}^2/2])/[F_G(\boldsymbol{q}^2] - \exp[a^2\boldsymbol{q}^2/2]$ appearing in $C_2^{(s)}(\boldsymbol{q})$. The total spin corrections are then in all cases less than 5 %, and generally appreciably smaller.

c) Here we shall show how the convection current effects may be calculated, and give estimates of some of the terms. If the nuclear Hamiltonian is of the form

$$H_0 = \sum_{i=1}^{A} \left(\frac{\boldsymbol{p}_i^2}{2M} + V(\boldsymbol{R}_i) \right)$$

the convection current operator is

$$J_{\mu i} = \left(1, \frac{\boldsymbol{p}_i}{M}\right).$$

The components of $T_{\nu\mu}$ are then

$$T_{00} = \sum_{i,j=1}^{Z} \langle 0 | \exp[i\boldsymbol{q}_2 \cdot \boldsymbol{R}_i] \frac{1}{H_0 - \boldsymbol{q}_{10} - i\eta} \exp[i\boldsymbol{q}_1 \cdot \boldsymbol{R}_j] + \frac{R}{H_0 + q_{10} - i\eta} | 0 \rangle ,$$

$$T_{0l} = \sum_{i,j=1}^{Z} \langle 0 | \exp[i\boldsymbol{q}_2 \cdot \boldsymbol{R}_i] \frac{1}{H_0 - q_{10} - i\eta} \frac{1}{2M} \{p_{jl}, \exp[i\boldsymbol{q}_1 \cdot \boldsymbol{R}_j]\} + \frac{R}{H_0 + q_{10} - i\eta} | 0 \rangle ,$$

2512

$$T_{l0} = \sum_{i,j=1}^{Z} \langle q | \frac{1}{2M} \{p_{il}, \exp[i\boldsymbol{q}_2 \cdot \boldsymbol{R}_i]\} \frac{1}{H_0 - q_{10} - i\eta} \exp[i\boldsymbol{q}_1 \cdot \boldsymbol{R}_j] + \frac{R}{H_0 + q_{10} - i\eta} |0\rangle ,$$

$$T_{lk} = \sum_{i,j=1}^{Z} \langle 0 | \frac{1}{2M} \{p_{il}, \exp[i\boldsymbol{q}_2 \cdot \boldsymbol{R}_i]\} \frac{1}{H_0 - q_{10} - i\eta} \frac{1}{2M} \{p_{jk}, \exp[i\boldsymbol{q}_1 \cdot \boldsymbol{R}_j]\} +$$
$$+ \frac{R}{H_0 + q_{10} - i\eta} |0\rangle - \frac{\delta_{lk}}{2M} \sum_{i=1}^{Z} \langle 0 | \exp[i\boldsymbol{q} \cdot \boldsymbol{R}_i] | 0 \rangle .$$

Again R denotes that the factors on each side of the denominators are interchanged. The last term in T_{lk} arises from the $e^2\boldsymbol{A}^2$ interaction term, when $\boldsymbol{P}_i$ in H_0 is replaced by $\boldsymbol{P}_i - e\boldsymbol{A}$.

The closure approximation cannot as yet be made without violation of gauge invariance. The gauge conditions are

$$q_{1\mu} T_{\nu\mu} = 0 , \qquad q_{2\nu} T_{\nu\mu} = 0 .$$

Since $[H_0, \exp[i\boldsymbol{q}_1 \cdot \boldsymbol{R}_i]] = (1/2M)\{\boldsymbol{P}_i \cdot \boldsymbol{q}_1, \exp[i\boldsymbol{q}_1 \cdot \boldsymbol{R}_i]\}$, $T_{\nu\mu}$ above satisfies these requirements. It is, however, essential that H_0 be an operator, and it cannot be replaced by a number ε.

To sidestep this problem we break the photon propagators into pure Coulomb and transverse terms [1]. After the breakup the closure procedure may be used, all terms violating the gauge conditions vanishing in the integrations. Referring to eq. (5), we can write

$$t_{\lambda\sigma} \frac{g^{\sigma\mu}}{q_1^2 + i\alpha} T_{\nu\mu} = - t_{\lambda 0} \frac{g^{00}}{\boldsymbol{q}_1^2} T_{\nu 0} - t_{\nu l} \frac{(\delta_{lk}\boldsymbol{q}_1^2 - q_{1l}q_{1k})}{\boldsymbol{q}_1^2(q_1^2 + i\alpha)} T_{\nu k} +$$
$$+ t_{\lambda 0} \frac{q_{10}^2}{\boldsymbol{q}_1^2(q_1^2 + i\alpha)} T_{\nu 0} - t_{\lambda l} \frac{q_{1l}q_{1k}}{\boldsymbol{q}_1^2(q_1^2 + i\alpha)} T_{\nu k} .$$

The last two terms vanish by virtue of the gauge conditions, and we may simply make the replacements

$$\frac{g^{00}}{q_1^2 + i\alpha} \to - \frac{g^{00}}{\boldsymbol{q}_1^2} , \quad \frac{g^{lk}}{q_1^2 + i\alpha} \to - \frac{(\delta_{lk}\boldsymbol{q}_1^2 - q_{1l}q_{1k})}{\boldsymbol{q}_1^2(q_1^2 + i\alpha)} .$$

The second-order Coulomb effects, involving T_{00}, then reduce to the forms given by SCHIFF [7] and LEWIS [8]; we shall quote their results below. Secondly in T_{0l}, the momentum P_{jl} may now be commuted through the exponential to operate directly on the nuclear wave functions

$$T_{0l} = \sum_{i,j=1}^{Z} \left\{ \langle 0 | \exp[i\boldsymbol{q}_2 \cdot \boldsymbol{R}_i] \frac{1}{H_0 - q_{10} - i\eta} \exp[i\boldsymbol{q}_1 \cdot \boldsymbol{R}_j] \frac{P_{jl}}{M} |0\rangle + \right.$$
$$\left. + \langle 0 | \frac{P_{jl}}{M} \exp[i\boldsymbol{q}_1 \cdot \boldsymbol{R}_j] \frac{1}{H_0 + q_{10} - i\eta} \exp[i\boldsymbol{q}_2 \cdot \boldsymbol{R}_i] | 0 \rangle \right\} .$$

$(P_{jl}/M)|0\rangle$ is the bound nucleon velocity (compared to c). In comparison with the Coulomb terms, all terms containing $(P_{jl}/M)|0\rangle$ may then be neglected. The final state has center-of-mass momentum $\boldsymbol{q}$, and again ignoring the bound nucleon velocity, $\langle 0|(P_{lj}/M) = (q_l/AM)\langle 0|$. Making the closure approximation, as is now permitted, we have

$$T_{0l} = \frac{q_l}{AM}\,\frac{1}{\varepsilon + q_{10} - i\eta}\sum_{i,j=1}^{Z}\langle 0|\exp\left[i(\boldsymbol{q}_1\cdot\boldsymbol{R}_j + \boldsymbol{q}_2\cdot\boldsymbol{R}_i)\right]|0\rangle\,.$$

Similarly

$$T_{l0} = \frac{q_l}{AM}\,\frac{1}{\varepsilon - q_{10} - i\eta}\sum_{i,j=1}^{Z}\langle 0|\exp\left[i(\boldsymbol{q}_1\cdot\boldsymbol{R}_j + \boldsymbol{q}_2\cdot\boldsymbol{R}_i)\right]|0\rangle\,.$$

and

$$T_{lk} = -\,\delta_{lk}\,\frac{F(q^2)}{2M}\,.$$

All quantities are of order q/M, rather than q^2/M^2, as might have been expected.

The results due to the spin effects indicate that the second-order corrections are predominantly due to the Coulomb interaction. Here we shall calculate only the single particle contribution arising from the center-of-mass motion, *i.e.*, T_{0l} and T_{l0}. Finding that this is much smaller than the single-particle Coulomb effects, we shall accept that in all cases, single- and two-particle terms, the Coulomb term is dominant.

The single-particle terms in T_{0l} and T_{l0} give

$$C_1^{(q)}(\boldsymbol{q}) = \frac{e^2\,\mathrm{tg}^2\,\theta/2}{4\pi^3}\,\frac{1}{AM}\,\mathrm{Re}\,i\int \mathrm{d}^4q_1\,\frac{\boldsymbol{q}_1^2 q_l - \boldsymbol{q}_1\cdot\boldsymbol{q}\,q_{1l}}{\boldsymbol{q}_1^2\boldsymbol{q}_2^2(q_1^2 + i\alpha)(\varepsilon + q_{10} - i\eta)}\,\cdot$$
$$\cdot\left\{\frac{\mathrm{Tr}\,\gamma_0 k_f\gamma\gamma_0(k_i\gamma - q_1\gamma)\gamma_l q_i\gamma}{(k_i - q_1)^2 + i\delta} + \frac{\mathrm{Tr}\,\gamma_0 k_f\gamma\gamma_l(k_f\gamma + q_1\gamma)\gamma_0 k_i\gamma}{(k_f + q_1)^2 + i\delta}\right\}.$$

The integrations over q_{10} and the angles of $\boldsymbol{q}_1$ are straightforward. The last integral over $|\boldsymbol{q}_1|$ is rather involved and two approximations will be made. First only terms not vanishing with ε are kept. Secondly, we expand the integrand in powers of $\cos^2\frac{1}{2}\theta$, keeping the first two terms. Within these approximations, the result is

$$C_1^{(q)}(\boldsymbol{q}) = -\,e^2\,\frac{q}{2M}\,J(\theta)\,,$$

with $J(\theta)$ given in Table IV. Since the expansion in $\cos^2\frac{1}{2}\theta$ is least adequate at $\theta = 90^\circ$, $J(\theta)$ at 90° is probably not too reliable. Otherwise within our

range of q-values, $q/M \leqslant 0.4$, this is much smaller than a one percent contribution.

TABLE IV. – *Center-of-mass momentum correction*, $C_1^{(q)}(\boldsymbol{q}) = -e^2(q/2M)J(\theta)$.

θ	$J(\theta)$
90°	2.28
120°	0.66
150°	0.30

The single-particle Coulomb correction in the static limit, $\varepsilon \to 0$, is (6-8)

$$C_1^{(C)}(\boldsymbol{q}) = \pi e^2 \, \frac{\sin\theta/2}{1+\sin\theta/2} \, .$$

At back angles this is about a one percent effect, but is appreciably larger than the orbital motion term, $C_1^{(q)}(\boldsymbol{q})$. We assume that the same holds for the two-particle terms.

The two-particle Coulomb terms have been evaluated in the static limit by LEWIS (9), using Yukawa and Gaussian form factors. His results with the Yukawa function are given in Table V, showing a correction of several percent

TABLE V. – *Lewis' results for percentage correction due to Coulomb effects. Form factor is Yukawa with r.m.s. radius*, $1.68\cdot 10^{-13}$ cm.

θ	$k=0.69\cdot 10^{13}\ \text{cm}^{-1}$		$k=1.04$	
	q	$C_1^{(C)}(\boldsymbol{q})$	q	$C_1^{(C)}(\boldsymbol{q})$
60°	0.69	−0.37	1.04	−0.92
90°	0.98	−1.18	1.47	−1.68
120°	1.20	−1.81	1.80	−2.14
150°	1.81	−2.11	2.00	−2.38

at large angles. LEWIS, unfortunately, has taken the Gaussian form factor only at momentum transfers much larger than those for which data are available. Since $C_1^{(C)}(\boldsymbol{q})$ is proportional to $\exp[a^2\boldsymbol{q}^2/2]$, at large angles and energies Lewis' results are quite large, becoming even greater than 100 %. In his range $\exp[a^2\boldsymbol{q}^2/2] \approx 300$, while at $q = 2\cdot 10^{13}\ \text{cm}^{-1}$, in ^{4}He $\exp[a^2\boldsymbol{q}^2/2] \approx 3$. Assuming $C_1^{(C)}(\boldsymbol{q})$ to scale, these corrections again become of the order of 5 %. We may therefore assume with some confidence that within our range of q-values all charge and convection current corrections are at best 5 % of the first-order cross-section.

3. – There are two conclusions to be drawn from these experiments. First we may say that in ^{4}He all second-order corrections to the first-order elastic scattering cross-section are at most 5% for $q = (1 \div 2) \cdot 10^{13}\,\text{cm}^{-1}$. BURLESON and KENDALL's results are that eq. (2) is satisfied for these q-values within experimental error of 6%. Therefore any large-angle anomalies due to electron dipole moments could not be masked or canceled by these dispersive effects, and their limits on λ and μ are valid.

In addition, the calculations of the spin and convection current contributions did not depend strongly on the particular target nucleus except through the parameters entering into the form factors. This dependence enters in the same way in the Coulomb terms. The conclusion that the Coulomb correction dominates then holds not only for ^{4}He, but for any nucleus, as long as q/M is not large. Thus in calculating the second-order corrections to elastic scattering, to a high order of accuracy only the Coulomb interaction need be considered.

* * *

Extreme gratitude is due Professor L. I. SCHIFF for suggesting this problem and for his guidance. I also wish to thank Dr. G. R. BURLESON for his discussions of his experiment. Lastly, I thank Drs. J. D. BJORKEN, J. FUJITA and C. N. LINDNER for innumerable interesting, enlightening and inspiring conversations.

RIASSUNTO (*)

Si valutano le correzioni dispersive di secondo ordine alla sezione d'urto per lo scattering elastico degli elettroni di alta energia da ^{4}He. Le correnti nucleari sono le correnti di convezione e di spin di ciascun nucleone. Per valutare l'ampiezza si usa un'approssimazione di chiusura. Gli effetti dello spin vengono calcolati esplicitamente supponendo un modello nucleare a particella indipendente per due differenti fattori di forma della carica. Si trova che questi sono inferiori al 4% della sezione d'urto di primo ordine. Si mostra come il contributo della corrente di convezione possa essere valutato entro le restrizioni dell'invarianza di gauge. Solo una parte dei termini di convezione vengono calcolati, si trova che questi ultimi sono molto più piccoli della correzione dovuta alla pura interazione Coulombiana. Si conclude che il contributo predominante alla correzione di secondo ordine è dovuto al potenziale di Coulomb, e che questo è vero in generale e non per il solo ^{4}He. Infine si fa menzione dell'importanza di queste correzioni negli esperimenti che misurano i fattori di forma del momento di dipolo elettrico e magnetico dell'elettrone.

(*) *Traduzione a cura della Redazione.*

A Note on Circular Gravitational Orbits (*).

P. GOLDHAMMER

Department of Physics, University of Nebraska - Lincoln, Neb.

(ricevuto il 20 Febbraio 1961)

SCHWARZSCHILD [1] has shown that the orbits provided by the general theory of relativity for a mass m circulating about a fixed mass M are described by

$$\frac{\mathrm{d}^2}{\mathrm{d}\varphi^2}\left(\frac{1}{R}\right)+\frac{1}{R}=\frac{1}{2\alpha\varrho}+6\varrho/R^2\,, \tag{1}$$

where

$$\varrho = kM/2c^2\,, \qquad a = (Lc/kMm)^2\,, \tag{2}$$

k is the gravitational constant, and L may be identified with the angular momentum. We wish to examine the circular orbits. Setting R=constant we obtain

$$R^2/2\alpha - R\varrho + 6\varrho^2 = 0\,. \tag{3}$$

Curiously we find that for a given angular momentum L we have two circular orbits:

$$R_\pm = \varrho\alpha[1 \pm (1-12/\alpha)^{\frac{1}{2}}]\,. \tag{4}$$

If L is large R_+ is slightly displaced from the usual Newtonian orbit:

$$R_+ \simeq 2\varrho\alpha - 6\varrho\,. \tag{5}$$

The orbits corresponding to R_- are obviously quite small, and have no classical analog.

We note further that there is a restriction on the admissible values of the angular momentum of circular orbits imposed by general relativity. One cannot

---

(*) Supported in part by a grant from the National Science Foundation.

[1] K. SCHWARZSCHILD: *Berl. Ber.*, (1916).

admit values of α less than 12, and so we have a minimum possible angular momentum for a particle in a circular orbit given by

$$L_{\min} = \sqrt{12}\,kMm/c\,. \tag{6}$$

For very large angular momentum one finds that R_- approaches 6ϱ while at $L_{\min}$ we have

$$(R_-)_{\max} = 12\varrho\,. \tag{7}$$

The ordinary classical orbit R_+ has value

$$(R_+)_{\min} = 12\varrho\,, \tag{8}$$

at $L_{\min}$. EINSTEIN [2] has previously noted that one cannot make the radius of a circular orbit arbitrarily small with the Schwarzschild metric since the particle begins to move with the speed of light before reaching the singularity. In this regard we note that there are also two circular orbits for a photon. The equation of motion is

$$\frac{\mathrm{d}^2}{\mathrm{d}\varphi^2}\left(\frac{1}{R}\right) + \frac{1}{R} = 6\varrho/R^2\,. \tag{9}$$

Circular orbits are found with $R=\infty$ which corresponds to the « classical » case; and $R=6\varrho$, which is the radius at which a massive particle would move with the velocity of light.

The energy of a particle in an orbit given by eq. 4 is

$$(E/mc^2)^2_\pm = 8/9 - (2/9)(1-\alpha/12)[1 \mp (1-12/\alpha)^{\frac{1}{2}}]\,. \tag{10}$$

The maximum binding is obtained where $\alpha=12$, and amounts to about 6% of the rest energy. If $\alpha \gg 12$ we find the usual classical values for the energy of the normal orbits ($R > 12\varrho$):

$$(E/mc^2)^2_+ \simeq 1 - \frac{1}{\chi} \simeq 1 - 2\varrho/R\,. \tag{11}$$

The energy of the relativistic orbits between 6ϱ and 12ϱ becomes greater than mc^2 for α greater than about 13.4 however, and consequently these orbits are unstable.

---

(2) A. EINSTEIN: *Ann. of Mathem.*, **40**, 922 (1939).

IL NUOVO CIMENTO   VOL. XX, N. 6   16 Giugno 1961

Modification of the Chew-Low Formula for the $(\frac{3}{2}, \frac{3}{2})$ π-$\mathcal{N}$ Resonance.

W. M. LAYSON (*)

CERN - Geneva

(ricevuto il 31 Marzo 1961)

The theory of Chew and Low for π-$\mathcal{N}$ scattering results in a formula, containing two parameters, which may be used to fit the observed phase shifts. It is most useful in the case of the $T=\frac{3}{2}$, $J=\frac{3}{2}$ state which contains the well-known resonance at approximately 2C0 MeV (lab.). The usual form ([1]) is

$$\frac{\eta^3}{\omega^*}\operatorname{ctg}\alpha_{33} = \frac{3}{4f^2}\left(1-\frac{\omega^*}{\omega_0}\right), \tag{1}$$

where $\eta = p/m_\pi c$ and p is the pion c.m. momentum, $(mc^2\omega^*)$ is the π-$\mathcal{N}$ c.m. energy less one nucleon mass, ω_0 is the resonance value and f is the coupling constant. For $\omega^* < \omega_0$ the straight line form of (1) agrees well with experiment, but for $\omega^* > \omega_c$ there is serious disagreement, as one might expect for a theory derived in a low energy approximation. However, it is possible to obtain good agreement with the data by noting that (1) actually ([2]) should contain $\eta^3[V(K)]^2$ in place of η^3. As explained by Wick

$$V(K) = \int \exp[i\boldsymbol{K}\cdot\boldsymbol{x}]\,\varrho(\boldsymbol{x})\,\mathrm{d}\boldsymbol{x}\,, \tag{2}$$

where K is the wave number

$$\left(K = \eta\left(\frac{\hbar}{m_\pi c}\right)\right),$$

and $\varrho(\boldsymbol{x})$ is the « extended source distribution » for the nucleon. In formula (1) $V(K)=1$ and $\varrho(\boldsymbol{x})=\delta(\boldsymbol{x})$. Actually, in a convergent theory one must introduce a cutoff. Instead of the usual sharp cutoff at $\omega^* = M/m_\pi$ (M=nucleon mass), I have considered the following:

$$\varrho(\boldsymbol{x}) = \frac{a^2\exp[-ar]}{4\pi r}\,. \tag{3}$$

This is a Yukawa source distribution, and yields a smooth cutoff for $V(K)$ or $V(\eta)$:

$$V(K) = \frac{1}{1+K^2a^{-2}}\,. \tag{4}$$

Introducing this into (1) it is possible to fit the data with $a^{-1}=0.38$ fermi

(*) National Science Foundation Fellow.

([1]) G. PUPPI and A. STANGHELLINI: *Nuovo Cimento*, **5**, 1305 (1957).

([2]) G. C. WICK: *Rev. Mod. Phys.*, **27**, 339 (1955).

($0.27(\hbar/m_\pi c)$ or $1.8(\hbar/Mc)$). The other constants are approximately in agreement with those of JOHNSON and CAMAC [7]:

$$f^2 = 0.087\,,$$

$$\omega_0 = 2.17\,.$$

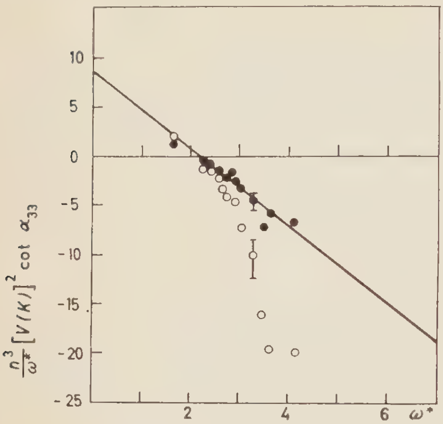

Fig. 1. – A Chew-Low plot for two values of $V(K)$ is shown above. The points are from the data of references [3-6]. The straight line is for $f^2 = 0.087$, $\omega_0 = 2.17$.

Since the Chew-Low theory is for a non-relativistic static nucleon problem and relies on the assumption that a complicated integral expression [8] can be approximated as a constant effective range (or equivalent ω_0), the agreement achieved with (4) may be fortuitous. Nevertheless it is interesting to note that the simple application of a more « realistic » nucleon source of approximately nucleonic dimensions brings theory and experiment together, as shown in the figure.

* * *

The author wishes to thank Professor B. T. FELD for advice and suggestions in this work.

---

[3] B. PONTECORVO: *Ninth Int. Annual Conf. on High Energy Physics*, p. 108.

[4] J. H. FOOTE, O. CHAMBERLAIN, E. H. ROGERS, H. M. STEINER, C. WIEGAND and T. YPSILANTIS: *Phys. Rev. Lett.*, **4**, 30 (1960).

[5] W. J. WILLIS: *Phys. Rev.*, **116**, 753 (1959).

[6] W. D. WALKER, J. DAVIS and W. D. SHEPHARD: *Phys. Rev.*, **118**, 1612 (1960).

[7] W. B. JOHNSON and M. CAMAC: The University of Rochester, NYO-2169.

[8] G. F. CHEW and F. E. LOW: *Phys. Rev.* **101**, 1570 (1956).

IL NUOVO CIMENTO Vol. XX, N. 6 16 Giugno 1961

Relativistic Pion-Nucleon Scattering with the Determinantal Method.

N. Bali, C. Garibotti, J. J. Giambiagi and A. Pignotti

Facultad de Ciencias Exactas y Naturales, Universidad de Buenos Aires - Buenos Aires

(ricevuto l'11 Aprile 1961)

It is a well known fact that a perturbation expansion of the scattering amplitude t is useless for large values of the coupling constant. Such is the case of the strong interactions. The determinantal method ([1]) offers an alternative procedure, based on the presumably better behaved expansion of a quantity $r(w)$ which can then be related to $t(w)$.

Let

$$\lim t(w+i\varepsilon) = t_+(w) = \frac{1}{\pi}\exp[i\delta(w)]\sin\delta(w) = \frac{r_+(w)}{D_+(w)}, \tag{1}$$

with

$$D_+(w) = 1 + \int \mathrm{d}w' \frac{r_+(w')}{w' - w - i\varepsilon}, \tag{2}$$

where the $+$ sign means that the limit is taken from above. It can then be shown that in potential theory $r(w)$ is an entire function of the coupling constant for very general potentials. No such proof exists in field theory, but it can be shown through unitarity that $r(w)$ has no discontinuities in the physical region of the real axis of the energy plane.

The method offers the possibility of improving the series for $t(w)$ once calculated up to a certain order in perturbation theory through the following expansions ([2]):

$$t_+(w) = [t_+^{(1)}(w) + t_+^{(2)}(w) + \ldots],$$

and

$$r_+(w) = [t_+^{(1)} + t_+^{(2)} + \ldots][1 + D_+^{(1)} + D_+^{(2)} + \ldots].$$

([1]) M. Baker: *Ann. Phys.*, **4**, 271 (1958).

([2]) See f.i. M. Baker and F. Zachariasen: *Phys. Rev.*, **118**, 1659 (1960) where the method is applied to π-π scattering.

One obtains, to first order (supressing + subscripts)

$$(3)\qquad \begin{cases} r^{(1)}(w) = t^{(1)}(w)\,, \\ D^1(w) = -\displaystyle\int \mathrm{d}w'\,\frac{r^{(1)}(w')}{w'-w-i\varepsilon} = -\,\mathrm{p.v.}\int \mathrm{d}w'\,\frac{r^{(1)}(w')}{w'-w} - i\pi r^{(1)}(w)\,, \end{cases}$$

to second order

$$r^{(2)}(w) = t^{(2)}(w) + t^{(1)}(w)D^{(1)}(w)\,,\quad \text{etc.}\,,$$

thus

$$(4)\qquad t(w) = \frac{1}{\pi}\,\frac{1}{\operatorname{ctg}\delta(w) - i} = \frac{r^{(1)} + r^{(2)} + \dots}{1 + D^{(1)} + D^{(2)} + \dots}\,.$$

The determinantal method was used to investigate the resonant behaviour of the π-$\mathcal{N}$ scattering in the 11, 13, 31 and 33 partial waves. The series for $t(w)$ was calculated to first order including the diagrams of Fig. 1. The derivation of the

Fig. 1.

different partial wave amplitudes is straightforward from Feynman rules and the appropriate projection operators ([3]). The result for the 33 wave is

$$(5)\qquad t_{33} = \frac{g^2}{64\pi^2 q}\left\{\left[-\alpha_1\frac{a}{q^2} + \alpha_2\left(1 - \frac{3}{4}\frac{a^2}{q^1}\right)\right]\ln\left|\frac{a+b}{a-b}\right| - 4\alpha_1 - \frac{3\alpha_2 a}{q^2}\right\},$$

where

$$\alpha_1 = \frac{w-M}{w^2}\left[(w+M)^2 - \mu^2\right]\,, \qquad a = 2\mu^2 + M^2 - w^2 + 2q^2\,,$$

$$\alpha_2 = \frac{w+M}{w^2}\left[(w-M)^2 - \mu^2\right]\,, \qquad b = -\,2q^2\,,$$

and similar expressions for the other partial waves. w is the total energy in the c.m. system and q the pion momentum. From eq. (3) and (4) one readily obtains, to first order

$$\operatorname{tg}\delta_{IJ}(w) = \frac{\pi t_{IJ}(w)}{1 + (w-M)\,\mathrm{p.v.}\displaystyle\int_{M+\mu}^{\infty}\mathrm{d}w'\left[t_{IJ}(w')/(w'-M)(w'-w)\right]}\,.$$

([3]) See f.i. S. C. FRAUTSCHI and J. D. WALECKA: *Phys. Rev.*, **120**, 1489 (1960).

where in order to renormalize the theory a subtraction has been performed at $w=M$ [1]. The integral in the denominator is convergent without the use of any cut-off factor. The energy of resonance w^0 will be given by the zeros of the denominator.

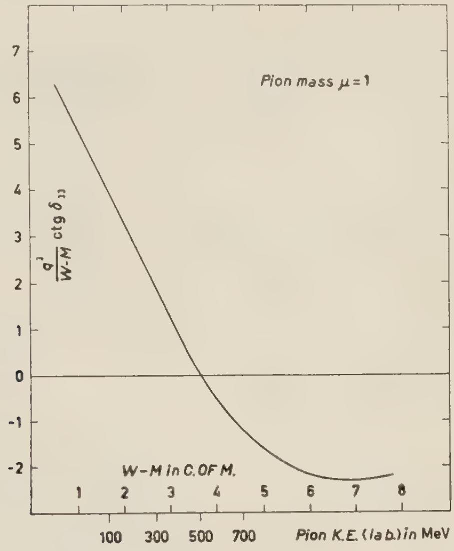

Fig. 2.

Calculations for the four partial waves were carried out numerically yielding a resonance in the 33 wave at $E^0_{\pi\,\mathrm{lab}}=500$ MeV while no resonances were found in the other waves up to this energy. The result is then qualitatively correct. Fig. 2 shows $q^3/(w-M)\,\mathrm{ctg}\,\delta_{33}$ as a function of the pion kinetic energy in the lab. system.

* * *

We are indebted to Prof. M. BAKER for suggesting this problem and for many valuable discussions.

2523

Very Preliminary Evidence for Even KΣ Parity from Associated Photoproduction (*).

J. J. Sakurai

The Enrico Fermi Institute for Nuclear Studies,
The Department of Physics, University of Chicago - Chicago, Ill.

(ricevuto il 20 Aprile 1961)

We wish to report an evidence in favor of even KΣ parity deduced from the angular distribution of associated photoproduction

$$\gamma + p \to K^+ + \Sigma^0 . \tag{1}$$

Our approach makes use of the well-known fact that the sign of the coefficient of the one-K-exchange pole term (1) is determined by the relative KΣ parity (2). In extracting the OKE term from the observed angular distribution, the only assumption we use is that only *s*-waves and *sp*-interference are significant for contributions *other* than the OKE term; this assumption may be justified since the de Broglie wavelength of the K particle in the c.m. system is as long as $1.0\cdot10^{-13}$ cm at the energy where the analysis is carried out. Our results are: (i) Odd KΣ parity is excluded by about two standard deviations. (ii) The resulting scalar $K\Sigma\mathcal{N}$ coupling constant is of the order of 0.6.

The photoproduction of charged K particles has been discussed by a number of authors (2,3). There are three salient features of practical interest common to all previous discussions (perturbative or dispersion-theoretic): (i) The OKE term gives rise to a retarded $\sin^2\theta$ distribution, and the sign of the coefficient of this term is positive for even KY parity (Y = Λ or Σ) but negative for odd KY parity. (ii) If the coupling constant is of the order of unity, the OKE term is expected to be much more pronounced in the even KY parity case than in the odd parity case as long as the differential cross-section at ∼100 MeV above the threshold is of the order of 10^{-31} cm² as experimentally observed. (iii) For the odd parity case the OKE term can never dominate in the physical region; otherwise the cross-section would become negative. Since we are interested only in the coefficient (both the sign and the magnitude) of the OKE term, we propose to treat the non-OKE con-

(*) This work was carried out under the auspices of the U. S. Atomic Energy Commission.

(1) Hereafter denoted by OKE.

(2) M. J. Moravcsik: *Phys. Rev. Lett.*, **2**, 352 (1959).

(3) M. Kawaguchi and M. J. Moravcsik: *Phys. Rev.*, **107**, 563 (1957); A. Fujii and R. E. Marshak: *Phys. Rev.*, **107**, 570 (1957); R. H. Capps: *Phys. Rev.*, **114**, 920 (1959).

tributions in an entirely phenomenological manner [4].

The angular distribution of reaction (1) has been measured by EDWARDS *et al.* [5,6] at $E_\gamma=1140$ MeV, 100 MeV above the threshold. At this energy the c.m. momentum of the K particle is 195 MeV/c, which corresponds to a de Broglie wavelength of $1.0\cdot10^{-13}$ cm. The range of forces associated with the non-OKE background is expected to be at most $(m_K+m_\pi)^{-1}=0.33\cdot10^{-13}$ cm; so it may be legitimate to assume that only *s*-waves and *sp*-interference are significant for the non-OKE contributions. It then becomes possible to characterize the angular distribution in terms of three constants [7]:

$$\frac{d\sigma}{d\Omega}=A+B\cos\theta+C\,\frac{\sin^2\theta}{(1-\beta_K\cos\theta)^2}, \tag{2}$$

where β_K is the velocity of the K particle in the c.m. system in units of c. The C term is the OKE contribution, and the sign and the magnitude of C are completely determined by the relative $K\Sigma$ parity and the coupling constant [2,3]. We have

$$C=\frac{1}{8}\left(\frac{1}{137}\right)\left(\frac{G^2_{K\Sigma\mathcal{N}}}{4\pi}\right)\frac{\beta_K^3\,\omega_K}{\omega_\gamma^3W^2}\cdot\left[(m_\Sigma\pm m_{\mathcal{N}})^2-m_K^2\right], \tag{3}$$

where ω_γ and ω_Σ are respectively the photon energy and the K particle energy in the c.m. system, and W stands for the total c.m. energy of the system. The upper (lower) sign is to be used for even (odd) $K\Sigma$ parity. $G^2_{K\Sigma\mathcal{N}}/4\pi$ is the scalar or pseudoscalar coupling constant for the $K\Sigma\mathcal{N}$ vertex defined in the usual manner.

Experimentally the observed angular distribution for $K^+\Sigma^0$ production is indeed similar to that of the OKE contribution with a *positive* value of C, indicating *even* $K\Sigma$ parity. We have analysed the experimental angular distribution in the following three ways, and in each case essentially the same value of the *scalar* coupling constant has been obtained.

(i) Assume that the pole term completely dominates (Set $A=B=0$). Then we obtain a value of C corresponding to the scalar coupling constant

$$\frac{G^2_{K\Sigma\mathcal{N}}}{4\pi}=0.75\pm0.08\,.$$

(ii) Forget about the form (2), and just extrapolate

$$(1-\beta_K\cos\theta)^2\frac{d\sigma}{d\Omega},$$

to $\cos\theta=\beta_K^{-1}$ using a *second* order polynomial *without any constraint*, just as MORAVCSIK [2] did for $K^+\Lambda^0$ production. Then we obtain the scalar coupling constant

$$\frac{G^2_{K\Sigma\mathcal{N}}}{4\pi}=0.63\pm0.36\,.$$

(iii) Assume the form (2), and obtain A, B and C, and $G^2/4\pi$. In Moravcsik's approach this way of determining the coupling constant amounts to extrapolating

$$(1-\beta_K\cos\theta)^2(d\sigma/d\Omega)$$

to $\cos\theta=\beta_K^{-1}$ using a third order polynomial such that only three of the four coefficients are independent because of (2)

---

[4] This makes our results independent of the validity of perturbation theory.

[5] D. A. EDWARDS, R. L. ANDERSON, F. TURKOT and W. M. WOODWARD: *Bull. Am. Phys. Soc.*, **6**, 39 (1961).

[6] F. TURKOT in *Proc. of the 1960 Annual International Conference on High Energy Physics at Rochester* (New York, 1960), p. 369.

[7] It is easy to show that in this approximation there is no interference between the OKE term and the non-OKE contributions. A similar analysis has been proposed by CAPPS [3] within the framework of perturbation theory.

We then obtain

$$(4)\quad \begin{cases} A & = (0.15 \pm 0.16)\cdot 10^{-31}\ \text{cm}^2, \\ B & = (0.19 \pm 0.12)\cdot 10^{-31}\ \text{cm}^2, \\ C & = (0.88 \pm 0.38)\cdot 10^{-31}\ \text{cm}^2, \\ \dfrac{G^2_{K\Sigma\mathcal{N}}}{4\pi} & = 0.62 \pm 0.27\,. \end{cases}$$

Note that in each case the experimental angular distribution favors a positive value of C, or equivalently a negative residue at $\cos\theta = \beta_K^{-1}$, which corresponds to *even* KΣ parity. It is also significant to note that the C term is very large compared to the A and B terms, which means that the OKE approximation is an excellent one even in the physical region. In Fig. 1 the quantity $(1-\beta_K\cos\theta)^2(d\sigma/d\Omega)$ is plotted against $\beta_K^{-1} - \cos\theta$ under the assumption (iii). We see that odd KΣ parity is excluded by 2.3 standard deviations.

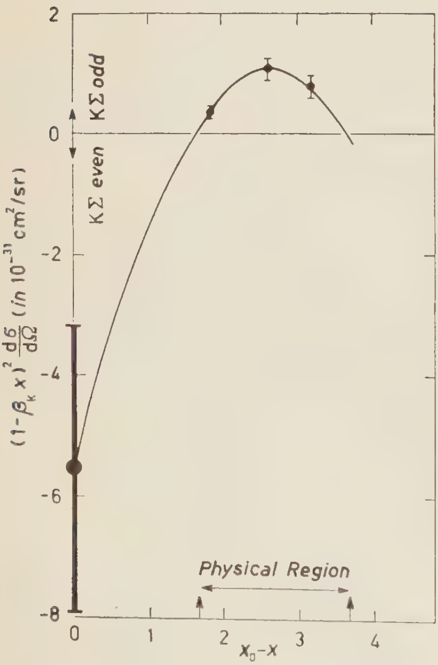

Fig. 1. – MORAVCSIK plot for $\gamma + p \to K^+ + \Sigma^0$. The quantity $(1-\beta_K x)^2(d\sigma/d\Omega)$ is plotted against $x_0 - x$ where $x = \cos\theta$ and $x_0 = \beta_K^{-1}$. The residue at $x_0 = x$ and the solid curves are obtained under the assumption that for the non-OKE contributions only s-waves and sp-interference are important (cubic extrapolation with one constraint). The experimental points in the physical region are taken from EDWARDS *et al.* [5].

We can now make predictions on the excitation function at 90°. Near threshold (say up to 110 MeV where the present analysis is carried out) the energy dependence must be given roughly by

$$(5)\qquad \left(\frac{d\sigma}{d\Omega}\right)_{90^\circ} = A\eta + C\eta^3,$$

where η is the c.m. momentum of the K particle measured in units of 195 MeV/c (the momentum at which the coefficients A and C are determined). Since the experimental value of A is vanishingly small, the 90° excitation function must be predominantly of the p^3 form. The available data are consistent with this prediction [6].

If we assume that the relation $A \ll C$ holds not only for $K^+\Sigma^0$ production but also for the reaction

$$\gamma + n \to K^+ + \Sigma^-,$$

then the $(K^+\Sigma^-)/(K^-\Sigma^0)$ ratio near 90° must be equal to two [8]. ($G^2_{K\Sigma\mathcal{N}}$ in (3) has to be replaced by $2G^2_{K\Sigma\mathcal{N}}$ in the $K^+\Sigma^-$ case). The predicted two-to-one ratio does not seem to be inconsistent with the observed ratios of 1.6 ± 0.7 (at 1122 MeV, 82°) and 0.8 ± 0.6 (at 1146 MeV, 75°) if corrections due to the momentum distribution of the neutron (estimated to be about +50%) are taken into account [6].

At comparable K particle momenta the angular distribution for

$$\gamma + p \to K^+ + \Lambda^0,$$

[8] Unfortunately in the $K^+\Sigma^-$ case the baryon exchange diagram might also result in a large $\sin^2\theta$-like term. In principle, but not in practice, one can distinguish the two terms, since the baryon exchange term has a pole in the $\cos\theta < -1$ region in contrast to the OKE term with a pole in the $\cos\theta > 1$ region.

is isotropic [6,9]; therefore the OKE term appears to be rather unimportant for $K^+\Lambda^0$ production at $p_K \sim 200$ MeV/c. If the coupling constant is of the order of unity, this feature is not surprising in the odd KΛ case but somewhat puzzling in the even KΛ case, as already pointed out by MORAVCSIK [2]. From our experience with photopion production [10], we may infer that for odd KΛ parity high energy data, rather than low energy data, may be more profitably used in extracting the OKE term in a reliable manner. Of course, at high energies the use of low-order polynomials cannot be justified *a priori* so that Moravcsik's criteria must be used in deciding how many powers of $\cos\theta$ are to be included in the extrapolation procedure.

One amusing point is that if we are just interested in determining the relative parity from low energy associated photoproduction experiments, the following simple rule can be used provided that the assumptions leading to eq. (2) can be justified. Plot $d\sigma/d\Omega$ as a function of $\cos\theta$. If the curvature

$$d^2\left(\frac{d\sigma}{d\Omega}\right)\Big/ d(\cos\theta)^2\,,$$

is negative in the forward hemisphere (which means that the angular distribution curves toward the axis), then the parity is even; if the curvature is positive, the parity is odd.

Coming back to the question of the KΣ parity and $G^2_{K\Sigma\mathcal{N}}/4\pi$, we may ask how the present analysis fits into our knowledge of other strange particle phenomena. In a previous communication [11], we have summarized various experimental indications in favor of odd ΛΣ parity. Since there is some evidence for odd KΛ parity from K^- He experiments [12], our evidence in favor of even KΣ parity fits well with odd ΛΣ parity.

From the dispersion relations for the $K\mathcal{N}$ interaction, KERTH [13] has estimated that K is « on the average » pseudoscalar, or more precisely speaking

$$(6)\quad P_{K\Lambda}X_\Lambda + P_{K\Sigma}X_\Sigma = -0.1 \text{ to } -0.4\,,$$

where $P_{K\Lambda}$ and $P_{K\Sigma}$ stand for the relative KΛ parity and the relative KΣ parity respectively (*i.e.* $P_{K\Lambda}$, $P_{K\Sigma} = \pm 1$ depending on even or odd parity), and

$$X_Y = \left(\frac{G^2_{KY\mathcal{N}}}{4\pi}\right)\cdot \left|\frac{4m_Y m_N}{(m_Y + P_{KY}m_{\mathcal{N}})^2 - m_K^2}\right|, \quad Y = \Lambda,\ \Sigma.$$

If we take both our value of the $K\Sigma\mathcal{N}$ constant and Kerth's result (6) seriously the K particle must be pseudoscalar with respect to Λ, and the pseudoscalar $K\Lambda\mathcal{N}$ constant must be at least as large as 10 and possibly 30. We believe that such an enormous value of the pseudoscalar $K\Lambda\mathcal{N}$ constant is unlikely. A $K\Lambda\mathcal{N}$ constant of the order of 10 would lead to a large positive value of the curvature in the $\gamma p \to K\Lambda$ angular distribution, and such an effect would have shown up even in very crude angular distribution measurements. It is possible that there are still a number of uncertainties (Y^*, etc.) associated with the $K\mathcal{N}$ dispersion relations [14].

---

(9) B. D. McDANIEL, A. SILVERMAN, R. R. WILSON and G. CORTELLESSA: *Phys. Rev.*, **115**, 1039 (1959); H. M. BRODY, A. M. WETHERELL and R. L. WALKER: *Phys. Rev.*, **149**, 1710 (1960).

(10) J. G. TAYLOR, M. J. MORAVCSIK and J. L. URETSKY: *Phys. Rev.*, **113**, 689 (1959).

(11) Y. NAMBU and J. J. SAKURAI: *Phys. Rev. Lett.*, **6**, 377 (1961). See also S. BARSHAY: *Phys. Rev. Lett.*, **1**, 97 (1958).

(12) G. PUPPI in *Proc. of the 1960 Annual International Conference on High Energy Physics at Rochester* (New York, 1960), p. 419.

(13) L. T. KERTH: *Rev. Mod. Phys.* (to be published).

(14) Recently a somewhat different approach to the $K\mathcal{N}$ dispersion relations has been proposed by Y. NOGAMI (to be published). His analysis seems to favor odd ΛΣ parity with a reasonable value of $(G^2_{K\Lambda\mathcal{N}}/4\pi)_{p.s.}$.

2527

This note is written not so much to present a decisive piece of evidence in favor of even $K\Sigma$ parity. Rather our main purpose is to point out that the existing very crude data (with only three points) already suggest that investigations along these lines are extremely promising. The magnitude of the coupling constant as well as the relative parity may be determined in a more conclusive manner when more precise measurements of the angular dependence of associated photoproduction become available.

IL NUOVO CIMENTO Vol. XX, N. 6 16 Giugno 1961

A Proposed Experimental Test of the Day, Snow and Sucher Argument Based on Antiproton Annihilation into Kaons.

B. d'Espagnat (*)

CERN - Geneva

(ricevuto il 4 Maggio 1961)

The purpose of this note is to stress the usefulness of the protonium annihilation modes

$$\bar{\mathrm{p}} + \mathrm{p} \rightarrow \begin{cases} \mathrm{K}_1^0 + \mathrm{K}_1^0\,, & (1a) \\ \mathrm{K}_2^0 + \mathrm{K}_2^0\,, & (1b) \\ \mathrm{K}_1^0 + \mathrm{K}_2^0\,, & (1c) \end{cases}$$

as tools for checking the validity of the Day, Snow and Sucher well-known general argument (1) on predominant S state absorption. If, as seems most likely (2), their argument does apply to protonium, then one expects all annihilations at rest to proceed from S states and therefore, all two-boson processes to take place from $^3S_1$ states [since, as is well-known (3-5), singlet states cannot decay into two charge conjugate spinless bosons (6)]. Now $^3S_1$ states, having $c=-1$ cannot annihilate through modes ($1a$) or ($1b$) for these final states have $c=+1$. If, therefore, the D.S.S. argument applies, *one expects that annihilations at rest into two neutral kaons* (and no pions) *should all be of type* ($1c$). If on the contrary the D.S.S. argument does *not* apply, then, as Bethe and Hamilton (4) have shown, the annihilations should occur predominantly from P states, *i.e.* from $^3P_{0,2}$ states in our case, with the opposite consequence ($c=+1$) that annihilations at rest into two neutral kaons and no pions *should all be of type* ($1a$) *or* ($1b$) (6).

It should be stressed that this very clear-cut distinction cannot be extended to the cases where charged or neutral pions are emitted together with the

(*) On leave from the University of Paris.

(1) T. B. Day, G. A. Snow and J. Sucher: *Phys. Rev. Lett.*, **3**, 61 (1959); hereafter abbreviated as D.S.S.

(2) B. P. Desai: *Phys. Rev.*, **119**, 1385 (1960).

(3) L. Michel: *Nuovo Cimento*, **10**, 319 (1953); D. Amati and B. Vitale: *Nuovo Cimento*, **2**, 719 (1955).

(4) H. Bethe and J. Hamilton: *Nuovo Cimento*, **4**, 1 (1956).

(5) P. Roman: *Theory of Elementary Particles* (Amsterdam, 1960).

(6) Process ($1a, b, c$) must conserve strangeness. The final state is therefore made of a kaon and an antikaon. According to whether the c value of the system is $+1$ or -1 this final state has to be symmetrized or antisymmetrized. In the case $c=-1$ one thus gets the final state ($1c$) whereas in the case $c=+1$ one gets a superposition of ($1a$) and ($1b$), the ($1a$):($1b$) branching ratio being always equal to unity.

kaons. This comes about because of the contributions from the singlet states, which have a c opposite to that of the triplet states of same angular momentum. When stopping antiprotons in hydrogen one should therefore expect appreciable numbers, both of double and of single K_1^0 events but — and this is the test of the D.S.S. argument — only *single* K_1^0 events having the kinetic energy $M - m_K$ (M, m_K, nucleon and K masses) which is characteristic of two-kaon annihilations (a margin of error smaller than 35 MeV being required in the measurement of this energy). Were the experiment to contradict these predictions, this would mean that the mechanism of quick Stark transitions to S states and absorption therefrom suggested by D.S.S. does not operate in this case, a fact which, in view of the calculations of Desai [2] on the capture rates of protonium, would presumably require some explanation of a general nature. An experimental confirmation, on the other hand, would prove the existence of such a mechanism, creating anomalously quick transitions.

* * *

It is a pleasure for me to thank Dr. Bouchiat, Prof. Gregory, Dr. Prentki, Prof. Van Hove and Prof. Yamaguchi for illuminating discussions on this and related topics.

IL NUOVO CIMENTO Vol. XX, N. 6 16 Giugno 1961

Corrélation du Champ Électrique dans un Plasma.

I. Fidone

Groupe de Recherches de l'Association Euratom-CEA - Fontenay aux Roses, Seine

(ricevuto il 4 Maggio 1961)

Récemment, Taylor [1] a appliqué le théorème de Nyquist généralisé [2] pour obtenir une évaluation de la résistivité d'un plasma. Taylor considère un ion lourd de charge Ze dans un gaz d'électrons en équilibre thermique. La relation (4.11) de la référence [2] donne la constante de frottement:

$$\mu = \frac{Z^2e^2}{kT}\int_0^\infty C(\tau)\,\mathrm{d}\tau\,, \tag{1}$$

où $C(\tau) = \langle E_x(t)E_x(t+\tau)\rangle$ est la fonction de corrélation temporelle du champ électrique fluctuant $\boldsymbol{E}(t)$ créé par les électrons (fluctuations d'équilibre) [*]. E_x est une composante de $\boldsymbol{E}$ et la moyenne envisagée est la moyenne d'ensemble. En calculant la moyenne, Taylor suppose les électrons indépendants les uns des autres. L'objet de cette note est d'essayer d'obtenir une meilleure approximation en introduisant l'effet des corrélations spatiales des électrons. Lewis [3] a donné une forme modifiée de la fonction de corrélation temporelle, dans le cadre du problème de l'élargissement Stark linéaire de la raie α de Lyman. L'expression de $C(\tau)$ obtenue par Lewis est applicable lorsque $2\varrho_c/\langle v\rangle \leqslant \tau \leqslant \tau_0$, où ϱ_c est la valeur critique du paramètre d'impact optique et τ_0 le temps de libre parcours moyen défini de façon que

$$\left\{\begin{aligned} &\langle(\Delta\boldsymbol{v})^2\rangle \sim \langle(\boldsymbol{v})^2\rangle\,,\\ &\Delta\boldsymbol{v} = \frac{e}{m_e}\int_0^\tau \boldsymbol{E}(t)\,\mathrm{d}t\,, \qquad \langle v\rangle = \sqrt{\frac{3kT}{m_e}}\,. \end{aligned}\right. \tag{2}$$

---

(1) J. B. Taylor: *Physics of Fluids*, **3**, 792 (1960).

(2) H. B. Callen and T. A. Welton: *Phys. Rev.*, **83**, 34 (1951).

(*) Monsieur Trocheris nous a fait remarquer que l'on pouvait obtenir l'éq. (1) en tenant compte de ce que le terme de Fokker-Planck $(\partial f/\partial t)_c$ est nul à l'équilibre. Si l'on suppose que $m(\langle\Delta v\rangle/\Delta t) = -\mu v$ et que la vitesse de l'ion est très petite par rapport à celle des électrons, on obtient l'éq. (1).

(3) M. Lewis: *Phys. Rev.*, **121**, 501 (1961).

Comme il n'y a pas dans notre problème de paramètre d'impact optique dépendant, par exemple, du nombre quantique principal de l'électron lié dans l'atome émetteur, il semble intéressant d'établir à nouveau l'expression de $C(\tau)$ afin de voir ce que deviennent dans notre cas les limites précédentes.

Nous voulons donc calculer

$$C(\tau) = \langle E_x(t)\,E_x(t+\tau)\rangle .$$

Nous avons

$$C(\tau) = \frac{1}{3}\langle \boldsymbol{E}(t)\cdot\boldsymbol{E}(t+\tau)\rangle = \tag{3}$$

$$= -\frac{16}{3}\pi^2 e^2 \sum_k{}' \sum_{k'}{}' \sum_{j\mu} \frac{\boldsymbol{k}\cdot\boldsymbol{k}'}{k^2 k'^2}\langle \exp[-i\boldsymbol{k}\cdot\boldsymbol{x}_j - i\boldsymbol{k}'\cdot\boldsymbol{x}_\mu(t+\tau)]\rangle_{(x,v)} =$$

$$= -\frac{16}{3}\pi^2 e^2 \sum_{kk'}{}' \sum_{j\mu} \frac{\boldsymbol{k}\cdot\boldsymbol{k}'}{k^2 k'^2} I_{j\mu} ,$$

où $\boldsymbol{x}_j$ désigne la position de l'électron j, (x, v) en indice une moyenne sur les positions et les vitesses et le symbole $\sum'$ désigne une sommation excluant le terme $k = k' = 0$. Apartir de maintenant, nous nous limiterons au cas où $\boldsymbol{x}_\mu(t+\tau) \simeq \simeq \boldsymbol{x}_\mu(t) + \boldsymbol{v}_\mu\cdot\boldsymbol{\tau}$ c'est-à-dire aux temps τ inférieurs à un certain temps caractéristique T_M que nous définirons plus loin. Avec cette simplification, on a

$$I_{j\mu} = \langle \exp[-i\boldsymbol{k}\cdot\boldsymbol{x}_j - i\boldsymbol{k}'\cdot\boldsymbol{x}_\mu\rangle_x \langle \exp[-i\boldsymbol{k}'\cdot\boldsymbol{v}\tau]\rangle_v . \tag{4}$$

Pour calculer

$$\langle \exp[-i\boldsymbol{k}\cdot\boldsymbol{x}_j - i\boldsymbol{k}'\cdot\boldsymbol{x}_\mu]\rangle_x = \iint \exp[-i\boldsymbol{k}\cdot\boldsymbol{x}_j - i\boldsymbol{k}'\cdot\boldsymbol{x}_\mu]\, P(\boldsymbol{x}_j, \boldsymbol{x}_\mu)\,\mathrm{d}\boldsymbol{x}_j\,\mathrm{d}\boldsymbol{x}_\mu , \tag{5}$$

il faut se donner une forme explicite de la fonction de distribution $P(\boldsymbol{x}_j, \boldsymbol{x}_\mu)$.

Nous utiliserons l'expression approchée de la théorie de Debye utilisée par BARANGER et MOZER [4] qui s'écrit

$$P(\boldsymbol{x}_j\,\boldsymbol{x}_\mu) = g_1(\boldsymbol{x}_j)g_1(\boldsymbol{x}_\mu) + g_2(\boldsymbol{x}_j, \boldsymbol{x}_\mu) , \tag{6}$$

avec

$$\left\{\begin{array}{l} g_1(\boldsymbol{x}) = 1 , \\[2mm] g_2(\boldsymbol{x}_j, \boldsymbol{x}_\mu) = \exp\left[-\dfrac{e^2}{kT}\varphi_{j\mu}\right] - 1 , \quad \varphi_{j\mu} = \dfrac{\exp[-|\boldsymbol{x}_j - \boldsymbol{x}_\mu|/\lambda]}{|\boldsymbol{x}_j - \boldsymbol{x}_\mu|} , \quad \lambda = \left(\dfrac{kT}{4\pi e^2 n}\right)^{\frac{1}{2}} , \end{array}\right. \tag{7}$$

en négligeant la correction due au fait qu'au point où nous calculons le champ électrique se trouve une charge Ze. En tenant compte de cette charge Ze, $g_1(\boldsymbol{x})$ ne serait pas égal à l'unité, mais vaudrait [4]

$$g_1(\boldsymbol{x}) = \exp\left[-\frac{Ze^2}{kT}\,\frac{\exp[-|x|/\lambda]}{|\boldsymbol{x}|}\right] .$$

---

[4] M. BARANGER and B. MOZER: *Phys. Rev.*, **115**, 521 (1959); **118**, 626 (1960).

Si les valeurs de $|\boldsymbol{x}|$ inférieures à Ze^2/kT donnent une contribution négligeable dans notre calcul, nous pouvons poser $g_1(\boldsymbol{x}) \sim 1$. En utilisant (6) et (7), on peut aisément calculer l'expression (5) et nous obtenons ainsi pour $I_{j\mu}$:
pour $j=\mu$

$$I_{j\mu} = \langle \exp[-i\boldsymbol{k}'\cdot\boldsymbol{v}\tau]\rangle_v \, \delta_{\boldsymbol{k},-\boldsymbol{k}'} , \qquad \delta_{\boldsymbol{k},-\boldsymbol{k}'} = \begin{cases} 1 , & \text{si } \boldsymbol{k} = -\boldsymbol{k}', \\ 0 , & \text{si } \boldsymbol{k} \neq \boldsymbol{k}', \end{cases}$$

pour $j \neq \mu$

$$I_{j\mu} = \langle \exp[-i\boldsymbol{k}'\cdot\boldsymbol{v}\tau]\rangle_v \iint \exp[-i\boldsymbol{k}\cdot\boldsymbol{x}_j - i\boldsymbol{k}'\cdot\boldsymbol{x}_\mu] \left[\exp\left[-\frac{e^2}{eT}\varphi_{j\mu}\right] - 1\right] \mathrm{d}\boldsymbol{x}_j \, \mathrm{d}\boldsymbol{x}_\mu .$$

Nous conservons à nouveau ici les distances de l'ordre de e^2/kT qui n'ont qu'une influence négligeable sur le calcul. Ceci implique évidemment que nous excluons des valeurs du temps inférieures à $(e^2/kT)/\langle v\rangle$. Le domaine des valeurs de τ pour lequel notre approximation est valable est donc

$$\tau_m = \frac{e^2/kT}{\langle v\rangle} \leqslant \tau \leqslant T_M .$$

Développant $\exp[-(e^2/kT)\varphi_{j\mu}]$ en série, on obtient

$$I_{j\mu} \simeq \frac{1}{n(1+\lambda^2k^2)} \langle \exp[-i\boldsymbol{k}'\cdot\boldsymbol{v}\tau]\rangle_v \, \delta_{\boldsymbol{k},-\boldsymbol{k}'} ,$$

où n est la densité électronique.

La relation (3) peut maintenant s'écrire

$$C(\tau) = \frac{16\pi^2e^2n}{3} \sum_k{}' \frac{\lambda^2}{1+\lambda^2k^2} \langle \exp[i\boldsymbol{k}\cdot\boldsymbol{v}\tau]\rangle_v .$$

On peut obtenir une expression simple pour $C(\tau)$ en prenant une fonction de Dirac pour la distribution de vitesses électroniques.

On a alors:

$$C(\tau) = \frac{4\pi e^2 n}{3} \frac{\exp[-(\langle v\rangle/\lambda)\tau]}{\langle v\rangle\,\tau} , \tag{8}$$

qui correspond à l'expression donnée par LEWIS [3]. Le cas d'une distribution Maxwellienne donne une expression plus compliquée. Si

$$P(\boldsymbol{v})\,\mathrm{d}\boldsymbol{v} = \left(\frac{m}{2\pi kT}\right)^{\frac{3}{2}} \exp[-mv^2/2kT]\, v^2 \sin\theta \, \mathrm{d}v \, \mathrm{d}\theta \, \mathrm{d}\varphi ,$$

on trouve

$$\langle \exp[i\boldsymbol{k}'\cdot\boldsymbol{v}\tau]\rangle_v = \exp\left[-\left(\frac{kT}{2m}\right) k'^2 \tau^2\right] ,$$

et

$$C(\tau) = \frac{16\pi^2 e^2 n}{3} \sum_{k'}{}' \frac{\lambda^2}{1 + k'^2 \lambda^2} \exp\left[-\left(\frac{kT}{2m}\right) k'^2\, \tau^2\right] = \tag{9}$$

$$= \frac{8\sqrt{\pi}\, e^2 n}{3\tau}\left(\frac{m}{2kT}\right)^{\frac{1}{2}} - \frac{4\pi e^2 n}{3\lambda} \exp\left[\frac{\omega_p^2}{2}\,\tau^2\right]\left[1 - \mathrm{erf}\left(\frac{\omega_p}{\sqrt{2}}\,\tau\right)\right],$$

où

$$\omega_p = \left(\frac{4\pi n e^2}{m}\right)^{\frac{1}{2}}, \qquad \mathrm{erf}\,(x) = \frac{2}{\sqrt{\pi}} \int_0^x \exp\,[-t^2]\, \mathrm{d}t\,.$$

Le premier terme de l'éq. (9) est la valeur de $C(\tau)$ donnée dans la référence (1) et représente $C(\tau)$ en l'absence de corrélation. Nous pouvons à présent calculer la constante de frottement. A l'aide de (8), on peut réécrire (1) sous la forme

$$\mu = \frac{4\pi Z^2 e^4 n}{3(kT)\,\langle v\rangle} \int_{\tau_m}^{T_M} \frac{\exp\,[-\,(\langle v\rangle/\lambda)\,\tau]}{\tau}\, \mathrm{d}\tau\,.$$

Il nous faut maintenant considérer la valeur de T_M. Dans la référence (1), on le prend de l'ordre de $1/\omega_p$, tandis que dans la référence (3) on utilise le temps de libre parcours moyen τ_0 défini par les relations (2). Approximativement, on a

$$\tau_0 \sim \frac{1}{\omega_p}\left(\frac{\lambda}{n^{-\frac{1}{3}}}\right)^3 \frac{36\pi}{\ln\,(\lambda/(e^2/kT))} \gg 1/\omega_p\,,$$

si bien que la valeur de T_M semble pouvoir être ajustée assez librement. Il nous semble que $T_M \sim \tau_0$ doit être considéré comme une valeur plus raisonnable parce que, dans un gaz près de l'équilibre, le temps au bout duquel la trajectoire réelle d'une particule a dévié de manière appréciable par rapport à une trajectoire rectiligne, est donné par

$$\langle(\Delta \boldsymbol{v})^2\rangle \sim \langle(\boldsymbol{v})^2\rangle\,.$$

De plus, comme $\tau_0 \gg 1/\omega_p$, on peut remplacer la limite supérieure de l'intégrale par l'∞ et l'on obtient

$$\mu = \frac{8\pi^{\frac{1}{2}} Z^2 e^4 n}{3(kT)}\left(\frac{m}{2kT}\right)^{\frac{1}{2}} \sqrt{\frac{\pi}{6}}\left[-E_i\left(-\frac{1}{\Lambda}\right)\right], \qquad \Lambda^{-1} = \frac{e^2/kT}{\lambda}\,. \tag{10}$$

Le calcul de μ à partir de l'expression (9) n'est pas aussi simple. En particulier, il faut être attentif au rôle joué par la limite supérieure. Si nous prenons $T_M \sim \tau_0 \gg 1/\omega_p$, le premier terme de l'éq. (9) ne donne pas la même valeur que celle obtenue dans la référence (1) pour la constante de frottement. Comme nous

voulons évaluer la correction due aux corrélations spatiales des électrons, nous suivrons le raisonnement de Taylor en supposant $T_M \sim 1/\omega_p$.

La constante de frottement devient alors

$$\mu = \frac{8\pi^{\frac{1}{2}} Z^2 e^4 n}{3(kT)} \left(\frac{m}{2kT}\right)^{\frac{1}{2}} \ln \Lambda - \frac{4\pi Z^2 e^4 n}{3(kT)\lambda} \int_{\tau_m}^{1/\omega_p} \exp\left[\frac{\omega_p^2}{2}\tau^2\right]\left[1 - \operatorname{erf}\left(\frac{\omega_p}{\sqrt{2}}\tau\right)\right] d\tau \,.$$

En développant l'intégrande en série et ne gardant que les termes d'ordre inférieur, on obtient

$$\mu = \frac{8\pi^{\frac{1}{2}} Z^2 e^4 n}{3(kT)} \left(\frac{m}{2kT}\right)^{\frac{1}{2}} \left[\ln \Lambda - 0.8 \sqrt{\frac{\pi}{2}}\right]. \tag{11}$$

Nous avons négligé une faible correction résultant de la limite inférieure de l'intégrale.

Finalement, la résistivité, suivant la définition de SPITZER [5] est donnée par

$$\eta_1 = \frac{16}{3} \frac{\pi^{\frac{1}{2}} m^{\frac{1}{2}} Z e^2}{(2kT)^{\frac{3}{2}}} \left[\ln \Lambda - 0.8 \sqrt{\frac{\pi}{2}}\right],$$

$$\eta_2 = \frac{16}{3} \frac{\pi^{\frac{1}{2}} m^{\frac{1}{2}} Z e^2}{(2kT)^{\frac{3}{2}}} \sqrt{\frac{\pi}{6}} \left[-E_i\left(-\frac{1}{\Lambda}\right)\right],$$

en utilisant les éq. (11) et (10) respectivement.

Pour les grandes valeurs de Λ l'expression de η_2 se réduit à

$$\eta_2 = \frac{16}{3} \frac{\pi^{\frac{1}{2}} m^{\frac{1}{2}} Z e^2}{(2kT)^{\frac{3}{2}}} \sqrt{\frac{\pi}{6}} [\ln \Lambda - 0.577] \,.$$

* * *

Nous désirons remercier MM. TROCHERIS et ENGELMANN pour avoir lu et commenté la présente note.

---

[5] L. SPITZER jr.: *Physics of Fully Ionized Gases* (New York, 1956).

IL NUOVO CIMENTO Vol. XX, N. 6 16 Giugno 1961

Pion-Hyperon Resonance from $\overline{\mathrm{K}}$ Nucleon Coulomb Constructive S-Wave Parameters.

G. Costa

Istituto di Fisica dell'Università - Padova
Istituto Nazionale di Fisica Nucleare - Sezione di Padova

F. Ferrari

Istituto di Fisica dell'Università - Bari

M. Pusterla

Istituto di Fisica dell'Università - Bari
Istituto Nazionale di Fisica Nucleare - Sezione di Napoli

(ricevuto il 9 Maggio 1961)

The elastic K-$\mathcal{N}$ and $\overline{\mathrm{K}}$-$\mathcal{N}$ scattering amplitudes exhibit a relevant long range interaction due to the possibility of exchanging pions between the K-mesons and the nucleons (1). To be more specific, by assuming double dispersion relations, it has been shown that the low angular momentum phase-shifts may be strongly affected by the presence of the dynamical branch cut related with the pion exchanges (2).

Because of the production of Λ- and Σ-hyperons connected with the $\overline{\mathrm{K}}$-$\mathcal{N}$ interaction, it is interesting to see whether a $\overline{\mathrm{K}}$-$\mathcal{N}$ scattering amplitude properly continued below the $\overline{\mathrm{K}}$-$\mathcal{N}$ physical threshold might provide information about the π-hyperon systems. Dalitz and Tuan (3) starting from a zero range solution do find a resonance in the $I=1$ π-hyperon S-wave amplitude, in agreement with the experimental data. Their scattering solution which behaves in this way has the peculiar character of producing destructive interference with the K^--p Coulomb force (4).

(1) F. Ferrari, G. Frye and M. Pusterla: *Phys. Rev. Lett.*, **4**, 615 (1960).

(2) F. Ferrari, G. Frye and M. Pusterla: *Long range interaction in* K-$\mathcal{N}$ *and* $\overline{\mathrm{K}}$-$\mathcal{N}$ *elastic amplitudes*, UCRL-9421, *Phys. Rev.* (to be published).

(3) R. H. Dalitz and S. F. Tuan: *Ann. of Phys.*, **8**, 100 (1959); *Phys. Rev. Lett.*, **2**, 425 (1959); *Ann. of Phys.*, **10**, 307 (1960).

(4) We remark that this solution does not explain the energy behaviour of the Σ^-/Σ^+ production rate suggested by the present data. See: R. H. Dalitz and S. F. Tuan: *Ann. of Phys.*, **10**, 307 (1960).

Experimental evidence, although not definite on this point, seems to favour a constructive interference ([5]).

In this note we like to emphasize that a Coulomb constructive $\bar{\mathrm{K}}$-$\mathcal{N}$ scattering amplitude can generate a resonance in the $I=1$ S-wave amplitude of the pion-hyperon system, if the long range force (due to the KK-$\pi\pi$ interaction) is taken into account.

In previous works the low energy behaviour of the K-$\mathcal{N}$ and $\bar{\mathrm{K}}$-$\mathcal{N}$ scattering has been interpreted in terms of a simple model in which a strong pion-pion interaction takes place in the $J=1$, $I=-1$ state. It has been found that a sharp resonance at $t_R \simeq 12$ (t=square of the total c.m. energy in pion mass units) gives results consistent with the present experimental data ([6,7]).

Recently, different pion production experiments ([8]) as well as theoretical analyses of the electromagnetic form factors of the nucleons ([9]) seem to be in favour of a resonant $J=1$, $I=1$ two-pion state at a higher energy $t_R \simeq 20$. Moreover, there is also some evidence of a $S=1$, $I=0$ three-pion bound state at $t'_R \simeq 5$ ([9,10]).

We are therefore led to consider two possible sources of the long range interaction. It is fortunate that their contributions are additive in the $I=1$ K-$\mathcal{N}$ and $\bar{\mathrm{K}}$-$\mathcal{N}$ systems ([11]), giving rise to long range forces similar to those obtained in ref. ([6]). This still allows an approximate description of the effects of the pion interactions along the dynamical branch cut in terms of a single pole, which would replace the separate contributions of the two- and three-pion states.

We point out that the two-pion forces are strongly repulsive in the $I=1$ K-$\mathcal{N}$ state, providing us with a simple interpretation of the low energy behaviour of the K^+-p scattering cross-section.

The amplitude for π-hyperon scattering is related to the K^--proton amplitude through the unitarity condition ([12,13]). In order to decide about the existence of a bound $I=1$ state, in the absence of a rigorous analitical continuation in the $\bar{\mathrm{K}}$-$\mathcal{N}$ elastic amplitude which was approximated in eq. (5) of ref. ([1]), we have to make sure that it reproduces dynamically as a resonance in the pion-hyperon elastic scattering.

([5]) L. W. ALVAREZ: *The interaction of strange particles*, UCRL-9354 (1960).

([6]) F. FERRARI, G. FRYE and M. PUSTERLA: *Energy dependence of the low energy* K^-p *and* K^+p *cross sections*, UCRL-9434; *Phys. Rev.* (to be published).

([7]) B. W. LEE: *Phys. Rev.*, **121**, 1550 (1961) and *Ph. D. Thesis*, University of Pennsylvania (unpublished); J. B. BJORKEN: *Proc. of the Ann. Intern. Conference on High Energy* (Rochester, 1960), p. 467; M. M. ISLAM: *Nuovo Cimento*, **20**, 546 (1961).

([8]) J. A. ANDERSON, U. X. BANG, P. G. BURKE, D. D. CARMONY and N. SCHMITZ: *Phys. Rev. Lett.*, **6**, 365 (1961); and B. MAGLIČ: private communication.

([9]) S. BERGIA, A. STANGHELLINI, S. FUBINI and C. VILLI: *Phys. Rev. Lett.*, **6**, 367 (1961).

([10]) A. ABASHIAN, N. E. BOOTH and K. M. CROWE: *Phys. Rev. Lett.*, **5**, 258 (1960); and G. F. CHEW: Communication at the Strong Interaction Conference (Berkeley, 1960).

([11]) The additivity of the contributions due to the two- and three-pion systems to the long range interactions can be argued from Sect. **5** of ref. ([2]).

([12]) The long range parts of the K-$\mathcal{N}$ and $\bar{\mathrm{K}}$-$\mathcal{N}$ potentials due to pion exchanges are simply related to each other, as long as the reactive effects of the absorption processes in the $\bar{\mathrm{K}}$-$\mathcal{N}$ system are not too strong in this region. This should be the case, since the absorption interactions take place at a shorter range, corresponding to the exchange of at least one pion and K-meson.

([13]) We notice that the $\bar{\mathrm{K}}$-$\mathcal{N}$ partial waves scattering amplitudes exhibit a peculiar superposition of the unitarity cut (in the s plane) with the branch cut due to the pion exchanges. The latter continues below the former up to the value $s=(\sqrt{M_{\mathcal{N}}^2+m_\pi^2}+\sqrt{m_{\mathrm{K}}^2+m_\pi^2})^2$. It can be easily shown that this overlapping does not forbid the possibility of writing dispersion relations for the partial waves, as the Mandelstam representation gives a unique prescription for separating the overlapping singularities. See also: S. MANDELSTAM: *Phys. Rev. Lett.*, **4**, 84 (1960).

We here develop an approximate form of the S-wave π-hyperon scattering amplitude valid within a small range below the $\bar{K}$-$\mathcal{N}$ threshold s_0. By calling δ_0 the π-hyperon phase-shifts at the $\bar{K}$-$\mathcal{N}$ physical threshold and by assuming

$$\lambda = \frac{k_Y(s)}{k_Y(s_0)} \sim 1 ,$$

we obtain, using a 2×2 scattering matrix [14],

$$\text{ctg}\,\sigma_Y - i = (\text{ctg}\,\sigma_0 - i)\,\frac{1 + (B - iA)[k_K + ih(s)]}{1 + (A - B\,\text{ctg}\,\delta_0)[h(s) - ik_K]}, \tag{1}$$

where [15]

$$A + iB = \frac{G(s_0)}{s_0^{\frac{1}{2}}(E_0 + M)} .$$

and

$$h(s) = -\frac{[l_{11}(s) - ik_K]^2 t(s)}{1 + [l_{11}(s) - ik_K] f_1(s)} ,$$

$$l_{11}(s) = \frac{s - s_0}{\pi} P\int_{s_0}^{\infty} ds' \frac{\text{Im}\,[G^{-1}(s')]_{11}}{(s' - s)(s' - s_0)} - \frac{a - s_0}{\pi}\int_{s_0}^{\infty} ds' \frac{\text{Im}\,[G^{-1}(s')]_{11}}{(s' - a)(s' - s_0)} .$$

k_Y is the c.m. momentum of the π-hyperon system, k_K is the c.m. momentum of the K-nucleon system. The function $f_1(s)$ is defined as in eq. (5) of ref. [1]:

$$f_1(s) = -\frac{1}{\pi}\left(\frac{1}{s - a} - \frac{1}{s_0 - a}\right)\frac{R^{(1)}_{KK,\pi\pi}}{1 + \beta R^{(1)}_{KK,\pi\pi}} .$$

$$\beta = \frac{1}{\pi^2}\int_{s_0}^{\infty} ds' \frac{\text{Im}\,[G^{-1}(s')]_{11}}{(s' - a)^2} .$$

We remark that the expression given above for $f_1(s)$ reproduces quite accurately the behaviour of the integral of the spectral function $[\text{Im}\,G_{11}(s)]_{\pi\pi}$ for values of s not close to $s=a$. In the region around $s=a$ it should be properly replaced by a Breit-Wigner type function.

Taking into account such requirement, the resonance condition is

$$1 + (B - iA)k_K + ih(s)] = 0 . \tag{2}$$

([14]) This approximation, made only for the sake of simplicity, does not weaken the conclusions. See also ref. ([3]).

([15]) The values used for the parameters A, B, are those obtained from ref. ([1]):

$$A + iB = (0.70 + i0.22)\ \text{fermi} .$$

2538

It can be seen that this condition is satisfied by a complex value of s on the unphysical sheet very close to the real axis around $s \simeq 95$ (this value of s in pion mass units corresponds to about 1360 MeV for the pion-hyperon total c.m. energy), if the parameters of the $\overline{\mathrm{K}}$-$\mathcal{N}$ approach outlined in the previous papers are assumed for the $I=1$ state [1]. The corresponding half-width is approximately 20 MeV.

In conclusion we have the possibility of creating enough attraction in the $I=1$ $\overline{\mathrm{K}}$-$\mathcal{N}$ state such as to obtain a resonance in the π-hyperon system if the two- and three-pion systems are taken into account. The absence of a three-pion bound state at low energy requires, to get agreement with experiments, a shift to lower values for the resonance in the P-wave two-pion system with respect to the value $t_R \simeq 20$ generally assumed, or a strong pion-pion scattering at lower energy behaving in the same direction of the resonance.

We finally notice that the pion-hyperon resonance appears from eq. (2) shifted to higher energy (a few pion masses) in comparison with the position of the bound state in the $\overline{\mathrm{K}}$-$\mathcal{N}$ amplitude.

A quantitative estimate of this resonance in terms of recent values for the pion systems and in terms of the latest $\mathrm{K}^-\mathcal{N}$ and $\mathrm{K}^+\mathcal{N}$ scattering data is in progress.

Note added in proof.

The same model has been suggested independently by G. Frye (private communication).

On the Symplectic Symmetry.

A. Salam
Imperial College - London

J. C. Ward
Institute for Advanced Study - Princeton, N. J.

(ricevuto il 10 Maggio 1961)

R. Utiyama [1] has shown in complete generality that if a set of elementary particles possesses a Lie symmetry, gauge transformations of the second kind lead directly to associated vector mesons whose number equals the number of generators of this particular Lie group. Recent theoretical speculations have centred around the investigation of possible Lie symmetries and the vector meson fields associated with these. The 3-dimensional isotopic rotation group was considered from this point of view by Yang and Mills, R. Shaw, S. Bludman, J. J. Sakurai and others [2], while the 3-dimensional unitary symmetry (introduced in conjunction with the Sakata-Thirring model) has been studied by Wess [3], Ikeda and Yamaguchi and its associated vector mesons by Neeman [4], Gell-Mann, Salam and Ward. Among these mesons are included four particles which look remarkably like the K* particles recently discovered at Berkeley [5]. This at present appears perhaps the most commendatory feature of the gauge ideas in connection with the unitary group.

The purpose of this note is to point out that the Salam-Polkinghorne [6] theory of elementary particles admits of the (unitary) symplectic group in 4-dimensions

(1) R. Utiyama: *Phys. Rev.*, **101**, 1597 (1956). Also see M. E. Mayer: preprint (Dubna, 1958).

(2) C. N. Yang and R. Mills: *Phys. Rev.*, **96**, 190 (1954); R. Shaw: *Cambridge Dissertation* (1954), unpublished; J. J. Sakurai: *Ann. of Phys.*, **11**, 1 (1960); S. Bludman: *Phys. Rev.*, **100**, 372 (1955); A. Salam and J. C. Ward: *Nuovo Cimento*, **11**, 568 (1959); **19**, 165 (1961); S. Glashow: *Nucl. Phys.*, **10**, 107 (1959).

(3) J. Wess: *Nuovo Cimento*, **15**, 52 (1960); M. Ikeda, S. Ogawa and Y. Ohnuki: *Progr. Theor. Phys.*, **22**, 715 (1959); Y. Yamaguchi: *Progr. Theor. Phys. Suppl.*, no. 11 (1959).

(4) M. Gell-Mann (preprint). We are grateful to Professor M. Gell-Mann for sending us a preprint before publication; Y. Neeman: *Nucl. Phys.* (to be published); A. Salam and J. C. Ward: *Nuovo Cimento*, to be published (1961).

(5) M. Alston, L. W. Alvarez, Ph. Eberhard, M. L. Good, W. Graziano, H. K. Ticho and S. G. Wojcicki: *Phys. Rev. Lett.*, **5**, 11, 520 (1960); C. H. Chan: *Phys. Rev. Lett.*, **6**, 383 (1961).

(6) A. Salam and J. C. Polkinghorne: *Nuovo Cimento*, **2**, 685 (1955).

and the associated vector mesons in this case also include vector particles similar to K*. Let us recall that this theory arose in the first place when one considers the internal symmetry space to be a 4-dimensional Euclidian space. The six independent rotations fall into two groups of three, leading to the quantum numbers $\boldsymbol{I}^+$, $\boldsymbol{I}^-$, where $\boldsymbol{I}^+$ corresponds to conventional isotopic spin and $2I_3^- = U$ (U is the hypercharge). Thus, for example, we obtain the classification,

I_3^+	I_3^-	Identification
0	0	Λ
$\frac{1}{2}$	$\frac{1}{2}$	(K, $\overline{\mathrm{K}}$); ($\mathcal{N}$, Ξ)
1	0	(π); (Σ)
0	1	(W); (X)

W⁺, W⁰, W⁻ are a (Bose) triplet with $S=2, 0, -2, I=0$ and X⁺, X⁰, X⁻ are Fermi particles with $I=0$, $S=1, -1, -3$ [7].

Now it can be shown that the ten particles π, W, K and $\overline{\mathrm{K}}$ (and likewise, Σ, X, $\mathcal{N}$, Ξ) correspond to the representations of the symplectic group. To see this we remark that this group has ten generators, the simplest realization of which is provided by the four Dirac matrices γ_μ and the six rotation matrices

$$\sigma_{\mu\nu} = \frac{1}{2i}(\gamma_\mu\gamma_\nu - \gamma_\nu\gamma_\mu)\,.$$

Since

$$[\gamma_\mu, \sigma_{\alpha\beta}] = \frac{2}{i}(\delta_{\mu\alpha}\gamma_\beta - \delta_{\mu\beta}\gamma_\alpha)\,,$$

and

$$[\sigma_{\alpha\beta}, \sigma_{\mu\nu}] = \delta_{\alpha\mu}\sigma_{\beta\nu} - \delta_{\alpha\nu}\sigma_{\beta\mu} + \delta_{\beta\mu}\sigma_{\alpha\nu} - \delta_{\beta\nu}\sigma_{\alpha\mu}\,.$$

if we are given two (4×4) matrices M_1 and M_2 of the type $M=(a_\mu\gamma_\mu + b_{\mu\nu}\sigma_{\mu\nu})$, their commutator $[M_1, M_2]$ is also a matrix of the same type [8]. In other words all ten-parameter matrices of the form $a_\mu\gamma_\mu + b_{\mu\nu}\sigma_{\mu\nu}$ generate a Lie algebra.

Among such matrices are the Bose matrix B and the Fermi matrix F, defined as

$$B = \begin{pmatrix} \boldsymbol{\tau}\cdot\boldsymbol{\pi} & \boldsymbol{K}\cdot\boldsymbol{\tau} + iK_4 \\ \boldsymbol{K}\cdot\boldsymbol{\tau} - iK_4 & \boldsymbol{\tau}\cdot\boldsymbol{\omega} \end{pmatrix}, \qquad \text{where} \qquad \boldsymbol{K}\cdot\boldsymbol{\tau} + iK_4 = \begin{pmatrix} -\overline{K}^0 & K^+ \\ K^- & K^0 \end{pmatrix},$$

$$F = \begin{pmatrix} \boldsymbol{\tau}\cdot\boldsymbol{\Sigma} & \boldsymbol{\tau}\cdot\boldsymbol{U} + iU_0 \\ \boldsymbol{\tau}\cdot\boldsymbol{U} - iU_0 & \boldsymbol{\tau}\cdot\boldsymbol{X} \end{pmatrix}, \quad \text{where} \quad \boldsymbol{\tau}\cdot\boldsymbol{\Sigma} = \begin{pmatrix} \Sigma^0 & \Sigma^+ \\ \Sigma^- & \Sigma^0 \end{pmatrix}, \quad \boldsymbol{\tau}\cdot\boldsymbol{U} + iU_0 = \begin{pmatrix} \Xi^0 & p \\ \Xi^- & n \end{pmatrix}.$$

(7) There is some evidence from Dubna for the existence of the W⁺ particle (Kiev Conference Report, 1959) (not to be published). There is no evidence so far, for the existence of the X-particles. If these particles are really missing, the considerations of the present note would become unrealistic and the 3-dimensional unitary symmetry (4) remains the nearest approximation to facts in either the form suggested by NEEMAN and GELL-MANN or in the Sakata form adopted by SALAM and WARD. The first form predicts the same (Λ, Σ) relative parity while for the second form this is not essential, but both predict the existence of eight vector bosons.

(8) For three such matrices M_1, M_2, M_3, $\mathrm{Tr}\,(M_1M_2M_3 + M_3M_2M_1) \equiv 0$.

In writing out B and F we have used for the Dirac matrices

$$\boldsymbol{\gamma} = \begin{pmatrix} & \boldsymbol{\tau} \\ \boldsymbol{\tau} & \end{pmatrix}, \quad \gamma_4 = \begin{pmatrix} & i \\ -i & \end{pmatrix}, \quad \sigma_{\mu\nu} = \begin{pmatrix} \boldsymbol{\tau} & \\ & \boldsymbol{\tau} \end{pmatrix}, \begin{pmatrix} \boldsymbol{\tau} & \\ & -\boldsymbol{\tau} \end{pmatrix}.$$

The kinetic energy terms in the free Lagrangian

$$L = -\tfrac{1}{2}\,\mathrm{Tr}\,(\partial_\mu B^+)(\partial_\mu B) - \mathrm{Tr}\, F^+\gamma_4\,\gamma_\mu(\partial_\mu F)\,,$$

are invariant for the infinitesimal unitary symplectic transformations

$$B \to (1 + iH)B\,,$$

$$F \to (1 + iH)F\,,$$

where H has the same form as B. Vector mesons can be introduced by defining a « covariant derivative » [4]

$$\nabla_\mu = (\partial_\mu + iH_\mu)\,.$$

The ten mesons which appear as elements of the matrix H_μ differ from the π, ω and K-mesons only in their spin; otherwise their symmetry properties are the same. Thus three of these mesons possess $I=1$, $S=0$; three possess $I=0$, $S=\pm 2$, 0 and four correspond to $I=\frac{1}{2}$, $S=\pm 1$ (like the K*-particles).

* * *

We would like to thank Professor R. G. SACHS for an invitation to the Summer School held at the University of Wisconsin where this work was done.

LIBRI RICEVUTI E RECENSIONI

Libri ricevuti.

L. R. B. Elton: *Nuclear Sizes*. Oxford University Press, 1961; pp. 114; 15 s.

N. Bohr: *Physique Atomique et Connaissance Humaine*. Gauthier-Villars, Paris, 1961; pp. 98; 15 NF.

P. Roman: *Theory of Elementary Particles*, 2nd ed. North Holland Publ., Amsterdam, 1961; pp. xvi-580; $ 50.00.

— *Infrared Physics*: an International Research Journal, vol. I, no 1 (March 1961)· Pergamon Press, 1961, pp. 104.

Recensioni.

E. M. Pugh and E. W. Pugh – *Principles of Electricity and Magnetism*. Addison-Wesley Publ. Co. Inc., Reading, Mass., U. S. A., London, England, 1960; $ 8.75.

Questo libro si propone di approfondire la conoscenza dei principi dell'elettricità e del magnetismo per studenti che indirizzano la loro attività verso i diversi rami della tecnica, principalmente, si può ritenere, verso l'ingegneria e la fisica applicata. Esso presuppone una conoscenza della fisica elementare e dei fondamenti dell'algebra e del calcolo infinitesimale, sino alle equazioni a derivate parziali.

Il primo capitolo è dedicato ai sistemi di unità di misura in uso per l'elettromagnetismo. Seguono tre capitoli sui fondamenti dell'elettrostatica, i quali servono a richiamare insieme le principali nozioni matematiche occorrenti, ed in particolare a introdurre i concetti e i metodi dell'analisi vettoriale, di cui è fatto poi uso sistematico nel libro. Gli A. rilevano come sia vantaggioso ai fini didattici presentare i principi della matematica insieme con le applicazioni fisiche di essi. Pur trovandoci d'accordo, in linea generale, su questo punto di vista, solleviamo qualche dubbio sulla opportunità di presentare la legge di Biot e Savart, come applicazione del prodotto vettoriale, ed il teorema di Stokes, come applicazione dell'operatore *rot*, in capitoli di elettrostatica: nel timore che questo possa generare qualche confusione d'idee.

L'inconveniente, se tale lo si vuol considerare, che il titolo dei capitoli non corrisponda sempre strettamente al contenuto, si riscontra anche più avanti. Al capitolo sesto sulle « Correnti continue » segue il settimo sulla « Induzione elettromagnetica », mentre l'ottavo soltanto è dedicato ai « Campi magnetici delle correnti elettriche »: ma le definizioni relative a questi campi si trovano nel capitolo settimo. È probabile, del resto, che l'allievo che fa uno studio sistematico del libro non abbia a risentire di questi inconvenienti; mentre egli troverà utili i frequenti ravvicinamenti fra argomenti diversi.

A parte questi rilievi non essenziali, ed altri che si potrebbero fare circa

qualche squilibrio nella trattazione, il libro ci sembra utile a quei fini didattici che esso si propone. L'impostazione generale e la scelta della materia sono quelle tradizionali. Il libro si conclude con un capitolo abbastanza esteso sui circuiti a corrente alternata, ed uno sulla radiazione elettromagnetica, che contiene la deduzione delle leggi della riflessione e rifrazione per un'onda piana e trattazioni sommarie dei problemi del dipolo oscillante e delle guide d'onda.

A. Rostagni

M. W. Wolkenstein – *Struktur und physicalische Eigenschaften der Moleküle.* B. G. Teubner Verlaggesellschaft, Leipzig, 1960; pagine XIV-770.

Il libro del noto strutturista sovietico Wolkenstein, apparso in Russia nel 1955, ed ora accessibile anche alla maggior parte dei cultori occidentali della materia nella nuova traduzione tedesca curata dal Dr. Heise di Berlino, contiene, nella forma di un tipico testo universitario la materia d'esame di uno dei corsi fondamentali di Chimica Fisica del nostro ordinamento universitario per la laurea in Chimica, quello dedicato alla strutturistica atomica e molecolare.

Il volume è evidentemente dedicato, anche nelle intenzioni dell'Autore, ad un pubblico di studenti universitari ed, a parere di chi scrive, è un modello del genere. Tutti i principali metodi e problemi della strutturistica molecolare moderna vi sono trattati in forma piana e molto aggiornata, con un minimo di descrizione matematica delle teorie e con grande dettaglio di illuminanti dati sperimentali.

Oltre agli argomenti classici di spettroscopia atomica e molecolare, a quelli sulla natura del legame chimico nelle molecole semplici e complesse, sulle proprietà elettriche ed ottiche dei sistemi molecolari e via dicendo, non manca la trattazione breve ma soddisfacente di metodi e problemi attualissimi come la risonanza magnetica elettronica e nucleare e le proprietà fisiche e strutturali delle macromolecole anche di interesse biologico.

I riferimenti bibliografici sono numerosissimi ed uno dei pregi del volume è che molti di questi sono dedicati ai contributi dei ricercatori sovietici poco citati nei testi occidentali. Non per questo mancano di essere ricordati gli autori occidentali nella giusta misura, se si esclude il capitolo introduttivo sulla «Teoria della costituzione chimica» nei quale domina la figura di Butlerov che è giustamente considerato un pioniere della strutturistica ma che non è certamente il solo.

Se si può fare un appunto all'Autore, è che forse si è un po' troppo dilungato in alcuni capitoli che trattano i suoi argomenti favoriti come l'attività ottica e la spettroscopia di vibrazione a scapito di qualche argomento pure importante, come la struttura dei complessi di coordinazione, che è troppo brevemente trattato.

Benchè, come ho detto sopra, il libro sia da considerarsi specialmente dedicato agli studenti (e per questo motivo sarebbe la benvenuta una traduzione italiana), esso può, per certi suoi aspetti, interessare anche il vasto pubblico di chimici e fisici impegnati in ricerche di struttura molecolare.

G. Giacometti